

UNIVERSITY OF ALBERTA

Compression Behaviour of Thixotropic Oil Sands Tailings

by

Silawat Jeeravipoolvarn

A thesis submitted to the Faculty of Graduate Studies and Research in partial fulfillment
of the requirements for the degree of Master of Science

in

Geotechnical Engineering

Department of Civil and Environmental Engineering

EDMONTON, ALBERTA

Spring 2005


ABSTRACT

Three ten meter high standpipe tests were initiated in 1982 to investigate the compression behaviour of oil sands tailings. The objectives of this research are to document and analyze the compression behaviour of these tailings in the ten meter standpipe tests and to use a finite strain consolidation theory to model the compression behaviour of these materials. The mature fine tailings (MFT) standpipe has been monitored for over 22 years and although it has compressed 3 meters by self-weight, very little or no effective stresses have developed. The MFT-sand standpipe with 82% sand content reached 100% consolidation in 8 years consolidating 1.5 m. Modeling with the finite strain consolidation theory does not predict the compression behaviour of the MFT. The theory, however, can forecast the consolidation progress of MFT-sand mixes which have a high percentage of sand. A nonsegregating MFT-sand mix should result in a tailings stream that consolidates rapidly to a sufficient density in a reasonable length of time.


University of Alberta

Faculty of Graduate Studies and Research

The undersigned certify that they have read, and recommend to the Faculty of Graduate Studies and Research for acceptance, a thesis entitled Compression Behaviour of Thixotropic Oil Sands Tailings submitted by Silawat Jeeravipoolvarn in partial fulfillment of the requirements for the degree of Master of Science in Geotechnical Engineering.



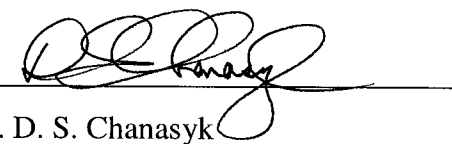
Dr. R. J. Chalaturnyk



Dr. J. D. Scott



Dr. D. C. Sego



Dr. D. S. Chanasyk

December 15th, 2004

Date of Approval by Committee

University of Alberta

Library Release Form

Name of Author: Silawat Jeeravipoolvarn

Title of Thesis: Compression Behaviour of Thixotropic Oil Sands Tailings

Degree: Master of Science

Year this Degree Granted: 2005

Permission is hereby granted to the University of Alberta Library to reproduce single copies of this thesis and to lend or sell such copies for private, scholarly or scientific research purposes only.

The author reserves all other publication and other rights in association with the copyright in the thesis, and except as herein before provided, neither the thesis nor any substantial portion thereof may be printed or otherwise reproduced in any material form whatever without the author's prior written permission.

Silawat J.

.....
9/1536 KlangMueng Rd., Amphur Mueng,
KhonKaen, 40000, THAILAND

December 22nd 2004

ACKNOWLEDGEMENTS

I would like to express my deepest gratitude to my supervisors, Dr. J.D. Scott and Dr. R.J. Chalaturnyk, for their guidance, patience, encouragement, and continual technical and financial support throughout my time at the university. Their help can never be forgotten.

Thank you to Ken Leung, Gilbert Wong and Steve Gamble for all the laboratory support and hard work. Thank you to Gordon Pollock, Dr. Yin Jianhua, Srbojib Masala, Chengmai Guo, Jen Wen Yang and Xieteng Liu for helpful technical discussions and recommendations.

Also I would like to thank all the faculty and staff in Geotechnical and Geoenvironmental Engineering and in the Department of Civil and Environmental Engineering at the University of Alberta for providing a pleasant and friendly environment which helped me through all the hard work. This research would not have been possible without them.

I would like to express my sincere gratitude to Syncrude Canada Ltd. who provided the initial funding to fabricate, install and fill the standpipes and perform the initial monitoring and to Suncor Energy Inc. who provided financial support for my research through the University of Alberta Oil Sands Tailings Research Facility (OSTRF).

Special thanks to my close friends, Changho Lim, WonJae Chang, Arash Eshraghian, and Khuram Mohib for their encouragement and the most refreshing moments. My thanks are extended to all my colleagues and friends in Canada and Thailand.

Finally, I would like to express my gratitude to my father, mother and brother for their love, and support.

TABLE OF CONTENTS

CHAPTER	PAGE
1. INTRODUCTION	1
1.1. Statement of Problem	1
1.2. Objectives and Scope of Thesis	1
1.3. Organization of Thesis	2
2. LITERATURE REVIEW	4
2.1. Oil Sands Tailings	4
2.1.1. Introduction	4
2.1.2. Extraction process	8
2.1.3. Tailing disposal method	10
2.1.4. Sedimentation and Consolidation in a pond	13
2.2. Sedimentation and Consolidation Considerations	14
2.3. Important Characteristics affecting Consolidation Behaviour of Fine Tailings	19
2.3.1. Compressibility	19
2.3.2. Hydraulic conductivity	20
2.3.3. Thixotropy	21
2.3.3.1. Clay mineralogy	24
2.3.3.2. Water content	25
2.3.3.3. Loading rate	25
2.3.3.4. Axial strain	26
2.3.3.5. Time	27
2.3.3.6. Thixotropy and consolidation	27
2.3.3.7. Comparison of thixotropy obtained from different clays	27
2.3.3.8. Thixotropic gain in strength tests and thixotropic strength evaluation	29
2.3.4. Creep behaviour of fine tailings	32
2.4. Scanning Electron Micrograph Technique and Fine Tailings Structure	35
2.4.1. Test procedure	36
2.4.2. SEM image analysis	37
2.5. Summary	38
3. TEN METER STANDPIPE TEST	40
3.1. Objectives of Large Standpipe Testing	40
3.2. The Ten meter Standpipe	41
3.3. Tailings Materials and Standpipe Filling	42
3.3.1. Filling Standpipe 1 with MFT	42
3.3.2. Filling Standpipe 2 with MFT-tailings sand mix	43
3.3.3. Filling Standpipe 3 with MFT-tailings sand mix	43

3.4. Monitoring ports	46
3.4.1. Sample ports	46
3.4.1.1. Solids content sampler	46
3.4.1.1.1. Solids content sampling procedures	48
3.4.1.2. Density sampler	48
3.4.1.2.1. Density sampling procedures	49
3.4.2. Pore water pressure ports	50
3.4.2.1. Procedure for reading piezometers in 10 m standpipes	51
3.5. History of Measurements on Standpipes	52
3.5.1. History of measurements on Standpipe 1	53
3.5.2. History of measurements on Standpipe 2	53
3.5.3. History of measurements on Standpipe 3	53
3.6. Summary	54
4. TEN METER STANDPIPE 1 MEASUREMENTS	59
4.1. Material Index Properties	59
4.1.1. Grain size distribution	60
4.1.1.1. recommended particle size analysis procedure	60
4.1.1.2. Methylene blue analysis	64
4.1.1.3. Particle size fraction profiles	66
4.1.2. Mineralogy	66
4.1.3. Water chemistry	67
4.1.4. Biological gas	70
4.1.5. Bitumen content	72
4.1.6. Specific gravity	73
4.1.7. Atterberg limits	73
4.2. Thixotropy	75
4.2.1. Determination of overconsolidation stress	76
4.3. Interface Measurements	78
4.4. Solids Content Measurements	80
4.5. Bulk Density Measurements	81
4.6. Pore Water Pressure Measurements	82
4.7. Scanning Electron Micrograph (SEM)	93
4.7.1. Energy dispersive X-Ray analysis	94
4.8. Summary	97
5. TEN METER STANDPIPE 2 MEASUREMENTS	100
5.1. Material Index Properties	100
5.1.1. Grain size distribution	100
5.1.2. Mineralogy	102
5.1.3. Bitumen content and specific gravity	102
5.2. Interface Measurements	103
5.3. Solids Content Measurements	107
5.4. Bulk Density Measurements	107

5.5. Pore Water Pressure Measurements	108
5.6. Summary	117
6. TEN METER STANDPIPE 3 MEASUREMENTS	119
6.1. Material Index Properties	119
6.1.1. Grain size distribution	119
6.1.2. Mineralogy	121
6.1.3. Bitumen content and specific gravity	121
6.2. Interface Measurements	122
6.3. Solids Content Measurements	125
6.4. Pore Water Pressure Measurements	127
6.5. Effective Stress Calculations	134
6.6. Comparison of settlement in Standpipes 1, 2 and 3.	141
6.7. Summary	144
7. CONSOLIDATION MODELING OF THIXOTROPIC SLURRIES	146
7.1. Consolidation and Hydraulic Conductivity Tests	146
7.1.1. Consolidation testing of oil sands fine tailings	147
7.1.1.1.Improved consolidation testing	147
7.1.1.2.The University of Alberta Geotechnical Centre large strain consolidation test	149
7.1.1.2.1. Large strain consolidation test procedure	149
7.1.2. Hydraulic conductivity test	158
7.1.2.1.Indirect methods of determining hydraulic conductivity	158
7.1.2.2.Direct methods of determining hydraulic conductivity	159
7.1.2.2.1. Constant head and falling head test	159
7.1.2.2.2. Flow pump test	160
7.1.2.2.3. Restricted flow test	160
7.1.2.2.4. Seepage test	160
7.1.2.3.Hydraulic conductivity test of the oil sands fine tailings	161
7.1.2.3.1. Testing equipments	161
7.1.2.3.2. Test procedure	161
7.2. Consolidation Test and Hydraulic Conductivity Test Results	162
7.2.1. Effective stress-void ratio relationship	162
7.2.2. Hydraulic conductivity-void ratio relationship	169
7.3. Theories of Consolidation	177
7.3.1. Finite strain theory	177
7.3.1.1.Finite strain consolidation model and variation of input relationships	180
7.4. Stress- Strain-Strain Rate relationship for the Compressibility of Clays	184
7.5. Consolidation modeling by Finite Strain Consolidation Theory	189
7.5.1. Consolidation prediction of the ten meter Standpipe 1	189

7.5.1.1.Procedure to obtain void ratio – effective stress relationship	189
7.5.1.2.Finite strain consolidation input parameters and analysis results	193
7.5.2. Consolidation prediction of the ten meter Standpipe 2	201
7.5.3. Consolidation prediction of the ten meter Standpipe 3	206
7.6. Summary	212
8. SUMMARY, CONCLUSIONS AND RECOMMENDATION	215
8.1. Summary	215
8.2. Observations and Conclusions	215
8.3. Major Conclusions of Research Project	219
8.4. Recommendations for Further Study	220
9. BIBLIOGRAPHY	222
10. APPENDIX A- ESTIMATION OF OIL SANDS TAILINGS STREAM VOLUME	231

LIST OF TABLES

	PAGE
Table 2.1 Reserves summary 2003 (EUB, 2004)	4
Table 3.1 Initial characteristics of mature fine tailings	45
Table 3.2 Tailings properties in the ten meter standpipes	46
Table 3.3 Measurements on Standpipe 1	55
Table 3.4 Measurements on Standpipe 2	57
Table 3.5 Measurements on Standpipe 3	58
Table 4.1 Major minerals of the mature fine tailings in Standpipe 1	67
Table 4.2 Compositions of pore water in ppm of the mature fine tailings from Standpipe 1.	68
Table 4.3 Index properties of the fine tailings.	74
Table 4.4 SEM image analysis results.	93
Table 5.1 Major minerals of the MFT-tailings sand mix in Standpipe 2	102
Table 6.1 Major minerals of the MFT-tailings sand mix in Standpipe 3	121
Table 7.1 MFT sample for large strain consolidation test	151
Table 7.2 Dead load	152
Table 7.3 Bellofram load	153
Table 7.4 Maximum head difference to be used for a permeability test	154
Table 7.5 Finite strain parameters	180
Table 7.6 Average strain rate results	190
Table 7.7 Finite strain parameters in pascals and m/s for Standpipe 1	195
Table 7.8 Finite strain parameters in pascals and m/s for Standpipe 2	201
Table 7.9 Finite strain parameters in pascals and m/s for Standpipe 3	207

LIST OF FIGURES

	PAGE
Figure 2.1 Alberta's oil reserves and production (Modified from EUB, 2004)	5
Figure 2.2 Alberta's three oil sands areas (Modified from EUB, 2004)	6
Figure 2.3 Scanning electron microscope of bitumen-free McMurray Formation oil sand (Modified from Touhidi, 1998)	8
Figure 2.4 Generalized scheme of Clark Hot Water Extraction Process (Modified from Chalaturnyk, R.J. et al. 2004)	9
Figure 2.5 Cross section of an oil sands tailings basin (Modified from FTFC, 1995)	10
Figure 2.6 Typical grain size distribution of oil sands fine tailings (Modified from FTFC, 1995)	12
Figure 2.7 The general characteristics of sedimentation of clay-water mixture (Modified from Imai, 1981)	16
Figure 2.8 Compressibility of oil sand fine tailings for various solids content (Modified from Suthaker, 1995)	19
Figure 2.9 Variation of flow velocity with time in the hydraulic conductivity testing (Modified from Suthaker, 1995)	20
Figure 2.10 Thixotropic ratio in some typical clays and the fine tailings	28
Figure 2.11 Thixotropic ratio in three clay minerals and the fine tailings	29
Figure 2.12 Total shear strength measurement of mature fine tailings	30
Figure 2.13 Solids content measurement of mature fine tailings	30
Figure 2.14 Thixotropic shear strength measurement of mature fine tailings	31
Figure 2.15 Creep index for fine tailings (Modified from Suthaker, 1995)	33
Figure 2.16 Comparison of creep index (Modified from Suthaker, 1995)	33
Figure 2.17 Creep index for fine tailing sand mixes (Modified from Suthaker, 1995)	34
Figure 2.18 Comparison of C_α and C_c relationship (Modified from Suthaker 1995)	34

Figure 2.19 Creep rate and void ratio	35
Figure 3.1 The ten meter standpipe	41
Figure 3.2 Ternary Diagram	44
Figure 3.3 Location of piezometer and sample ports of a ten meter standpipe test	47
Figure 3.4 Solids content sampler	48
Figure 3.5 Density sampler	49
Figure 4.1 Grain size distribution measured in 1985	63
Figure 4.2 Grain size distribution measured in 2003	63
Figure 4.3 Particle size fraction profiles	65
Figure 4.4 pH profiles	69
Figure 4.5 Conductivity profiles	69
Figure 4.6 Methanogen profiles	71
Figure 4.7 SRB profiles	71
Figure 4.8 Measured degree of saturation in 1997 and 2003	71
Figure 4.9 Plasticity of oil sand fine tailings	74
Figure 4.10 Thixotropic strength	76
Figure 4.11 Interface measurement with arithmetic time	79
Figure 4.12 Interface measurement with log time	79
Figure 4.13 Initial interface measurement to 900 days	80
Figure 4.14 a) solids content profiles b) fines void ratio profiles	81
Figure 4.15 Comparison of bulk density	82
Figure 4.16 Initial excess pore water pressure measurements	85
Figure 4.17 Excess Pore water dissipation rate profiles	88
Figure 4.18 Total stress, pore pressure and effective stress profiles at 2 days	89
Figure 4.19 Total stress, pore pressure and effective stress profiles at 2.4 years	90
Figure 4.20 Total stress, pore pressure and effective stress profiles at 9.8 years	91
Figure 4.21 Total stress, pore pressure and effective stress profiles at 20.6 years	92
Figure 4.22 The fine tailings structure at 3.5 m depth (39.9% solids).	95

Figure 4.23 The fine tailings structure at 6.5 m depth (37.0% solids).	95
Figure 4.24 The fine tailings structure at 9.5 m depth (46.2% solids).	95
Figure 4.25 Energy dispersive X-Ray analysis at 3.5 m depth (39.9% solids).	96
Figure 4.26 Energy dispersive X-Ray analysis at 6.5 m depth (39.9% solids).	96
Figure 4.27 Energy dispersive X-Ray analysis at 9.5 m depth (39.9% solids).	96
Figure 5.1 Particle size distribution of MFT-tailings sand mix in Standpipe 2	101
Figure 5.2 Transition zone at the top of Standpipe 2	103
Figure 5.3 Interface settlement of a transition zone	104
Figure 5.4 Fines content profile in the top 2 meters	105
Figure 5.5 Fines content profile of Standpipe 2	105
Figure 5.6 Interface measurement with arithmetic time	106
Figure 5.7 Interface measurement with log time	106
Figure 5.8 Solids content profiles of MFT-tailings sand mix in Standpipe 2	108
Figure 5.9 Initial excess pore water pressure measurements for standpipe number 2	110
Figure 5.10 Total stress, pore pressure and effective stress profiles at 0 day	113
Figure 5.11 Total stress, pore pressure and effective stress profiles at 183 days	114
Figure 5.12 Total stress, pore pressure and effective stress profiles at 339 days	115
Figure 5.13 Total stress, pore pressure and effective stress profiles at 650 days	116
Figure 6.1 Particle size distribution of MFT-tailings sand mix in Standpipe 3	120
Figure 6.2 Initial interface measurement with time (100 day period)	122
Figure 6.3 Interface measurement with arithmetic time	123
Figure 6.4 Interface measurement with log time	123
Figure 6.5 Compressibility function for Standpipe 3	124
Figure 6.6 Solids content profiles of fine tailings-sand mix in Standpipe 3	126
Figure 6.7 Initial excess pore water pressure measurements	129
Figure 6.8 Excess pore water measurements in Standpipe 3	132
Figure 6.9 Normalized depth of Excess pore water pressure in Standpipe 3	133
Figure 6.10 Solids content profiles at 100% consolidation	135

Figure 6.11 Total stress, pore pressure and effective stress profiles at 3 days	136
Figure 6.12 Total stress, pore pressure and effective stress profiles at 335 days	137
Figure 6.13 Total stress, pore pressure and effective stress profiles at 872 days	138
Figure 6.14 Total stress, pore pressure and effective stress profiles at 1529 days	139
Figure 6.15 Total stress, pore pressure and effective stress profiles at 100% consolidation	140
Figure 6.16 Solids content increases with time	142
Figure 6.17 Fines void ratio changes with time	143
Figure 6.18 Rate of compression of fines matrix with sand content	143
Figure 7.1 Initial set up of the Large Strain Consolidation Test before loading sample	155
Figure 7.2 Sample loaded with piston and dead loads up to about 8 kPa	156
Figure 7.3 Sample in loading frame and loaded by bellofram up to 1000 kPa.	157
Figure 7.4 Compressibility of oil sands tailings (Modified from Pollock, 1988)	163
Figure 7.5 Compressibilities of fine tailings with sand	164
Figure 7.6 Compressibility of oil sand tailings SFR 3:1 with different additives	166
Figure 7.7 Compressibility of oil sand tailings SFR 4:1 with different additives	166
Figure 7.8 Compressibility of oil sand tailings SFR 5:1 with different additives	167
Figure 7.9 Compressibility of oil sand tailings SFR 6:1 with different additives	167
Figure 7.10 Selected compressibilities of fine tailing with sands	168
Figure 7.11 Hydraulic conductivity of mature fine tailings	169
Figure 7.12 Hydraulic conductivity - fines void ratio relationship of tailings materials in the ten meter standpipes	171
Figure 7.13 Hydraulic conductivity – void ratio relationships for the tailings materials in the ten meter standpipes	172
Figure 7.14 Hydraulic conductivity – void ratio of various oil sand tailing materials	174
Figure 7.15 Hydraulic conductivity – fines void ratio of various oil sand tailing materials	175

Figure 7.16 Hydraulic conductivity – fines void ratio of chosen oil sand tailing materials	176
Figure 7.17 Varied Compressibility and interface settlement prediction for short term	182
Figure 7.18 Varied Permeability and interface settlement prediction for short term	182
Figure 7.19 Varied Compressibility and interface settlement prediction for long term	183
Figure 7.20 Varied Permeability and interface settlement prediction for long term	183
Figure 7.21 Instant and delayed compression compared with primary and secondary compression (Modified from Bjerrum 1967).	184
Figure 7.22 Compressibility and shear strength of clay exhibiting delayed consolidation (Modified from Bjerrum 1967).	185
Figure 7.23 Schematic of pore water pressure increase during relaxation (Modified from Yin et al. 1994)	186
Figure 7.24 Suggested rheological model (Modified from Leroueil et al. 1985)	188
Figure 7.25 Stress-strain curve	191
Figure 7.26 Normalized stress-strain curve	191
Figure 7.27 Preconsolidation-average strain rate	191
Figure 7.28 Strain – time –sample height	192
Figure 7.29 The 10 m standpipe void ratio-effective stress arithmetic curve	194
Figure 7.30 The 10 m standpipe void ratio-effective stress log curve	194
Figure 7.31 Interface settlement for 10 m standpipe 1	197
Figure 7.32 Interface settlement for 10 m standpipe 1 (log time)	197
Figure 7.33 Solids content profile for 10 m standpipe 1	198
Figure 7.34 Excess pore water pressure profile for 10 m standpipe 1	199
Figure 7.35 Effective stress profile for 10 m standpipe 1	200
Figure 7.36 Interface settlement for 10 m standpipe 2	202
Figure 7.37 Interface settlement for 10m standpipe 2 (log time)	202
Figure 7.38 Solids content profile for 10m standpipe 2	203

Figure 7.39 Excess pore water pressure profile for 10m standpipe 2	204
Figure 7.40 Effective stress profile for 10m standpipe 2	205
Figure 7.41 Measured and selected compressibility relationship of Standpipe 3	207
Figure 7.42 Interface settlement for 10m standpipe 3 (arithmetic time)	209
Figure 7.43 Interface settlement for 10m standpipe 3 (log time)	209
Figure 7.44 Excess pore water pressure profile for 10m standpipe 3	210
Figure 7.45 Effective stress profile for 10m standpipe 3	211

1. Introduction

1.1 Statement of problem

The oil sands mining operations in Alberta produce large volumes of tailings composed of sand, silt, clay and a small amount of bitumen. Upon deposition the tailings segregate with the sand dropping out to form dykes and beaches and about one-half of the fines and the bitumen running into the tailings pond as a fine tails which are only about 8% solids. After deposition, the fine tails settle to about 30% solids within 2 years and the tailings at this point are called mature fine tails (MFT). The MFT exhibits significant cohesion and after reaching 30% solids the MFT does not appear to be consolidating in the tailing ponds, that is, the excess pore pressures are not dissipating. Volume decreases appear to be taking place by a creep mechanism.

To investigate these phenomena, two ten meter standpipes were fabricated and erected with an access scaffold in 1982 with MFT in one standpipe and a mix of MFT and tailings sand in the second standpipe. The MFT standpipe has been monitored for over 21 years and although the MFT has compressed 3 meters by self-weight, very little or no effective stresses have developed. Pore water pressures throughout the height of the standpipe are equal to the total stress. Geotechnical analyses such as finite strain consolidation theory, coupled sedimentation-consolidation theory, and an extension of finite strain consolidation theory incorporating creep have been used to model these test results. None of these theories can predict the consolidation and pore water pressures in the standpipe or in the large scale tailings pond deposits containing this cohesive slurry.

1.2 Objective and Scope of Thesis

The first objective of the research in this thesis is to study and document the compression behaviour of the oil sand tailings slurries in the ten meter standpipe tests which include mature fine tailings (MFT) and MFT-tailings sand mixes. The study includes measurements in the 10 m self-weight consolidation standpipe tests and in large strain consolidometer tests of these oil sand tailings materials. The equipment, materials and testing methods are described and test results are analyzed. The results are used to improve the understanding of the compression behaviour of these materials. The second

objective is to use a finite strain consolidation theory to model the compression behaviour of these materials in the 10 m standpipes and to provide limitations and suggestions on using the finite strain theory.

1.3 Organization of the Thesis

The thesis is organized into 8 chapters.

Chapter 2 presents a review of existing literature on related topics. This chapter begins with information on the oil sands deposits in Alberta followed by a brief description of the geology of the Athabasca oil sands. The bitumen extraction process used by the oil sands mining companies and the tailings disposal methods are outlined. This chapter continues with the sedimentation and consolidation aspects of fine tailings and factors affecting the consolidation behaviour are discussed.

Chapter 3 presents the background information on and the descriptions of the ten meter self-weight consolidation standpipe tests. The chapter includes the objectives of the test program, the general material properties, the methods used to fill the standpipes, the monitoring procedures, and the history of the measurements.

Chapter 4 provides detailed measurements on the mature fine tailings in ten meter standpipe 1. The measurements include index properties, settlement of the interface, solids content, bulk density, pore pressure measurements, thixotropic gain in strength, and scanning electron microscopy. The present understanding of the fine tailings compression behaviour is then discussed.

Chapter 5 provides detailed measurements on the MFT-tailings sand mix with 48% sand in ten meter standpipe 2. The measurements include index properties, settlement of the interface, solids content, bulk density, and pore pressure measurements. The chapter concludes with a summary of the observations and with conclusions on the compression behaviour of this MFT-tailings sand mix.

Chapter 6 provides detailed measurements on the MFT-tailings sand mix with 82% sand in ten meter standpipe 3. The measurements include index properties, settlement of the interface, solids content, bulk density, and pore pressure measurements. The chapter is finalized with a summary of the compression behaviour of this tailings and a comparison of the rate of settlement in the three standpipes.

Chapter 7 presents a review of the large strain consolidation test followed by the compressibility and permeability characteristics of oil sands tailings materials. The finite strain consolidation theory is outlined and the importance of the stress-strain-strain rate relationship for the compressibility of clays is discussed. Consolidation modeling using a finite strain consolidation theory is performed to model the performance of the materials in the three ten meter standpipes. Limitations and suggestions on the finite strain consolidation theory to model oil sand tailings materials are given at the end of this chapter.

Finally in Chapter 8, a summary of the observations and conclusions on the compression behaviour of the oil sand tailings developed throughout the thesis is shown.

2. Literature Review

This chapter begins with a brief review of the origin of the oil sands fine tailings, followed by a more detailed presentation of sedimentation and consolidation behaviour and important properties related to compressibility of the oil sands fine tailings. The chapter is finalized with a brief re-consideration of consolidation behaviour and important properties that relate to this behaviour.

2.1 Oil Sand Tailings

2.1.1 Introduction

In northern Alberta, Canada, oil sands have been known since the 1760s in the Fort McMurray area. The need for energy has brought these deposits into production and they have become a major industry in Northern Alberta.

According to the EUB (2004) raw bitumen production, which surpassed conventional crude oil production in 2001 for the first time, is continuing its growth. Nonupgraded bitumen and synthetic crude oil production accounted for 53% of Alberta's crude oil and equivalent production in 2003. Increased bitumen production and upgrading from oil sands mining was the main contributor to this growth. In situ bitumen production increased modestly compared to 2002. The following table summarizes Alberta's energy reserves at the end of 2003.

Table 2.1 Reserves summary 2003 (EUB, 2004)

	Crude Bitumen		Crude Oil		Natural Gas		Coal	
	(million cubic metres)	(billion barrels)	(million cubic metres)	(billion barrels)	(million cubic metres)	(billion barrels)	(million cubic metres)	(billion barrels)
Initial in place	258,900	1,629	9,852	62	7,504	261	94	103
Initial established	28,392	179	2,634	16.6	4,401	156	35	38
Cumulative production	667	4.2	2,380	15	3,279	116	1.21	1.3
Remaining established	27,726	174	254	1.6	1,122	40	34	37
Annual production	56	0.352	37	0.23	135	4.8	0.029	0.032
Ultimate potential (recoverable)	50,000	315	3,130	19.7	5,600	200	620	683

From Table 2.1, the total in situ and mineable remaining established reserves are 27.7 billion cubic metres. To the present date, only about 2% of the initial established crude bitumen reserve has been produced. In 2003, Alberta produced 35.6 million cubic metres from the mineable area and 20.3 million cubic metres from the in situ area for a total of 55.9 million cubic metres. The bitumen produced from mining was upgraded, yielding 31.2 million cubic metres of synthetic crude oil (SCO). The in situ production was sold as nonupgraded crude bitumen. This bitumen production was continuing to increase in 2003. On the other hand, Alberta's remaining established reserves of conventional crude oil was estimated at 254 million cubic metres which is only about 0.9% of the crude bitumen in situ and mineable remaining established reserves. The following figure shows annual production and remaining established reserves for crude bitumen and crude oil.

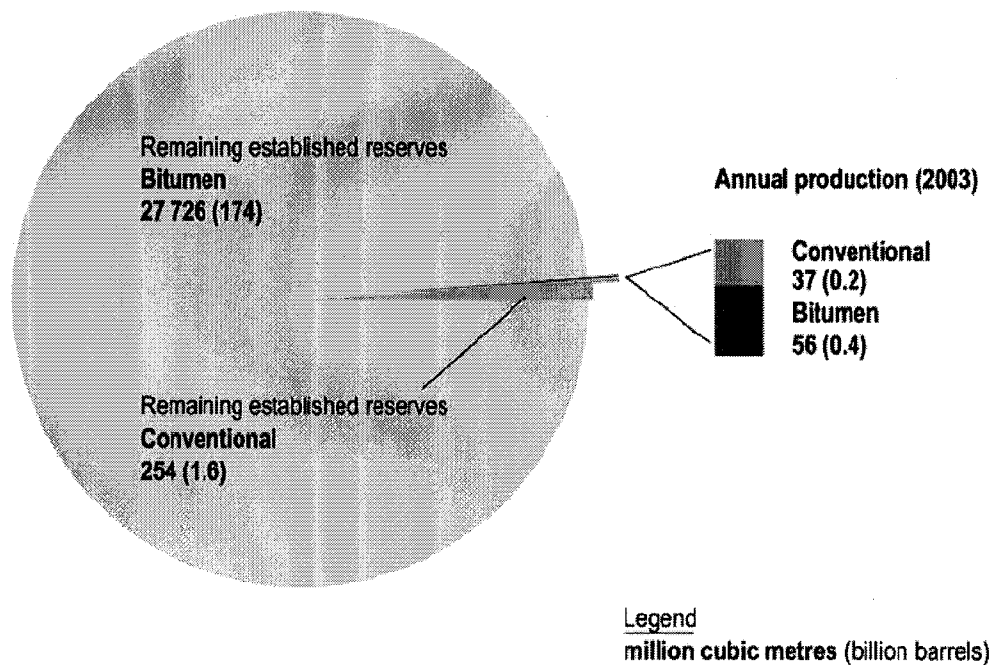


Figure 2.1 Alberta's oil reserves and production (Modified from EUB, 2004)

A comparison of conventional oil production and bitumen production over the last 10 years clearly shows bitumen's increasing contribution to Alberta's oil production. This ability to change from conventional oil to bitumen is unique to Alberta, allowing the province to offset the expected decline in conventional oil with bitumen production. It is expected that the share of nonupgraded bitumen and synthetic crude oil production in the overall Alberta crude oil to increase from 53% in 2003 to 80% by 2013 (EUB, 2004). The economic outlook for Alberta (EUB, 2004) and the above statement show that the expansion of the oil sands industry will offset the economic impact of declining conventional production activities and Alberta will continue to be the most important Canadian producer of crude oil and bitumen.

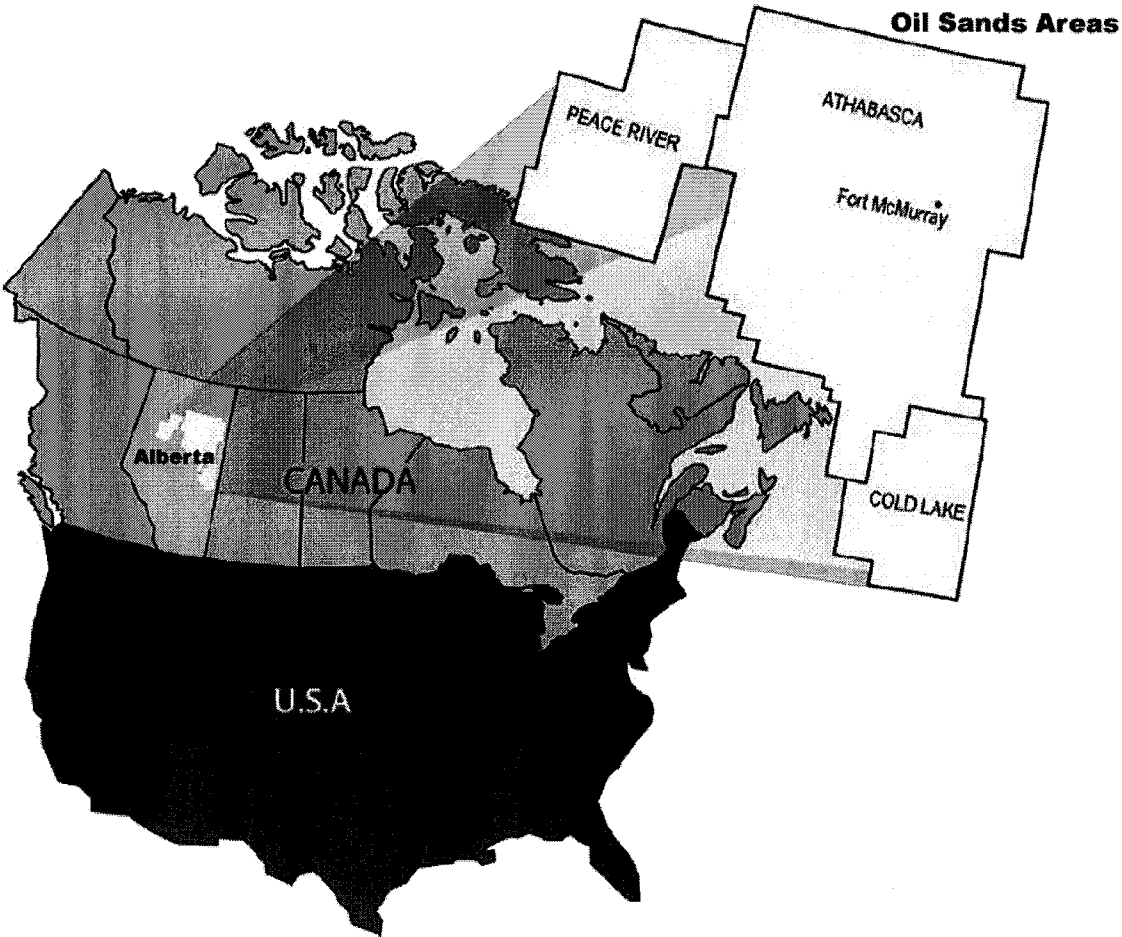


Figure 2.2 Alberta's three oil sands areas (Modified from EUB, 2004)

The Alberta oil sands consist of three deposits as shown in Figure 2.2 (Athabasca, Cold Lake and Peace River). These deposits contain in-place reserves of approximately

258.9 billion cubic metres of mineable and in situ crude bitumen with 28.4 billion cubic metres as initial established reserves.

Of the three deposits, the Athabasca deposit is the largest deposit and it contains an initial volume of crude bitumen of about 206.4 billion cubic metres. Essentially more than half of the bitumen reserves in the deposit are contained within the Lower Cretaceous Wabiskaw-McMurray Formation. About 18.0 billion cubic metres of crude bitumen in this deposit has overburden of less than 75 meters which makes these deposits suitable for the use of surface-mining techniques, unlike the rest of Alberta's crude bitumen area, where recovery will be through in situ methods (EUB, 2004). For the surface-mining techniques, it can be estimated that 1.0 m³ of the in place oil sands will produce a tailings stream volume of 3.3 m³ if the solids content of the tailings stream is 40% or a tailings stream volume of 1.9 m³ when the tailings solids content is 60% (Appendix A).

In detail, the sediments generally consist of uncemented quartzose sands and associated finer grained lithologies. The sand grains, predominately quartz, are covered by a layer of water with bitumen filling the pores. The sand was deposited in these layers approximately 100 million years ago. In this period, streams flowed from the Rocky Mountains in the west and from the Precambrian Shield in the east. These streams brought sand and shale which filled in between the ridges running through Alberta and Saskatchewan. Eventually the area was the location of an ancient inland sea which spread the sand more widely. How the sands became saturated with oil can be explained by a theory that the oil originated elsewhere and then flowed into the sand deposits that were filled with water.

The structure of the oil sands can be illustrated as in Figure 2.3. The sand grains in the formation are locked sands with some fines filling between particle contacts. However, the amount of the fines is very small and will not have a significant contribution to the total amount of fines in tailings. The fines in tailings originate from interbedded clay-shale which is broken up by the mining and extraction processes. In the

surface mineable area of the Athabasca oil sand deposit, the average bitumen content is about 9.7% by total mass or 20.7% by total volume. The amount of water relative to the bulk mass averages about 4.2% (EUB, 2004).

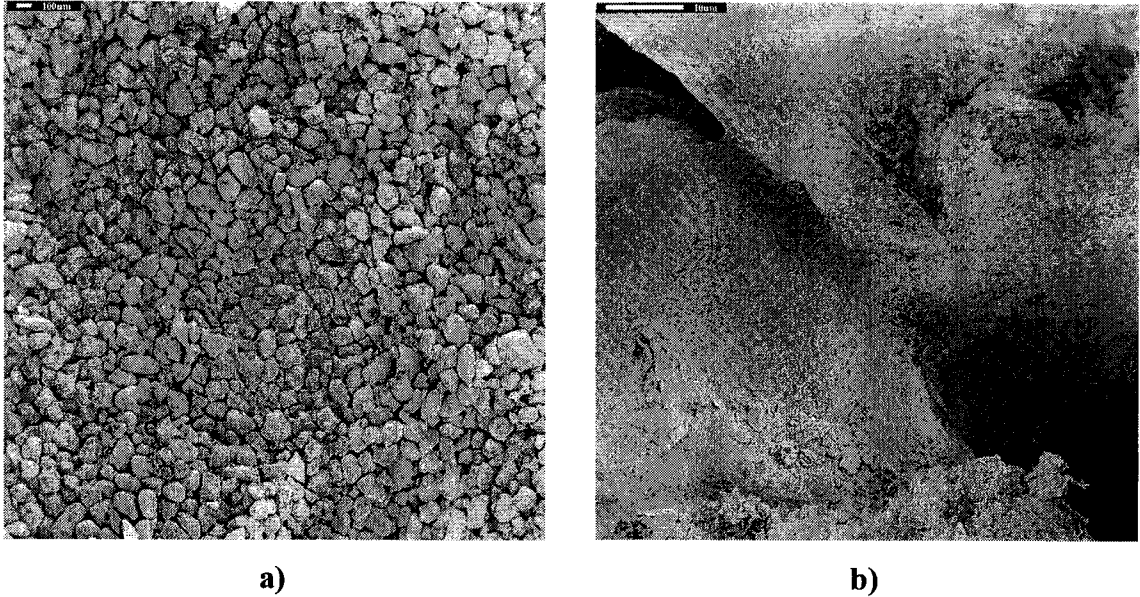


Figure 2.3 Scanning electron microscope of bitumen-free McMurray Formation oil sand a) overview of sand structure b) fines in sand structure

(Modified from Touhidi, 1998)

2.1.2 Extraction process

There are many processes that have been considered for extracting bitumen from the oil sands (Fuhr et. al., 1993). A schematic flow diagram of the oil sands process, from open pit to final product is shown in Figure 2.4. The initial extraction process is based on the pioneer work of Dr. Karl Clark, who used a combination of hot water, steam and caustic to separate bitumen from oil sands and the process is called the Clark Hot Water Extraction Process (CHWE). This process adds sodium hydroxide to the oil sands slurry to aid in the extraction process. The sodium hydroxide disperses the clay-shale stringers and seams in the oil sands and the process breaks the clay-shale down to small booklets or clay flakes. The particle size distribution is therefore affected by the extraction process. New oil sand plants such as Albion Sands Energy Inc. use a nondispersive bitumen extraction process and therefore their tailings will contain less clay-size material. This research is limited to tailings from the CHWE process.

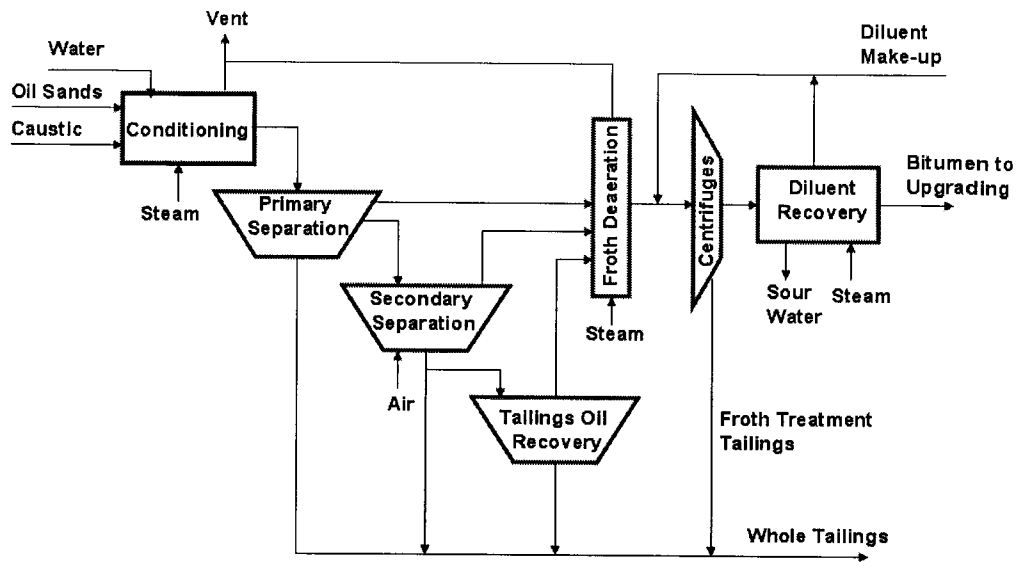


Figure 2.4 Generalized scheme of Clark Hot Water Extraction Process (Modified from Chalaturnyk, R.J. et al. 2004)

In today's commercial plants, oil sands are mined at Suncor and Syncrude by a truck and shovel method. From the truck discharge, the oil sands are partially conditioned in transport pipelines and at the extraction plant are digested and conditioned in large tumblers with the addition of hot water, steam and caustic soda to separate the bitumen from the oil sand. This is the first stage of extraction called conditioning. During this stage caustic soda (NaOH) is used to assist in maintaining the pH of the solution between 8.0 and 8.5 in order to separate the bitumen from the mineral solids. As a result the bitumen can be easily separated and the silt and clay particles become well dispersed. In the second stage, called separation, hot water is added to the solution to better separate the sand particles and to float the bitumen. The bitumen is separated as a froth which floats to the surface in large vessels known as primary separation vessels. The sands settle to the bottom and are then removed as a tailings stream.

After the first two stages, a portion of the slurry, known as middlings, is removed from the central portion of the vessels and is further processed to recover the fine oil droplets which remain unfloated in the first two stages. This stage is called scavenging.

At Suncor, this stream is processed in conventional flotation cells, and a small amount of bitumen is added to the primary settling vessels. At Syncrude, the tailings and middlings streams from the primary separation vessels are combined and further processed in large deep cone vessels where additional bitumen is recovered from both tailings and middlings. The additional bitumen is then added into the primary separation vessels. Both oil sand companies produce bitumen froth which contains significant amounts of water and fine soils, mainly clays, which must be removed prior to the upgrading process where bitumen is converted into a light synthetic crude oil.

2.1.3 Tailing disposal method

Tailings from the extraction process are composed of solids and water with small residual quantities of bitumen. In general, the tailings are a warm aqueous suspension of sand, silt, clay, residual bitumen and naphtha at a pH between 8 and 9.

The tailings are pumped into large tailing ponds where the coarse solids settle out to form dykes and beaches while much of the fines and residual bitumen are carried out into the ponds as a thin slurry stream with approximately 8% solids. Once the stream slows down, sedimentation of the clastic particles begins. Stokian and hindered settling of the fines takes place leaving a supernatant water layer on the top. This water will be recycled as extraction water. A schematic cross section of an oil sands tailings pond is shown in Figure 2.5.

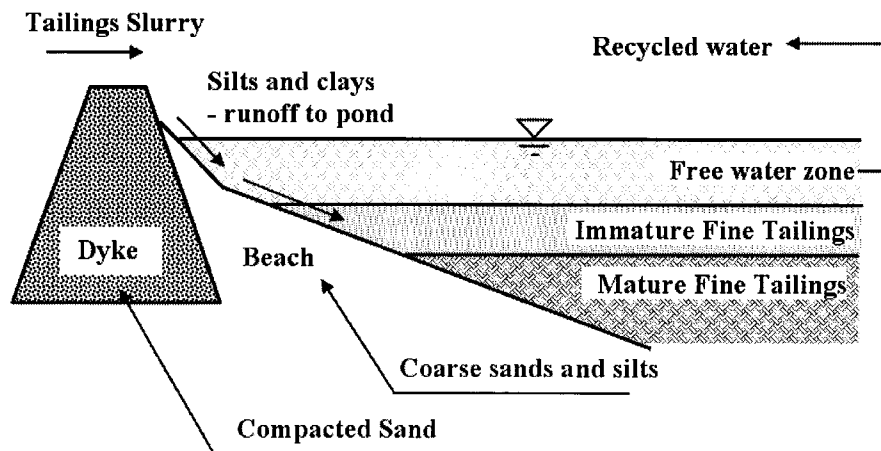


Figure 2.5 Cross section of an oil sands tailings basin (Modified from FTFC, 1995)

Over time, three zones have developed in the tailing ponds. From Figure 2.3, the top 1 to 3 m of the pond will be clear water which is continuously pumped back to the extraction processes. Under the clear water is the immature fine tailing zone - a transition zone of water and settling particles and this zone is about 1 to 2 m thick. Below this zone is the mature fine tailings (MFT) zone, a layer of silts and clays, fine sands, bitumen, and water which increases in density with depth due to sand settling through the MFT. The sands are wind blown sands from the dyke of the tailings pond. The depth of the mature fine tailings zone can vary from 15 to 20 m not including the higher sand content material at the bottom. The pond can have a maximum depth of about 50 m in some areas (Guo, 2004).

Generally, for the CHWE process, about half of the fine tails are in the clay-size range ($<2 \mu\text{m}$) with more than 90% of the material being silt or clay-size particles. Typical grain size distributions of the fine tailings are shown in Figure 2.6. Various studies have determined that the clay minerals typically consist of 80% kaolinite, 15% illite, 1.5% montmorillonite, 1.5% chlorite and 2% mixed clay layers (FTFC, 1995). Bitumen contents vary from 2 to 30% but is probably more typically in the range of 2% to 10% by dry weight (FTFC, 1995). The water in the fine tailings contains a number of organic compounds, for instance, naphthenic acids. Most of these organic compounds are believed to be released from the bitumen during the extraction processes.

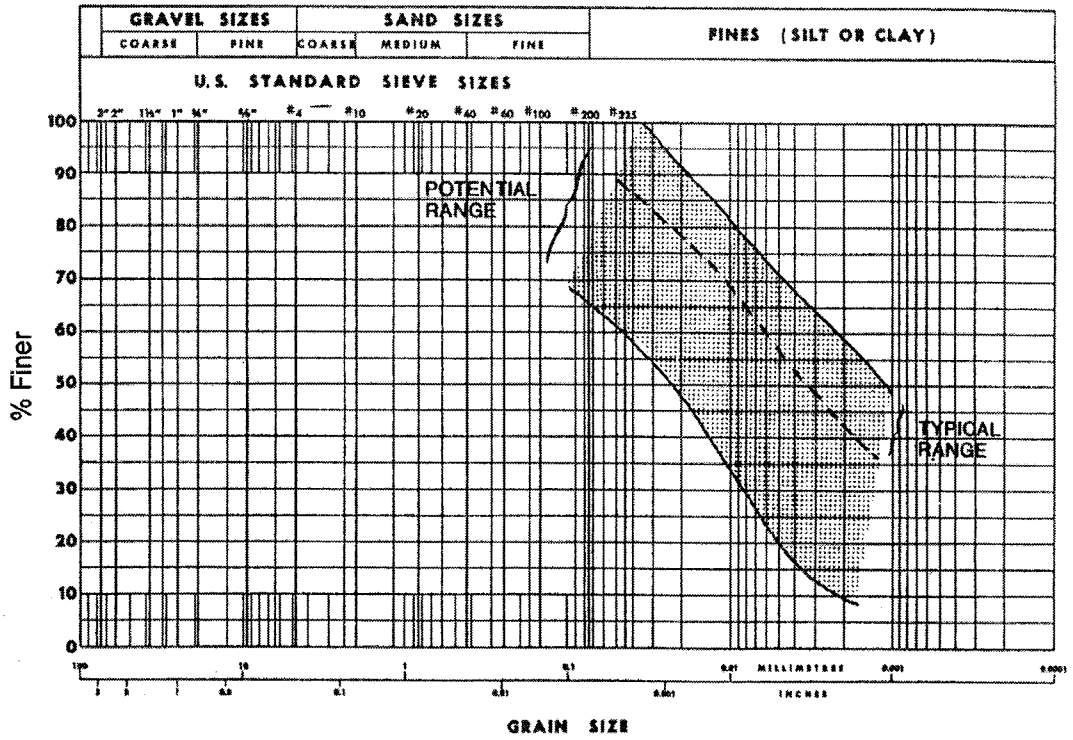


Figure 2.6 Typical grain size distribution of oil sands fine tailings
(Modified from FTFC, 1995)

2.1.4 Sedimentation and consolidation in a pond

In a tailings pond, after the whole slurry is pumped into it, the slurry travels on the top of the coarse grained beach, into a clear water zone and finally stops in a sedimentation region. During this traveling, the slurry separates into a sand density current and thin fine particle current. The thin fine particle slurry which has a relative density around 1.05 and a solid content around 8% travels down the beach into a sedimentation zone until it reaches a zone of similar density.

Sedimentation is occurring in this region by the solid particles falling through the water, during which there is no stress transfer between particles except for collision of the particles. For this type of a material, both Stokian and hindered settling can be observed. During this process some of the free bitumen separates from the slurry and forms a layer of bitumen on the top of the fine tails. This is because the bitumen is slightly denser than water with a density of 1.03 g/cm^3 . However most of the bitumen remains in the slurry (Scott and Dusseault, 1982).

After the solids content of the slurry reaches about 15 to 20%, the slurry begins to form a matrix such that stress can be transferred within the solid particles. After the slurry reaches this solids content, any increase in density arises from the process of self-weight consolidation (Scott and Dusseault, 1982). This process is controlled by the hydraulic conductivity and compressibility of the matrix, and is induced by the buoyant weight of the particles. The slurry compresses under self-weight and reaches a solids content about 30% within several years. The slurry at this point is known as “mature fine tailings” or MFT and by this stage has released approximately 65 % of the original water volume.

The rate of compressibility after this point decreases dramatically (Dusseault and Scott, 1982, Yong et al., 1982). Because of this phenomenon, laboratory testing and field observations result in the conclusion that the mechanism controlling the pond management is consolidation not sedimentation (Scott and Dusseault, 1980). However, considerable research efforts have been made to improve the sedimentation process but little research has been done on ways to improve the consolidation process.

Changing the pH of the MFT has improved the settling of the fines. The optimum pH has been found to be 2 where the clay particles will have zero charge which improves the settling process (Hocking and Lee, 1977). Another finding is that a pH of 11.3 is also an optimum pH (Ripmeester and Sirianni, 1981). In order to change the pH of the materials, chemical additives are used. However, there are problems working with chemical agents and gel is formed upon the addition of chemical agents which results in a bulkier product after sedimentation (Van Olphen, 1977).

Many researchers have shown evidence of developing thixotropic gel strength in the tailings materials (Van Olphen, 1977, Kessick, 1979, Burchfield and Hepler, 1979, Ignasiak et al. 1982, Banas, 1991, Miller, 2004). This gel strength is thought to be one of the reasons that the MFT compresses so slowly.

2.2 Sedimentation and Consolidation Considerations

Solids and/or soils suspended in a fluid when left alone will fall under their own weight until an equilibrium state has arrived. This process is a combination of two processes which are sedimentation and consolidation. Sedimentation and consolidation become one of the most significant problems in geotechnical engineering because the need to reclaim coastal land, deep sea lanes near ports to facilitate shipping, and tailing ponds from mining operations have an increasing need to deal with clay slurry. However there are many difficulties in developing a good understanding of sedimentation to consolidation. This is mainly because it involves an area of research in many disciplines, such as chemical, environmental, and geotechnical engineering and the settling phenomenon is dependent on so many factors, for example, grain size, shape, chemical content and suspension medium.

In general, sedimentation is an accumulation process of geologic or organic material deposited by air, water, or ice. In a geotechnical process, sedimentation occurs when a dilute slurry is allowed to settle freely under gravity. At this time, particulate settling starts. Particulate settling is defined as heavier particles settling faster than lighter

particles. Therefore during this phenomenon, segregation can happen, some heavier particles such as sand-sized particles will settle to the bottom leaving lighter particles floating and/or settling slowly in the solution.

After particulate settling finishes, flocculation may take place. Flocculation is the agglomeration of destabilized particles into microflocs and after into bulky floccules, called floc, which can be settled. Floc is mainly caused by ions on surfaces of solid particles that attract each other. After the particles form flocs, the whole system of flocs will settle and the concentration of the floc system will increase with time and a layer of supernatant water will appear on the top. This stage is referred to hindered settling.

In this hindered settling zone, settling behaviour is not well defined and it can be sedimentation or consolidation (Tan et al. 1990). Studies suggest that there may be a transition zone where effective stresses are partially developed (Tan et al. 1990, Been and Sills 1981). Studies by Tan et al. (1990) have shown that there is a specific water content at which a transition from particulate to hindered settling will take place which depends on the electrolytic concentration and the initial grain size distribution. It should be noted that in some tailing materials during this stage a very small effective stress can be observed which is usually assumed to be zero. This is due to the very weak floc structure which can tolerate little stress. Even though this structure will collapse by applied pressure, it is not possible to do because of engineering and economic considerations. This floc structure is undesired in most tailing ponds because this stage takes considerable time before it changes to a more stable structure.

The process of sedimentation to consolidation has been well described by Imai (1981) as consisting of three stages which are shown in Figure 2.7. It is explained that “*at the first stage no settling takes place but the flocculation yields flocs. In a second stage, the flocs gradually settle and form a layer of sediment, which undergoes consolidation and reduction in water content. The boundary between the upper settling zone and the sediment is the birth place of new sediment. While the sediment grows, the settling zone becomes thinner and finally vanishes. In the last stage, all of the sediment thus formed undergoes self-weight consolidation and finally approaches an equilibrium state*”.

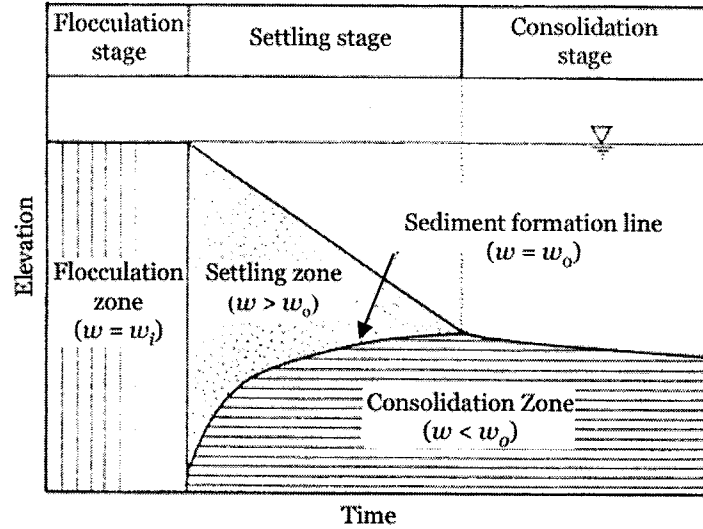


**Figure 2.7 The general characteristics of sedimentation of clay-water mixture
(Modified from Imai, 1981)**

Engineering interests are based on the total mechanism of settling including flocculation. As the concentration of flocs during hindered settling increases, interactions and effective stresses will occur. At this stage the soil structure can be explained by Terzaghi's effective stress principle.

Terzaghi's effective stress principle states that volume change and deformation depend not on the total stress applied but on the difference between the total stress and the fluid pressure in the pore space. Shear strength depends not on the total normal stress on the shearing surface considered but on the effective stress on the potential shear surface. The principle requires effective stress not only to exist but to control the deformation. However, any interaction stress which carries load will manifest itself in the form of the difference between the total stress and pore pressure. This kind of effective stress may not control deformation and thus the effective stress principle can not be applied (Tan, 1995).

Considering the transition point where slurry turns to a Terzaghi soil, a typical value of void ratio at the end of settling is usually around 6 to 7 while the void ratio when effective stress can be first measured is usually around 9 to 10 (Tan, 1995). Tan illustrated that the existence of a difference in total stress and pore pressure may result in the development of an effective stress which contributes to equilibrium but does not cause compression. It was explained that in the initial stage when the clay particles come close together, it is the chemical bonding as a result of the electrolytic concentration and Van der Waal's forces which is more important and not any physical contact. The presence of this interactive stress may not imply the formation of a Terzaghi soil.

Tan (1995) suggested that it will be clearer to think of effective stress as the stress that is controlling deformation, and it may not be equal to the difference between total stress and pore pressure. Thus the effective stress expression may be in the form:

$$\sigma' = \sigma - u - \sigma_r(t) \quad [2.1]$$

$\sigma_r(t)$ is the contribution from electrochemical forces that have no effect on deformation and may be time dependent. According to this discussion, it can be explained why there is a conflict of the first appearing point of effective stress and the observed transition boundary. From work done on Singapore marine clay and reported by Sills and co-workers, it seems that the surface density, as measured by non-destructive means suggests a transition to a Terzaghi soil occurs around a water content of 250% or a void ratio of about 6.5 (Been and Sills, 1981 and Tan et al., 1988). It is noted that this transition can be different for other soils due to other factors such as grain size distribution, chemical compositions, suspension medium and initial water content.

Considering fine tailings material, it is stated by Scott and Dusseault (1982) that after the solids content of the slurry reaches about 15 to 20% (void ratio of 12.9 to 9.1), the slurry begins to form a matrix such that stress can be transferred within the solid particles. This statement implies that effective stress can be first measured around this solids content whether the effective stress controls deformation or not. It is noted that this

range of solids content is very similar to values reported by Tan (1995) on Singapore marine clays. Interestingly, the point where the fine tailings appear to stop settling or the transition point is at a solids content of 30% (water content of 233% and void ratio of 5.3). This value is similar to that reported by Tan (1995) for a typical value of void ratio at the end of settling. All this evidence indicates that fine tailings start to have an effective stress at a solids content of about 15 to 20%. These effective stresses are very small and difficult to measure. At a solids content of about 30%, the soil particles become sufficiently close and can be considered as the end of settling. After this point, physical and chemical effects play the most important role in controlling deformation. It is at a solids content of close to 50% (void ratio of 2.3) that the particles become close enough for physical contact to govern the deformation behaviour and for the effective stress principle to apply (Chapter 4).

It is concluded that the MFT tailings slurry has passed the point that is called particulate settling and is in a hindered settling process. During hindered settling the floc system forms and settles and the solids content rises from 8 to 20% (Dusseault and Scott, 1982) and the solid particles begin to form a matrix such that stress can be transferred. This is the process by which the slurry will reach a solid content of about 30%. After this point the settling process is dramatically reduced. The slurry at this solids content is the initial material used in a 10 meter standpipe at the University of Alberta. Therefore, in the 10 meter standpipe, the probable behaviour of the slurry is that the matrix is already there and the structure is under self-weight compression. Because there is a structure formed a little amount of effective stress should be present whether it is measurable by our sampling technique or not. Whether the effective stress is very small or zero depends on the pore water pressure.

This structure has a high void ratio and high water content. As it decreases in volume, the particles will come closer and result in a reduction of water content. The deformation may not be controlled by effective stress or by electrochemical attraction and repulsion forces on clay surfaces alone but may be both. From laboratory and field observations, the settlement which is effective stress independent seems to be the major

characteristic which is occurring and the soil compression behaviour is governed by creep or time dependent effects. Eventually the structure will reach a specific void ratio or strain where Terzaghi's effective stress principle becomes valid.

2.3 Important Characteristics affecting Compression Behaviour of Fine Tailings

In this section, important characteristics of fine tailings, compressibility, hydraulic conductivity, thixotropy and creep, are reviewed. The discussion is confined to the consolidation behaviour of the fine tailings.

2.3.1 Compressibility

Compressibility of fine tailings can be determined from large strain consolidation tests. A typical change of void ratio with effective stress is shown in Figure 2.8.

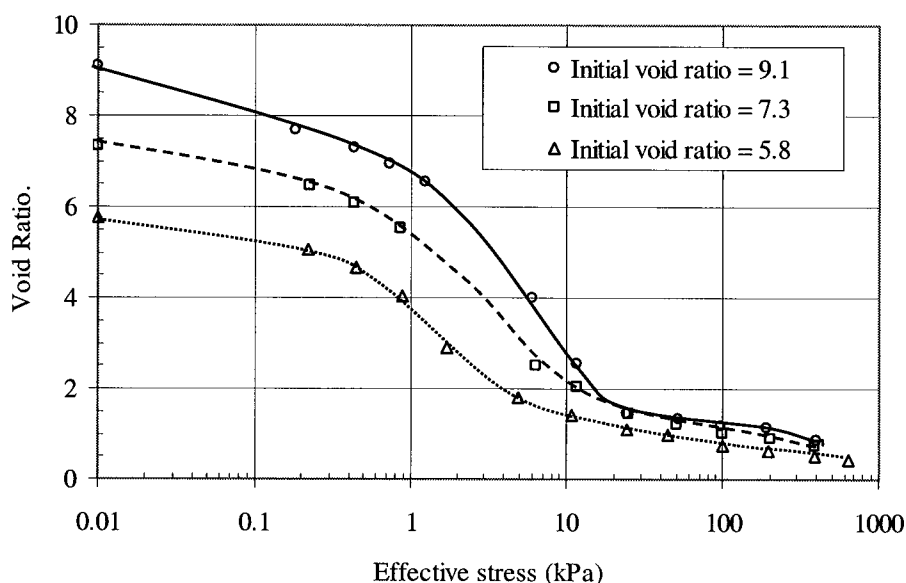


**Figure 2.8 Compressibility of oil sand fine tailings for various solids content
(Modified from Suthaker, 1995)**

Unlike normal soils, the compressibility of the fine tailings is controlled by the initial void ratio of the sample. It suggests that aging changes the microstructure of the fine tailings and hence the compressibility (Suthaker, 1995). This suggests that there is a time dependent parameter involved in the compressibility of fine tailings. The older the

fine tailings, the longer they have settled in the tailings pond, the smaller the void ratio they will reach under an applied effective stress. As a result, Suthaker (1995) concluded that a single void ratio-effective stress relationship is not sufficient to describe the consolidation behaviour.

Myint Win Bo et al. (2003) also showed that for ultra-soft soils, a large change in void ratio happened with little gain in effective stress. The change in void ratio was dependent on the initial void ratio. However, for the same applied stresses, the final void ratios were about the same at large effective stresses, regardless of the initial solids content. It was also suggested that the transition point from an ultra soft soil into a Terzaghi soil was approximately at an effective stress of 10 kPa where the compressibility was independent of initial void ratio.

2.3.2 Hydraulic conductivity

The measurement of hydraulic conductivity of this tailings material is performed in the consolidation test. Typical results showed that the measured flow velocities during the hydraulic conductivity testing were not constant but decreased with time to a steady state. A typical flow velocity is shown in Figure 2.9.

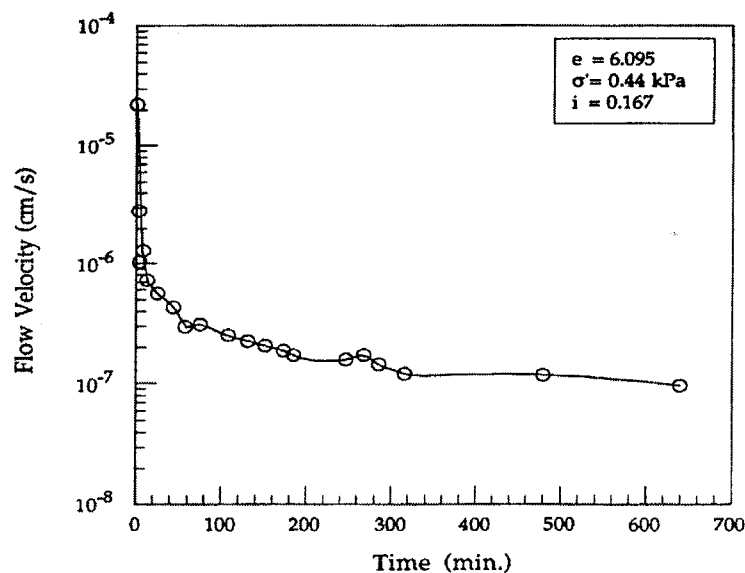


Figure 2.9 Variation of flow velocity with time in the hydraulic conductivity testing
(Modified from Suthaker, 1995)

According to Suthaker (1995), the time to reach the steady state varied between 30 minutes and 15 hours, increasing with the void ratio and decreasing with the hydraulic conductivity. The repeatability of this behaviour was excellent and it only took 5 to 10 minutes after the flow was stopped for the tested material to return to the original state.

It was concluded that the transient behaviour is caused by the movement of particles under the seepage stress which would rearrange the distribution of pore space. The ratio of initial flow velocity to steady state velocity for the fine tailings is about 300 to 400 at void ratios around 6 and is about 20 at a void ratio of about 1.5. This variation is compatible with the possibility of movement of fine particles into pore throats between coarser particles, which would occur more readily at high void ratios. High bitumen content is also suggested to be a contributing cause to this transient behaviour. Although considered as solid in calculations, the bitumen is not totally rigid and can deform under stress. This deformable quality of the bitumen could allow it to move to block the pore throats while being subject to a seepage stress. However, the bitumen effect on the transient behaviour is considered low.

In the tailing ponds, there is a continuous upward flow due to compression. Fine particle and bitumen blocking of pore throats would be occurring and the tailings pond field hydraulic conductivity would be similar to the laboratory steady state hydraulic conductivity. As a result, the steady state flow velocity is used to determine hydraulic conductivity for use in flow calculations.

2.3.3 Thixotropy

In this section thixotropic gain in strength which is believed to be an important property of the mature fine tailings is discussed. Then evaluation and measurement of thixotropic gain in strength are summarized.

Thixotropy is defined as an isothermal, reversible time dependent process occurring under conditions of constant composition and volume whereby material stiffens while at rest and softens or liquefies by remolding (Mitchell, 1993). In the geotechnical

context, the thixotropic phenomenon can be generally described as a continuous decrease of shear strength or softening caused by remolding, followed by a time-dependent return to the original harder state at a constant water content and constant porosity (Mitchell, 1960). This phenomenon takes place in the majority of clay-water systems.

Study of this phenomenon is separated into two main parts; one microscopic and the other macroscopic. Research in the Geotechnical Centre at the University of Alberta has concentrated more on the macroscopic part. The microscopic approach is of greater interest to colloidal physicists. However, both microscopic and macroscopic approaches will be discussed.

Osipov et al. (1984) suggested interesting thixotropic phenomena in clay soils. Rotary viscometer tests were conducted on clay samples which had water contents ranging from 0.8 to 2.2 of the liquid limit. Scanning electron micrographs were used to explain the mechanisms of thixotropic gain in strength. The findings showed that under static shear the soil reacted immediately by showing minor displacement. At this stage reversible elastic deformations dominate as a result of partial tilting of particles and micro aggregates in the direction of the shear force without displacement relative to one another (Osipov et al. 1984). Load removal at this stage will lead to elastic restoration to the initial state of particle arrangement with time. As the maximum strength is approached and deformation increases, the elastic deformation gradually changes to visco-plastic deformation leading to rebuilding of the soil microstructure. In the case of bentonite paste, the rebuilding is manifested through partial micro aggregate disruption. In the case of coarser systems such as kaolinite, reorientation of the micro aggregates also occurs along the direction of shear force. After that the process is followed by a decrease of micro aggregate size, an increase in porosity in the shear zone, the development of a negative pore pressure and an increase in moisture content. The micro structural rebuilding and the development of the shear zone results in a reduction in shear strength of the system during continuous deformation. As the stress increases to the maximum shear strength, a shear zone is formed with weakened structural bonds between particles

and the micro aggregates. As a result, the moisture content increases and partial reorientation of the structural elements along the shearing zone occurs.

These micro structural changes are directly related to the value of the maximum and minimum shear strength of the soils. It is important to note that in a shear test of a system of clay containing small particle sizes, such as bentonite, the deformation is volumetric in character which does not lead to a disruption of structural continuity or to shear planes. It is obvious that the mechanism of the deformation of such systems is relaxation or thixotropy, that is, the micro structure cells are ruptured at shear and instantaneously restored without forming a defect. For coarser materials such as kaolinite, volumetric deformation and local disruption of the structure occurs along developing shear planes. At the rest stage, strengthening of the system occurs and a number of processes lead to an enlargement of the micro aggregates and a reduction in soil porosity. As a result, the SEM structure will look similar to the initial state before the shear tests. A subsequent increase in thixotropic soil strength with time is evidently related to the gradual establishment of thermodynamic equilibrium and complete restoration of the initial microstructure.

For oil sand fine tailings, in which kaolinite is a major clay mineral, the thixotropic gain in strength process is likely to be similar to the above discussion and can be explained that when the tailings are sheared, a volumetric deformation and local disruption of the clay structure occurs. During this stage the porosity is increased due to a decrease of micro aggregate size and the moisture content is increased. The micro structural rebuilding and the development of the shear zone results in a reduction in shear strength of the system during continuous shearing. At the rest stage, strengthening of the clay system occurs and micro aggregate and soil porosity are restoring to the initial state. The fine tailings structure will change to a structure similar to the initial state before shearing. A subsequent increase in soil strength with time will gradually occur to complete restoration of the initial microstructure and thermodynamic equilibrium.

Mitchell (1993) gave the following explanation on the mechanism of thixotropic hardening. Sedimentation, remolding and compaction produce soil structures compatible with the processes that are acting. Once the externally applied energy of remolding or compaction is removed, the structure is no longer in equilibrium with the surroundings. If the inter-particle force balances, such that the attraction is somewhat in excess of repulsion, there will be a tendency toward flocculation of particles and particle groups and for reorganization of the water-cation structure to a lower energy state.

Thixotropic effects in remolded natural clays have been studied by several researchers (Moretto, 1948, Skempton and Northey, 1952, Locat et al., 1985, Bently, 1979). Most of the discussion is related to sensitivity of clays. Seed and Chan (1957) focused their attention on compacted clays and found that compacted clays can also exhibit appreciable thixotropic gain in strength with time. Ripple and Day (1966) show that shear of thixotropic clay pastes causes an abrupt drop in pore water tension resulting in an increase in pore water pressure followed by a slow regain of pore water tension during periods of rest. It is mentioned that a concurrent increase in effective stress also has to be considered to explain the increase in undrained shear strength.

Banas (1991) and Suthaker (1995) summarize several factors affecting the thixotropic gain in strength. These factors include clay mineralogy, water content, rate of loading, axial strain and time. A discussion of these factors follows.

2.3.3.1 Clay mineralogy

Clay mineralogy is one factor in thixotropic gain in strength. Skempton and Northey (1952) tested three clay minerals: illite, kaolinite and bentonite. Bentonite showed the most thixotropic effect, followed by illite, while kaolinite had the least thixotropic effect. It was concluded that clays which have high content of bentonite should exhibit high thixotropy. However, it has been shown that kaolinite can be made very thixotropic by the use of dispersing agents in order to reduce the degree of flocculation present in the natural material (Mitchell, 1960). In MFT, the clay mineralogy analysis has shown that the MFT generally consists of 80% kaolinite, 15% illite, 1.5%

montmorillonite, 1.5% chlorite and 2% mixed clay layers (FTFC, 1995). It appears that the thixotropic effect in MFT does not relate entirely to the clay mineralogy. The addition of sodium hydroxide during the extraction process of the oil sands and the presence of organic matter (bitumen) are important factors in the material's thixotropic behaviour.

2.3.3.2 Water content

Water content is of primary importance in thixotropic gain in strength of clays. In general, the thixotropic effect increases as the water content increases. Seed and Chan (1957) showed soils with a water content approaching the plastic limit exhibited very little or no thixotropy. However, Mitchell (1960) showed that thixotropy can be significant at low water contents. Skempton and Northey (1952) found that some soils had slightly lower thixotropic at lower water contents while others showed significant increase in thixotropy. There is no conclusion on this phenomenon presently available in the literature. Seed and Chan (1957) also made a suggestion that the magnitude of the thixotropic effect was not related directly to the Atterberg limits and the liquidity index was the only parameter that could be related to the thixotropic gain in strength of clays.

2.3.3.3 Loading rate

It has long been known that for saturated clays, strength increases with an increase of loading rate and vice versa. Bjerrum (1967) proposed that the compression of clay sediment can be divided into two components: instantaneous compression and delayed compression. Regarding the effect of time, it was argued that the compressibility characteristic of a clay with delayed compression or creep can not be described by a single $e\text{-log}\sigma'$ curve, but by a family of similar curves, each of which corresponds to a specific time of sustained loading.

Imai (1992) provided findings based on consolidation experimental evidence that the $e\text{-log}\sigma'$ state path followed by each clay element in a consolidating layer is different. The experiments show that the nearer the clay element is to the drainage boundary, the greater the curvature of $e\text{-log}\sigma'$ relationship. Nevertheless, all the starting points and ending points of different samples fall at almost the same position. Strain rate was

extracted from the data to show that there is a unique constitutive relation of the clay skeleton for a constant strain rate value. It was also shown that the change in void ratio with increasing effective stress is initially very small but becomes large over a certain effective stress level. This different in state paths was interpreted to be a result of the viscosity inherent in the soil skeleton. It can be postulated that from these findings that in a large or high sample consolidation test, such as the 10 m standpipe test in the Geotechnical Centre at the University of Alberta, MFT at different elevations will trace different $e\text{-log}\sigma'$ paths. This postulation will be valid during the consolidation phase and may or may not be applied to the initial creep compression phase. That is, different elevations will have different compressibility relationships due to different strain rates.

However, in thixotropic materials this could be different. Seed and Chan (1957) suggested that for this class of material, the longer the duration of the test, the greater the thixotropic gain in strength in a sample. Thus in standpipe consolidation tests, the total effect of an increase in loading time will be a combination of two factors:

- A tendency for strength to decrease because of the increasing time of loading available for creep deformation.
- A tendency for strength to increase due to thixotropic gain in strength because of the increasing time available for thixotropic gain in strength to develop.

2.3.3.4 Axial strain

Seed and Chan (1957) investigated thixotropic gain in strength for different axial strains. It was concluded that the thixotropic gain in strength becomes increasingly significant at smaller strains. For instance, the thixotropic strength ratio after one week for saturated samples was close to 1.9 for 1% axial strain and only 1.3 for 10% axial strain. This could be the effect of the restoration time and the degree of changes in the microstructure. When a clay structure is changed, it takes time to be able to come back to the initial stage. It can be said that the greater the change, the more is the time to restore to the initial condition. However, if some disorientation happens in the structure or some defect occurs, the maximum and minimum shear strengths which directly depend on

change in microstructure, may not be the same as initially. In this case the result may be that the structure needs more restoration time or that the microstructure has changed.

2.3.3.5 Time

Time plays a major role in the thixotropic gain in strength behaviour of clays. Tests on marine clays indicate two stages of strength recovery; the 1st stage is a rapid one with duration of about 15 minutes and the 2nd stage is longer duration (Locat et al. 1985). Osipov et al. (1984) showed that after the application of vibration, there was a rapid gain in strength within some seconds due to mutual fixation of particles and the creation of coagulation contacts between them followed by a slow restoration of strength which was related to the gradual establishment of thermodynamic equilibrium and restoration of microstructure. Mitchell (1960) suggested that there appears to be no relationship between thixotropic strength ratio and time. Tests on MFT and clay samples performed in the Geotechnical Centre at the University of Alberta (Banas, 1991, Suthaker, 1995, Miller, 2004) showed substantial increasing shear strength with time.

2.3.3.6 Thixotropy and consolidation

The consolidation of clays is related to time and thixotropy is a time dependent effect. Mitchell (1960) argued that it would seem reasonable that thixotropic effects during consolidation lead to a smaller compression index. As a result thixotropic gain in strength will retard the consolidation process by building up strength and holding the soil particles together. Mitchell (1960) recommended more detailed investigation on this subject.

2.3.3.7 Comparison of thixotropy obtained from different clays

In this section, the fine tailings will be compared to other soils which display various degrees of thixotropy.

Moretto (1948) tested four different natural clays that had water contents at or close to their liquid limit. Unconfined compression tests were conducted on the clay samples with constant water content at different time intervals ranging from 0 to 610 days

after remolding. Skempton and Northey (1952) reported test results on three different sensitive clays and three clay minerals. To compare the oil sand fine tailings to other soils exhibiting thixotropy, the results of Moretto (1948) and Skempton and Northey (1952) were plotted with the shear strength test results of the fine tailings at the liquid limit (Banas, 1991).

Figure 2.10 shows the gain in strength with time for different soils in form of thixotropic ratio versus time. It can be seen that the fine tailings have the highest thixotropic ratio and only the Beauharnois clay shows a relatively close increase. In Figure 2.11, the thixotropic ratios of three clay minerals; kaolinite, illite, bentonite are given in comparison to the fine tailings at the liquid limit. Kaolin shows almost no thixotropy and illite shows only a small effect. On the contrary, bentonite shows a high gain in strength at a very short time. Compared to the fine tailings, the clay minerals show significantly lower thixotropic gain in strength.

The oil sands fine tailings appear to be a highly thixotropic soil. It exhibits higher relative thixotropic gain in strength than typical clays and clay minerals.

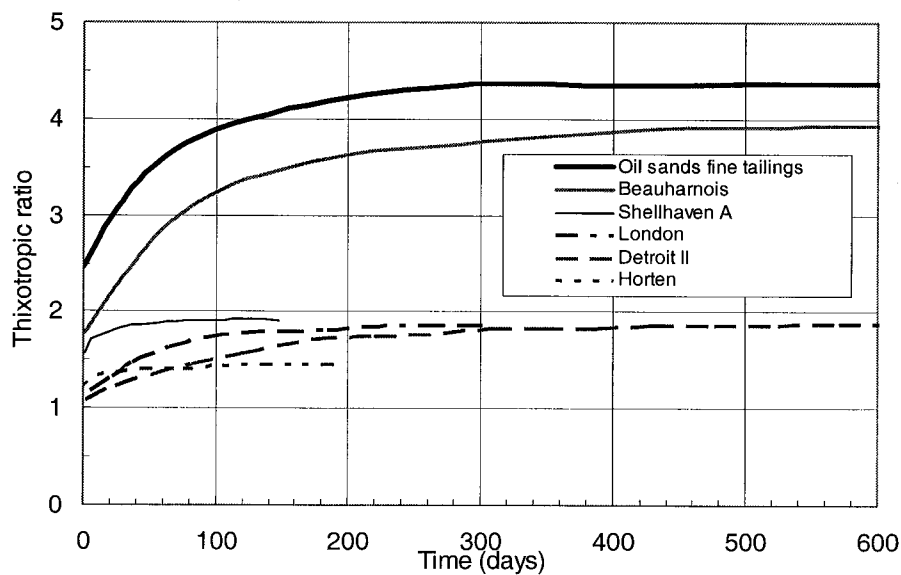


Figure 2.10 Thixotropic ratio in some typical clays and the fine tailings

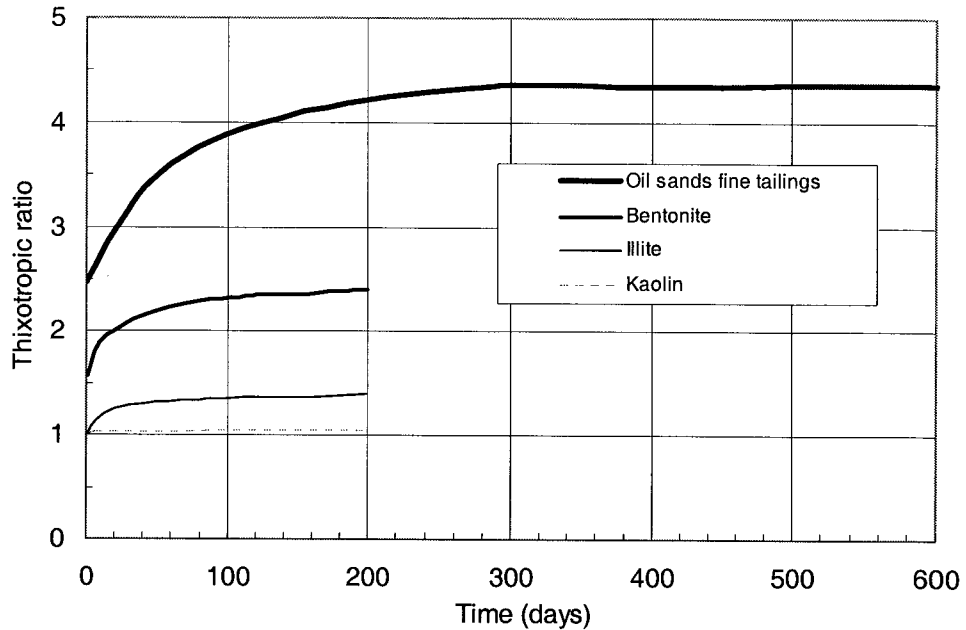


Figure 2.11 Thixotropic ratio in three clay minerals and the fine tailings

2.3.3.8 Thixotropic gain in strength tests and thixotropic strength evaluation

Thixotropic tests by Banas (1991) and by Miller (2004) are summarized here. The objective of the shear strength tests performed on the fine tailings was to investigate the absolute and relative gain in strength of the material with time. The increase in strength of the fine tails was not solely due to the thixotropic behaviour of the material but also to a slight decrease of void ratio due to self-weight consolidation of the material during the long test program. Interpolation techniques were used to correct for any change in void ratio.

In Figure 2.12, the measured total shear strength with time of mature fine tailings at solids contents of 28% and 40% (void ratios of 5.86 and 3.42 respectively) is shown. The measured solids contents at different times are also shown (Figure 2.13).

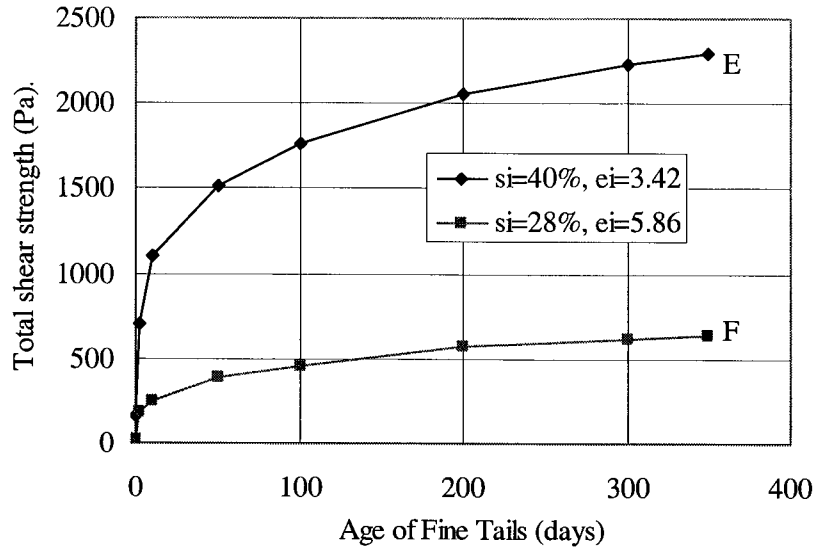


Figure 2.12 Total shear strength measurement of mature fine tailings

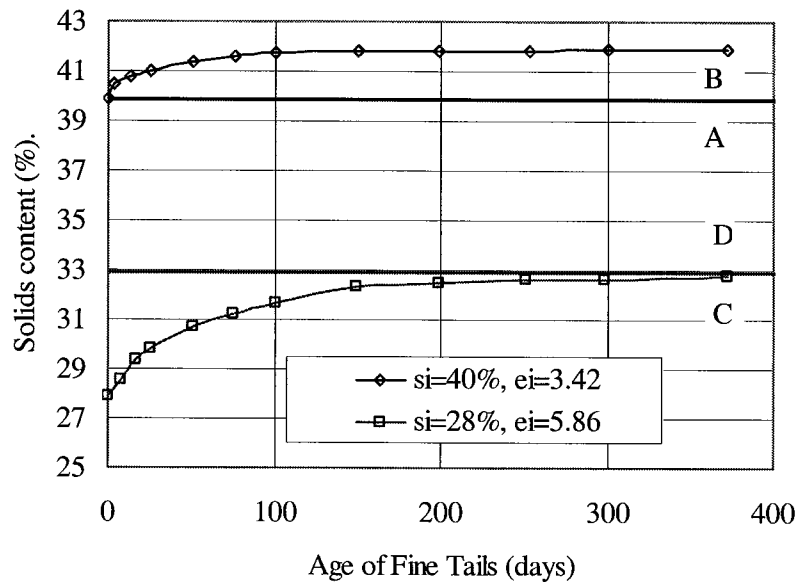


Figure 2.13 Solids content measurement of mature fine tailings

From Figures 2.12 and 2.13, an interpolation to obtain thixotropic strength values at solids contents of 40% and 33% can be made by following procedure (Miller, 2004). It is noted that the letter symbols (A, B, C, D, E, and F) are shown in Figures 2.12 and 2.13.

Interpolation to get thixotropic strength at 40% solids (void ratio of 3.42)

- From Figure 2.13 obtain values of B and C
- Calculate AB by using value B subtracted by A (40% solids)
- Calculate BC by using value B subtracted by C
- Correction value by interpolation = $(AB/BC) \times (E-F)$
- Then the thixotropic strength at 40% solids = E - Correction value

Interpolation to get thixotropic strength at 33% solids (void ratio of 4.63)

- Calculate DC by using value D (33% solids) subtracted by C
- Calculate BC by using value B subtracted by C
- Correction value by interpolation = $(DC/BC) \times (E-F)$
- Then the thixotropic strength at 33% solids = F + Correction value

The results of the interpolation (Figure 2.14) shows the gain in thixotropic strength with time of fine tailings at solids contents of 33% and 40% without the effect of the increase in shear strength due to consolidation. The initial strengths after remolding were small, 18 Pa and 165 Pa respectively. Within 2 days the strength had increased to 182 Pa and 702 Pa respectively. At 350 days the strengths were 635 Pa and 1941 Pa respectively and the 40% solids shear strength was still increasing.

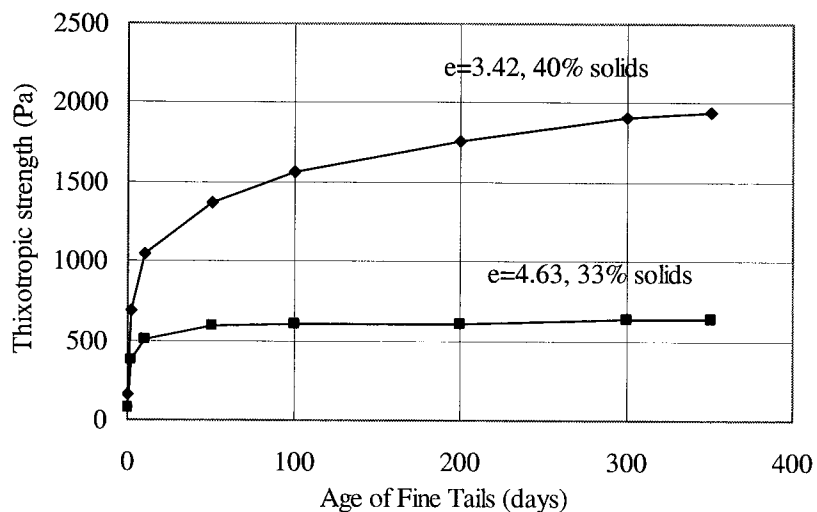


Figure 2.14 Thixotropic shear strength measurement of mature fine tailings

2.3.4 Creep behaviour of fine tailings

Creep behaviour is another property of the mature fine tailings that relates to consolidation or reduction in volume. Mitchell (1993) defined creep as the time dependent volumetric strains and/or shear strains that develop at a rate controlled by the viscous resistance of the soil structure. Secondary compression or secondary consolidation is the specific case of the creep that follows primary consolidation and is also controlled by the viscous resistance.

For oil sand fine tailings which appear to settle in the tailings ponds, the in situ measured effective stresses are very small. As well, the consolidation observation of mature fine tailings in the ten meter standpipe at the University of Alberta shows a reduction of volume under constant zero effective stress. This suggests that much of the decrease in void ratio must be due to a creep mechanism.

Suthaker and Scott (1995) studied the creep behaviour of the fine tails (Figure 2.15) using secondary consolidation measurements from 0.2 m high large strain consolidation tests. The creep index (C_α) is calculated using the slope of the void ratio – log time curve after primary consolidation is complete. For fine tailings, it appears that the creep index decreases with a decrease in end of primary (EOP) void ratio. The creep index of the fine tailings can be estimated from $C_\alpha(\%) = 3.689 e_p$ (Figure 2.16). It is reported that at high effective stress levels the effect of initial void ratio becomes insignificant. Suthaker and Scott (1995) also studied the creep behaviour of mixtures of fine tailings and sands (Figure 2.17). It appears that for fine tailing sand mixes, the creep index increases rapidly with a decrease in void ratio to a maximum value and then decreases. Suthaker (1995) suggested that the void ratio at maximum creep index might represent the void ratio at an apparent preconsolidation stress caused by the sand content. From their study, it was also found that there is a limiting fines content that separates the creep behaviour of MFT from MFT-sand mixes because at high fines contents the sand grains in the mixes are not touching each other and the fines control the geotechnical behaviour. The ratio of C_α and C_c of the fine tailings was found to be 0.085 which is very high compared to other clayey soils but is similar to other organic soils (Figure 2.18).

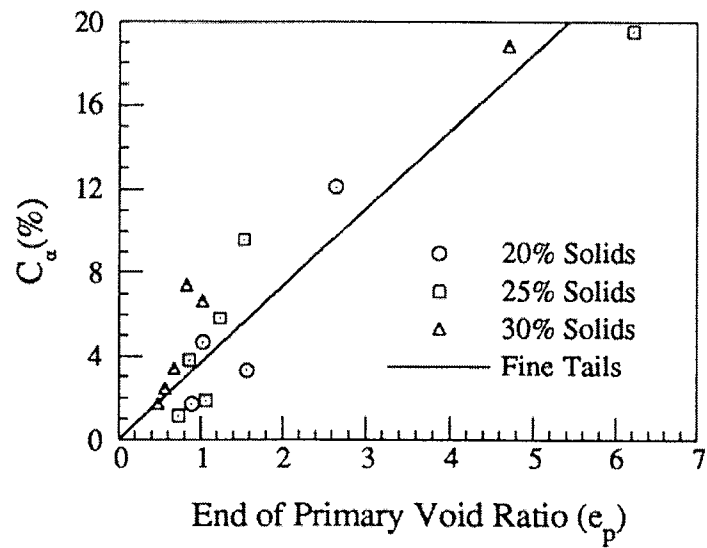


Figure 2.15 Creep index for fine tailings (Modified from Suthaker, 1995)

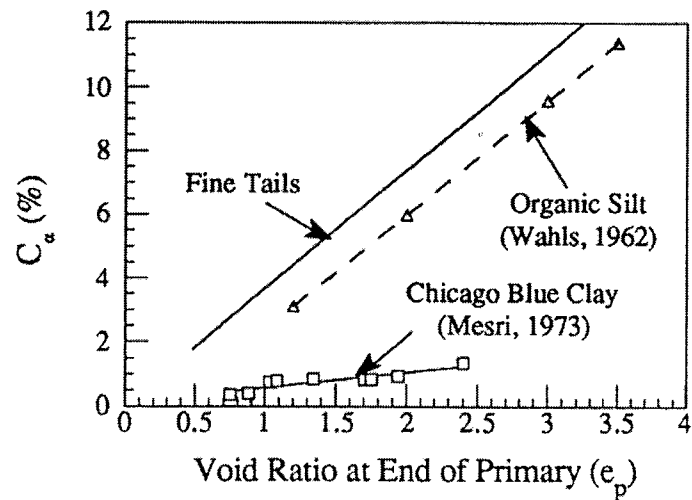


Figure 2.16 Comparison of creep index (Modified from Suthaker, 1995)

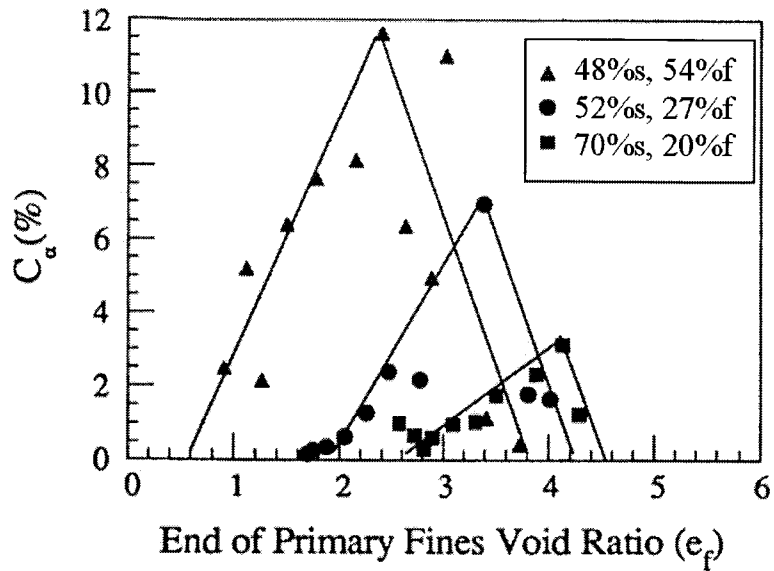


Figure 2.17 Creep index for fine tailing sand mixes (Modified from Suthaker, 1995)

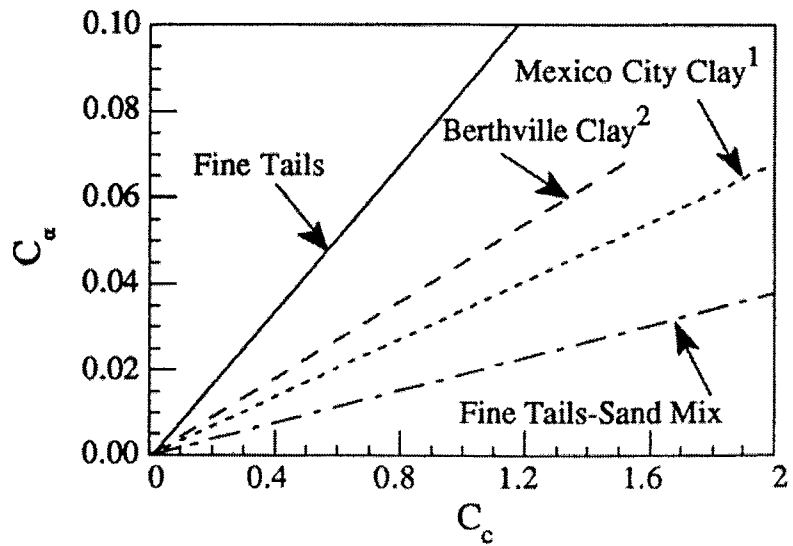


Figure 2.18 Comparison of C_α and C_c relationship (Modified from Suthaker 1995)

However, the creep occurring in the tailings ponds and in ten meter standpipe 1 is the creep during primary consolidation not the creep at the end of primary consolidation. The creep rates for MFT in a two meter standpipe and in the ten meter standpipe 1 have been estimated as the rate of interface settlement and are shown in Figure 2.19. Assuming that the MFT hydraulic conductivity is high enough that water flow from volume change by creep is not retarded, the interface settlement by creep in a 10 m standpipe will be 5

times greater than that in a 2 m standpipe because the height of material is 5 times greater. The measured values in Figure 2.19 are in this range. These creep rates are several orders of magnitude faster than those from a large strain consolidation test, also give in Figure 2.19, at the same void ratios. As the 10 m standpipe is 50 times higher than the 0.2 m consolidation sample, its creep rate should only be 50 times faster not 500 times faster.

As creep is also occurring during primary consolidation in the consolidation tests, it is this creep stage which should be studied, not the creep stage during secondary consolidation. It is necessary, therefore, to separate the void ratio change due to creep from the total void ratio change during primary consolidation in large strain consolidation tests.

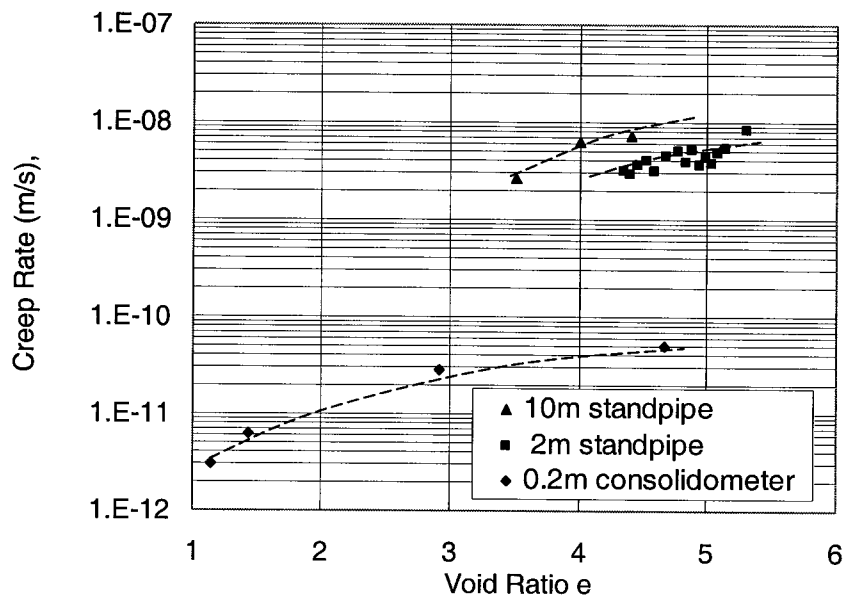


Figure 2.19 Creep rate and void ratio

2.4 Scanning Electron Micrograph Technique and Fine Tailings Structure

The scanning electron microscope used was a JSM6301FXV made by Japan Electron Optics Limited. It is equipped with an energy dispersive X-ray analysis (EDXA) system containing a Noran pioneer light element detector and a TN5500 analyzer. The SEM is also equipped with a Emitek K1200 cryo system. It is important to outline the test

procedure in order to discuss the image analysis measurements. The test procedure is as follows.

2.4.1 Test procedure

The slurry samples are drawn into 5 mm diameter straws and flash frozen in liquid nitrogen slush at a temperature of $-208\text{ }^{\circ}\text{C}$ which freezes the slurry almost instantaneously. If water in the sample can be frozen fast enough the ice is amorphous not crystalline and freezing artifacts will be small. Then the frozen samples are put into liquid nitrogen at a temperature of $-196\text{ }^{\circ}\text{C}$. The straws are then peeled off the samples and the samples are set into the sample holder using a silver paste (glue). Then the samples are fractured under liquid nitrogen to avoid condensation on the fracture surface. The fractured samples are placed in the cryo sublimation stage for about 30 minutes at $-40\text{ }^{\circ}\text{C}$ to remove the surface ice. Then the samples are placed in the SEM cold stage at $-40\text{ }^{\circ}\text{C}$ and examined at low voltage (2.5 KV) until it appeared that enough ice had been removed. This is usually done until an ablation depth of about $10\text{ }\mu\text{m}$ is obtained. Although greater depths may be observed in the SEM, there is a danger that the unsupported microfabric may collapse if too great a depth of sublimation is allowed to occur. Sublimation removes all water from the sample including pore water and interlayer water; precipitating the salts on the mineral surfaces. The removal of interlayer water may shrink the face to face clay aggregates and affect the microfabric. This effect will vary with different salt concentrations. It has also been postulated that some of the weakly bonded cross-linking clay particles may be plucked off during fracturing and by the applied vacuum during ablation or in the SEM chamber. As a result, the clay particles may appear to be aligned mainly in a face-to-face chain-like pattern and less in a edge-to-face pattern.

The samples are then cooled to -155°C and transferred to the cryo chamber and sputtered with gold. Then the samples are returned to the SEM cold stage at -155°C for visual and photographic examination at a voltage of 2.5 to 5KV and for energy dispersive X-Ray analysis (EDXA) at a voltage of 10 to 15 KV. Digital photographic scans are taken at representative locations at different powers of magnification.

2.4.2 SEM image analysis

Since the electron-microscopic observation technique requires a high vacuum, only dry or frozen samples can be observed. There is no guarantee, therefore, that the electron micrograph reflects the shape and size of the particles when they are in a dispersed condition. In most cases there is little doubt that plates remain plates and needles remain needles when suspended in water.

However, SEM tests provide good qualitative information or comparative information for analyzing oil sand fine tailings. In general, for oil sands tailings, the SEM analysis is performed to obtain information on fine tailings structure and X-Ray analysis is performed to obtain elemental information on clay mineralogy and other compositions in the tailings.

Tang et al. (1997) examined the structure of mature fine tailings. The SEM tests were performed to investigate the effects of bicarbonate, NaOH, organic matter, sodium naphthenate, gypsum, and processing temperature on the structure of MFT. The results showed that the bicarbonate and the NaOH in the tailings water are dominant agents which cause the card-house structure of kaolinite clay-water systems similar to those in the oil sands tailings. The bicarbonate comes from the connate water in the oil sands, the make-up water from the Athabasca River and from the adsorption of CO₂ during the aeration process in the plant. The NaOH is added during the Clark Hot Water Extraction process. The high temperature used in the extraction process enhances the card-house structure. It was observed that the bitumen and strongly bound organic matter in MFT may also have an effect on the card-house structure. The addition of gypsum to MFT did not change the structure but made it finer and much stronger. The addition of sodium naphthenate did not affect the structure of the kaolinite clay-water system which retained a flocculated structure. It appears that this surfactant is not responsible for the dispersed structure. The exchangeable sodium ratio (ESR) of a clay-water system resulting from different bitumen extraction processes can be used to forecast and identify whether a fine tailings will have a flocculated structure or a dispersed card-house structure.

2.5 Summary

After fine tailings reach a solids content of about 30%, the rate of volume decrease of the fine tailings decreases dramatically. The fine tailings at this point are called mature fine tailings. In order for effective tailings management, the behaviour of the mature fine tailings must be understood.

The Clark Hot Water Extraction Process has a major impact on tailings properties. Sodium and bicarbonate ions in this extraction process are a major contributor to the stabilization of the fines matrix.

It appears that the fine tailings settling behaviour is initially governed by a hindered sedimentation process and then by self-weight compression. Settling behaviour of this material can be explained that at a solids content of about 15%, the slurry begins to form a matrix such that stress can be transferred between the solid particles. However, at this stage the effective stress principle can not be applied. The slurry then compresses under self-weight and reaches a solids content of about 30% within several years. At this stage the soil particles become sufficiently close that physical and chemical effects play the most important role in controlling deformation. The transition point of this tailings to a Terzaghi soil is at a solids content close to 50% when the particles become close enough for physical contact to govern the deformation behaviour and for the effective stress principle to apply.

During the mature fine tailings stage, the fine tailings form a fines matrix that has a structure which is overconsolidated and thus results in a resistance to a reduction in volume. The fine tailings card-house structure is mainly caused by bicarbonate ions and the NaOH in the tailings water. The fine tailings volume behaviour appears to be controlled by the thixotropic gain in strength in the fines matrix. The reduction of volume under little or no effective stress appears to be caused by slow bond yielding or creep.

Important characteristics affecting the compression behaviour of the mature fine tailings are not only the void ratio-effective stress and hydraulic conductivity-void ratio relationships but also creep and thixotropic behavior.

The ten meter standpipe tests at the University of Alberta were conducted to investigate the consolidation behaviour of the oil sand tailings. The test results are used to evaluate the predictive capabilities of laboratory large strain consolidation tests and finite strain consolidation models.

3. The Ten Meter Standpipe Test

Oil sands mining companies in northern Alberta produce large volumes of fine tailings which create challenges for containment and land reclamation. After the fine tailings reach a solids content of about 30%, the water release process appears to almost cease. The need to understand the volume reduction behaviour of the fine tailings led to large standpipe testing at the University of Alberta. The large standpipe testing program was initiated and conducted under the supervision of Dr. J.D. Scott with funding by Syncrude Canada Ltd. The objective of the program was to provide verification of laboratory tests and theoretical models on consolidation of the fine tailings in the Syncrude tailings pond. The purpose was to allow planning for the long term performance of the tailings pond. Details about this large scale testing program are presented in Chapters 4, 5 and 6.

3.1 Objectives of Large Standpipe Testing

The ten meter standpipe tests were performed to study and model the consolidation behaviour of the mine tailings materials in the oil sands tailings ponds.

In order to predict consolidation behaviour of a slurry material by the use of the finite strain consolidation theory, two important relationships (void ratio-effective stress and hydraulic conductivity-void ratio) are needed. These two relationships can be obtained from a large strain consolidation test in the laboratory. With the use of the numerical model, long term consolidation behaviour of tailings can be predicted. The use of the numerical model with the small laboratory tests to estimate the long term behaviour in the field however requires verification so that the modeling results can be used with confidence for long term planning and design. The large, self-weight consolidation standpipe tests due to their large scale and the undisturbed environment have provided an excellent opportunity to examine the ability of the finite strain consolidation theory to predict the progress of self-weight consolidation of oil sand fine tailings.

If the small laboratory test and the finite strain consolidation theory can mathematically model the ten meter standpipe performance, this model should also be able to predict consolidation behaviour of the fine tailings in the ponds. If the mathematical model does not model the standpipe test then the experimental measurements from the ten meter standpipe can be used to modify the numerical model for this class of material.

3.2 The Ten Meter Standpipe

Two ten meter standpipes were fabricated and erected with an access scaffold in 1982. The ten meter standpipes are made of high density polyethylene with walls 25 mm thick, 914 mm inside diameter and are 10.5 m in height. The standpipes were supplied by PROLITE Company. The bottom 0.5 m of the standpipes are encircled by a series of steel bands covered in fiberglass reinforcement to prevent any bulging of the plastic due to creep. The bases of the standpipes are 13 mm thick high density polyethylene plates which are welded to the sides of the standpipes. The pore water pressure monitoring ports and sample ports are aligned at 0.5 m spacing down the side of the standpipes. The ten meter standpipe diagram (Figure 3.1) shows the alignment of all the measurement ports. The standpipes are located in the University of Alberta Structures Laboratory which has a fairly consistent temperature around 21°C.

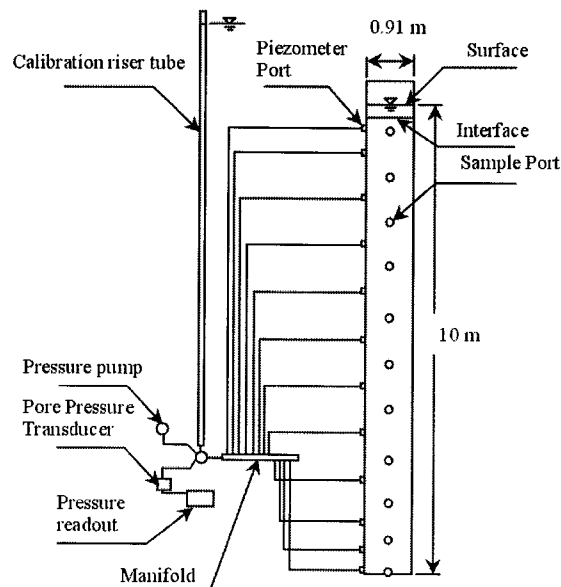


Figure 3.1 The ten meter standpipe

3.3 Tailings Materials and Standpipe Filling

Tailings placed in the standpipes are mature fine tailings and fine tailings-sand mixes. The MFT material was pumped from the center of Syncrude's Mildred lake tailings pond from a depth of about 25 m below the surface in the mature tailings region in the fall of 1982 into a total of seventy two barrels – approximately 200 liters each. These barrels were then transported to the University of Alberta to investigate their geotechnical properties prior to filling. The initial characteristics of the mature fine tailings in each of the barrels used for Standpipe 1 are shown in Table 3.1. The properties showed in Table 3.1 indicate that the material in different barrels did not vary significantly in both bitumen content and solid content. This allowed the mixing and placing of the material to be done by pumping from different barrels in a sequence so a consistent material was placed. The properties of material filled in Standpipes 1, 2 and 3 are shown in Table 2 and on the ternary diagram in Figure 3.2 (Morgenstern and Scott, 1995).

3.3.1 Filling Standpipe 1 with MFT

In order to fill Standpipe 1 to a 10 meter height, 6.57 m³ of mature fine tailings was needed. The mature fine tailings in the barrels were mixed thoroughly with a mixing blade extension attached to a power drill. This was done to achieve a uniform material throughout the barrel. A small sample, of known mass and a volume, was extracted and laboratory tests were performed on the material for solids content and bulk density. It was then possible to determine how much additional pond water was required to dilute the fine tailings to the desired solids content for Standpipe 1. From Table 3.1, barrel numbers 1 to 30, 32, 34, 1a, 2a, and 6a were used by mixing them thoroughly to reach the properties shown in Table 3.2.

After the mature fine tailings were mixed, they were pumped into the standpipe. Standpipe 1 was filled on October 4th in 1982 by pumping with a tremie hose discharging below the surface to prevent air entrainment.

3.3.2 Filling Standpipe 2 with a MFT-tailings sand mix

Standpipe 2 was designed for studying the effects of entrained sand on the consolidation behaviour. Tailings sand from the tailings pond was used for the mixing material in both Standpipe 2 and 3 tests. The tailings sand had an initial water content of approximately 20% and had to be dried before mixing with the MFT. A sand drying platform consisting of several pallets covered with a geotextile fabric was used to allow the tailings sand to gravity drain and air dry to a lower water content. Standpipe 2 was designed for a fine tailings-sand mix with 48% sand and a solids content of 45%. The mix was done by mixing 6480 kg of MFT (30.6% solids, 90% fines) with 2210 kg of tailings sand (92% solids, 15% fines) and 238 liters of process water. The designed properties of the material are showed in Table 3.2. By mixing tailings sand and process water with mature fine tailings in each barrel and placing the material following the same manner as Standpipe 1, Standpipe 2 was started on November 4th in 1982. After approximately 2 years of operation, Standpipe 2 was discontinued as its progress was similar to Standpipe 1 and potential field applications would use more sand. The mix was pumped out, mixed with more sand and pumped back into the standpipe. This new mix was termed Standpipe 3.

3.3.3 Filling Standpipe 3 with a MFT-tailings sand mix

In Standpipe 3, the percent of sand was changed from Standpipe 2 from 48 % to 82 % on November 30th, 1984. The material properties of the material in Standpipe 3 are shown in Table 3.2. In order to get the new mix for Standpipe 3, the material in Standpipe 2 was pumped out of the standpipe completely and remixed with sand to reach 82 % sand. The mix was done by mixing 1630 kg of fine tailings-sand mix (45% solids, 48% fines) with 9450 kg of tailing sands (88% solids, 15% fines) and 1018 liters of process water. A contractor, Titan Pumping Services Ltd, with an oil well servicing truck, was hired to do the mixing. Due to the unusual and unexpectedly cold weather at the arranged date, the sand pile froze solid and had to be moved inside a heated area to thaw before mixing could proceed. The sand was also dried to lower the water content so the mix would be a nonsegregating mix.

The mixing method was a vacuum truck that drained off all the tailings in the standpipe and temporarily stored it in its holding tank. A separate blending unit took on a predetermined volume of tailings and blended in the correct amount of tailings sand. A density sample was taken when mixing of each batch was completed to confirm that the mix was correct. Three or four batches were required to completely fill the standpipe. The blending unit discharged the mix into the 4 inch valve at the bottom of the standpipe (that is, filling from the bottom up). The whole changeover process took approximately four hours. The new 82 % sand mix was pumped back to the standpipe which has been continually monitored for interface settlement until 1997 when it was verified that the mix was fully consolidated under self-weight.

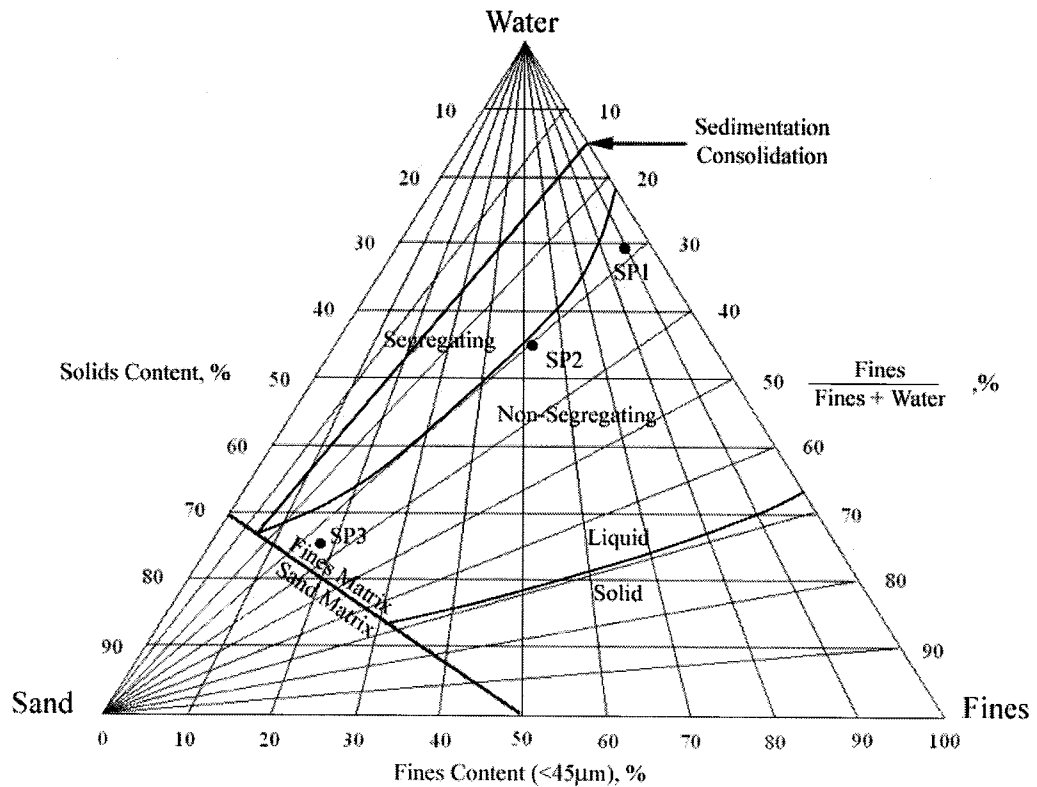


Figure 3.2 Ternary diagram

Table 3.1 Initial characteristics of mature fine tailings

Barrel Number	Density (g/cm ³)	Solids Content (%)	Geotechnical Bitumen Content (%)	Percent by Total mass			Remarks
				Water (%)	Bitumen (%)	Mineral Solids (%)	
1	1.22	31.7	12.5	68.3	3.5	28.2	Used in Standpipe 1
2	1.22	31.7	12.1	68.3	3.4	28.3	Used in Standpipe 1
3	1.21	31.8	14.3	68.2	4.0	27.8	Used in Standpipe 1
4	1.21	31.2	12.0	68.8	3.4	27.9	Used in Standpipe 1
5	1.22	31.5	11.0	68.5	3.2	28.4	Used in Standpipe 1
6	1.22	31.7	12.0	68.3	3.4	28.3	Used in Standpipe 1
7	1.21	30.6	12.0	69.4	3.3	27.3	Used in Standpipe 1
8	1.21	30.5	11.0	69.5	3.0	27.3	Used in laboratory
9	1.21	30.7	13.5	69.3	3.7	27.0	Used in Standpipe 1
10	1.21	30.4	13.1	69.6	3.5	26.9	Used in Standpipe.1
11	1.21	30.7	13.9	69.3	3.8	26.9	Used in Standpipe 1
12	1.21	31.2	12.8	68.8	3.5	27.7	Used in Standpipe 1
13	1.21	30.3	10.2	69.7	2.8	27.5	Used in Standpipe 1
14	1.21	30.6	10.2	69.4	2.8	27.9	Used in Standpipe 1
15	1.21	30.3	10.9	69.7	3.0	27.4	Used in lab
16	1.21	30.6	10.1	69.4	2.8	27.9	Used in Standpipe 1
17	1.21	31.0	9.5	68.6	2.7	28.7	Used in Standpipe 1
18	1.21	30.6	9.7	69.4	2.7	27.9	Used in Standpipe 1
19	1.21	30.1	10.6	69.9	2.9	27.2	Used in Standpipe 1
20	1.20	29.6	11.4	70.4	3.0	26.6	Used in Standpipe 1
21	1.20	29.6	11.0	70.4	2.9	26.7	Used in Standpipe 1
22	1.20	29.6	11.8	70.4	3.1	26.4	Used in Standpipe 1
23	1.20	29.0	10.8	71.0	2.8	26.1	Used in Standpipe 1
24	1.20	29.3	10.6	70.1	2.8	26.4	Used in Standpipe 1
25	1.20	30.1	12.2	69.9	3.3	26.8	Used in Standpipe 2
26	1.21	30.6	13.6	69.4	3.7	26.9	Used in Standpipe 1
27	1.21	30.2	11.1	69.8	3.0	27.2	Used in Standpipe 1
28	1.20	30.1	12.8	69.9	3.4	26.7	Used in Standpipe 1
29	1.20	29.8	11.9	70.2	3.2	26.6	Used in Standpipe 1
30	1.20	30.0	12.4	70.0	3.3	26.6	Used in Standpipe 1
31	1.20	29.8	12.7	70.2	3.3	26.3	Sent to Syncrude
32	1.20	30.1	12.5	69.9	3.3	26.6	Used in Standpipe 1
33	-	-	-	-	-	-	-
34	1.21	30.4	12.6	69.6	3.4	26.9	Used in Standpipe 1
35	1.21	30.7	11.9	69.3	3.3	27.3	Used in Standpipe 2
1a	1.23	32.4	11.0	67.6	3.2	29.5	Used in Standpipe 1
2a	1.23	32.4	9.8	67.6	2.9	29.6	Used in Standpipe 1
3a	1.19	27.8	9.3	72.2	2.4	25.4	Sent to Syncrude
4a	1.23	32.1	9.9	67.9	2.9	29.3	Used in Standpipe 2
5a	1.19	28.9	12.8	71.1	3.3	25.4	Sent to Syncrude
6a	1.20	29.3	12.1	70.7	3.2	25.9	Used in Standpipe 1
7a	1.20	29.5	12.1	70.5	3.2	26.1	Sent to Syncrude

Table 3.2 Tailings properties in the ten meter standpipes

Standpipe No.	1	2	3
Initial Solids Content (%)	30.6	45.0	74.8
Initial Water Content (%)	226.8	122.2	33.7
Sand Content (% by dry weight)	11.0	48.0	82.0
Fines Content (% by dry weight)	89.0	52.0	18.0
Bitumen Content (% by dry weight)	10.2	5.6	1.6
Bitumen Content (% by total weight)	3.1	2.5	1.2
Initial Bulk Density (g/cm ³)	1.21	1.36	1.85
Initial Void Ratio	5.17	2.98	0.87
Initial Fines Void Ratio	5.80	5.37	4.26
Initial Fines-Water Ratio (FWR)	28.2	29.8	34.8
Specific Gravity, G _s	2.28	2.44	2.58
Sand -Fine Ratio (SFR)	0.12	0.92	4.56

3.4 Monitoring Ports

The monitoring ports on the ten meter standpipes are ports where solids content, density and pore water pressures are measured. These ports are aligned along the sides of the standpipes as shown in Figure 3.3. In this section different purposed ports and sampling devices used with the ports as well as the test procedures are presented.

3.4.1 Sample ports

Sample ports on the ten meter standpipes are used to obtain solid content and bulk density measurements of the material. These data are mainly used to calculate total stress, effective stress and degree of saturation. The sample ports are aligned at 1 m intervals along the sides of the standpipe (Figure 3.1, Figure 3.3). Samples are collected with two types of samplers; a solids content sampler and a density sampler. These two samplers are discussed in detail below.

3.4.1.1 Solids content sampler

A solids content sampler (Figure 3.4) is an apparatus used to collect samples from the ten meter standpipe by allowing materials in the standpipe to flow into a sample bottle. Suction can be used in the case of high solids content samples. The solids content

sampler is used to obtain density of the tailings by assuming the degree of saturation is equal to 100%. The sampling procedure is as follows.

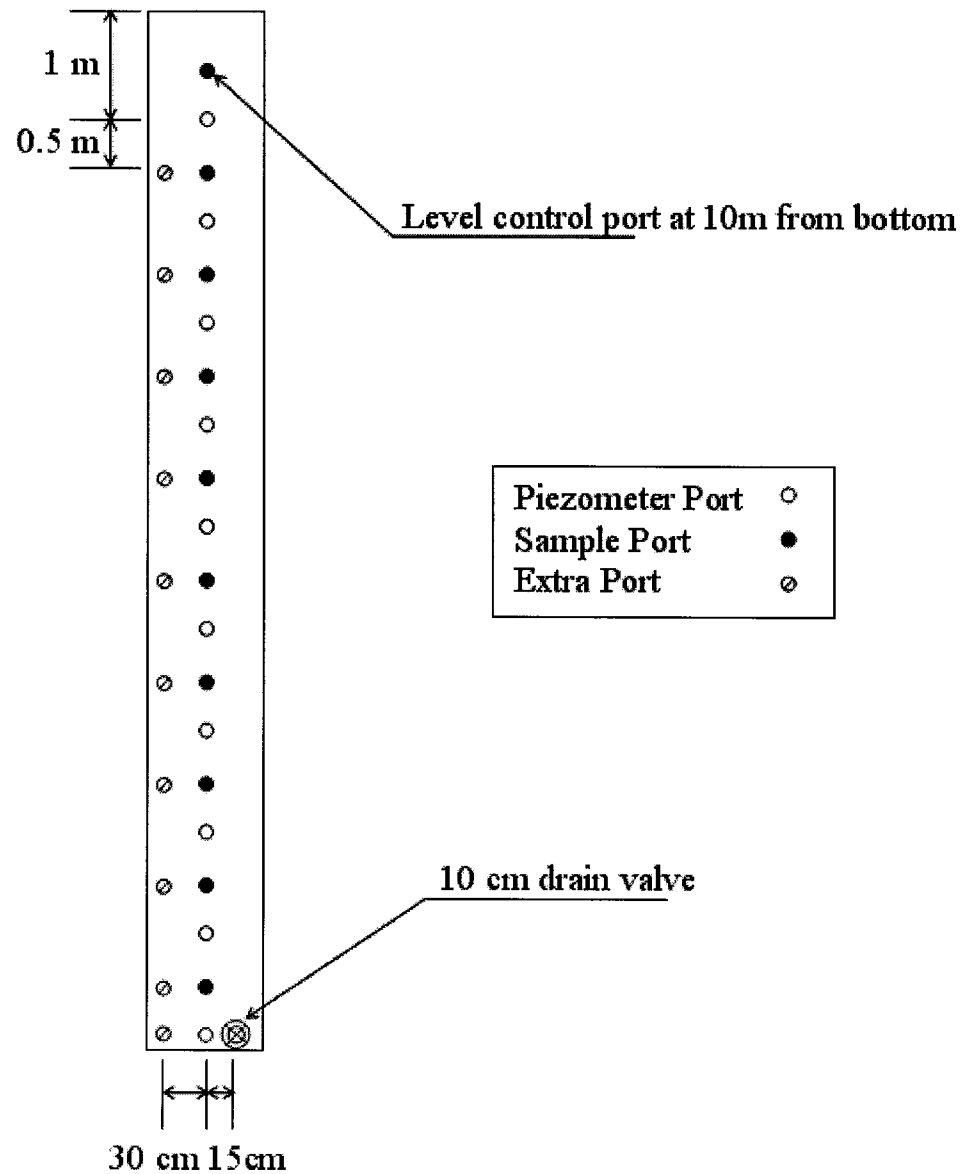


Figure 3.3 Location of piezometer and sample ports on a ten meter standpipe test

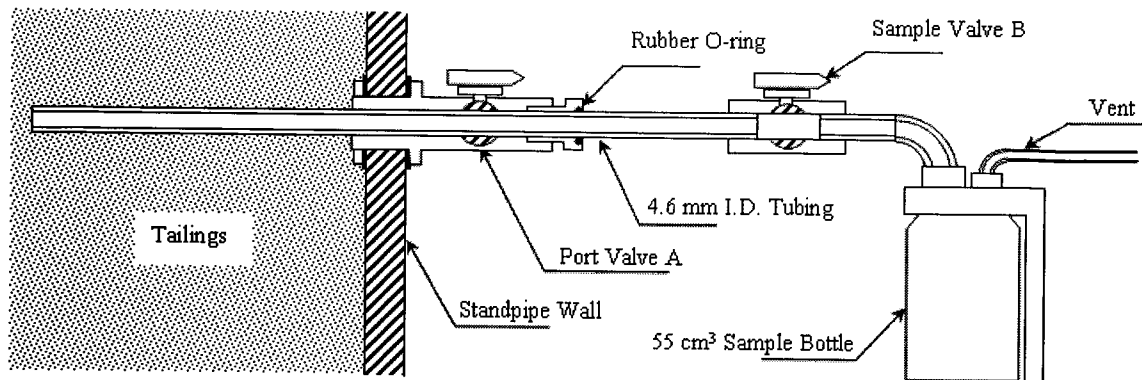


Figure 3.4 Solids content sampler

3.4.1.1 Solids content sampling procedure

1. Insert the sampler tube into the sample port with the port valve A and sampler valve B closed (Figure 3.4).
2. Open port valve A and sample valve B and push the sampler tube slowly into the middle of the standpipe.
3. Let the material freely flow into a sample bottle with about 30 - 40 ml capacity.
4. Close sample valve B and remove the sampler tube out of the standpipe slowly.
5. Let a very small amount of the material flow out and close valve A to minimize air that may be introduced into the system during sampling procedures.
6. From the weight of the material and the volume of the bottle, a density of the tailings can be calculated.
7. Move to next sampling port for the next test.

3.4.1.2 Density sampler

The density sampler allows the soil density to be measured under in situ pore pressure conditions to prevent gas coming out of solution or gas bubbles to increase in volume. This type of sampler is more complex than the solids content sampler in both operation procedures and in the sampling device itself, however, it yields a better measurement of density. Moreover by using both samplers together, the degree of saturation can be calculated and comparative studies between these two samplers can be made.

The density sampler (Figure 3.5) sampling procedures are divided into 2 sections, saturation and sampling, which are discussed in detail below.

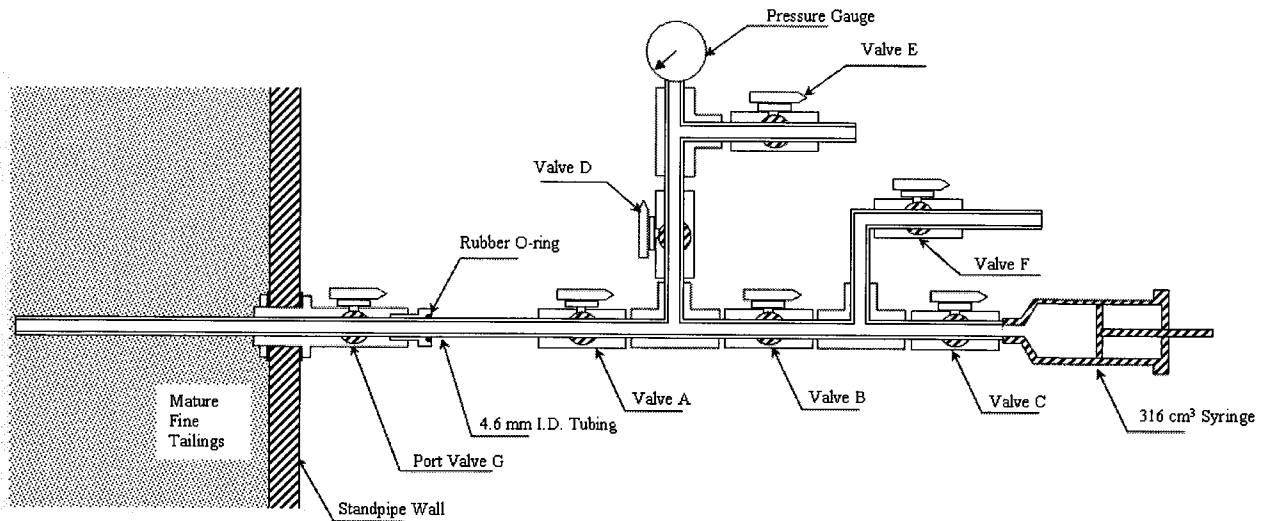


Figure 3.5 Density sampler

3.4.1.2.1 Density sampling procedures

a. Saturate the system.

1. Open sampler valves A, B, and C. Close sampler valves D and F.
2. Open port valve G. Insert a sampler into the standpipe about 2 - 3 cm inside standpipe wall.
3. Let fine tailings freely flow into the syringe or pull the syringe out steadily and slowly to fill the line and syringe with 30 - 40 ml of fine tailings.
4. Close valve A and open valve D and E. Push fine tailings out into a waste pail through valve E. Close valve D and E.
5. Open valve F and flush fine tailings out into the waste pail. Then close valve F and C.
6. Detach the syringe from valve C and empty the syringe. Then attach it back to the sampler. Avoid introducing any bubbles into the system.

b. Sampling

1. Make sure that all valves on the sampler are closed.
2. Open valve A and push the sampler tube into the middle of the standpipe.
3. Open valves C, D and B then record the fluid pressure from the pressure gauge.
This pressure should be similar to the pore pressure at that point in the standpipe.
Do not allow any movement of the syringe.
4. Extract sample by allowing syringe piston to move at a rate that maintains the initial pore pressure measured by the gauge.
5. Once the piston has reached the end of travel, close valve C.
6. Remove sampler, closing valves D and A once the sampling rod is clear of the port valve G. Close valve G.
7. Break sampler upstream of valve C.
8. Measure weight of syringe tube assembly including sample (syringe tube assembly must be weighted prior to sampling).
9. Expel sample into a jar. Flush sampler with water ensuring all solids are transferred to jar. Jar contents should be transferred to drying pans and dried overnight to determine the dry mass of the sample.
10. Clean all components of the sampler and repeat procedure at next sample port.

3.4.2 Pore water pressure ports

Pore water pressure ports are used to measure pore water pressure inside the standpipes (Figures 3.1 and 3.3). The pore water pressure ports are aligned along the sides of the standpipe similar to those of sampling ports, however, they are at depths of 0.5, 1, 2, 3, 4, 5, 6, 7, 8, 9, 9.5 and 10 m. This alignment allows sampling without disturbance to the pore water pressure. The pore water pressure and the measured density from the sampling ports are used to calculate total stress and effective stress throughout the depth of the standpipe. These data measured at different time periods provide pore water pressure profiles, excess pore water pressure profiles and effective stress profiles that can be used to evaluate the consolidation behaviour of the fine tailings material.

Pore water pressures are measured at the pore water pressure ports usually at 1 m intervals. Before any measurements are taken, the water level is measured to ensure that the water level is at 10 m, otherwise, water filling is needed. If water is added, generally the standpipe is left for over a month before pore water pressure measurements are taken to make sure that the pore water pressures are stabilized. A pore pressure transducer is calibrated with a riser tube every time measurements are performed. The pore water pressure testing procedure is as follows:

3.4.2.1 Procedure for reading piezometers in 10 m standpipes

a. Checking and saturating the system.

1. Make sure all valves are closed on standpipe.
2. Check for air bubbles or gas bubbles in clear plastic piezometer lines.
3. If bubbles are in the lines, flush out by using the water reservoir and hand screw pump.
4. Close all valves on manifold.
5. Pressurize manifold to maximum pore pressure expected. That pore pressure is at the bottom piezometer. For the first reading, the maximum pressure of a fluid column with a density equal to the initial density and height of 10 m minus height of pressure transducer above bottom (inside) can be assumed. For Standpipe 1:

$$\begin{aligned}u &= \rho \cdot g \cdot h \\ &= (1.21 \times 9.81) \times (10 - 1.36) \\ &= 102.6 \text{ kPa.}\end{aligned}$$

6. Open all manifold valves to see if pressure drops. This is done for checking for air bubbles in lines. Re-pressurize manifold and lines with the hand screw pump. Then close all valves.

b. Calibration of transducer.

1. A calibration tube in the pore pressure reading system is used to calibrate the pore pressure transducer. Water is forced up the calibration tube with the screw pump until it overflows. The transducer is read and the pressure is checked against the height of the tube.

2. Vary the height of water in the calibration tube and take a reading from the transducer for every height of water.
3. Make a plot of the height of water and transducer voltage readings.
4. Obtain the transducer calibration factor from the plot.

c. Reading pore pressure.

1. Check level of water in standpipe and fill standpipe with water up to the 10 m height port. Leave it for a month to let the pore pressure stabilize.
2. Open all standpipe piezometer valves. Keep all manifold valves closed.
3. To start readings; pressurize the manifold with the screw pump to maximum expected pore pressure. Open manifold valve to bottom piezometer. Read immediately and every minute until reading stabilizes.
4. After the pressure stabilizes, close manifold valve and open the next piezometer manifold valve.
5. Repeat the procedures for all remaining piezometers.

3.5 History of Measurements on Standpipes

The ten meter standpipe test program performed at the University of Alberta consists of a total of three ten meter standpipes. They were started at different times and they contain different tailings material but with the same objective which is to study the self-weight consolidation behaviour of tailings. The measurements taken in the standpipes are listed below. Each of the measurements has a different importance, which is used to study the consolidation behaviour of these tailings materials and they are discussed in detail in the next three chapters for each standpipe.

1. Grain size distribution test
2. Bitumen content measurement
3. Specific gravity test
4. Atterberg limits
5. Scanning Electron Microscopy
6. Degree of saturation

7. Biological test
8. pH measurement
9. Mineralogy
10. Pore water chemistry
11. Solids content and density measurements
12. Pore water pressure measurements

In this section, all records of the different measurements taken in all three standpipes are shown.

3.5.1 History of measurements on Standpipe 1

Standpipe 1 was started on October 4th, 1982. The material inside the standpipe is mature fine tailings. This standpipe has been monitored since 1982. It is this standpipe that has been extensively monitored more than the other standpipes for over 21 years of operation. The measurements shown in the list above are restated in Table 3.3 for Standpipe 1.

3.5.2 History of measurements on Standpipe 2

Standpipe 2 was started on November 4th, 1982 and stopped on October 12th, 1984 when it had fulfilled its objective. During the 2 years of operation, Standpipe 2 was operating satisfactorily. All measurements taken for Standpipe 2 are shown in Table 3.4.

3.5.3 History of measurements on Standpipe 3

After it was considered that no further investigation on Standpipe 2 was needed, Standpipe 3 was started on November 30th, 1984 by remixing the material inside Standpipe 2 with additional sand. The last reading on this standpipe was on February 20th, 1997. The types of measurements taken for this standpipe are very similar to Standpipe 2 and are shown in Table 3.5.

Information on soil structure by SEM, mineralogy by XRD and pore water chemistry was obtained in recent years. The reason for these measurements is because

studies have shown that mineralogy and pore water chemistry play a significant role on the behaviour of the fine water-clay structure. Extensive studies on these subjects help explain clay-water interaction related to consolidation. Discussion on this topic is presented in the next three chapters.

3.6 Summary

The large ten meter standpipe tests at the University of Alberta have been performed to understand the self-weight consolidation behaviour of fine tailings and MFT-sand mixes. A total of three standpipe tests have been conducted with different tailings materials. Standpipe 1 was filled with mature fine tailings, Standpipe 2 was filled with a fine tailings-sand mix of 48% sand and Standpipe 3 was filled with a fine tailings-sand mix of 82% sand. Only Standpipe 1 is currently under observation.

Measurement of interface settlement and stress profiles are mandatory for all standpipe tests. The presented methods of measurements are considered to be effective and give good resolution of measured data for soft slurries. Monitoring of the large scale, self-weight consolidation test in Standpipe 1 will be continued for further evaluation of the consolidation behaviour of this class of material. The ten meter standpipe test results could be used to develop a theory for the settlement behaviour of large void ratio highly thixotropic slurries.

Table 3.3 Measurements on Standpipe 1

Depth (m)	Grain Size Distributions						Bitumen Content				Specific gravity		Atterberg Limit		Scanning Electron Micrograph (SEM)	Degree of saturation s%		Biological test		pH and conductivity		Mineralogy and Pore water chemistry	
	1982		1985		2000		2003		1982	1983	1984	1987	2003	1982	2003	2003	1997	2003	2000	2003	1992	2000	2000
	a	c	a	c	a	c	a	c	c	c	c	c	i	a	a						x		
0.0	a	c	a	c	a	c							i	a							x		
0.5	a	c	a	c	a	c							i	a									
1.0	a	c	a	c	a	c							i	a									
1.5	a	c	a	c	a	c							i	a									
2.0	a	c	a	c	a	c							i	a									
2.5	a	c	a	c	a	c							i	a									
3.0	a	c	a	c	a	c							i	a									
3.5	a	c	a	c	a	c							i	a									
4.0	a	c	a	c	a	c							i	a									
4.5	a	c	a	c	a	c							i	a									
5.0	a	c	a	c	a	c							i	a									
5.5	a	c	a	c	a	c							i	a									
6.0	a	c	a	c	a	c							i	a									
6.5	a	c	a	c	a	c							i	a									
7.0	a	c	a	c	a	c							i	a									
7.5	a	c	a	c	a	c							i	a									
8.0	a	c	a	c	a	c							i	a									
8.5	a	c	a	c	a	c							i	a									
9.0	a	c	a	c	a	c							i	a									
9.5	a	c	a	c	a	c							i	a									
10.0	a	c	a	c	a	c							i	a									

a - average value, x - measured values, c - calculated values

Remarks:

Table 3.3 Measurements on Standpipe 1 (Continued)

Depth (m)	Solids Content, Bulk Density										Pore water pressure										Interface measurements				
	1982	1983	1984	1985	1992	1997	2000	2003	1982	1983	1984	1985	1992	1997	2003	1982-1987	1989	1992	1997	2000	2003				
0.0	x	x	x	x																					
0.5	x	x	x	x				x	x	x															
1.0																									
1.5	x	x	x	x																					
2.0																									
2.5	x	x	x	x				x	x	x			x	x											
3.0																									
3.5	x	x	x	x				x	x	x			x	x											
4.0																									
4.5	x	x	x	x				x	x	x			x	x											
5.0																									
5.5	x	x	x	x				x	x	x			x	x											
6.0																									
6.5	x	x	x	x				x	x	x			x	x											
7.0																									
7.5	x	x	x	x				x	x	x			x	x											
8.0																									
8.5	x	x	x	x				x	x	x			x	x											
9.0																									
9.5	x	x	x	x				x	x	x			x	x											
10.0								x	x	x			x	x											
Remarks:	a - average value, x - measured values, c - calculated values																								

Table 3.4 Measurements on Standpipe 2

Depth (m)	Grain Size Distributions		Bitumen Content		Specific gravity		Solids Content, Bulk Density		Pore water pressure		Interface measurements	
	1982	1984	1982	1984	1982	1984	1982	1984	1982	1984	1982	1984
0.0	a	c	c	c	i		x	x				
0.5	a	c	c	c	i		x	x				
1.0	a				i				x	x		
1.5	a	c	c	c	i		x	x				
2.0	a				i				x	x		
2.5	a	c	c	c	i		x	x				
3.0	a				i				x	x		
3.5	a	c	c	c	i		x	x				
4.0	a				i				x	x		
4.5	a	c	c	c	i		x	x				
5.0	a				i				x	x		
5.5	a	c	c	c	i		x	x			x	x
6.0	a				i				x	x		
6.5	a	c	c	c	i		x	x				
7.0	a				i				x	x		
7.5	a	c	c	c	i		x	x				
8.0	a				i				x	x		
8.5	a	c	c	c	i		x	x				
9.0	a				i				x	x		
9.5	a	c	c	c	i		x	x			x	x
10.0	a				i				x	x		

a - average value, x - measured values, c - calculated values

Remarks:

Table 3.5 Measurements on Standpipe 3

Depth (m)	Grain Size Distributions	Specific gravity	Solids Content, Bulk Density		Pore water pressure										Interface measurements				
	1984	1984	1984	1985	1984	1985	1986	1987	1989	1992	1997	1984	1985	1986	1987	1989	1992	1997	2004
0.00	a	a	x	x															
0.25	a	a	x	x															
0.50	a	a	x	x															
0.75	a	a	x	x															
1.00	a	a	x	x															
1.50	a	a	x	x															
2.00	a	a																	
2.50	a	a	x	x															
3.00	a	a																	
3.50	a	a	x	x															
4.00	a	a																	
4.50	a	a	x	x															
5.00	a	a																	
5.50	a	a	x	x															
6.00	a	a																	
6.50	a	a	x	x															
7.00	a	a	x	x															
7.50	a	a	x	x															
8.00	a	a																	
8.50	a	a	x	x															
9.00	a	a																	
9.50	a	a	x	x															
10.00	a	a	x	x															

a - average value, x - measured values, c - calculated values, XX - this measurements was done after surface water had evaporated

4. Ten Meter Standpipe 1 Measurements

Ten meter standpipe 1 initially contained 6.57 m³ of mature fine tailings whose general properties have been shown in Table 3.2. The material was pumped from the Mildred Lake tailings pond and transported to Edmonton and pumped into the standpipe in October 1982. These mature fine tailings in the tailings pond appear to be consolidating very slowly and thus are very challenging for reclamation planning of the tailings pond. Extensive studies on mature fine tailings are therefore needed to improve the approach to manage the oil sand tailings operations in Northern Alberta.

In this chapter, measurements taken on this standpipe are shown and the present understanding of the consolidation behaviour is elaborated. The measurements include index properties, settlement of the interface, solids content, bulk density, pore water pressure, thixotropic gain in strength, and scanning electron micrograph.

4.1 Material Index Properties

The mature fine tailings are a unique and complex material. There are many factors that influence the compression behaviour of this material. A comprehensive description and explanation of their physical and chemical properties is essential for understanding their behaviour and for explaining differences between materials. However, an evaluation of the fine tailings from a single perspective is inadequate to fully understand their true nature. Comprehensive approaches in geotechnical engineering, soil and water chemistry and the environmental sciences are all necessary to obtain a fundamental understanding of how the characteristics of the fine tailings will govern behaviour.

In this section, a description of the index properties is presented and a discussion on how these fundamental properties have an influence on the compressibility and permeability of the material is given. Due to the existing bitumen in the mature fine tailings, measurements of index properties of this class of material are modified from the standard geotechnical measurements in order to be able to capture the most reasonable values.

4.1.1 Grain size distribution

Mature fine tailings are very fine materials (approximately 95% fines depending on the depth). The fine material ($< 45 \mu\text{m}$) in the fine tailings originated from inter-bedded clay shale in the oil sands formations. The extent that these clay bands are broken up depends on the mining methods, the bitumen extraction processes, and the composition of the oil sands ore.

The mature fine tailings are generally composed of 5% sands, 45% of silt size particles and 50% of clay size particles. The average grain size distributions of the fine tailings in Standpipe 1 are shown in Figures 4.1 and 4.2, which are the grain sizes measured in 1985 and 2003, respectively. The two sets of measurements are the same within experimental error. The recent measurement (2003) was done for investigating changing of the particle size distribution by segregation settling of the coarser grains. These two particle size distributions were measured by the same method which was the dispersed hydrometer-sieve (ASTM D422-63). Due to the bitumen content, the ASTM standard for the hydrometer-sieve test can not be performed effectively and a modified hydrometer test is conducted. Extraction of bitumen and drying of the samples are avoided as heavy hydrocarbons left in the sample tend to cement the finer particles together resulting in smaller measurements of clay-size material. Moreover, breaking up by grinding or pulverization will exert a considerable influence on the particle size distribution. Initial wet weights are chosen based on the solids content measurements and dry weights are measured after sieving. Excess bitumen is skimmed off the sample after mixing. Detailed procedures are showed in Section 4.1.1.1.

4.1.1.1 Recommended particle size analysis procedure

Two methods are used to determined grain size distribution; dispersed tests (ASTM D422-63) and nondispersed tests (ASTM D4221-99). It was found that there was little difference between the particle size distributions determined from the dispersed and nondispersed methods for Clark Hot Water Extraction (CHWE) fine tailings for material coarser than approximately $1.7 \mu\text{m}$ and both methods showed 100% dispersion (Miller, 2004). This dispersed state is expected because sodium hydroxide is added in the CHWE

extraction process as a conditioning agent to disperse the clay lumps as much as possible to optimize the separation of bitumen from the mineral solids. However, Miller (2004) showed that while the majority of the CHWE fine tailings were dispersed during the extraction process, some of the finer sized material remained as small lumps from the original clay bands. These small clay band lumps are perhaps best described as clay particle aggregates. As it is important to determine the field grain size distribution, the recommended method for determining the nondispersed particle size distribution of this class of material does not change the chemistry of the clay minerals or pore water.

1. Measure solids content of a sample and calculate weight of wet sample to get a dry mass of about 25 g.
2. Put the prepared wet sample in a dispersion cup. Wash any residue in the sample container into the dispersion cup with process water. Mix the slurry for a period of 5 minutes.
3. After mixing, some bitumen will float on the top of the mix. Skim bitumen on the top of the mix as much as possible and put the bitumen in a tare which is weighed earlier. Let the tailings sit about 6 to 12 hours and skim bitumen one more time.
4. Transfer the soil-water slurry from the dispersion cup into the glass sedimentation cylinder and add process water until the volume is 1000 ml.
5. Using the rubber stopper in the open end, turn the cylinder upside down and back for a period of 1 minute. After mixing, replace the cylinder on the table, insert the hydrometer, and start the timer.
6. Take hydrometer readings at total elapsed times of $\frac{1}{4}$, $\frac{1}{2}$, 1 and 2 minutes without removing the hydrometer.
7. After the 2 minute reading, remove the hydrometer, remix and restart the test, but take no reading until 2 minutes. For this reading and all the following ones insert the hydrometer just before reading and remove it after the reading.
8. Take hydrometer readings at total elapsed time intervals of 2, 4, 8, 15, 30, ... minutes etc., approximately doubling the previous time interval until the 1440 minute (24 hours) reading is taken.

9. After the hydrometer test is finished, perform a standard test method for wet sieve analysis with a range of sieve sizes from 2 mm to 0.045 mm.
10. Collect all soil including that washed through the 0.045 mm sieve. Dry soil to obtain the dry mass used in the hydrometer test.
11. Retain all soil for future analyses.

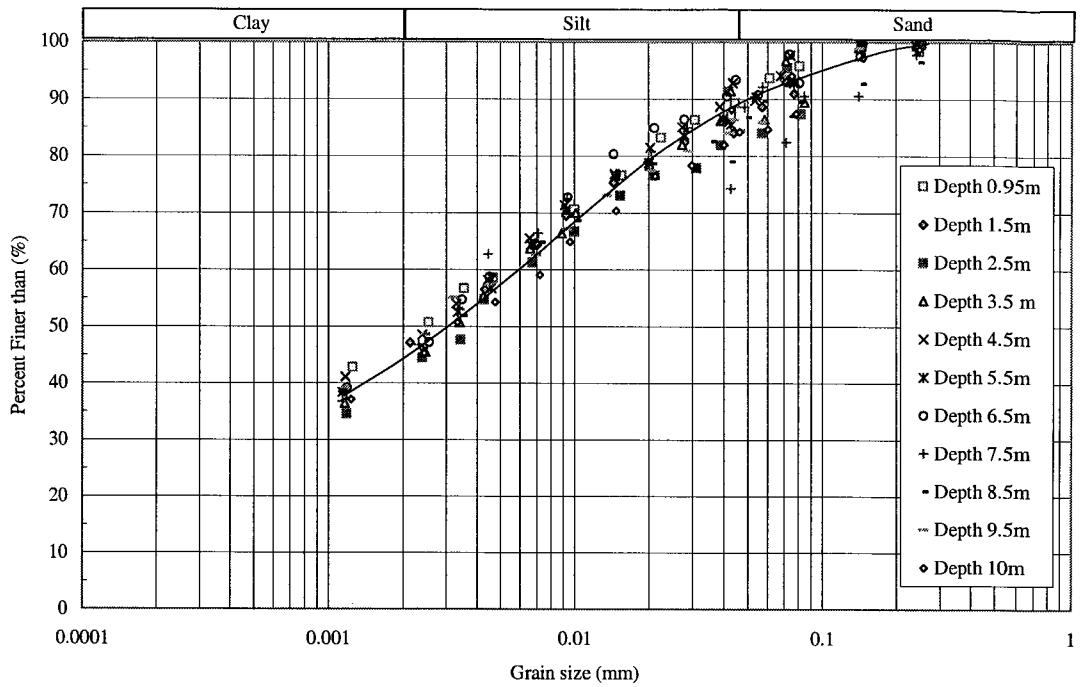


Figure 4.1 Grain size distribution measured in 1985

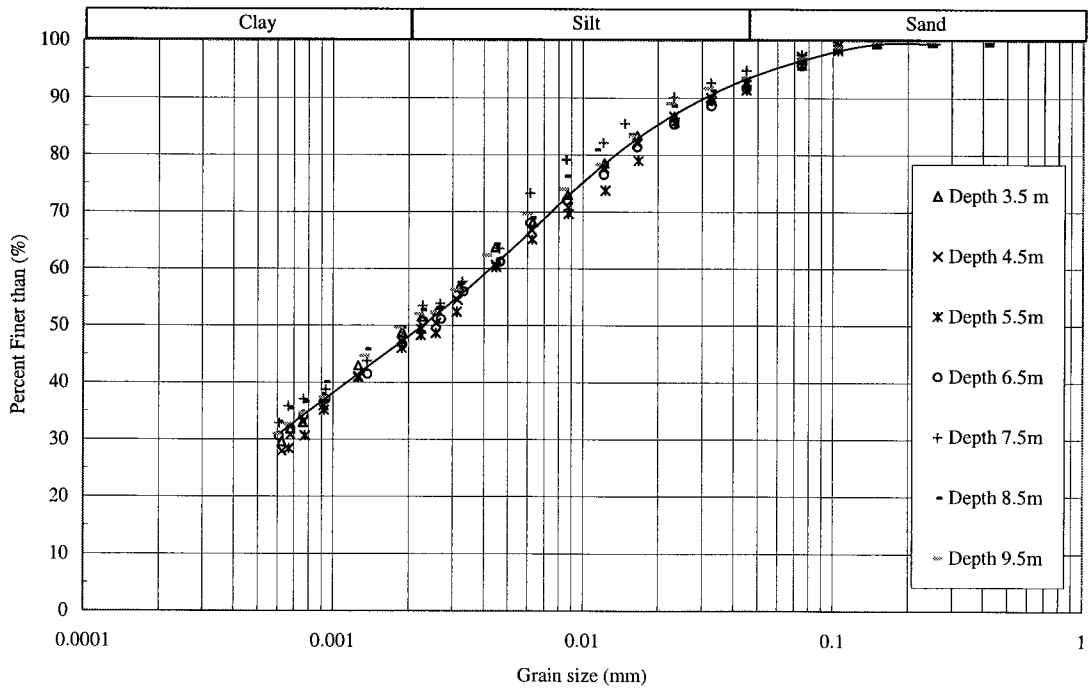


Figure 4.2 Grain size distribution measured in 2003

4.1.1.2 Methylene blue analysis

Another common method used in the oil sands mining industry for determining clay size fraction is the Methylene Blue Test. Methylene blue adsorption values are determined for both chemically dispersed and non dispersed fine tailings solids to assess the degree of dispersion of active clays (Sethi, 1994). Methylene blue is a cationic dye that can be adsorbed on the exposed negatively charged surfaces of clays and is a standard used to measure exposed surface area of clays in soils. The quantity of exposed clay mineral can be calculated using an empirical relationship developed for the oil sands tailings (Tang, 1997) given as:

$$\text{Clay Mineral Fraction (\%)} = \{(0.006) \times (\text{MB value}) + 0.04\} / 0.14 \quad (4.1)$$

where MB value = methylene blue number

The methylene blue test only detects clay surfaces that are exposed. Therefore, the dispersed methylene blue test is an effective tool to determine the total amount of clay material present in fine tailings, but does not provide any information regarding the form of the clay particles prior to dispersion. As a result, when completely dispersed, the clay sized fractions of fine tailings determined by methylene blue and hydrometer give a good correlation (Miller, 2004). A dispersed methylene blue test then should give similar results to those of a dispersed hydrometer test and represents the total amount of clay-size material existing in the fine tailings. Methylene blue test results showed that the clay fraction at depths of 4.5 m and 6.5 m are 50% and 53%, respectively, while the hydrometer tests measured 48% and 49% for the same depths. These results indicate that the modified hydrometer test procedure works effectively.

The standard methylene blue test procedure specifies the use of bitumen extracted and dried tailings samples. As mentioned earlier, drying and grinding changes both the chemical and physical characteristics of the fine tailings. When dried, the mineral solids of the fine tailings become cemented together. Grinding is then required to break up the sample. The intensity and duration of the grinding will determine to what degree the solids are broken apart and the proportion of clay surfaces exposed. It is unlikely that the

fine tailings can be consistently returned to a condition representative of fine tailings in their natural state.

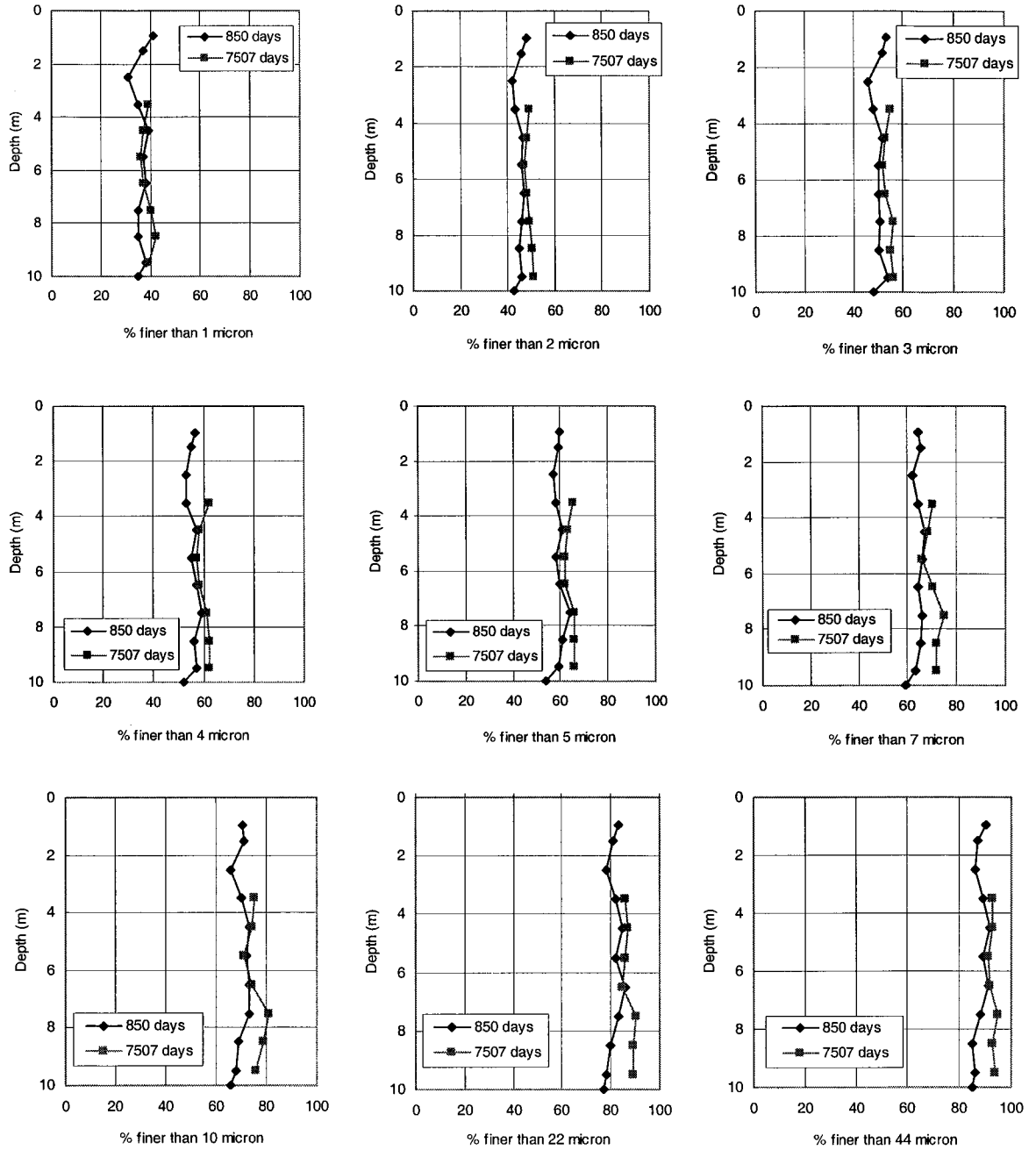


Figure 4.3 Particle size fraction profiles

4.1.1.3 Particle size fraction profiles

Segregation or settling of the sand through the fines matrix is evaluated in Figure 4.3. Nine particle size fraction profiles at 850 days (1985) and 7507 days (2003) are shown. The fraction profiles do not show a significant change in particle size or migration of coarse grain particles and are within the range of experimental error. These results in Figure 4.3 agree with the particle size distributions in Figures 4.1 and 4.2. It is concluded that there was no segregation or changing in particle size distribution in Standpipe 1 during this period.

4.1.2 Mineralogy

Soil behaviour is directly related to the mineralogy of soils. Soil particles and interaction between the particles controls the compressibility as well as the hydraulic conductivity of a soil. The clay minerals of the fine tailings typically consist of 80% kaolinite, 15% illite, 1.5% montmorillonite, 1.5% chlorite and 2% mixed clay layers (FTFC, 1995). The existence of the fines in the tailings results from the dispersion of clay-shale stringers and layers in the ore during mining and extraction.

Bulk and clay X-Ray diffraction analysis performed on clay samples from the ten meter standpipe has confirmed the clay mineralogy of the fine tailings in the standpipe. Table 4.1 shows the major minerals of the fine tailings samples at depths of 6.5 m and 9.5 m. It appears that the major mineralogy of the fine tailings is generally kaolinite followed by quartz and illite respectively while the clay-size minerals are entirely kaolinite and illite in approximately equal amounts. From Table 4.1 it appears that the clay particles are not fully dispersed, some of the kaolinite is in the form of aggregates and booklets which have a large particle size and appear as silt size particles. Kaolinite, which is the major clay mineral in the fine tailings, is typically one of the least active clay minerals in thixotropic gain in strength. However, an addition of a dispersing agent to kaolinite can make kaolinite very thixotropic (Mitchell, 1960).

Table 4.1 Major minerals of the mature fine tailings in Standpipe 1

Minerals (%)	Sand-size (>45 µm)		Silt-size (45 µm-2 µm)		Clay-size (<2 µm)		Total minerals in mineral category	
	6.5	9.5	6.5	9.5	6.5	9.5	6.5	9.5
Depth in standpipe (m)	6.5	9.5	6.5	9.5	6.5	9.5	6.5	9.5
Quartz and other minerals	5	7	29	31	0	0	34	38
Kaolinite	0	0	19	9	25	28	44	37
Illite	0	0	0	0	22	25	22	25
Total minerals in size	5	7	48	40	47	53	100	100

4.1.3 Water chemistry

Several investigations have found that the pore water chemistry has a major influence on the fine tailings structure. Tang et al. (1997) showed that the bicarbonate and sodium hydroxide in the tailings water are the dominant agents which cause the card-house floc structure of kaolinite clay-water systems as in the CHWE tailings.

Recycled pond water from the Mildred Lake tailings pond and Athabasca River make up water is used for the CHWE process. Sodium hydroxide was originally added during the extraction process as a dispersing agent and exists in the recycled pond water and bicarbonate comes from the river water, the connate water in the oil sands and from the adsorption of CO₂ during aeration processes. Similarly, studies (FTFC, 1995) on the effect of the compositions of the tailings water concluded that the repulsive and attractive forces between the clay particles dominate the behaviour of the fine tailings-water structure and that the electro-kinetic behaviour is mainly caused by the presence of bicarbonate ions. Major ions in the fine tailings pore water samples from five different depths in the ten meter standpipe are shown in Table 4.2. The significant presence of bicarbonate (HCO₃⁻) is shown. Conductivity and pH measurements at different depths taken in 2000 are shown in Figures 4.4 and 4.5 respectively. The values are similar to those in the Syncrude and Suncor tailings ponds in 1992 and indicate that no significant change in water chemistry in the ten meter standpipe has likely occurred from 1982 to 2000.

Table 4.2 Compositions of pore water in ppm of the mature fine tailings from Standpipe 1.

Depth (m)	Na	K	Mg	Ca	F	Cl	SO ₄	CO ₃	HCO ₃	NH ₄	IC ₅₀	IC ₂₀	Nap Acid
4.5	258	7.5	4.1	5.9	5.0	87.0	BDL	24.6	864	8.7	23	7	41
6.5	260	7.9	4.3	6.0	9.0	97.0	3.0	25.8	878	9.4	N/A	N/A	N/A
7.5	260	7.8	4.0	5.7	6.0	90.0	3.0	67.2	775	9.3	20	5	45
8.5	254	7.7	4.0	5.7	12.0	100	5.0	13.8	873	8.6	N/A	N/A	N/A
9.5	257	7.9	4.1	6.0	9.0	96.0	8.0	33.0	839	8.1	25	8	42

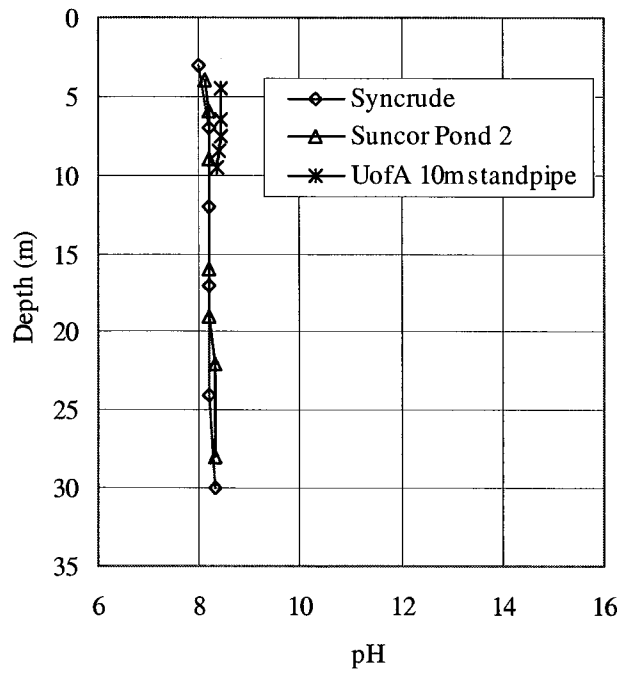


Figure 4.4 pH profiles

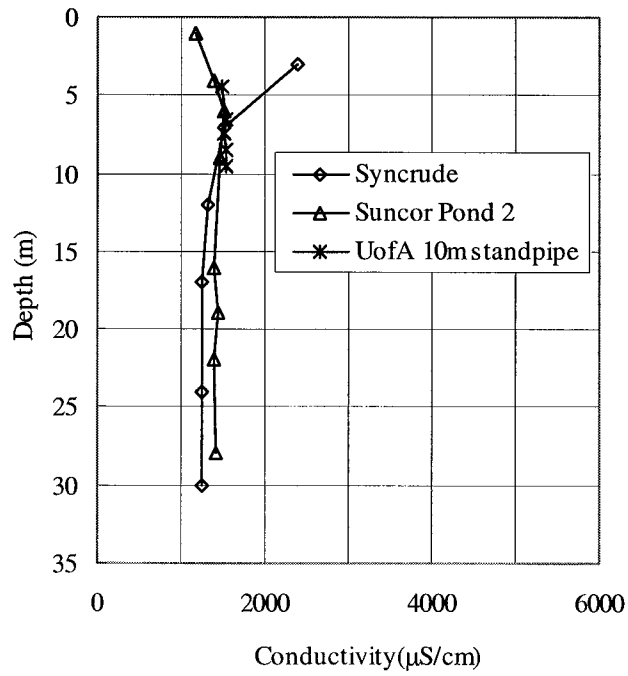


Figure 4.5 Conductivity profiles

4.1.4 Biological gas

Biological gas generation can cause a process of rapid consolidation by opening up water flow channels by gas bubble migration towards the surface of the deposit and therefore increase hydraulic conductivity. To investigate this effect, the presence of methanogens (methane producing microorganisms) and sulfate reducing bacteria (SRB) (inhibiting methane generation microorganisms) were determined in 2000 and 2003. Figures 4.6 and 4.7 show profiles of methanogen and SRB maximum possible numbers (MPN) respectively in the ten meter standpipe. The MPN values are determined by the standard five-tube MPN method (American Public Health Association, 1985).

In overview, the lack of methanogens (Figure 4.6) indicates gas generation should be negligible and no gas bubbles have been observed in the standpipe. The 1997 and 2003 average degree of saturation is about 99% to 100% (Figure 4.8). Therefore from the beginning to the latest measurements, gas generation has not affected the consolidation process in this standpipe test. However, methanogens are starting to have a higher population at the surface of the MFT. The sulfate (SO_4) measurements (Table 4.2) from pore water show that at the MFT surface the amount of sulfate is very low and below the determination limit. Because the inhibition of methanogenesis by sulfate arises from the competition of methanogens and SRB for substrates such as H_2 and acetate and SRB needs sulfate, the lack of sulfate directly reflects the low amount of SRB and the increasing of the methanogens. With low sulfate, methane generation is not inhibited and as shown in Figure 4.6, the methanogens are now large at the MFT surface compared to other depths. As there is quite a number of methanogens at the MFT surface, there is potential for microbial activity which produces gas. These measurements are supported by the degree of saturation measurements showing a smaller degree of saturation or a small amount of gas existing in the top part of the standpipe. However, the effect of methanogens is still very low and negligible in most of the standpipe. The presence of methanogens and gas in the ponds is much greater than that detected in the standpipe.

Details about effects of sulfate on methanogens and SRB can be found elsewhere (Fedorak et al. 2002 and Holowenko et al. 2000) and the influence of gas generation in parts of the Syncrude tailings pond is discussed by Guo et al. (2004).

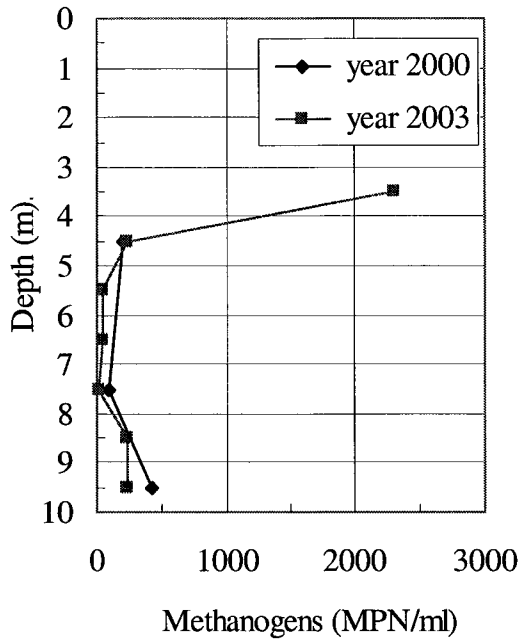


Figure 4.6 Methanogen profiles

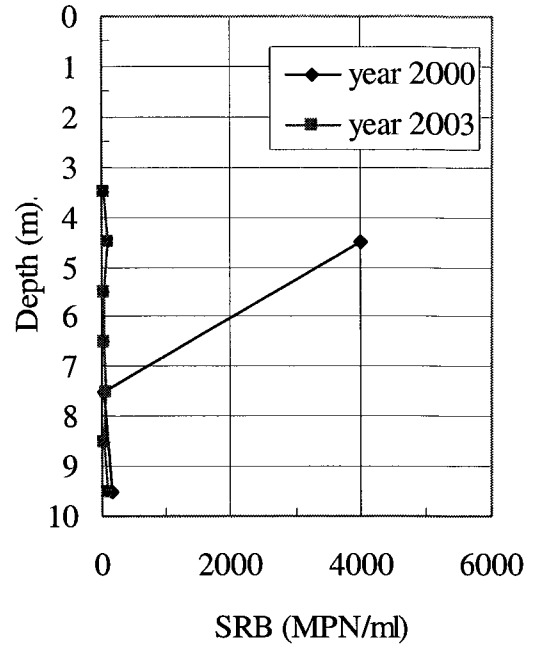


Figure 4.7 SRB profiles

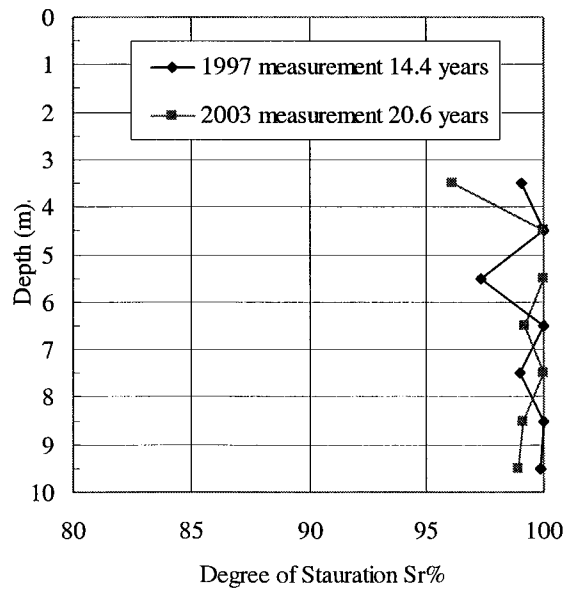


Figure 4.8 Measured degree of saturation in 1997 and 2003

4.1.5 Bitumen content

Bitumen exists in the tailings as free and adsorbed bitumen. The amount of bitumen in the ten meter standpipe averages around 3% of the total mass or 10% of the dry mass which is higher than the present bitumen content in the tailings ponds. It is typically greater in finer tailings than coarser tailings (Scott et al. 1985).

Bitumen content can be defined by two definitions which are bitumen content in geotechnical terms and in mining terms. The geotechnical and mining bitumen contents are expressed in Equations 4.2 and 4.3 respectively. It is noted that bitumen content can also be back calculated from the specific gravity of the fine tailings solids by using the specific gravities of the mineral solids and the bitumen. The bitumen is assumed to be a solid because its very high viscosity prevents it from flowing at ambient temperature.

$$b = \frac{M_b}{M_s} \quad (4.2)$$

$$b_m = \frac{M_b}{M} \quad (4.3)$$

where

b = geotechnical bitumen content

b_m = mining bitumen content

M_b = mass of bitumen

M_s = mass of bitumen and mineral solids = mass of solids

M = mass of water, bitumen, and mineral solids = total mass

While the geotechnical definition of bitumen content means that the parameter is fixed with the amount of solids, the mining definition means that the bitumen content will change with the amount of solids. In geotechnical analyses, the geotechnical definition is preferred.

Scott et al. (1985) suggested that bitumen has a significant influence on the consolidation process. The clay adsorbed organic layers and bitumen's affinity for water are a factor in decreasing the tailings hydraulic conductivity which controls the rate of consolidation. It also appears that the bitumen acts like a very viscous solid which at particle contacts can affect water flow through pore throats. Under high hydraulic gradients, such as in large strain consolidation tests, the bitumen tends to flow and block the pore throats resulting in a lower measured hydraulic conductivity.

4.1.6 Specific gravity

The specific gravity of the fine tailings was measured initially in 1982 and again in 2003 and the values in both cases were 2.28 which is quite low compared to natural clay soils. The low specific gravity value of the fine tailings is caused by the amount of bitumen attached to the fine mineral particles. The bitumen which has a specific gravity of about 1.03 is considered part of the solids and results in this low specific gravity of the total solids.

In the specific gravity test procedure, there are two common methods to remove air bubbles. One is boiling and another is vacuuming. If boiling is chosen, special care must be applied because existing bitumen will froth and fill the specific gravity jar. If bitumen is extracted prior to the specific gravity test, the back calculation to get the natural state specific gravity can be in error. Therefore, for the oil sand fine tailings vacuuming is preferable.

4.1.7 Atterberg limits

The Atterberg limits of the oil sand fine tailings are shown in Figure 4.9. The liquid limit of the tailings ranges from 44% to 53% and the plasticity index is in the range of 23% to 32%. The tailings with more bitumen (usually finer tailings) tend to have higher liquid limits (Scott et al. 1985). Studies have indicated a consistently lower plasticity index value for bitumen-free tailings (Scott et al. 1985). Thus bitumen has an effect on the clay-water interaction which affects both hydraulic conductivity and compressibility of the fine tailings. Table 4.3 shows index properties of the fine tailings

in 1982 and 2003. There does not appear to have been a significant change in the index properties throughout the 21 years of the standpipe operation.

Because of the rapid thixotropic gain in strength of the fine tailings, liquid limit samples have to be mixed thoroughly and tested quickly or high values of liquid limit will be measured as the material gains strength rapidly after mixing.

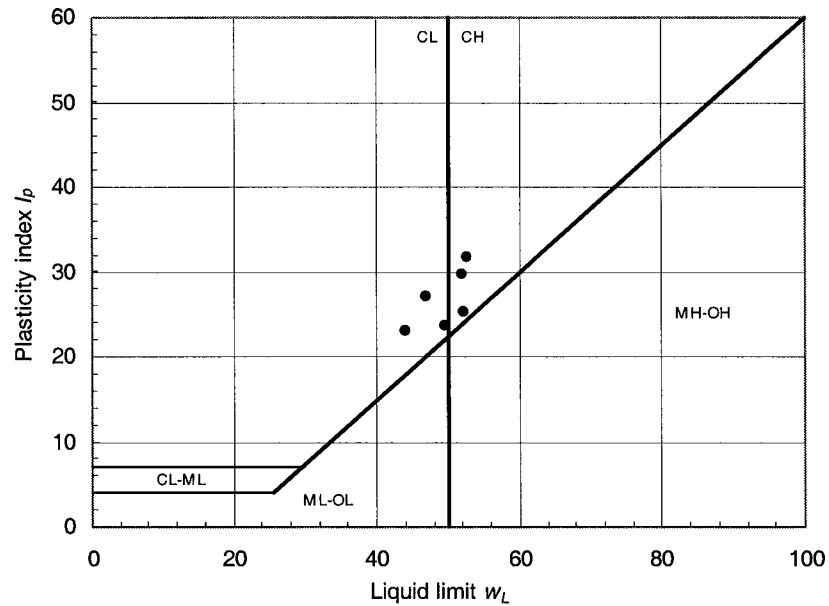


Figure 4.9 Plasticity of the oil sand fine tailings

Table 4.3 Index properties of the fine tailings.

Year	1982	2003
Average Water Content (%)	227	146
Liquid Limit (%)	46	52
Plastic Limit (%)	21	21
Plasticity Index (%)	25	31
Liquidity Index	8.24	4.03
Activity	0.53	0.65
Specific Gravity	2.28	2.28

4.2 Thixotropy

As stated in Chapter 2, thixotropy is defined as an isothermal, reversible time dependent process occurring under conditions of constant composition and volume whereby material stiffens while at rest and softens or liquefies by remolding (Mitchell, 1993). For geotechnical engineering, the thixotropic phenomenon can be generally described as a continuous decrease of shear strength or softening caused by remolding, followed by a time-dependent return to the original harder state at a constant water content and constant porosity. This phenomenon takes place in the majority of clay-water systems. As the consolidation process in clays is related to time and thixotropy is a time dependent effect, Mitchell (1960) argued that it would seem reasonable that thixotropic effects during consolidation lead to a smaller compression index. As a result, a thixotropic gain in strength will retard the consolidation process by building up bond strength and not allowing the soil to compress.

In general, kaolinite has minor thixotropic behaviour compared to bentonite and illite but the fine tailings, in which kaolinite is the main clay mineral, exhibits a very high thixotropic gain in strength. As discussed above, the mineralogy is not the main factor of this phenomenon but the addition of sodium hydroxide as a dispersing agent during the oil sands extraction process and the presence of bicarbonates and organic matter (bitumen) give the material its thixotropic behaviour.

In order to evaluate this phenomenon for geotechnical applications, thixotropic strength tests on fine tailings samples have been performed by several researchers at the University of Alberta. The objective of the thixotropic shear strength tests performed on the fine tailings was to investigate the absolute and relative gain in strength of the material with time. The increase in strength of the fine tailings in the experimental programs was due both to the thixotropic behaviour of the material and to a decrease of void ratio due to self-weight consolidation. The strength values were then corrected for the change in void ratio as described previously in Chapter 2. Thixotropic strength tests on the fine tailings were conducted by both the cavity expansion test and the vane shear test. Here the results of the cavity expansion test are presented (Figure 4.10).

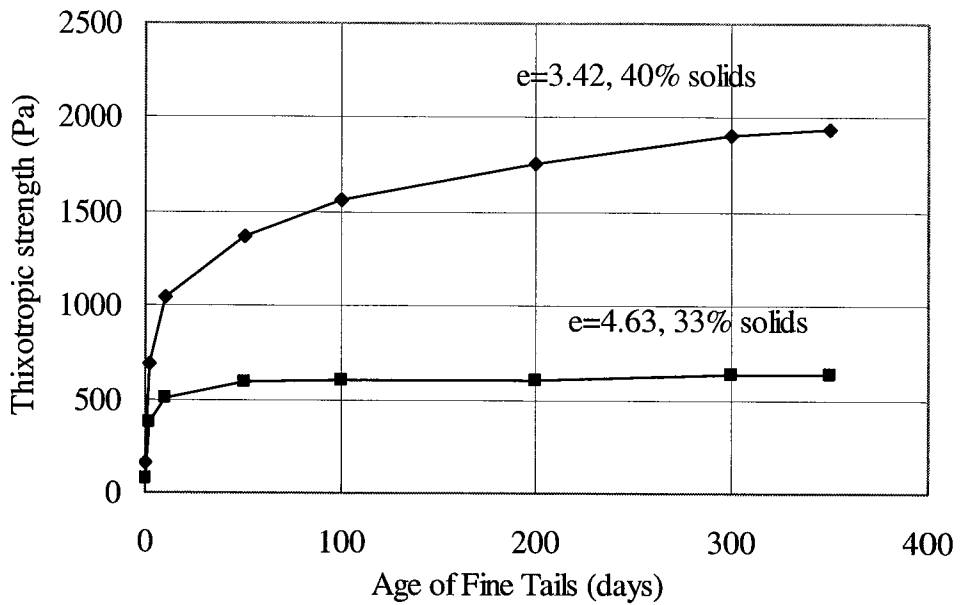


Figure 4.10 Thixotropic strength

The cavity expansion test procedure uses a cavity expansion theory to calculate the undrained shear strength of a soil from applied pressure in an expanding sphere. The initial cavity expansion test procedure was established by Banas (1991), who refined Elder's (1985) work, and which became the procedure presently used at the University of Alberta. Figure 4.10 shows thixotropic strengths measured from the cavity expansion test at void ratios of 4.63 and 3.42 or solids contents of 33% and 40% (Miller, 2004). The initial strengths after remolding were small, 18 and 165 Pa respectively. Within 2 days the strength had increased to 182 Pa and 702 Pa respectively. At 350 days the strengths were 635 Pa and 1941 Pa, respectively, and still increasing in the 40% solids MFT.

4.2.1 Determination of overconsolidation stress

From the above discussion, the influence of thixotropy on consolidation of the fine tailings has to be evaluated. In this section, overconsolidation stress due to thixotropic strength is discussed.

Thixotropy is directly related to the physio-chemical effect as shown by the repulsive-attractive forces in the clay water system, $R-A$, where R is repulsive force and A

is attractive force (Chatterji and Morgenstern 1989). The R and A forces are the direct result of the pore water ionic chemistry and the clay mineralogy. The equation of true effective stress is

$$\sigma'_i = \sigma - u - (R - A) \quad (4.4)$$

where σ'_i = true intergranular stress or true effective stress

σ = total stress

u = pore water pressure

$(R - A)$ = repulsive and attractive stresses

The more common equation for effective stress is

$$\sigma' = \sigma - u \quad (4.5)$$

where σ' = apparent effective stress or when the $R-A$ forces are small enough to be neglected, it is simply called the effective stress.

Field measurements in fine tailings ponds appear to show that the apparent effective stress is zero. However, because of sand settling through the fine tails, the difficulty in determining the total stress and pore pressure in these deep ponds and the more recent development of gas in the fine tailings makes the determination of the apparent effective stress difficult. If the apparent effective stress is zero, then Equation 4.4 reduces to Equation 4.6.

$$\sigma'_i = -(R - A) \quad (4.6)$$

In natural deposits of sedimentary clays the undrained shear strength has been found to increase with time (Bjerrum, 1967). It has also been found that the undrained shear strength is proportional to the increase in effective overburden stress. The fines-water structure has gone through the same process and therefore can be treated similarly.

Mesri (1975) developed a relationship between plasticity index and τ_f/σ'_p for recently deposited clays. The fine tailings plasticity index is about 25 and from Mesri's results the relationship in Equation 4.7 is obtained.

$$\frac{\tau_f}{\sigma'_p} = 0.22 \quad (4.7)$$

Where τ_f = undrained shear strength

σ'_p = overconsolidation stress

Overconsolidation stress is usually associated with a previous loading on a clay deposit that has subsequently been eroded leaving the clay overconsolidated with respect to its present vertical effective stress. Thixotropic changes in structure and improved interparticle bonding through chemical changes will also contribute to the magnitude of overconsolidation stress in a clay deposit (Terzaghi et al. 1996). A vertical effective stress greater than the overconsolidation stress must be applied to the deposit to cause the breakdown of interparticle bonds which would then result in consolidation settlement.

Using Mesri's relationship, the fine tailings at void ratios of 4.63 and 3.42 (solids contents of 33% and 40% with thixotropic strengths of 635 Pa and 1941 Pa, respectively) have overconsolidation stresses of 2.9 and 8.8 kPa, respectively. Therefore fine tailings deposits at these solids contents must have vertical effective stresses greater than these amounts for significant virgin consolidation to take place. Volume decreases that take place at lower effective stresses must be mainly caused by creep mechanisms.

4.3 Interface Measurements

Interface settlement or water-fine tails interface settlement of the material in the ten meter standpipe shows settling behaviour of the material with time. It has been measured frequently to determine the amount of compression of the mature fine tailings. The interface settlement measurements are shown in Figures 4.11 and 4.12 for arithmetic

time and log time respectively. Initial interface settlement through 900 days is also shown in Figure 4.13. This information is used to validate a consolidation model.

The interface settlement during the past 21 years shows that the settlement of the fine tailings has reached approximately 3.0 m and has settled at a uniform rate during the last 10 years. The average solids content has increased from its initial value of 30.6% to its present value of 40.6%.

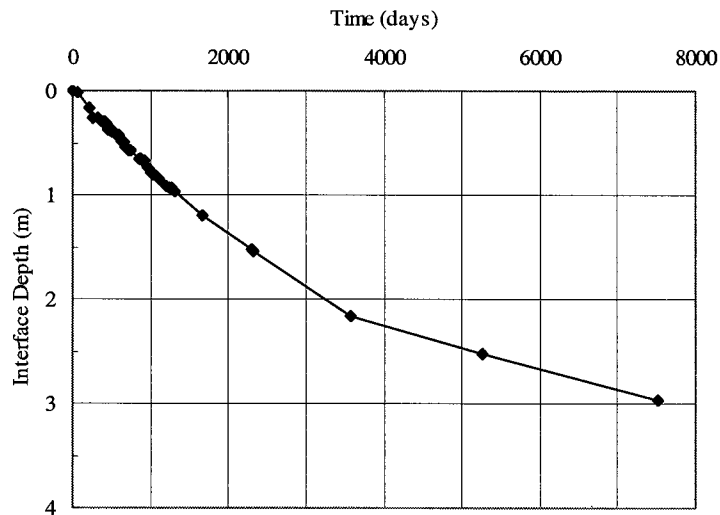


Figure 4.11 Interface measurement with arithmetic time

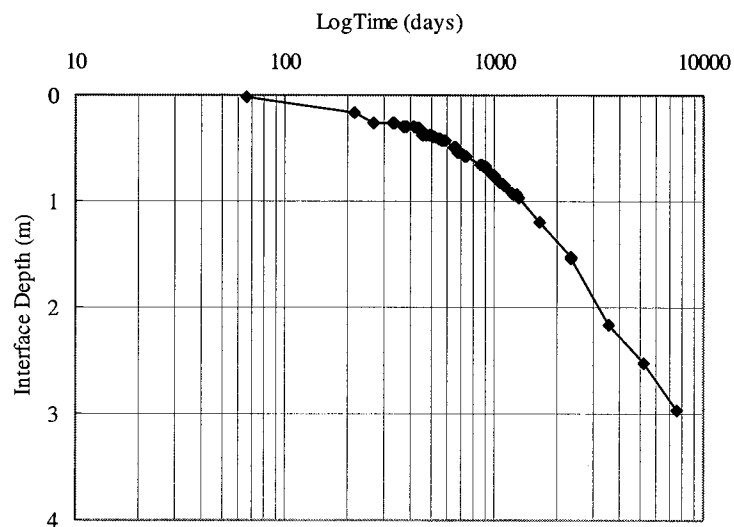


Figure 4.12 Interface measurement with log time

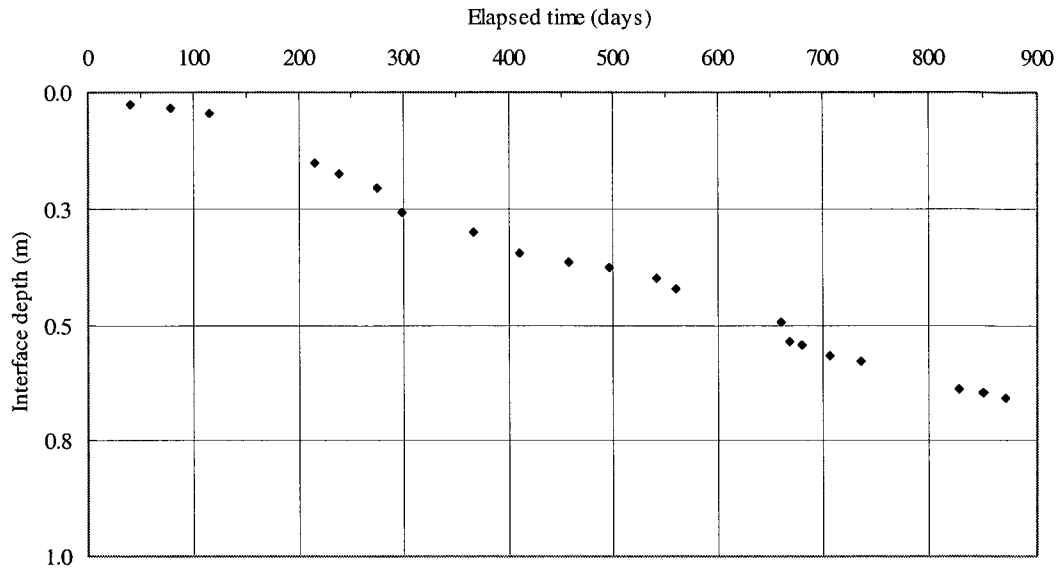


Figure 4.13 Initial interface measurement to 900 days

From Figure 4.13 the initial interface measurements are shown. It can be observed that the settlement rate has changed rapidly from a lower rate to a higher rate at around 150 days. This behaviour is believed to be the effect of thixotropic behaviour of the mature fine tailings as is discussed in the previous section. It will be discussed more with the discussion on the pore water pressure measurements.

4.4 Solids Content Measurements

In the oil sands industry, solids content is commonly used to express the solids-water composition of tailings. For geotechnical purposes, solids content is defined as the mass of tailings solids (the non-water portion of the tailings consisting of bitumen and mineral solids) divided by the total mass of the tailings. Generally, in the rest of the industry, the bitumen is extracted and solids content is defined as the mass of mineral solids divided by the total mass. Solids content was determined by oven drying samples of fine tailings at 105 °C for 24 hours. The method of solids content sampling in the ten meter standpipe is presented in Chapter 3.

The solids content appears to be increasing fairly uniformly with depth and only the bottom meter to a meter and a half appears to be consolidating (Figure 4.14a). The

average solids content has increased from its initial value of 30.6% to its present value of 40.6% (void ratios of 5.17 and 3.34, respectively). Fines void ratios (see Section 7.22 for calculation) with depth are also shown in Figure 4.14b.

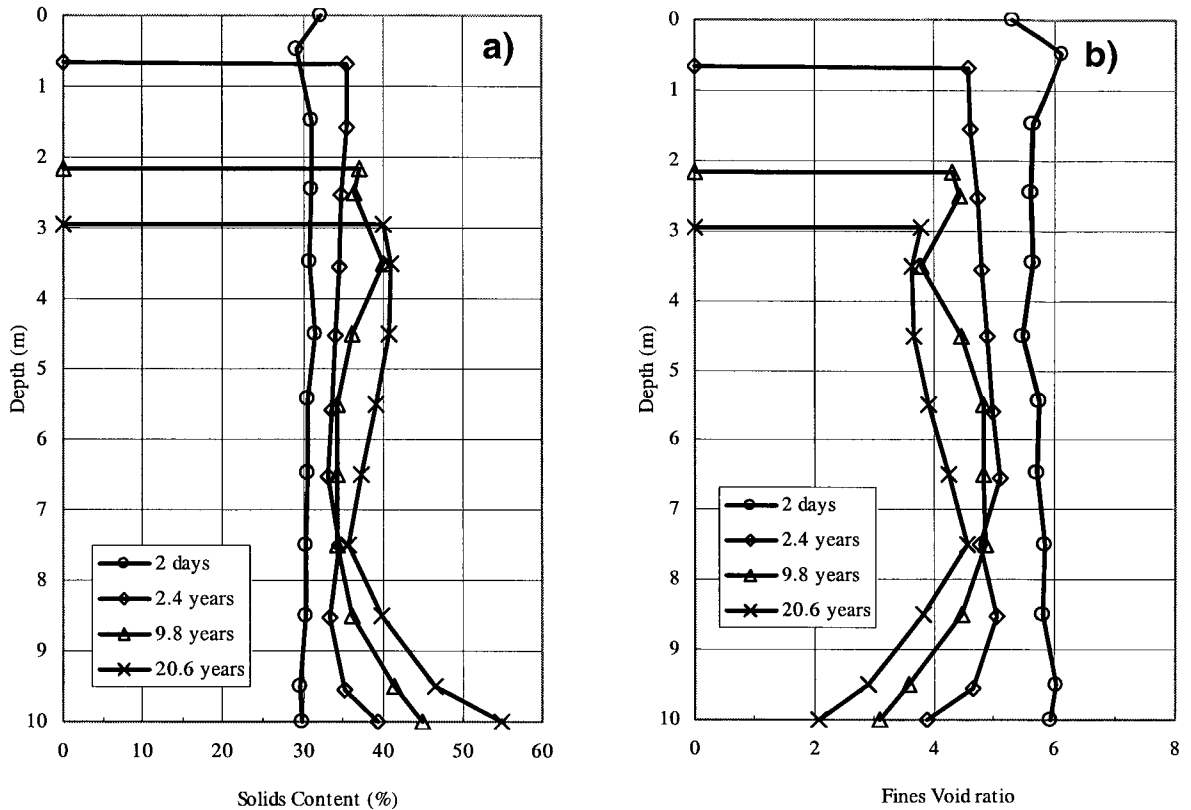


Figure 4.14 a) solids content profiles b) fines void ratio profiles

4.5 Bulk Density Measurements

The density sampler mentioned in Section 3.4.1.2 allows the soil density to be measured under in situ pore pressure conditions to prevent gas coming out of solution or gas bubbles to increase in volume. The average degree of saturation determined from this sampler is found to be about 99% to 100% which indicates that there are very few to no gas bubbles in these fine tailings. Bulk density is used to plot total stresses which are shown in the next section with pore water pressure measurements.

The latest measurements on Standpipe 1, as expected, show very little difference between the density measured by the solids content sampler and by the density sampler. The comparison is shown in Figure 4.15. The results are similar because the degree of

saturation is close to 100%. At a depth of 3.5 m the pressurized solids content measurement is slightly different from the other measurements because at this depth the degree of saturation is 96%, low compared to the other depths (Figure 4.8). The bulk densities calculated from the water content measurements assuming 100% saturation are similar to the other measurements (Figure 4.15).

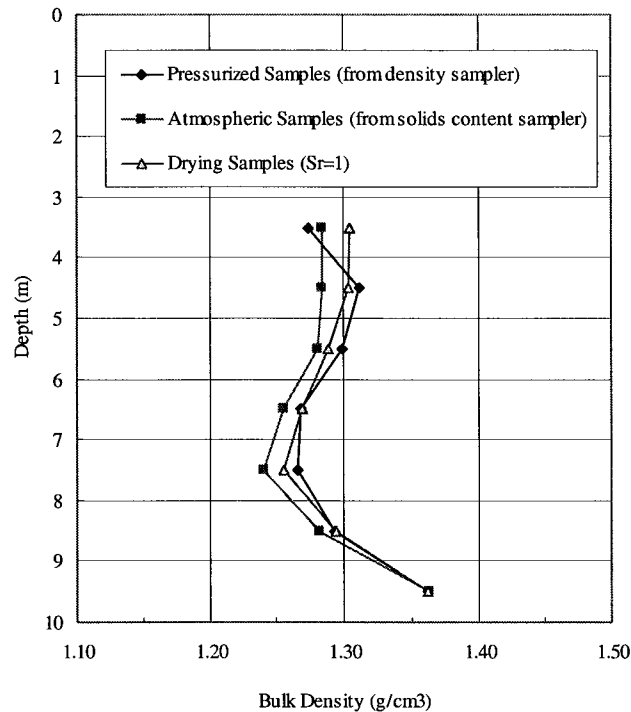


Figure 4.15 Comparison of bulk density

4.6 Pore Water Pressure Measurements

Pore water pressures are measured at the piezometer ports usually at 1 m intervals. A pore pressure transducer is calibrated with a riser tube every time measurements are taken. Details on measuring the pore water pressure can be found in Section 3.4.2. In this section the measurements of pore water pressure and stresses in the ten meter standpipe at 2 days, 2.4 years, 9.8 years and 20.6 years are shown.

Initial measurements of excess pore water pressures (Figure 4.16) indicate a rapid drop followed by a slight increase and then the excess pore water pressures reduce gradually. A hypothesis on this behaviour is that the settlement and pore water pressure

dissipation are initially controlled by hydraulic conductivity, compressibility and thixotropy. Within a short time the thixotropic gel strength builds up, resulting in a stronger soil structure behaving like an over consolidated soil. The initial rapid drop of excess pore pressure was caused by pore water pressure tension due to thixotropy. After the gel strength sets up, settlement can occur in two possible ways; one by destroying the gel strength with applied pressure and another is settlement by creep compression where particles slide and get closer to each other under a constant effective stress. Figure 4.16 shows initial excess pore water pressure measurements and Figure 4.13 shows the initial interface settlement. At an elapsed time around 100 to 150 days, the excess pore water pressure stopped decreasing rapidly, increased again and then changed to a lower dissipation rate. At the same period the interface settlement changed the rate of settlement to a higher rate. It is suggested that the increasing thixotropic gel strength initiated the decrease and then around this period a creep phenomenon or bond yielding of the fine matrix occurred, which increased the excess pore pressure again. The low dissipation rate is due to the decrease in total stress as the interface settles. Note that in Figure 4.16 the continuous low dissipation rate is greatest at 0.5 m depth where the change in total stress is greatest and does not occur at the bottom of the standpipe at the 10 m depth because the total stress does not change at this depth as the interface settles. The comparison of the excess pore water dissipation rate profiles are shown in Figure 4.17.

In Figures 4.18, 4.19, 4.20 and 4.21, total stresses, effective stresses and pore pressures at elapsed times of 2 days, 2.8 years, 9.8 years and 20.6 years are shown. Pore water pressure measurements show that the pore pressure remains very high and close to the total stress. The effective stresses as shown are very low to zero. Only the bottom 1 m of the standpipe shows a small effective stress about 5 kPa. The average void ratio at this time is about 3.34. During the last 10 years no additional effective stress has developed while the interface has settled about 80 cm. Therefore the decrease in void ratio throughout most of the depth of the standpipe is not due to consolidation, that is, a decrease in pore pressure with a subsequent increase in effective stress but is a creep phenomenon at a constant effective stress of zero.

The increase of effective stress at the bottom of the standpipe as shown in Figure 4.21 is not due to segregation of coarse materials in the fine tailings. The fines content ($<45\ \mu\text{m}$) is consistent throughout the depth of the standpipe and is about 90% as shown in Figure 4.3.

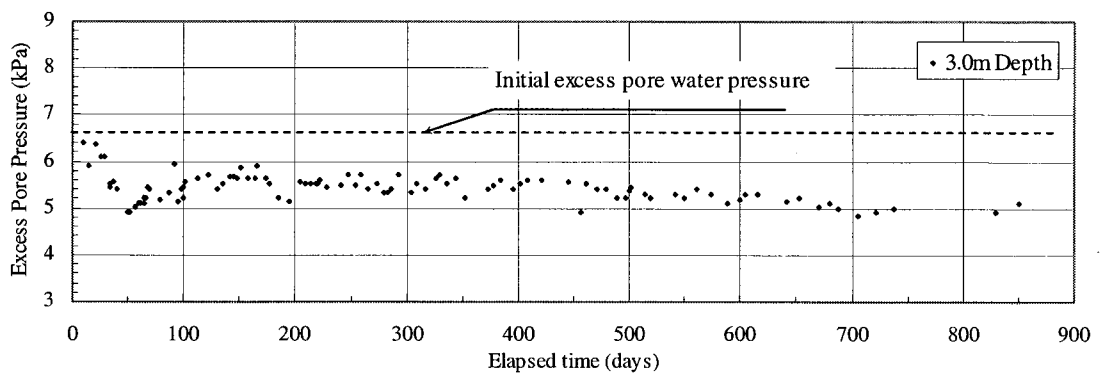
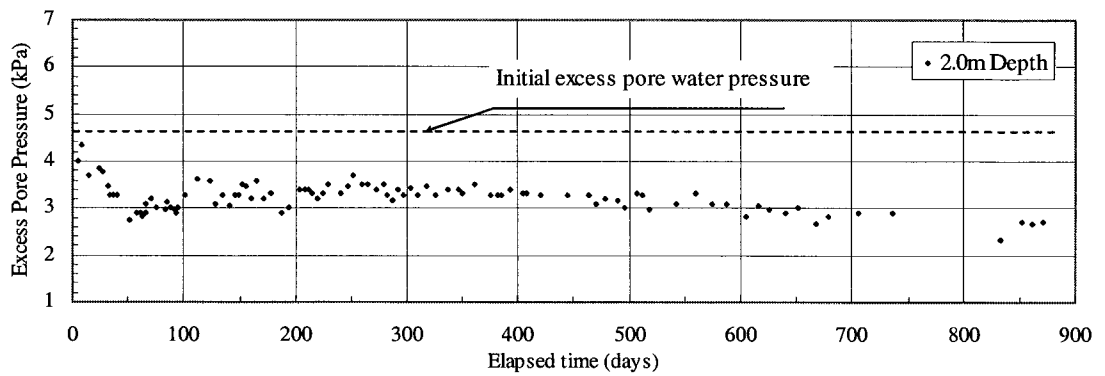
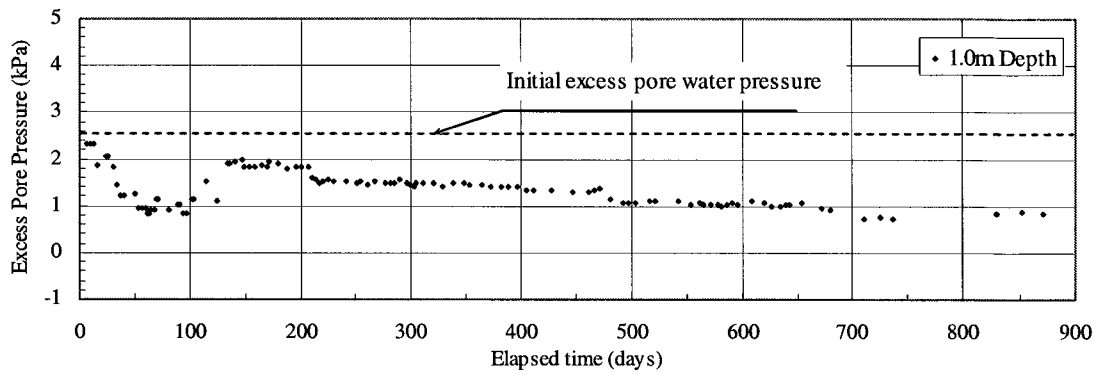
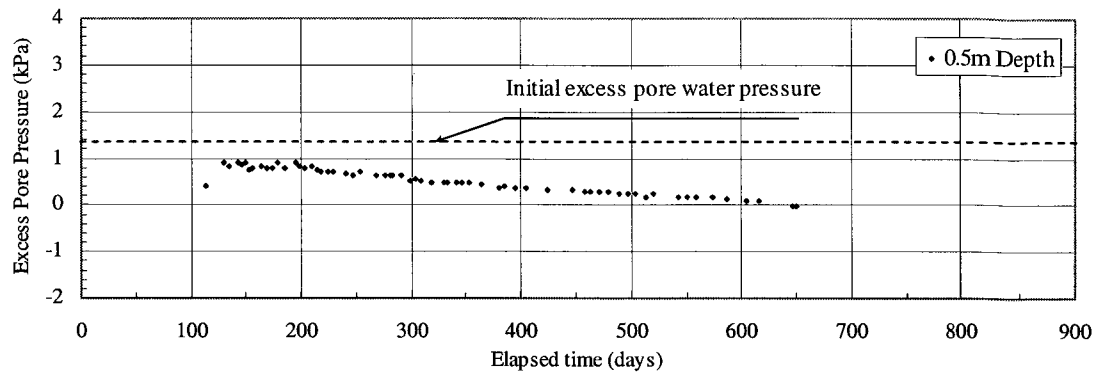


Figure 4.16 Initial excess pore water pressure measurements

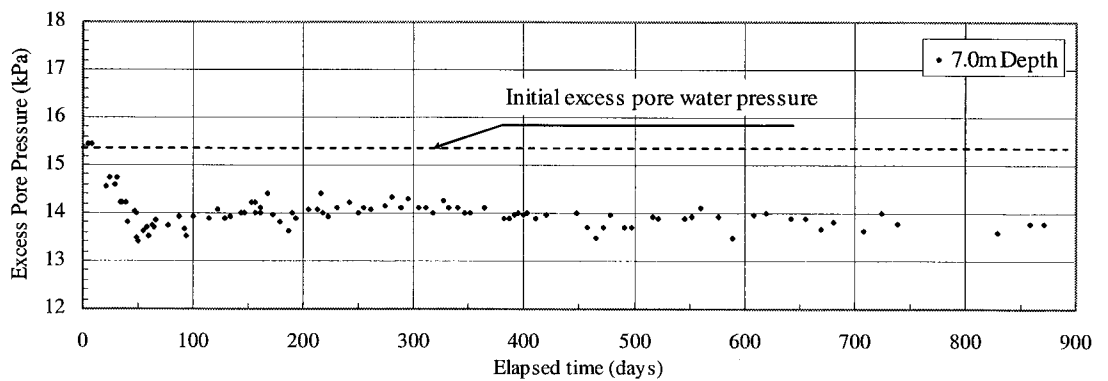
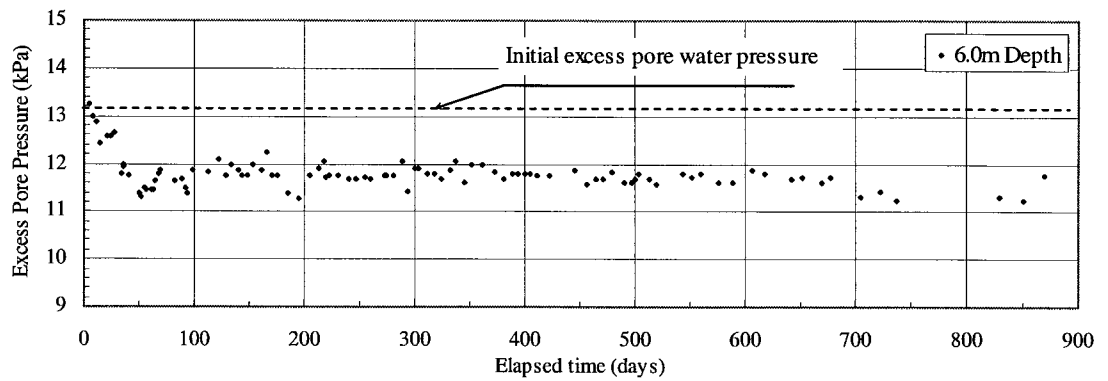
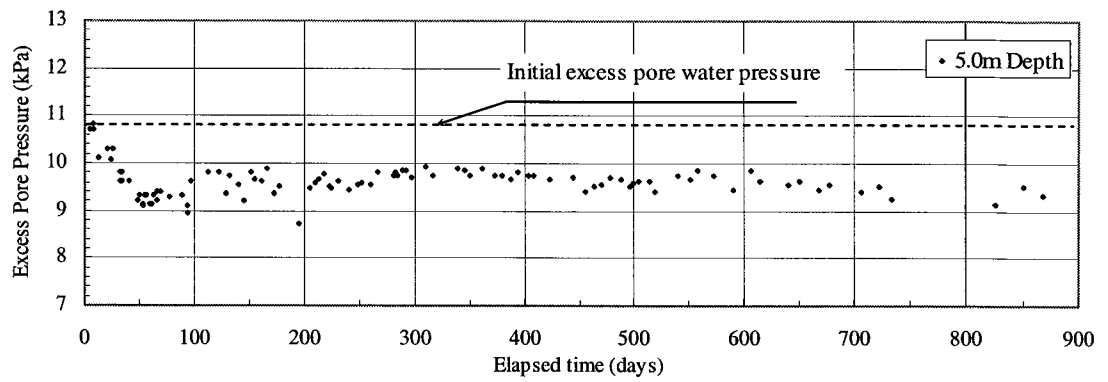
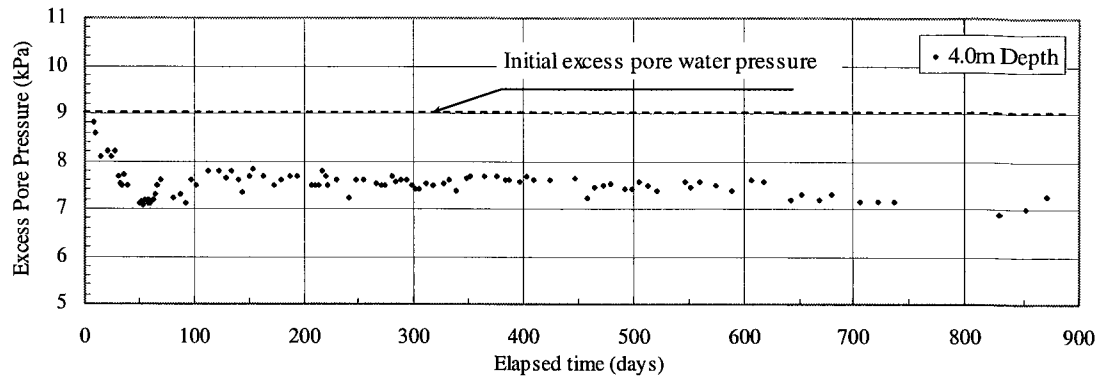


Figure 4.16 Initial excess pore water pressure measurements(continued)

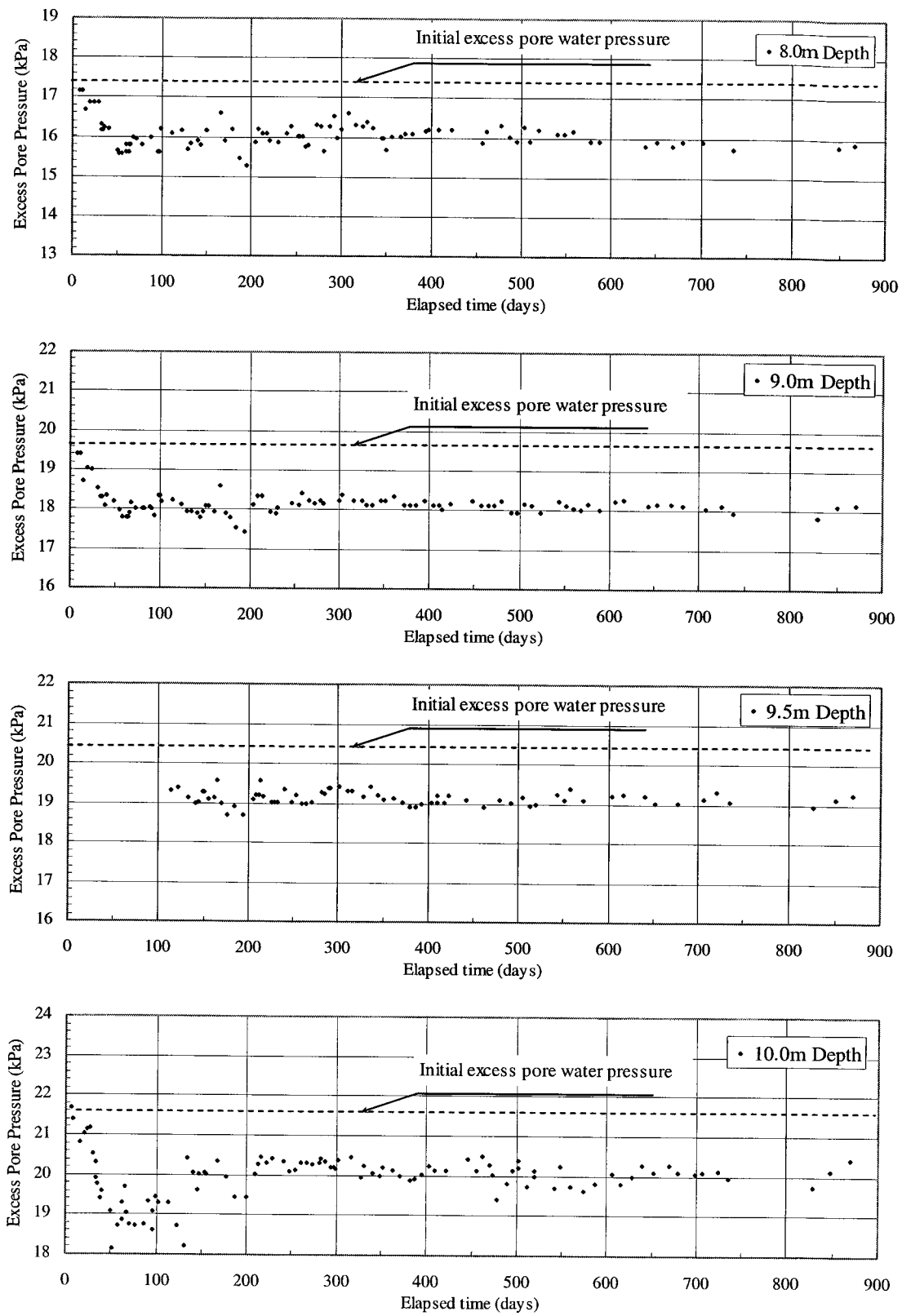


Figure 4.16 Initial excess pore water pressure measurements (continued)

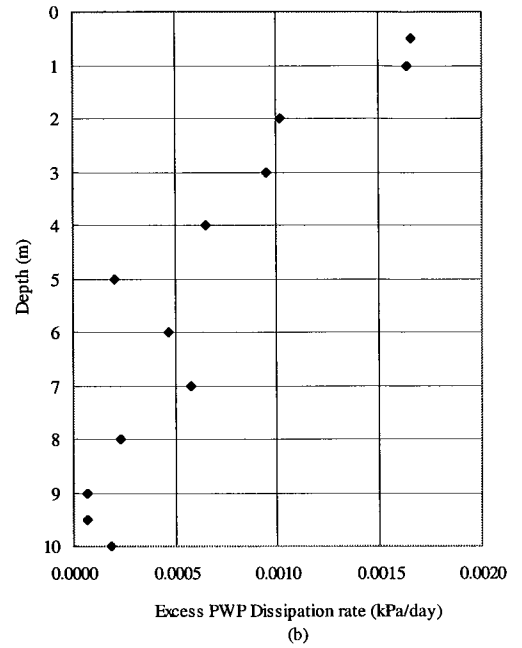
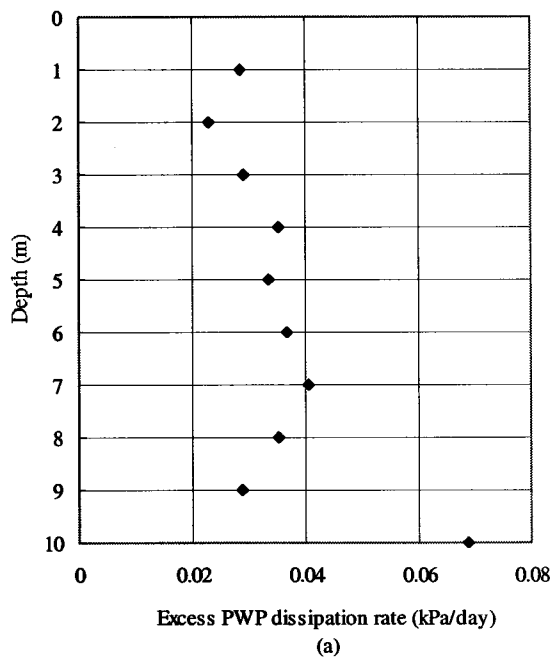


Figure 4.17 Excess Pore water dissipation rate profiles
a) settlement rate of 2.49×10^{-4} m/day (0-50days)
b) settlement rate of 7.87×10^{-4} m/day (150-900 days)

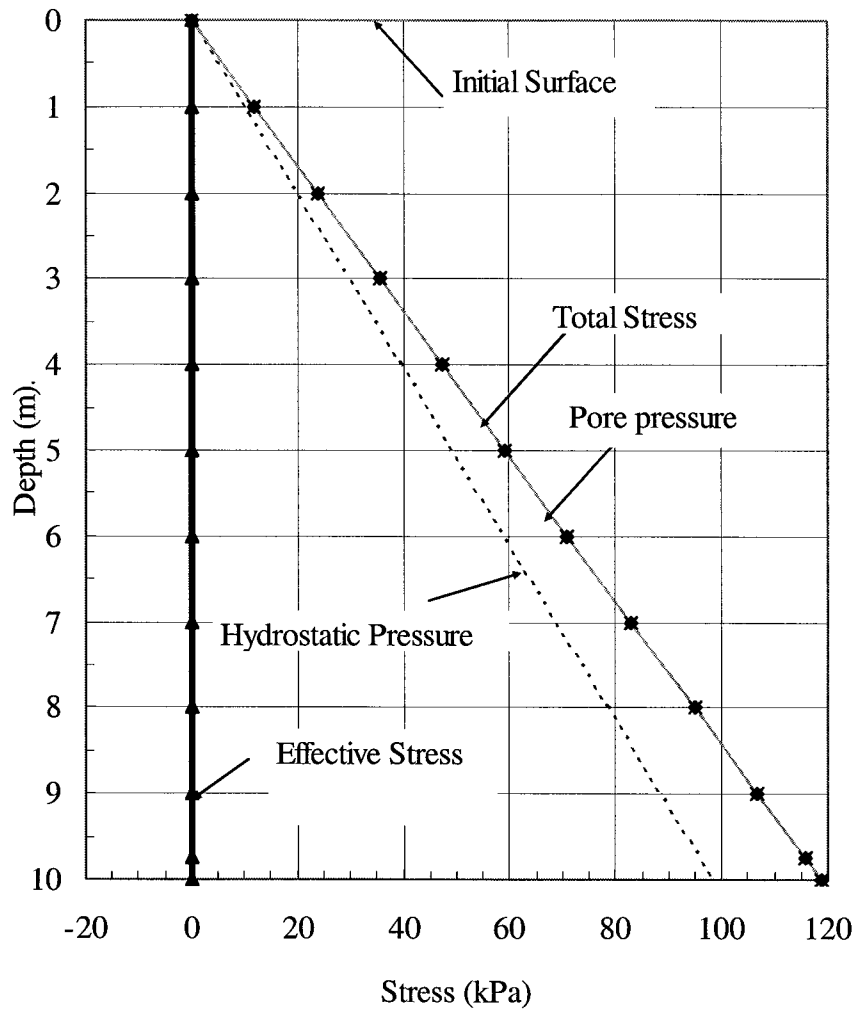


Figure 4.18 Total stress, pore pressure and effective stress profiles at 2 days

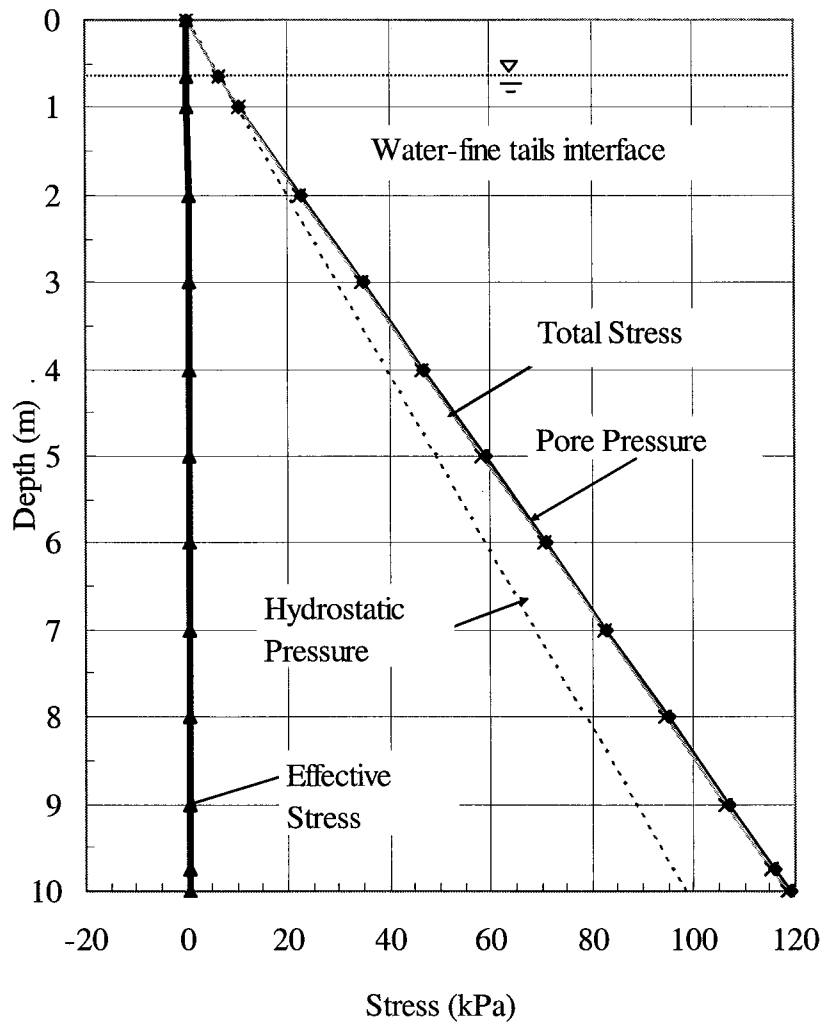


Figure 4.19 Total stress, pore pressure and effective stress profiles at 2.4 years

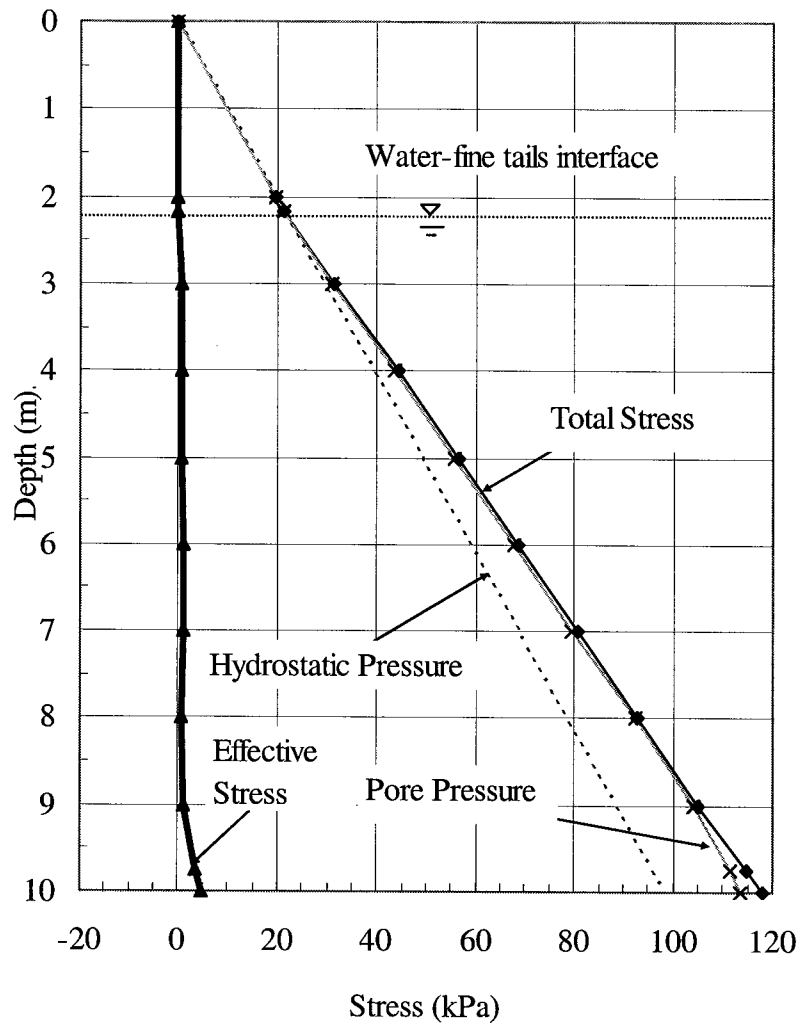


Figure 4.20 Total stress, pore pressure and effective stress profiles at 9.8 years

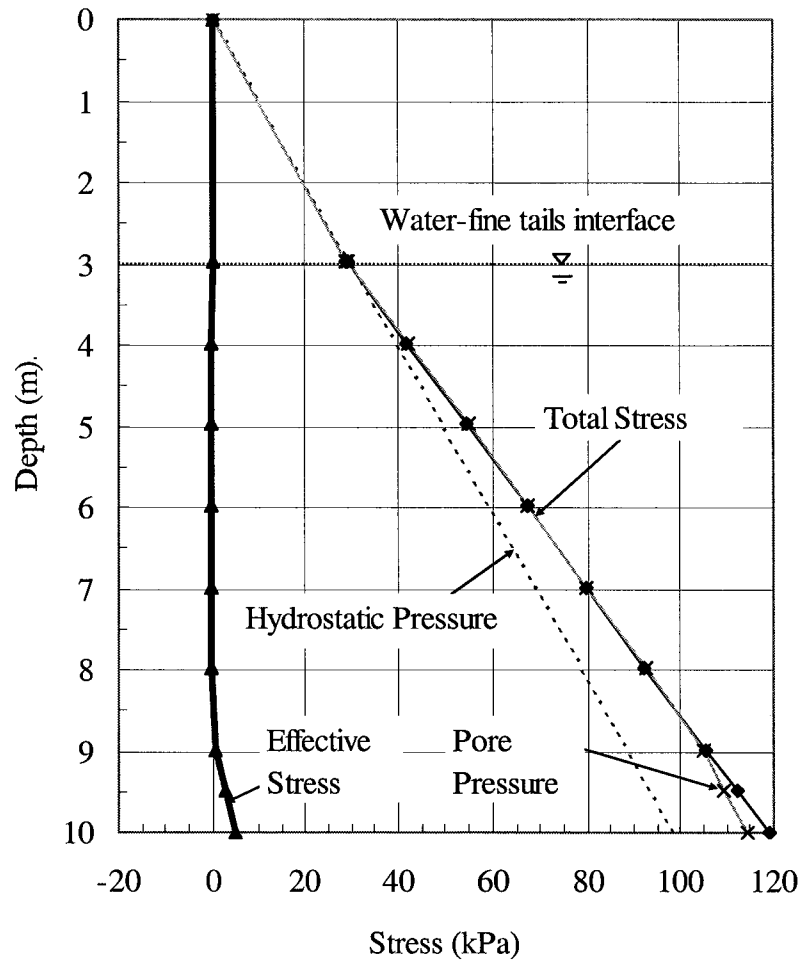


Figure 4.21 Total stress, pore pressure and effective stress profiles at 20.6 years

4.7 Scanning Electron Micrograph (SEM)

Studies on SEM images have shown that the fine tailings card-house floc structure is directly related to the pore water chemistry (Tang et al. 1997).

In Figures 4.22, 4.23 and 4.24 the card-house floc structure is clearly shown. At 9.5 m depth close to the bottom of the standpipe, the card-house structure is compressed while at the middle and at the top of the standpipe, the card-house structure is similar to that found in the tailings ponds (FTFC, 1995). Gas at the depth of 3.5 m was not discovered in any of the SEM images at this depth. The possibility of gas at this depth as indicated by the degree of saturation measurements must be very low and probably does not have a significant effect on settling behaviour.

An image analysis on the SEM micrographs has been performed based on a total of 60 images (20 images at each depth). These analyses are based on the blacking-in or out technique (Smart and Tovey, 1980) and the results are shown in Table 4.4.

Table 4.4 SEM image analysis results.

Depth (m)	Void ratio from density samples	Void ratio from image analysis	Average floc spacing (μm)
3.5	3.43	3.50	7.43
6.5	3.88	3.58	6.62
9.5	2.65	2.52	3.70

The void ratio values calculated from the image analysis show a close agreement with the sample measurements. The MFT in the major part of the standpipe has a card-house structure which is where creep occurs. The creep or slow bond yielding will have less effect when the soil particles approach a void ratio around 3. After this the creep will not significantly maintain the excess pore water pressure because the creep rate is much slower at lower void ratios (Figure 2.15). Therefore, further reduction in volume will be caused mainly by consolidation, that is, a decrease in excess pore water pressure or an increase in effective stress.

4.7.1 Energy dispersive X-Ray analysis

Energy dispersive X-Ray testing was performed on each SEM sample to evaluate the solids mineralogy. The results of this testing on SEM samples should be analyzed in conjunction with the mineralogy measurements in Section 4.12. The energy dispersive spectrometer with the SEM, however, only provides a qualitative analysis of the elements present. More thorough elemental analysis can be done but takes considerable more time and expertise. In addition, any elements with a lower atomic number than carbon are difficult to pick by for this method. Nevertheless the test is valuable and the results provide assurance of the sample mineralogy in Section 4.12.

Figures 4.25, 4.26 and 4.27 show the energy dispersive X-Ray analysis from the SEM for the mature fine tailings material at depths of 3.5 m, 6.5 m, and 9.5 m respectively. The electron beam in the SEM covers the entire photomicrograph viewed. Therefore the elemental analysis is an average of the mineralogy of all the particles in the photomicrograph. The traces in the figures show that there is little difference in mineralogy in the three depths investigated.

From Section 4.12, it is shown that the major mineral in the MFT samples is kaolinite (aluminum silicate hydroxide, $\text{Al}_4\text{Si}_4\text{O}_{10}(\text{OH})_8$) followed by quartz (silicon dioxide, SiO_2) and illite ($\text{KAl}_2(\text{OH})_2[\text{AlSi}_3(\text{O},\text{OH})_{10}]$). Figures 4.25, 4.26 and 4.27 show an aluminum: silica ratio of about 1:2. Kaolinite has this ratio equal to 1:1 and illite's ratio is about 1:2. The overall ratio of about 1:2 is the result of silica from quartz sand and quartz silt-size material contributing to the high silica reading. The small amount of potassium is likely from the illite and the trace of iron is probably from siderite (iron carbonate, FeCO_3). These elemental analyses agree with the mineralogy reported in Section 4.12.

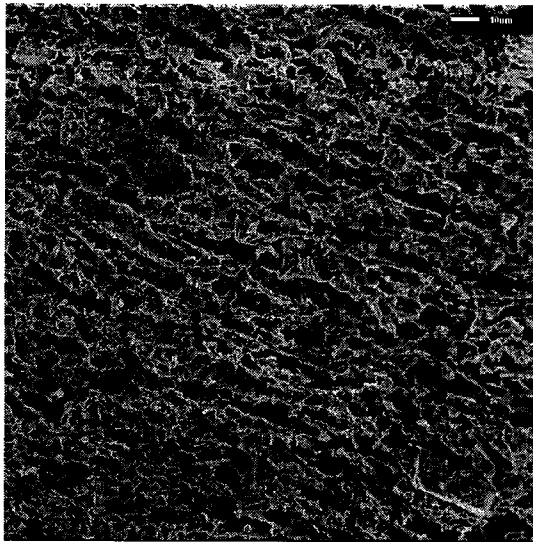


Figure 4.22 The fine tailings structure at 3.5 m depth (39.9% solids).

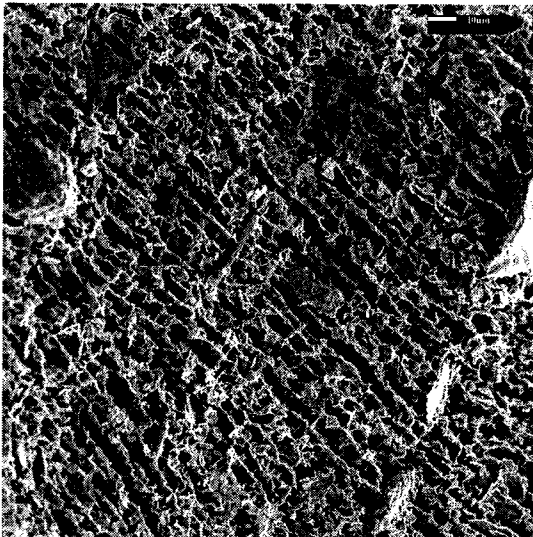


Figure 4.23 The fine tailings structure at 6.5 m depth (37.0% solids).

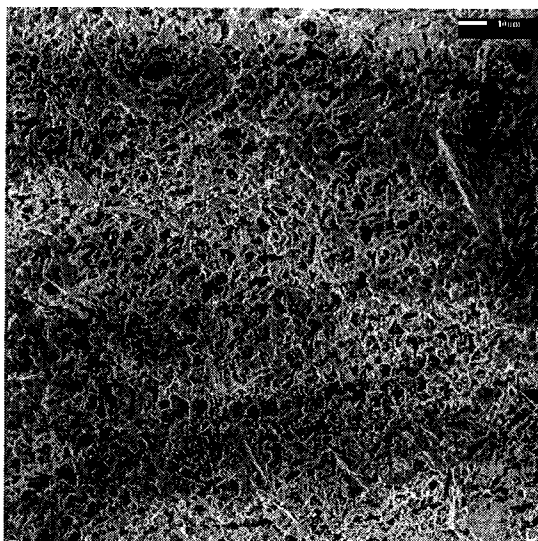


Figure 4.24 The fine tailings structure at 9.5 m depth (46.2% solids).

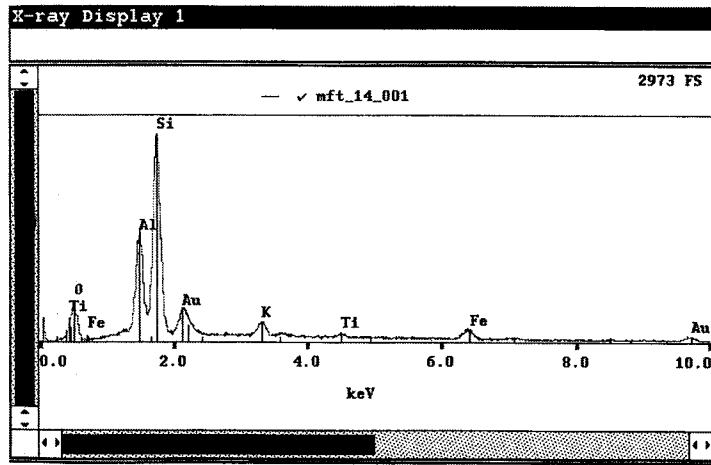


Figure 4.25 Energy dispersive X-Ray analysis at 3.5 m depth (39.9% solids).

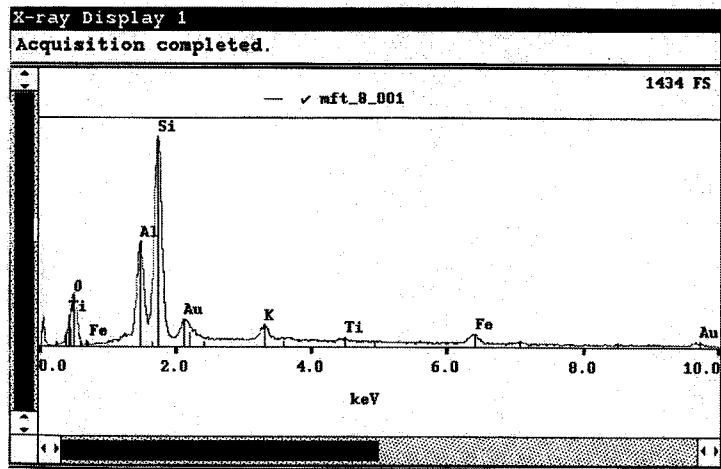


Figure 4.26 Energy dispersive X-Ray analysis at 6.5 m depth (39.9% solids).

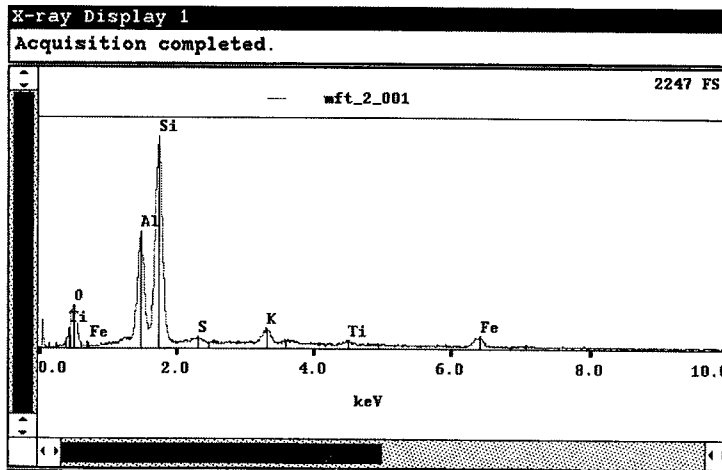


Figure 4.27 Energy dispersive X-Ray analysis at 9.5 m depth (39.9% solids).

4.8 Summary

The ten meter standpipe 1 test was commenced in 1982 at the University of Alberta to evaluate the long term consolidation behaviour of the mature fine tailings in the tailings ponds. By 2003, the MFT in the standpipe had settled 3 meters and the average void ratio had decreased from 5.18 to 3.34 but the pore pressures have remained approximately equal to the total stress.

The following observations and conclusions on the standpipe measurements have been reached.

1. Grain size distributions on samples from the full height of the standpipe were performed in 1985 and in 2003. The two sets of measurements were essentially the same indicating no change in grain size during this period.
2. Dispersed hydrometer tests and dispersed methylene blue tests agreed on the clay fraction amounts.
3. Particle size fraction profiles show that no segregation of coarse particles has occurred in the 1985 to 2003 period.
4. The clay-sized ($<2 \mu\text{m}$) minerals in the MFT are entirely kaolinite and illite in approximately equal amounts. Some of the kaolinite is in the form of aggregates and booklets which have a large particle size and appear as silt-size ($45 \mu\text{m} - 2 \mu\text{m}$) particles.
5. It has been concluded that the repulsive and attractive forces between the clay particles dominate the behaviour of the fine tailings-water structure and that the electro-kinetic behaviour is mainly caused by the presence of sodium and bicarbonate ions in the tailings water. Chemical analysis of the mature fine tailings pore water samples shows the significant presence of bicarbonate and sodium ions. Conductivity and pH measurements in 2000 show values similar to those in the Syncrude and Suncor tailings ponds measured in 1992 which indicate that no significant changes in water chemistry in the standpipe have occurred during this period.

6. The lack of methanogens in the MFT indicates gas generation should be negligible and no gas bubbles have been observed in the standpipe. Measurements in 2003 indicate the potential for microbial activity which produces gas at the surface of the MFT.
7. The bitumen content of the MFT in Standpipe 1 is slightly higher at 3% of the total mass than the present bitumen content in the tailings ponds.
8. The specific gravity of the MFT solids is 2.28. This low specific gravity is caused by the amount of bitumen attached to the fine mineral particles.
9. The liquid limit of the MFT ranges from 46% to 52% and the plasticity index from 25% to 31%.
10. There does not appear to have been a significant change in the index properties of the MFT during the 21 years of the standpipe operation.
11. MFT which is predominately kaolinite exhibits a very high thixotropic gain in strength. This is caused by the addition of dispersing agent during extraction process and the presence of bicarbonates and bitumen.
12. MFT at solids contents of 33% and 40% has overconsolidation stresses of 2.9 kPa and 8.8 kPa respectively because of thixotropy. Therefore fine tailings deposits at these solid contents must have vertical effective stresses greater than these amounts for significant consolidation to take place. Settlement that takes place at lower effective stresses must be mainly caused by creep phenomenon.
13. The interface settlement measurements during the past 21 years show that the settlement of the fine tailings has reached approximately 3.0 m and has settled at a uniform rate during the last 10 years.
14. The solids content in the 10 m standpipe is increasing fairly uniformly with depth and only the bottom meter appears to be consolidating. The average solids content has increased from 30.6% to 40.6% during the 21 years.
15. The bulk densities measured by the density sampler and solids content sampler are similar because the degree of saturation is close to 100%.
16. Pore water pressure measurements in the standpipe have shown that the settlement and decrease in void ratio are not due to consolidation but are a creep phenomenon at a constant effective stress of zero.

17. SEM micrographs of the MFT from various depths clearly show the card-house structure typical of MFT in the tailings ponds. At the 9.5 m depth, the card-house structure is compressed.

Monitoring of the large scale self-weight consolidation test of mature fine tailings in Standpipe 1 will be continued for further evaluation of the compression behaviour of this class of materials. The 21 years of measurements show that the standpipe instrumentation performs with no problems and the fine tailings are still undergoing compression with approximately zero effective stress

5. Ten Meter Standpipe 2 Measurements

Ten meter standpipe 2 contains 6.57 m³ of a slurry of mature fine tailings and tailings sand whose general properties have been shown in Table 3.2. This MFT-tailings sand mix was performed to investigate the effect of sand on the consolidation behaviour or, in other words, to study the effect of a large increase in density on consolidation. Since the consolidation stress is self-weight, the added sand is added density and this should increase the rate and magnitude of consolidation. The Standpipe 2 test was started on November 4th, 1982 and stopped on October 9th, 1984. During the 708 days of operation, Standpipe 2 provided information on the consolidation behaviour of a MFT-tailings sand mix.

In this chapter, measurements taken on the MFT-tailings sand mix in the ten meter standpipe 2 are shown. The measurements include index properties, settlement of the interface, solids content, bulk density and pore water pressure.

5.1 Material Index Properties

In this section, a description of the index properties are presented and a discussion on how these fundamental properties have an influence on the compressibility and permeability of the material is given. Due to the bitumen in the mix, the measurements of the index properties for this class of material are partly modified from the standard geotechnical measurements in order to be able to capture the most reasonable measured values.

5.1.1 Grain size distribution

For the MFT-tailings sand mix in Standpipe 2, the total solids contained 48% sand. In Figure 5.1 the particle size distribution of the fine tailings-sand mix shows that there is 18% clay-size (< 2 µm), 34% silt-size (2 µm – 45 µm) and 48% sand (> 45 µm).

Particle size analysis for this material was expected to be less difficult compared to the mature fine tailings installed in Standpipe 1 because of a lower bitumen content

and higher sand content. However it is recommended to follow the procedures suggested in Section 4.1.1. for dispersed and nondispersed particle size analysis.

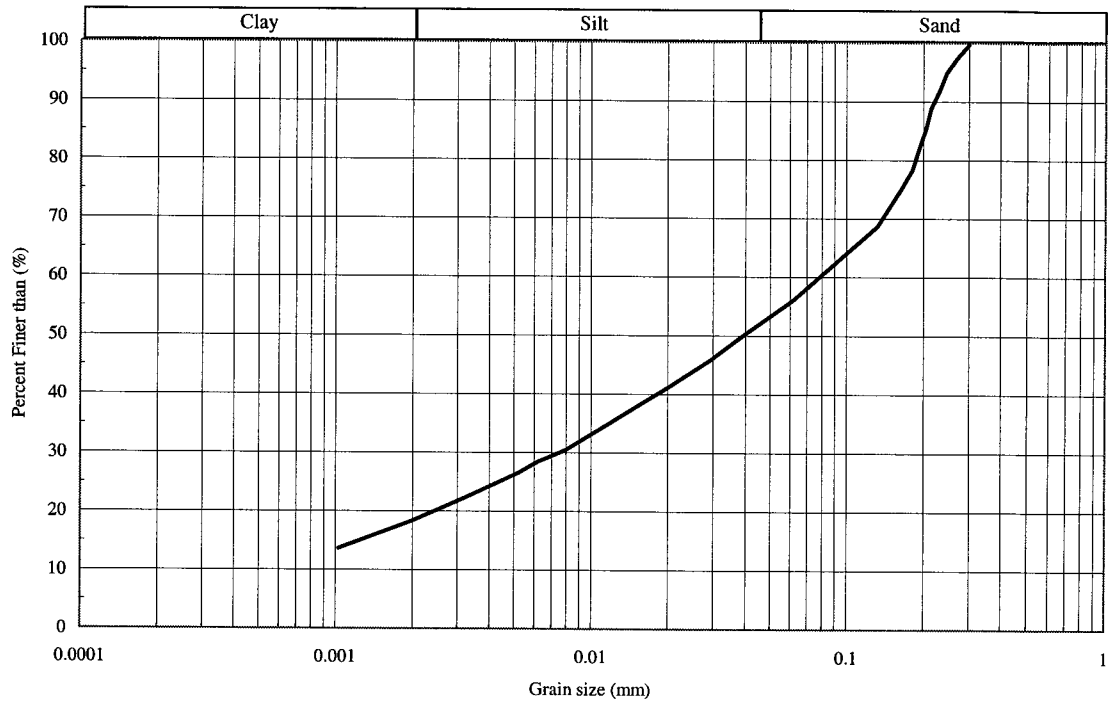


Figure 5.1 Particle size distribution of MFT-tailings sand mix in Standpipe 2

5.1.2 Mineralogy

For the MFT-tailings sand mix in Standpipe 2, there was no X-Ray diffraction analysis performed on the material. As a result, in this section, mineral compositions of the material are calculated from available data on the mature fine tailings by adding sand up to 48% into the mix and assuming that all sands are quartz or other rock forming minerals.

According to Bulk and clay X-Ray diffraction analyses performed on the mature fine tailing samples from Standpipe 1 in Table 4.1 and by using 48% of sand from the particle size analysis in Figure 5.1, the mineralogy of the MFT-tailings sand mix can be approximated and is shown in Table 5.1. It appears that the major mineralogy of the fine tailings is generally quartz followed by kaolinite and illite respectively. The clay-size material is equal amounts of kaolinite and illite. One-third of the silt-size material is large aggregates or booklets of kaolinite.

Table 5.1 Major minerals of the MFT-tailings sand mix in Standpipe 2

Mineral (%)	Sand-size (>45 µm)	Silt-size (2 µm-45 µm)	Clay-size (<2 µm)	Total minerals in mineral category
Quartz and other minerals	48	17	0	65
Kaolinite	0	8	14	22
Illite	0	0	13	13
Total minerals in size	48	24	28	100

5.1.3 Bitumen content and specific gravity

With the addition of sand, the bitumen content was reduced and measured to be 2.5% by total mass and 5.6% by dry mass and the specific gravity was 2.44 (Table 3.2). The lower bitumen content and higher sand content of the mix made the material have a higher specific gravity, which affected the self-weight consolidation behaviour of this material.

5.2 Interface Measurements

Interface settlement or tailings-water interface settlement in the ten meter standpipe shows the settling behaviour of this material with time. It was measured frequently to determine the amount of settlement of the MFT-tailings sand mix in Standpipe 2.

A surface zone of varying density was formed in the standpipe and was termed a transition zone. This zone was not found until after 48 days when the interface had settled and the density measured at the top port indicated a lower density than the initial density. This zone made accurate measuring of the tailings-water interface difficult and direct measurement was abandoned. The zone had solids contents lower than the initial solids content (45% solids). This zone and its settlement are shown in Figure 5.2. The zone had a thickness of about 30 to 40 cm.

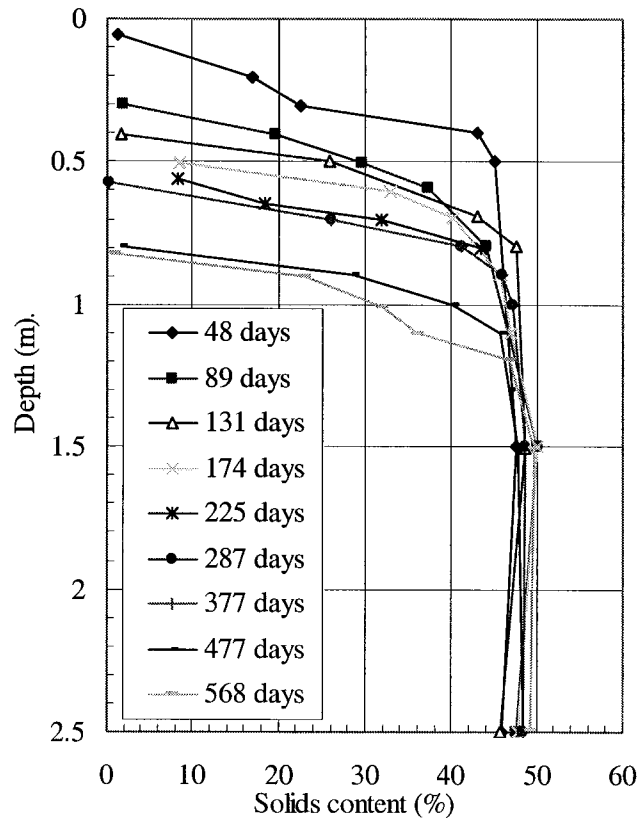


Figure 5.2 Transition zone at the top of Standpipe 2

This transition zone led to the question of where the interface has to be plotted. The interface settlements of the transition zone are plotted in Figure 5.3. This transition zone was likely formed by segregation when fines were washed to the top during the filling process.

From measurements of solids content (Figure 5.2) and fines content (Figure 5.4) in the transition zone, there is a variation of the sand in this zone as the fines content varies from about 95% to 65% from top to bottom. During the removal of the material at the end of the test, there was an approximately 2.5 cm thick layer of bitumen located at some depth within the transition zone. This indicated that there was a migration of bitumen to the top of the standpipe and this might have led to a layering problem or nonhomogeneous material in the standpipe. This layering might have changed the hydraulic conductivity as well as the bulk density of the material at some locations. However, as it was only in the top 30 cm to 40 cm of the standpipe, its effect on the rate and amount of settlement and the pore pressure dissipation would be small.

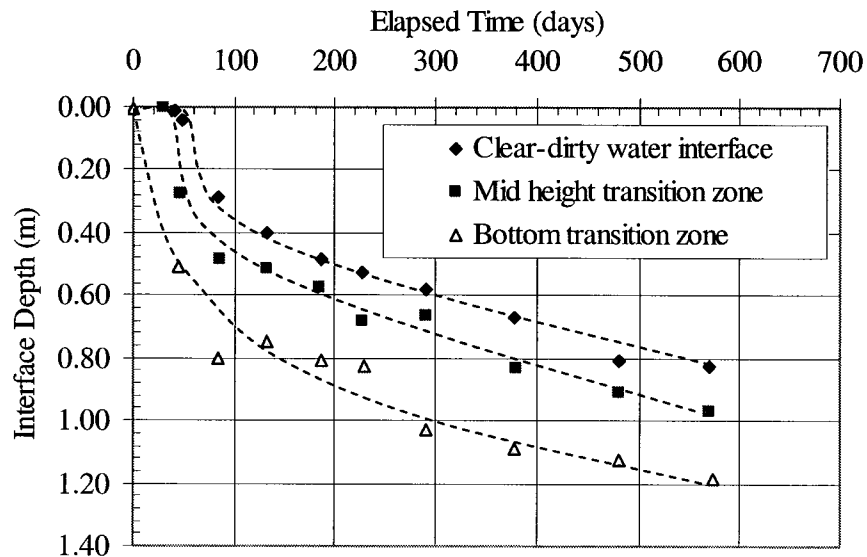


Figure 5.3 Interface settlement of the transition zone

It was concluded that the settlement measurement, however, should use the top clear-dirty water interface to indicate interface settlement as it is indicating the whole

self-weight consolidation. Therefore, these interface settlement measurements are plotted in Figures 5.6 and 5.7 with arithmetic scale time and log scale time respectively.

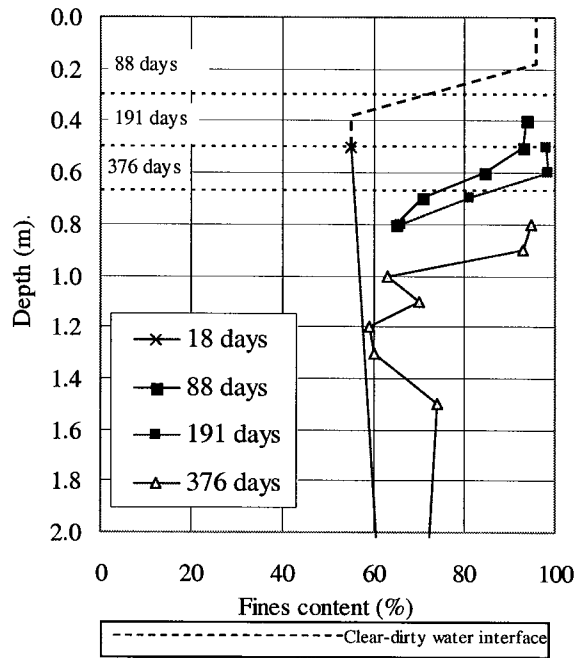


Figure 5.4 Fines content profile in the top 2 meters

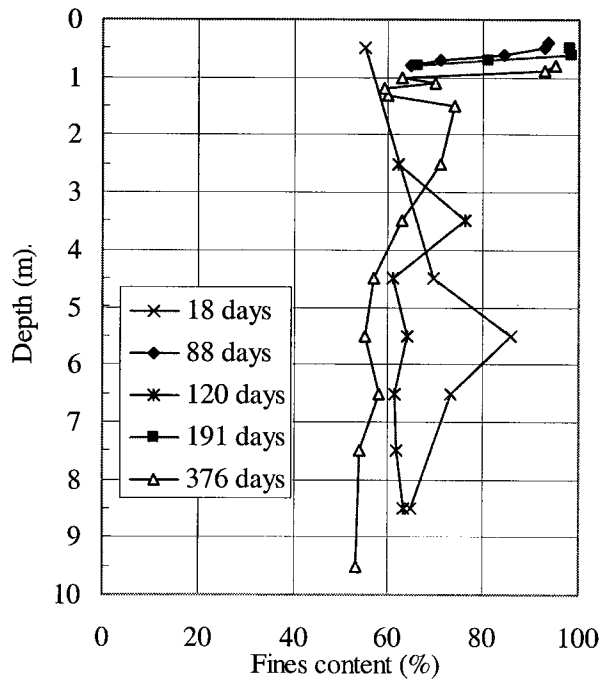


Figure 5.5 Fines content profile of Standpipe 2

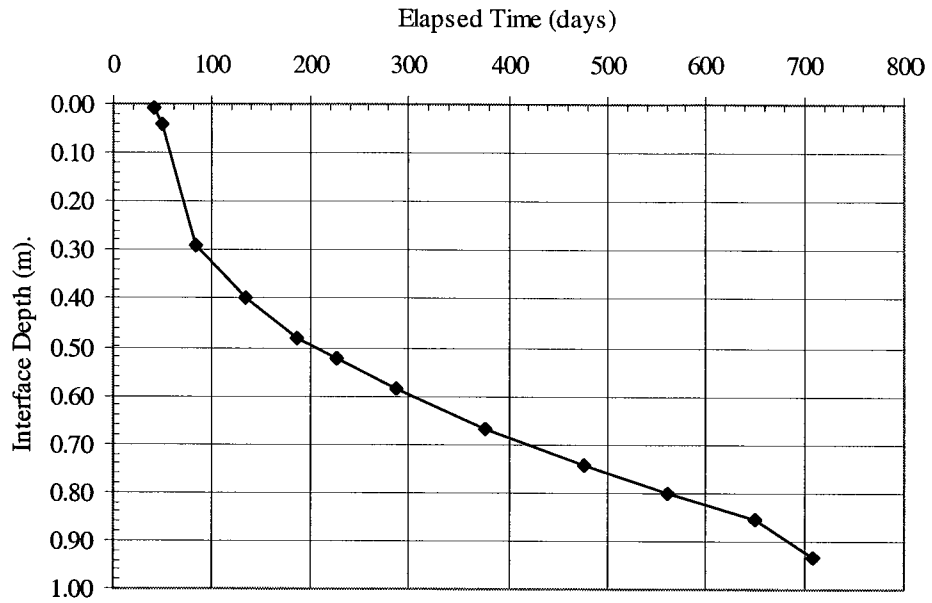


Figure 5.6 Interface measurement with arithmetic time

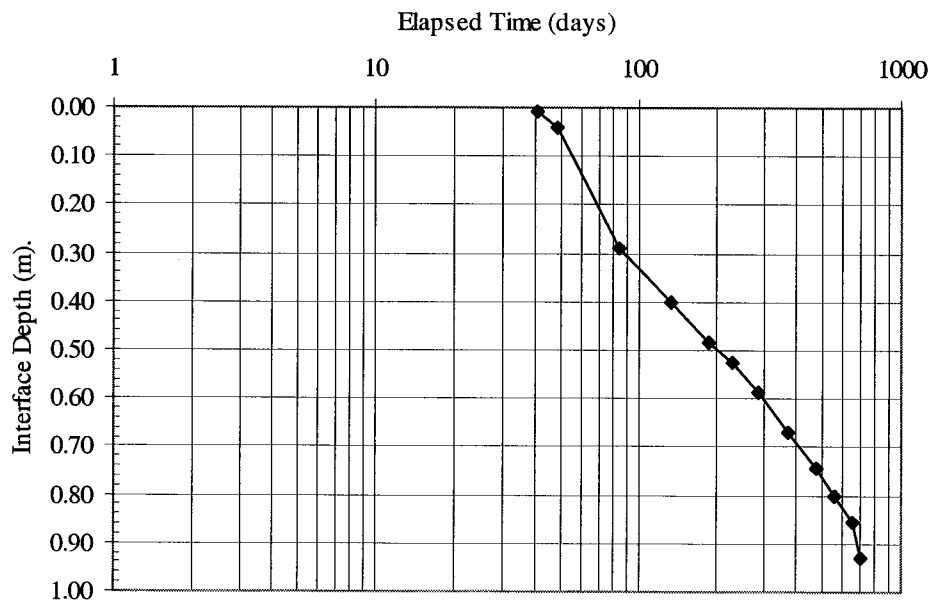


Figure 5.7 Interface measurement with log time

The interface settlement during the approximately 2 year operational period of Standpipe 2 shows that the settlement of the MFT-tailings sand mix reached 0.93 m which is about 1.6 times greater than the interface settlement of the mature fine tailings in Standpipe 1 (about 0.57 m for the same elapsed time).

A discrete change in settlement was found at about 80 days (Figures 5.6 and 5.7). Although the cause for this change in rate remains unknown, Scott and Chichak (1985b) postulated that it was related to the sand segregation which was present in the top 30 cm for the first two days of the test. Since the MFT-tailings sand mix initial solids content is so close to the segregation boundary as shown in Figure 3.2, coarse sand particles settling through the fines matrix may have opened drainage channels and these may not have been shut off until enough settlement had occurred.

5.3 Solids Content Measurements

Solids content was determined by oven drying samples of the MFT-tailings sand mix at 105 °C for 24 hours and the method of solids content sampling for the ten meter standpipe is presented in Chapter 3.

Solids content profiles are shown in Figure 5.8. The average solids content increased from its initial value of 45% to its 2 year value of 48.3% (void ratio 2.98 and 2.61 respectively). Increasing of solids in the bottom third of the standpipe was suspected to be caused by segregation of sand particles from the middle third of the standpipe. Increasing of the solids content in the top third of the standpipe may have been caused by settling sand at the surface opening up drainage channels resulting in consolidation. Figure 5.3 shows a small effective stress at this location.

5.4 Bulk Density Measurements

The solids content sampler mentioned in Section 3.4.1.1 was used in all the solids content measurements for Standpipe 2. By assuming that the degree of saturation is 100%, it allows the slurry bulk density to be calculated. Calculated bulk density is then used to calculate total stresses which are shown in the next section with pore water pressure measurements.

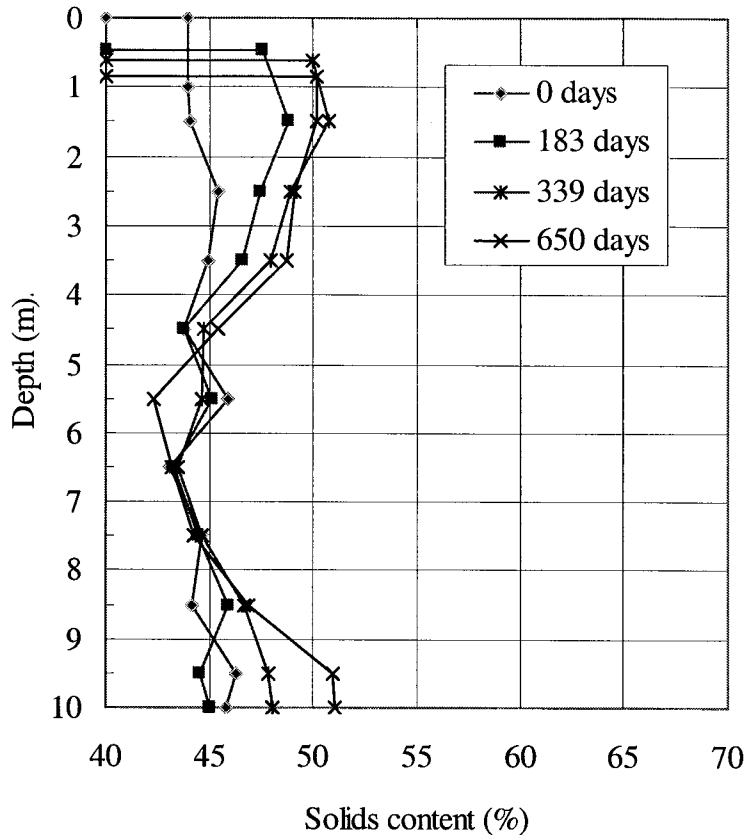


Figure 5.8 Solids content profiles of MFT-tailings sand mix in Standpipe 2

5.5 Pore Water Pressure Measurements

Pore water pressures are measured at the piezometer ports usually at 1 m intervals. A pore pressure transducer is calibrated with a riser tube every time measurements are taken. Details on measuring pore water pressure can be found in Section 3.4.2.

The initial excess pore water pressure measurements (Figure 5.9) show similar behaviour to the mature fine tailings in Standpipe 1. These measurements indicated a rapid drop in excess pore water pressure with almost no settlement caused by thixotropic gain in strength and a slight increase in excess pore water pressure immediately afterward due to creep compression. However, in this MFT-tailings sand mix, the increase in excess pore water pressure is not as obvious as in the mature fine tailings. This implies that the creep mechanism might be affected by sand content as well as by channeling from sand segregation.

Figures 5.10, 5.11, 5.12 and 5.13 show total stresses, effective stresses and pore pressures at 0 days, 183 days, 339 days and 650 days respectively. Pore water pressure measurements show that the pore pressure remains very high and close to the total stress. The effective stresses as shown are very low to no effective stress. The effective stress appears to occur where segregation of sand has taken place. The average void ratio at 650 days is about 2.61. From 0 to 650 days, there was little significant effective stress at the bottom or at any specific location while the interface had settled about 93 cm. It appears that creep compression took place in this material similar as in the mature fine tailings in Standpipe 1.

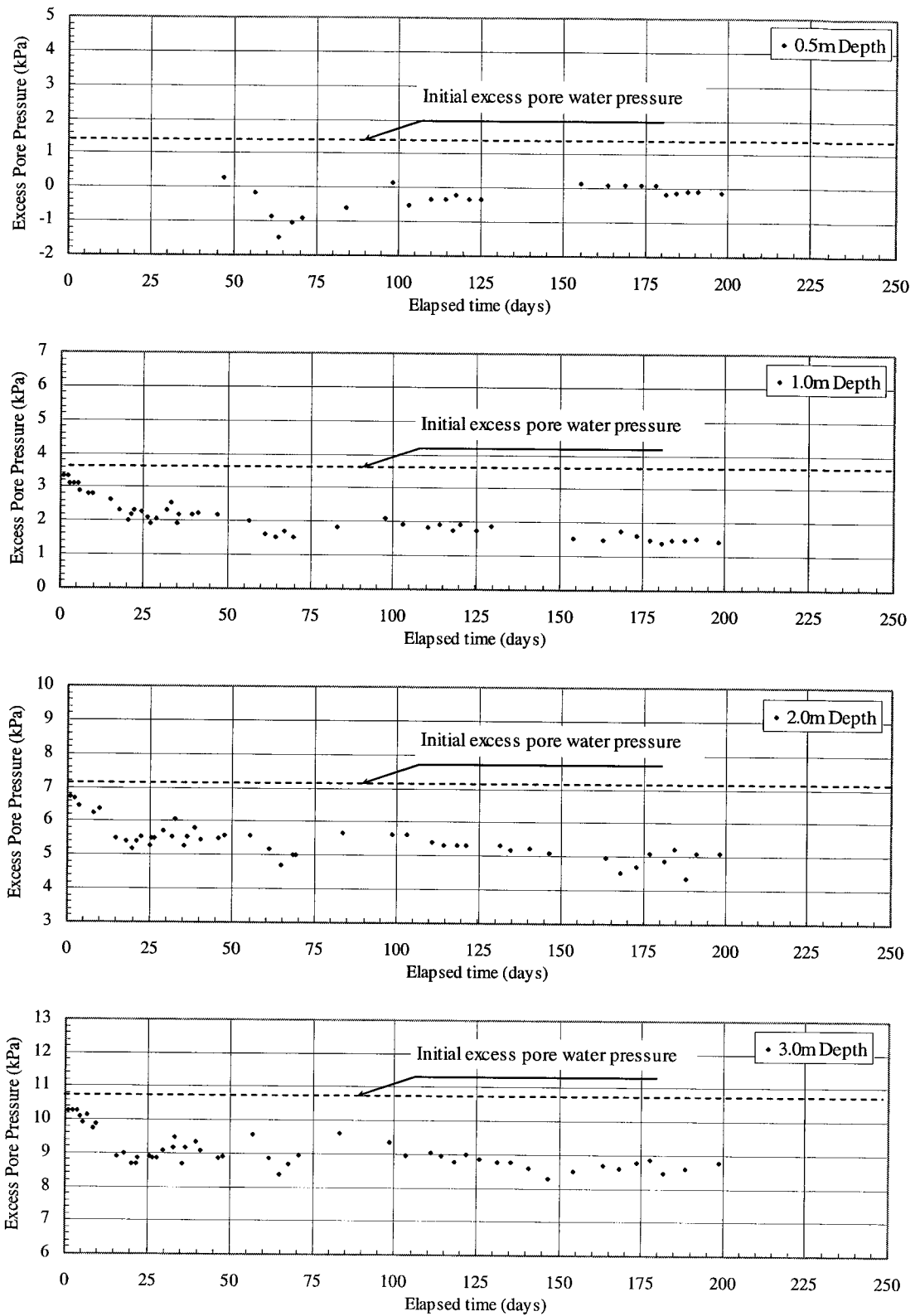


Figure 5.9 Initial excess pore water pressure measurements

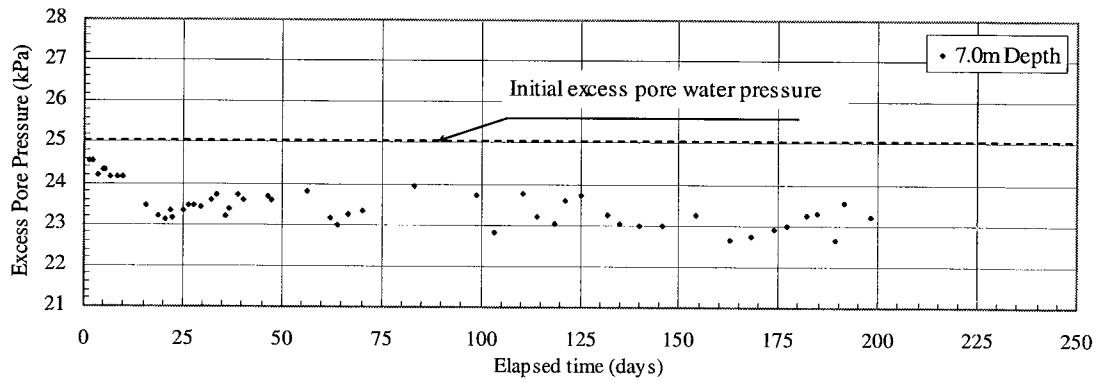
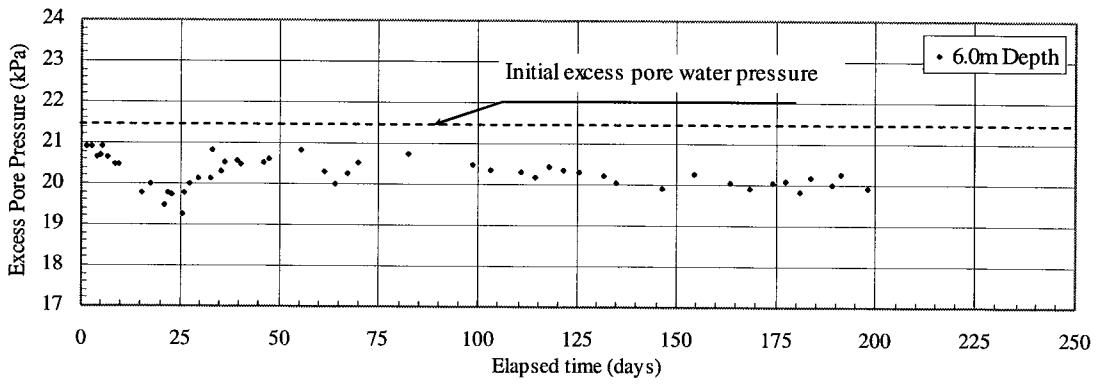
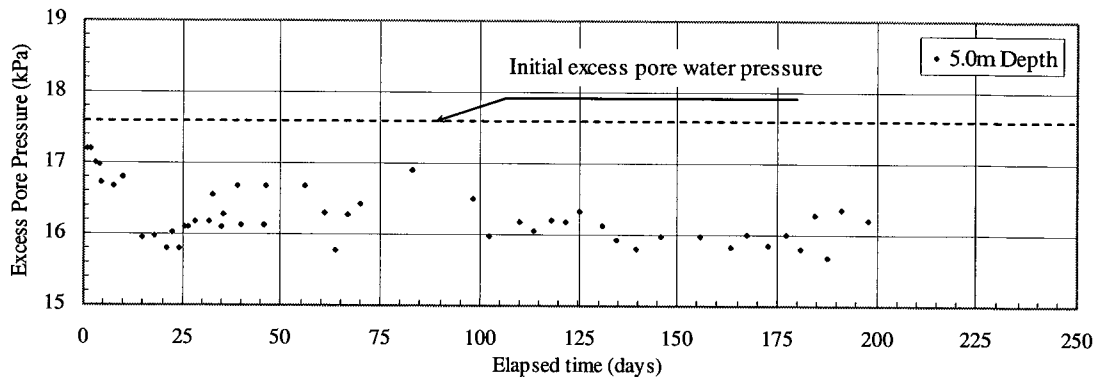
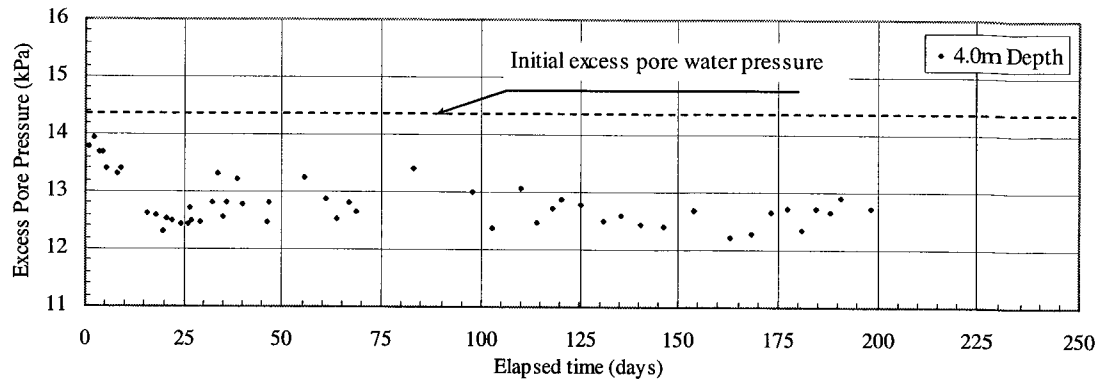


Figure 5.9 Initial excess pore water pressure measurements(continued)

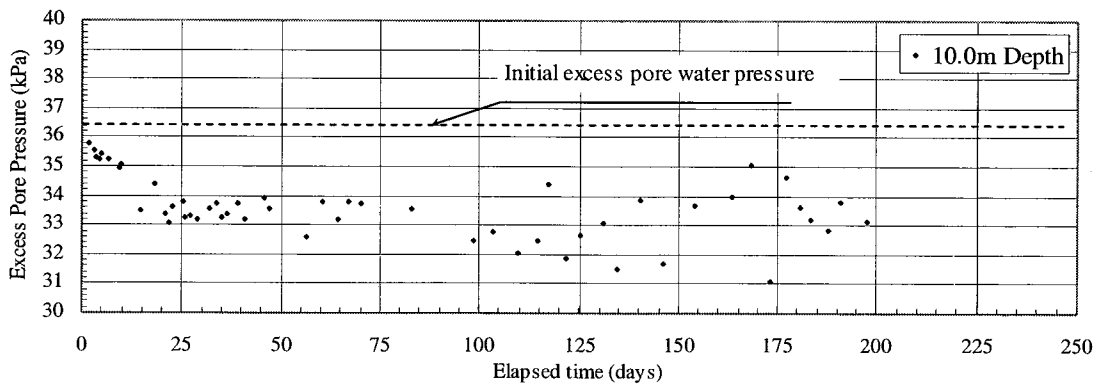
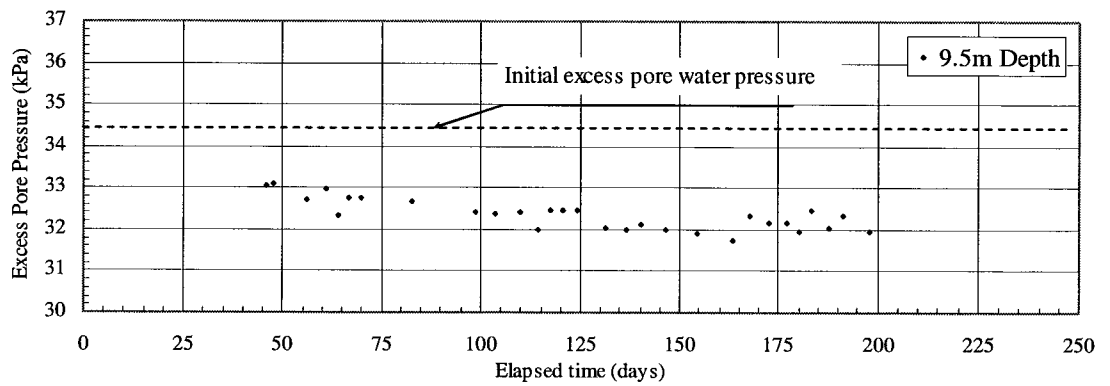
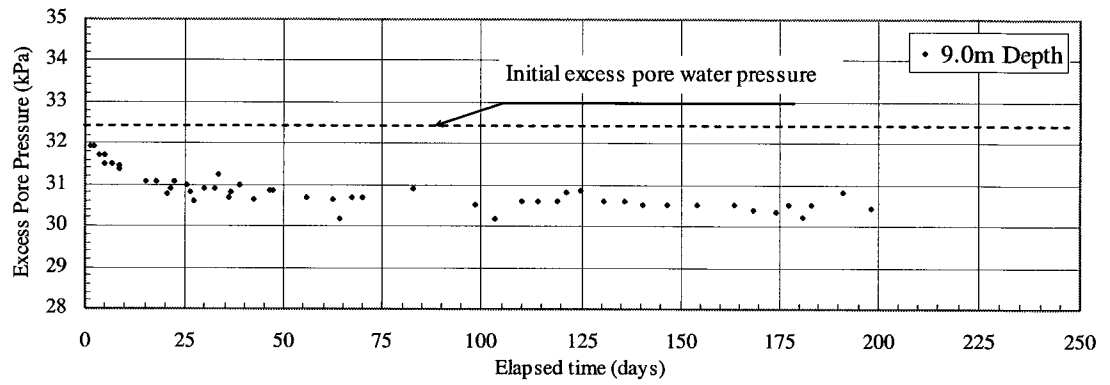
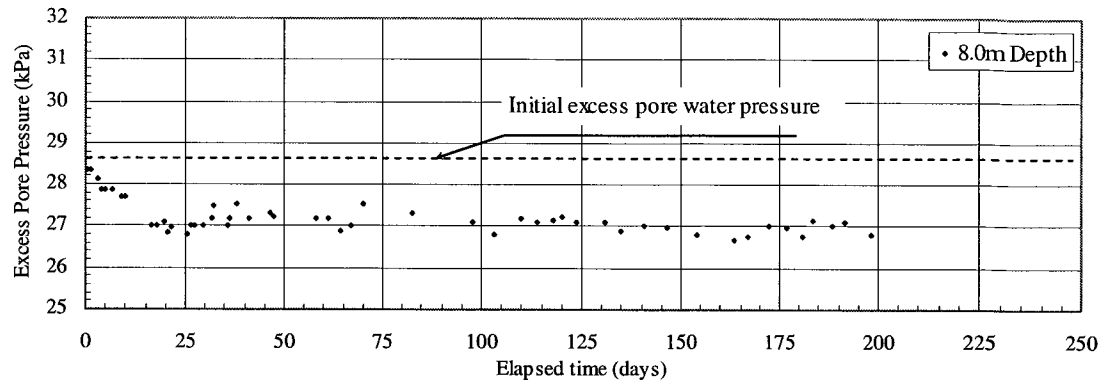


Figure 5.9 Initial excess pore water pressure measurements(continued)

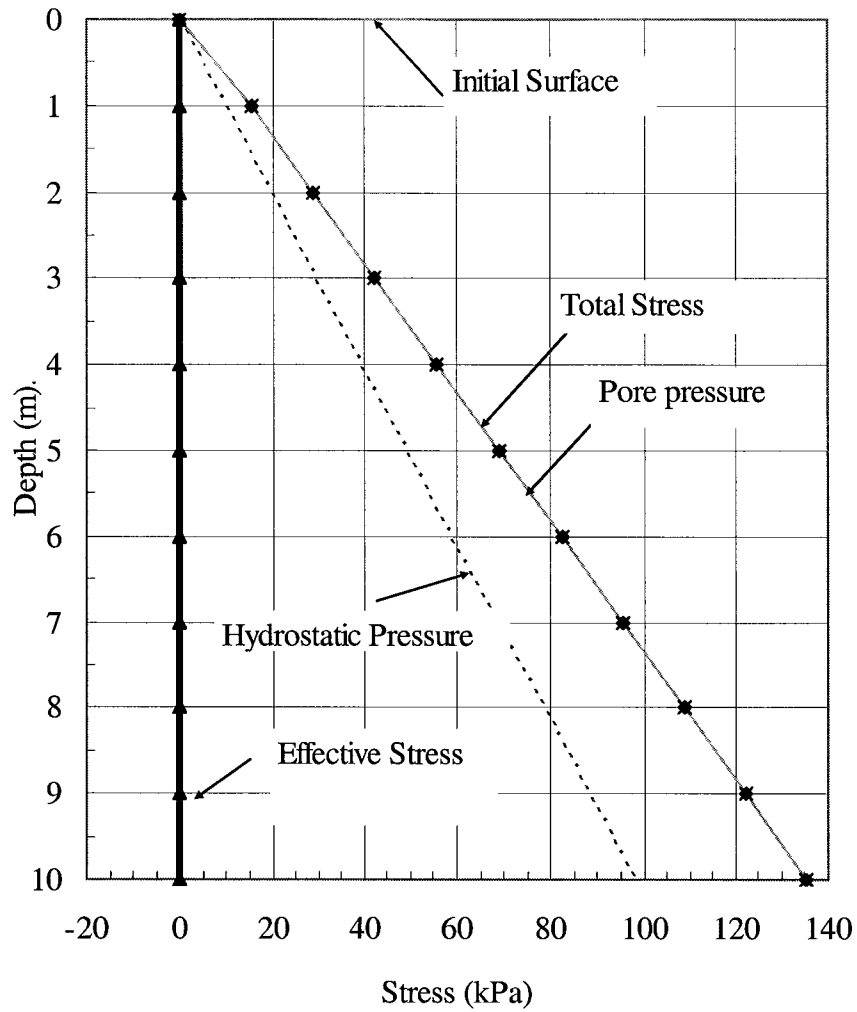


Figure 5.10 Total stress, pore pressure and effective stress profiles at 0 day

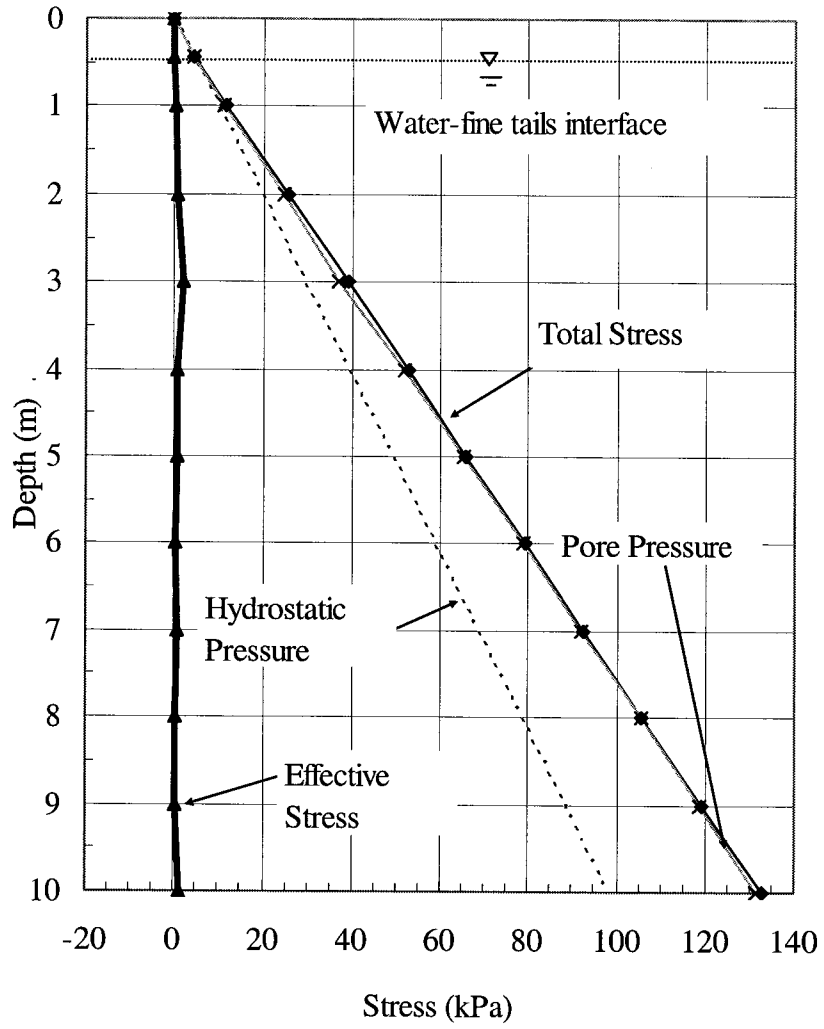


Figure 5.11 Total stress, pore pressure and effective stress profiles at 183 days

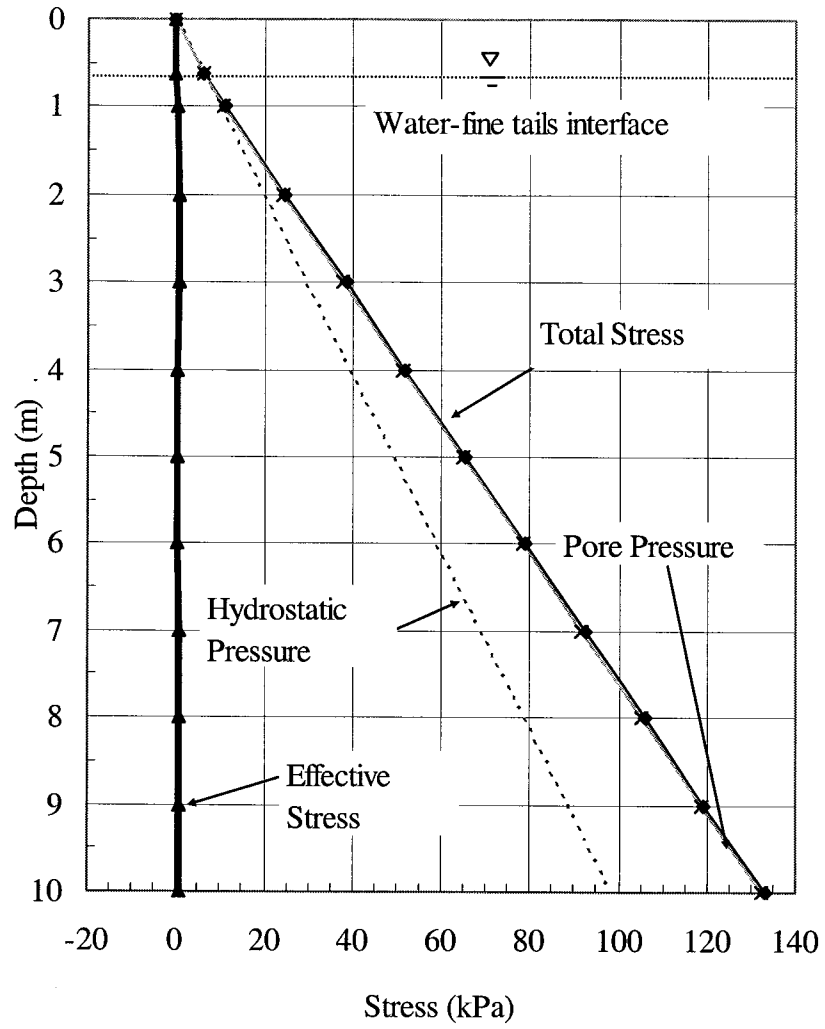


Figure 5.12 Total stress, pore pressure and effective stress profiles at 339 days

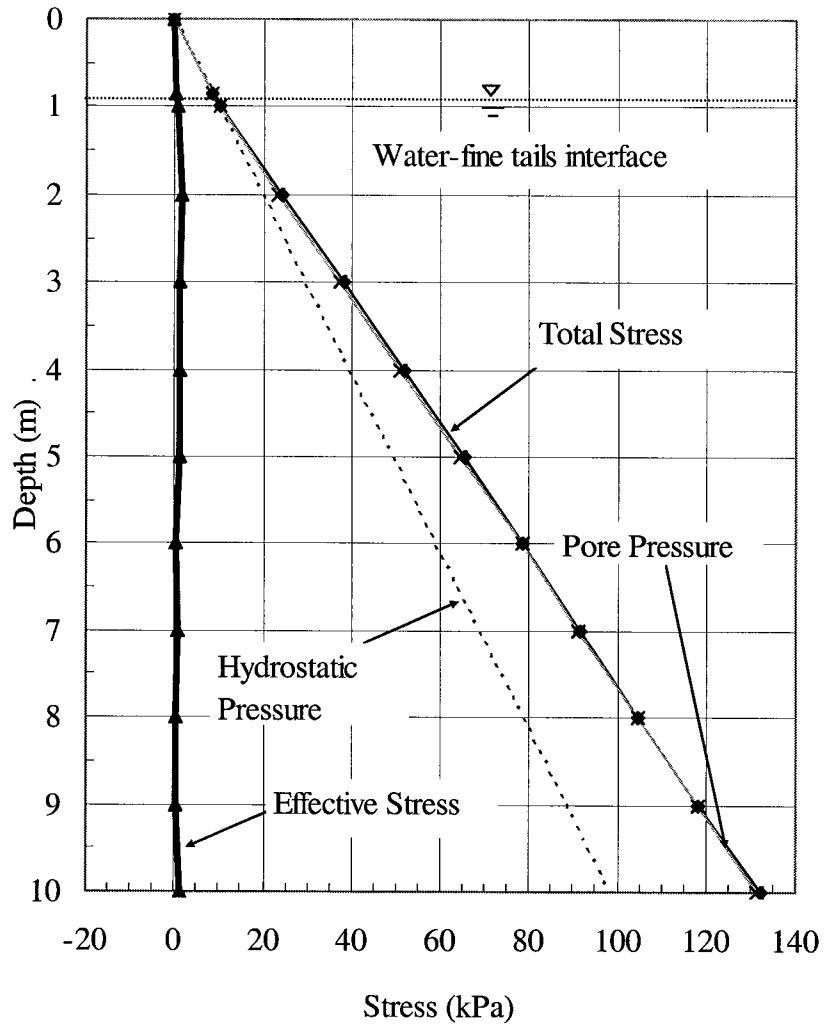


Figure 5.13 Total stress, pore pressure and effective stress profiles at 650 days

5.6 Summary

Standpipe test 2 was conducted to investigate the effect of additional sand on consolidation behaviour of mature fine tailings. The test was continued for only 2 years as its progress was similar to Standpipe 1 and potential field applications would use more sand. The test, however, provided valuable information on the consolidation behaviour of this MFT-tailings sand mix.

When sand is added into the slurry, the creep mechanism and thixotropic properties of mature fine tailings will still be there. This is because the additional sand is only floating in the fines matrix and has little to do with the interparticle action of the fines. The thixotropic strength of the fine tailings results in the soil structure being overconsolidated and pore pressure dissipation will not significantly occur until effective stresses are sufficient to shear the interparticle bonds. Meanwhile, submerged self-weight stresses are sufficient to result in slow yielding of inter particle bonds or creep. The creep maintains the excess pore pressure and results in settlement under zero effective stress.

The following observations and conclusions on the standpipe measurements have been reached.

1. Standpipe 2 contained a MFT-tailings sand mix with an initial solids content of 45% that was 18% clay-size, 34% silt-size and 48% sand.
2. The major minerals in the standpipe mix are 65% quartz and other rock forming minerals and 35% clay minerals. The clay-size material contains equal amounts of kaolinite and illite. One third of the silt-size material is large aggregates or booklets of kaolinite.
3. The bitumen content of the mix was 2.5% of the total mass and the specific gravity of the solids was 2.44.
4. The interface settlement during the approximately two year operational period of Standpipe 2 was 0.93 m which was about 1.6 times greater than that in Standpipe 1 for the same elapsed time.

5. The average solids content increased from its initial value of 45% to its 2 year value of 48.3%.
6. Solids content and fines content profiles showed possible sand segregation from the middle third of the standpipe to the lower third and an increase in solids in the top third of the standpipe possibly from consolidation.
7. Excess pore water measurements show there was little significant effective stress in the standpipe after 650 days. It appears that creep compression took place in this MFT-tailings sand mix similar as in the mature fine tailings in Standpipe 1.

The effect of addition of sand appears to be only increasing bulk density of the material which does have a role in self-weight consolidation. Therefore by adding sand to mature fine tailings and using a mix design so there will be no segregation, the MFT-tailings sand mix will consolidate faster and more than the consolidation of the mature fine tailings.

6. Ten Meter Standpipe 3 Measurements

Ten meter standpipe 3 contains 6.57 m^3 of mature fine tailings mixed with tailings sand whose general properties have been shown in Table 3.2. This standpipe test containing a MFT-tailings sand mix with 82% sand was performed to investigate the effect of sand on the consolidation behaviour of MFT similar to Standpipe 2. The sand content of 82% by mass of solids or about 42% sand by total volume was chosen to be a MFT-tailings sand mix which would consolidate to a sufficient density in a reasonable length of time and may be technically and economically better than other MFT-tailings sand mixes (Scott and Dusseault, 1981). This sand content of 82% by mass of solids resulted in a mix with a solids content of 74.8% by total mass (Table 3.2).

The ten meter standpipe 3 test was started on November 30th, 1984 and its last measurement was made on February 20th, 1997 when consolidation appeared to be completed. During the 12.2 years of operation, Standpipe 3 has provided good data on the settling behaviour of this MFT-tailings sand mix. In this chapter, measurements taken on the tailings in the standpipe and on the standpipe settlement behaviour are shown. The measurements included index properties, settlement of the interface, solids contents and pore water pressures.

6.1 Material Index Properties

The material properties of the fine tailings-sand mix in Standpipe 3 are quite different from the material in Standpipe 2 due to the much greater amount of added sand. In this section, a description of the physical characteristics of the material with reference to the index properties is presented. How these fundamental properties have an influence on the compressibility and permeability of the material are discussed. Due to the bitumen in the mix, tests to determine the index properties of this class of material are partly modified from the standard geotechnical measurements.

6.1.1 Grain size distribution

In Figure 6.1 the particle size distribution of the fine tailings-sand mix shows that there is 5% clay-size ($<2 \mu\text{m}$), 13% silt-size ($2 \mu\text{m} - 45 \mu\text{m}$) and 82% sand ($>45 \mu\text{m}$).

Particle size analysis on this material was less difficult compared to the mature fine tailings installed in Standpipe 1 because of the lower bitumen content and higher sand content. However it is recommended to follow the procedures given in the Section 4.1.1.

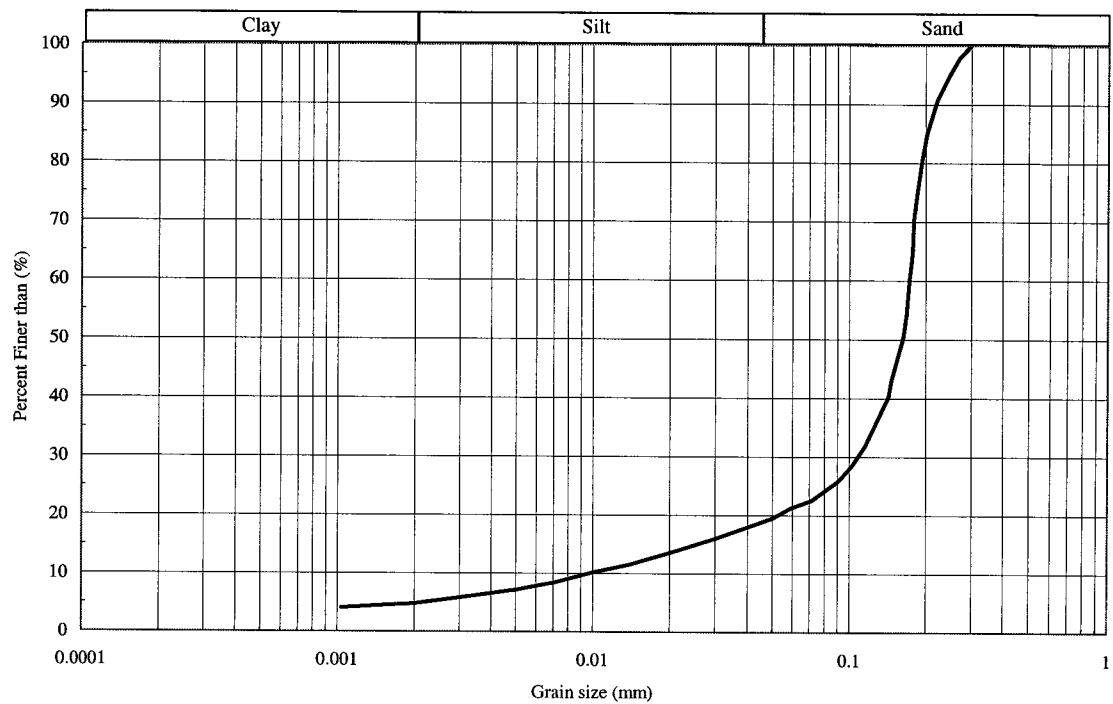


Figure 6.1 Particle size distribution of MFT-tailings sand mix in Standpipe 3

6.1.2 Mineralogy

Similar as for Standpipe 2 tailings, there was no X-Ray diffraction analysis done on the material in Standpipe 3. As a result, the mineral composition of the material is calculated from available mineralogy data on the mature fine tailings by adding sand up to 82% into the mix and assuming that all sand is quartz or other rock forming minerals.

From the bulk and clay X-Ray diffraction analyses performed on the mature fine tailings given in Table 4.1 and by adding 82% of quartz sand, the mineralogy of the MFT-tailings sand mix in Standpipe 3 can be approximated and is shown in Table 6.1. It appears that the major mineralogy of the fine tailings-sand mix is generally quartz followed by kaolinite and illite respectively. The clay-size material is composed of equal amounts of kaolinite and illite and large aggregates or booklets of kaolinite make up one-third of the silt-size material. From the ternary diagram in Figure 3.2, the material is close to the sand structure boundary.

Table 6.1 Major minerals of the MFT-tailings sand mix in Standpipe 3

Mineral (%)	Sand-size (>45 µm)	Silt-size (2 µm-45 µm)	Clay-size (<2 µm)	Total minerals in mineral category
Quartz and other minerals	82	5	0	87
Kaolinite	0	3	5	8
Illite	0	0	5	5
Total minerals in size	82	8	10	100

6.1.3 Bitumen content and specific gravity

With 82% sand by total weight of solids, the bitumen content is 1.2% by total mass and 1.6% by dry mass of solids. The specific gravity of the mix in Standpipe 3 is 2.58 as shown in Table 3.2. The much lower bitumen content and higher sand content of the mix gave the material a higher specific gravity which will affect the self-weight consolidation behaviour of this material.

6.2 Interface Measurements

The first 100 days of the interface settlement in Standpipe 3 is shown in Figure 6.2 to examine the initial performance of the material for signs of thixotropy and creep as was seen in Standpipe 1 and to a lesser extent in Standpipe 2. At about 20 days there is a change in settlement rate to a slightly faster rate but other anomalies can not be observed. Other variations appear to be experimental error.

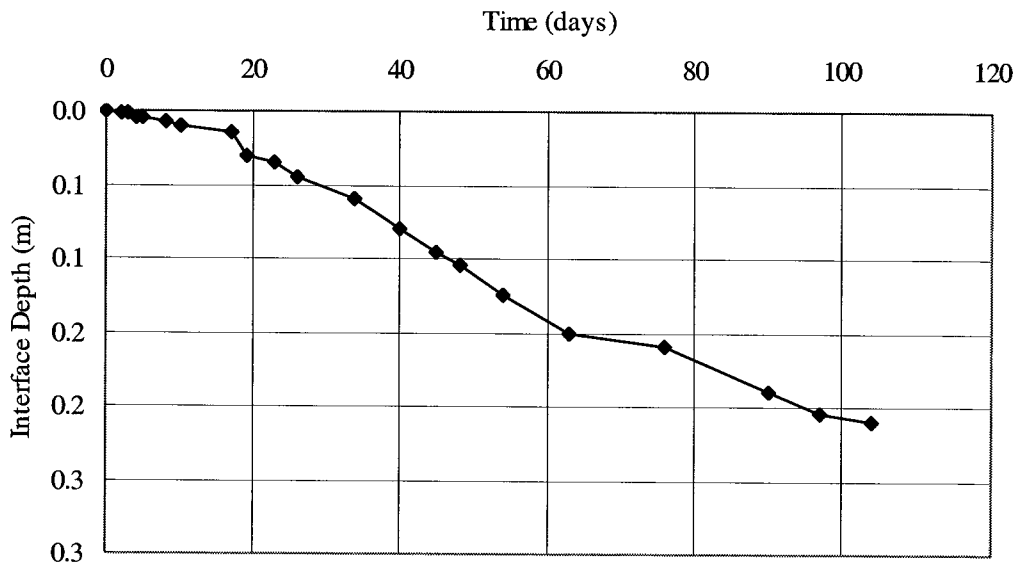


Figure 6.2 Initial interface measurement with time (100 day period)

The full interface settlement history of Standpipe 3 is shown in Figures 6.3 and 6.4 for arithmetic time scale and log time scale respectively. Both plots show typical settlement patterns for a consolidating material. The interface settlement ceased rather abruptly at a depth of 1.46 m when the average solids content reached 81% or an average void ratio of 0.60. To check whether this depth indicated full consolidation, after 12.2 years the surface water was allowed to evaporate so the surface of the solids could be observed. A recent measurement at 19.6 years showed the solids surface at 1.48 m.

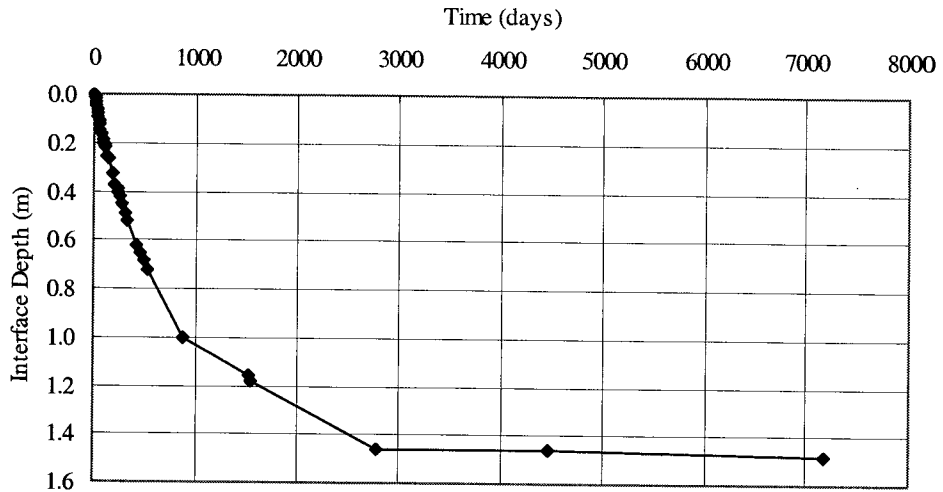


Figure 6.3 Interface measurement with arithmetic time

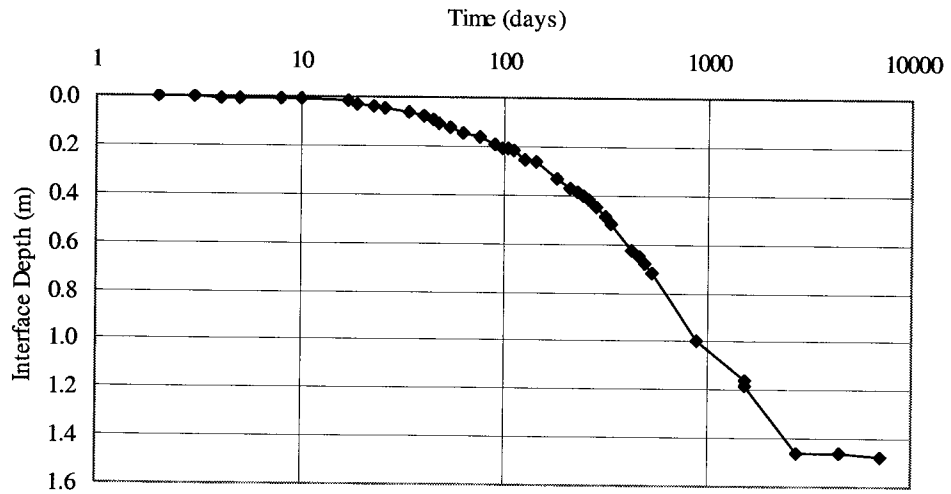


Figure 6.4 Interface measurement with log time

The abrupt stop at a depth of 1.46 m occurred because the sand particles start to contact at a solids content of about 79% (average void ratio of about 0.68) as shown in the ternary diagram (Figure 3.2). At higher solids or lower void ratios, the sand matrix structure must be compressed as well as the fines matrix. Therefore, the nature of the compressibility properties changes at a void ratio of approximately 0.68 (solids content of about 79%).

To elaborate on the settlement-void ratio relationship during consolidation, the effective stress-void ratio relationship for this material shown in Figure 7.10 has been replotted from an effective stress of zero to an effective stress of 100 kPa in Figure 6.5. At full consolidation the effective stress at the bottom of the standpipe is 83.4 kPa. From Figure 6.5, the void ratio at the bottom would be 0.54 and the void ratio at the solids surface would be the initial void ratio of 0.87. However, the density of the consolidated material increases with depth. Therefore, using the relationship in Figure 6.5, the effective stress profile, the void ratio profile and the average void ratio were calculated. This calculated average void ratio at the end of consolidation was 0.58. This calculated average void ratio compares well to the average void ratio of 0.60 determined from the final settlement of the interface at 1.46 m.

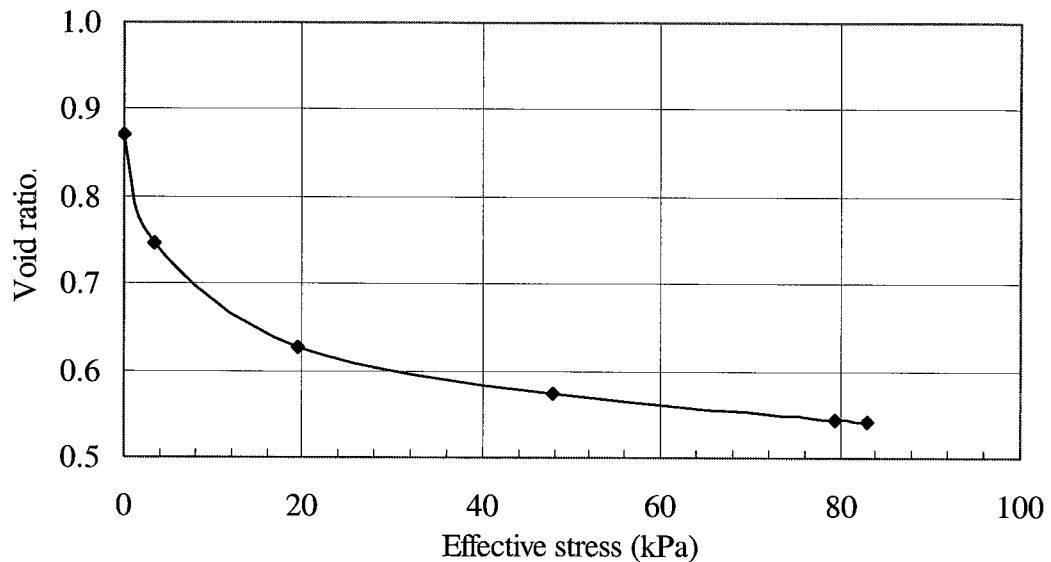


Figure 6.5 Compressibility function for Standpipe 3

6.3 Solids Content Measurements

For Standpipe 3, due to the high 82% sand content of the new mix, it was necessary to increase the inside diameter of all sample ports from 6.3 mm to 9.5 mm. This allowed the use of a 3/8" diameter sample tube and resulted in better sample recovery. The solids content and bulk density measurements for this standpipe, however, were ended 229 days after the start because the very high sand content prevented accurate sampling by the sampling methods mentioned in Chapter 3.

Measured solids content profiles are shown in Figure 6.6. The solids content profiles reflect the difficulty in measurement and the variability in values prevents detailed analysis. The initial solids content of the tailings was fairly uniform varying from 74 to 76% with an average of 74.8%; close to the design solids content of about 75%. The data indicate, however, that the solids contents were still fairly constant with depth at 229 days. At this time the interface had settled 0.39 m and the average solids content had only increased to 76.4%. The settlement up to this time appears to be mainly by creep although excess pore pressures have shown some dissipation in the bottom 2 m of the standpipe (Figure 6.8).

The average solids content calculated from the amount of settlement has increased from its initial value of 74.8% to a 12.2 year value of 81.2%. According to the mix design and the initial material properties in Figure 3.2, segregation should not be the cause of the solids increase at the bottom. Fines content measurements conducted at the beginning of the test also reported that there was no segregation measured in Standpipe 3 (Scott and Chichak, 1985c).

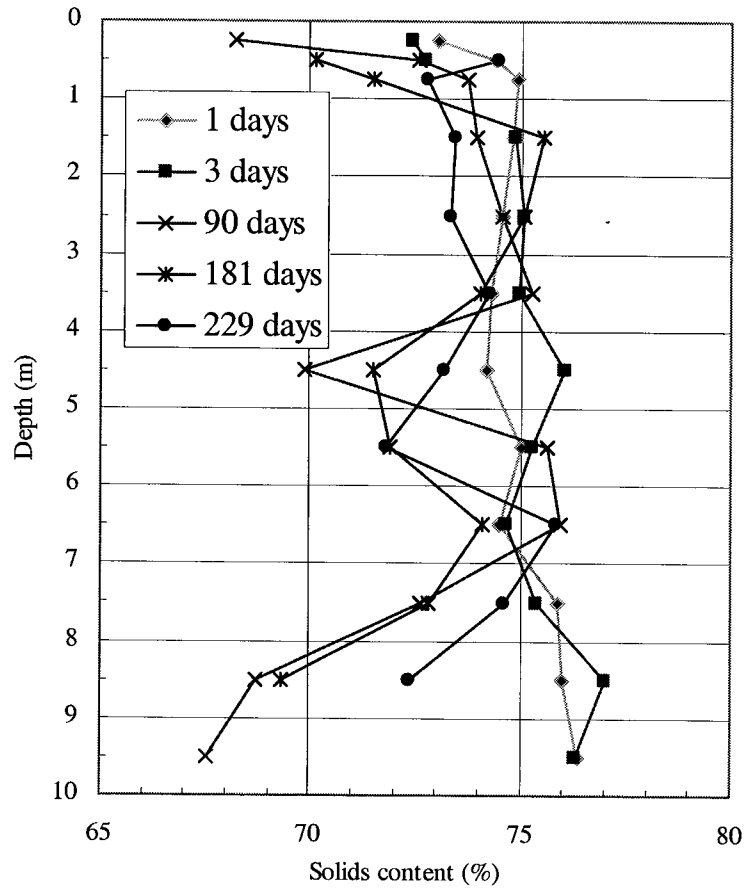


Figure 6.6 Solids content profiles of fine tailings-sand mix in Standpipe 3

6.4 Pore Water Pressure Measurements

The pore water pressure behaviour, as a result of the problem in measuring solids content, is used to calculate the consolidation progress. Pore water pressures were measured at the piezometer ports at 1.0 m intervals. Measurements were also taken at the 0.5 m depth as the readings at this depth are sensitive to a decrease in total stress as the interface settles (see Section 4.6) and at the 9.5 m depth as the readings at this depth are sensitive to the dissipation of the excess pore water pressure during the consolidation process. Details on measuring pore water pressure can be found in Section 3.4.2.

The first 100 days of the pore pressure measurements at all 12 of the piezometer ports in Standpipe 3 are shown in Figure 6.7 to examine the initial performance of the material for signs of thixotropy and creep. As discussed for Standpipe 1 in Section 4.6, thixotropy manifests itself by a rapid drop in pore pressure due to pore water tension. Creep manifests itself by a subsequent increase in pore water pressure as the thixotropic bonds are destroyed by creep shear.

Also shown in Figure 6.7 the initial excess pore pressure calculated from the bulk density and assuming the initial pore pressure was equal to the total stress. There was generally a time lag of 1 to 2 days for the pore water pressures to reach a steady state. A variation in readings of 1 to 2 kPa appears to be caused by inaccuracies in the monitoring system as the variations only occur for one reading. The most noticeable aspect of these initial measurements is that in the top half of the standpipe they are about 1 kPa lower than the calculated values and approach the calculated values with depth. This may be caused by slightly lower densities in the top half meter of the column (Figure 6.6); the effect of which would taper out with depth.

No significant effect of thixotropy or creep can be seen in the initial excess pore water pressure measurements. Dissipation of the excess pore pressure, that is, consolidation can already be seen at 9.5 m and 10.0 m depths after 30 days. The increase in rate of settlement after 20 days (Figure 6.2) may also be related to the onset of consolidation.

Measurements of pore water pressures profiles in Standpipe 3 at various elapsed times are shown in Figure 6.8. Other periodical measurements not shown on the figure fall in between these presented values. To indicate dissipation of excess pore water pressure, the excess pore pressure profiles are normalized from the water-tailings interface (Figure 6.9). It appears that significant pore pressure dissipation started immediately at the bottom of the standpipe. By 530 days the interface settlement had reached 0.72 m and the average solids content increased from 74.8% to 77.8% and the degree of consolidation at the 10 m depth had reached 30%. From the fact that there is no segregation in Standpipe 3, the dissipation of pore pressure at the bottom of the standpipe must be by a self-weight consolidation mechanism.

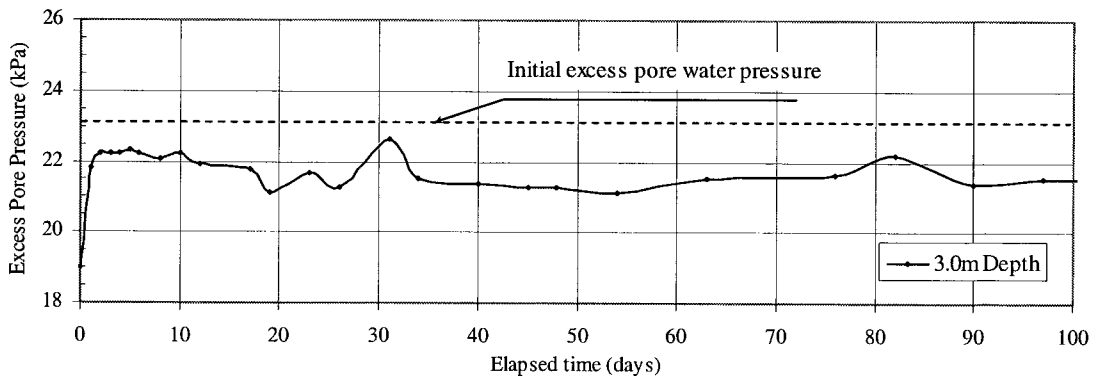
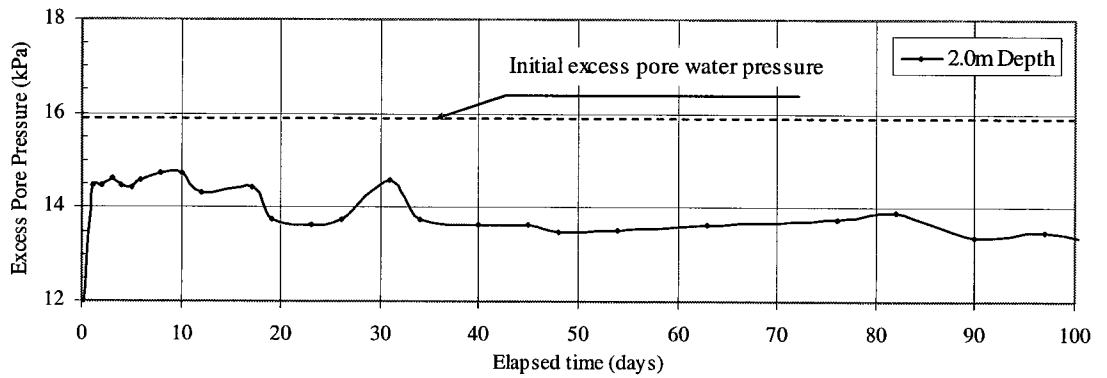
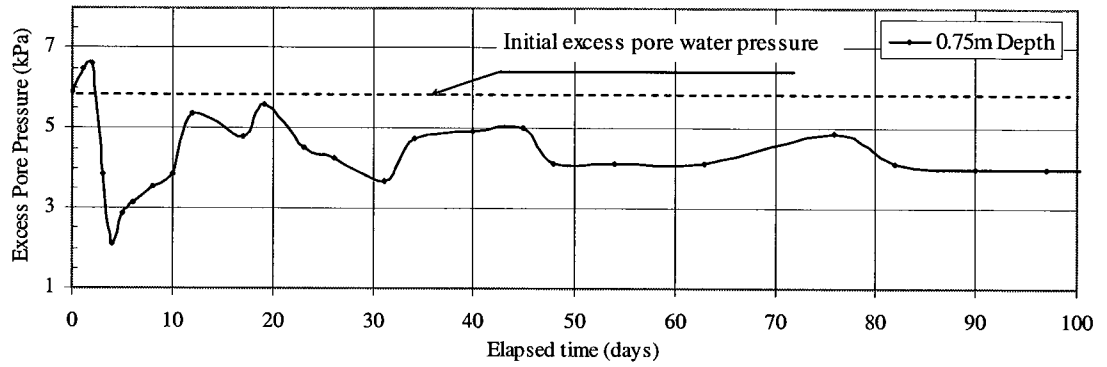
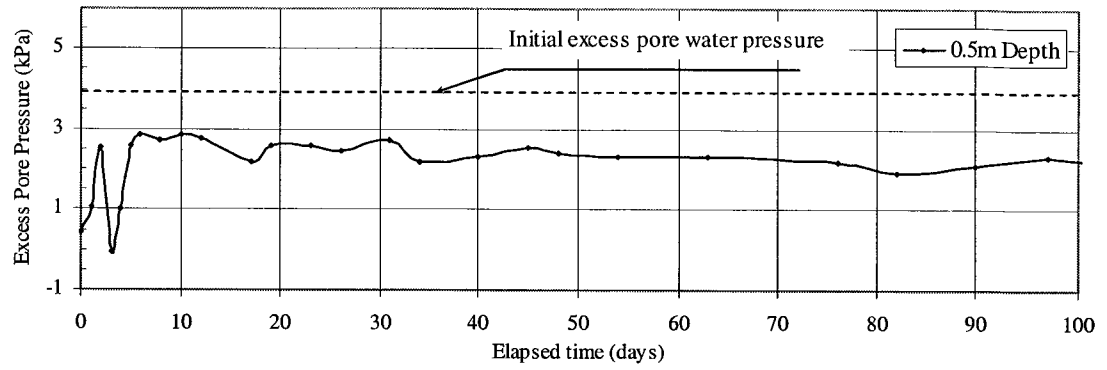


Figure 6.7 Initial excess pore water pressure measurements

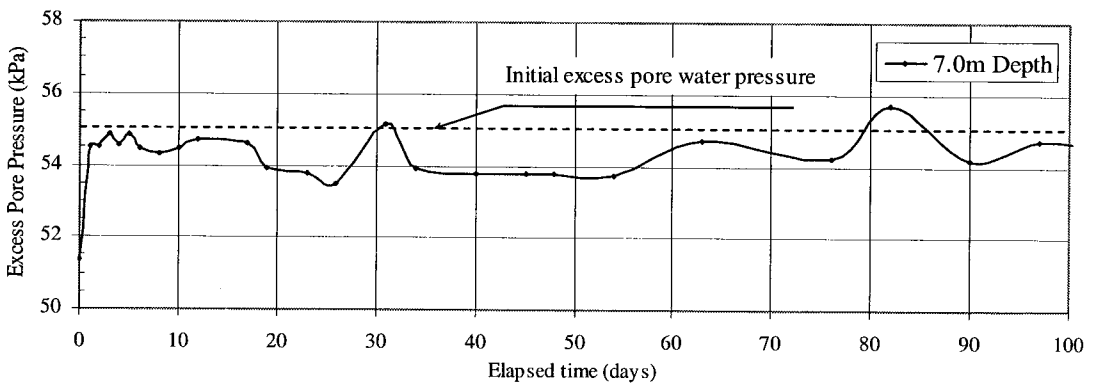
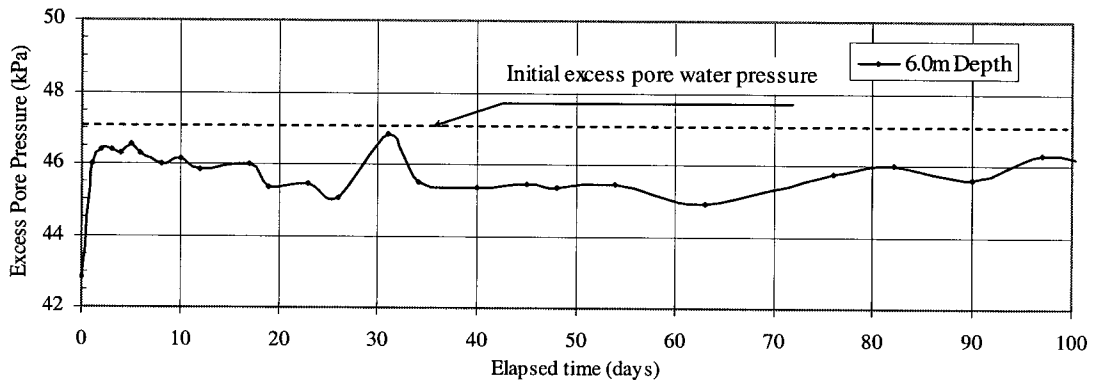
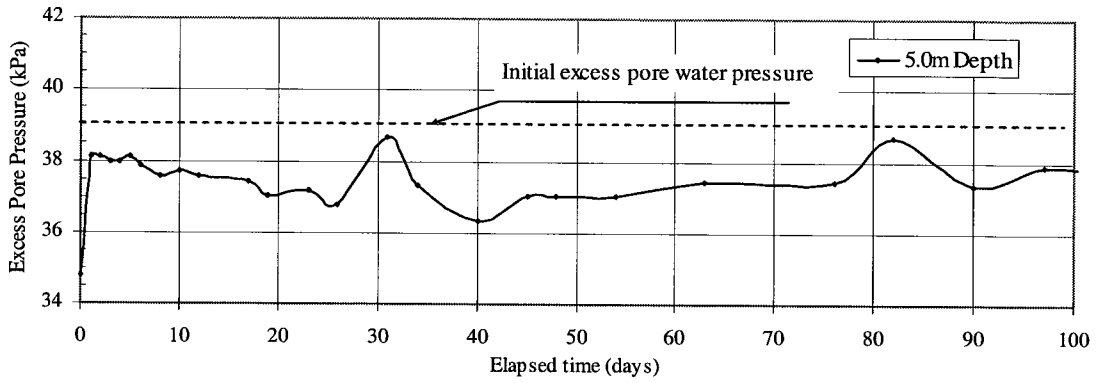
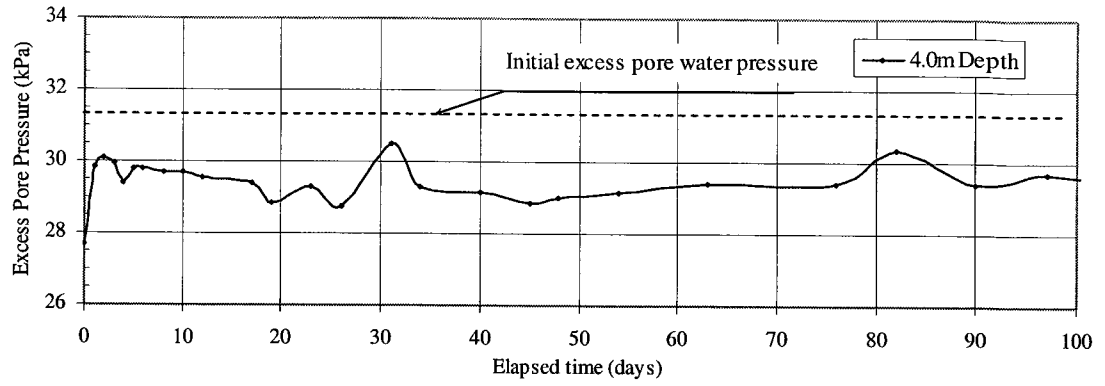


Figure 6.7 Initial excess pore water pressure measurements (continued)

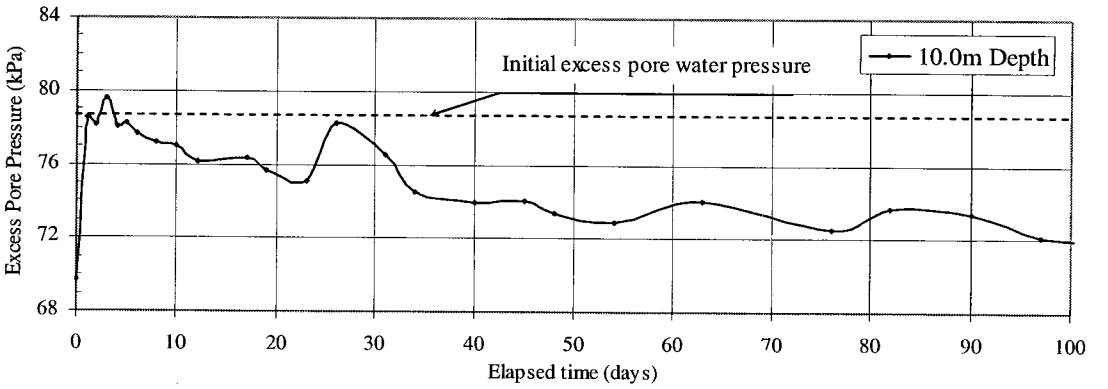
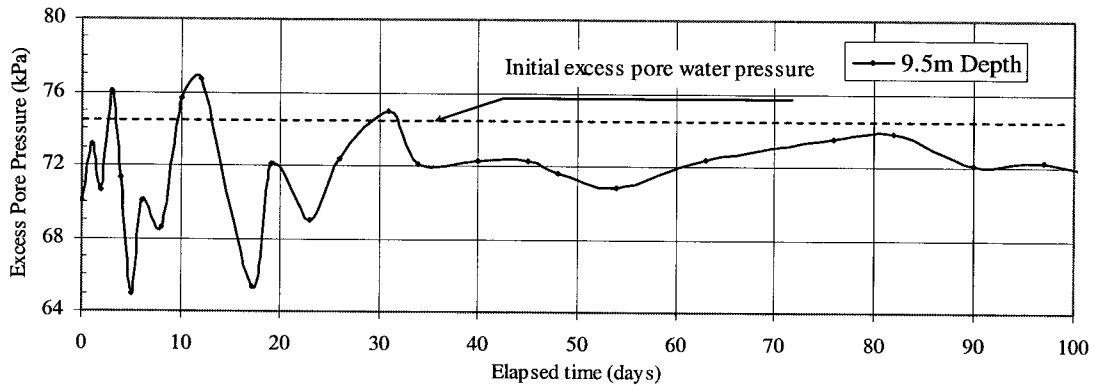
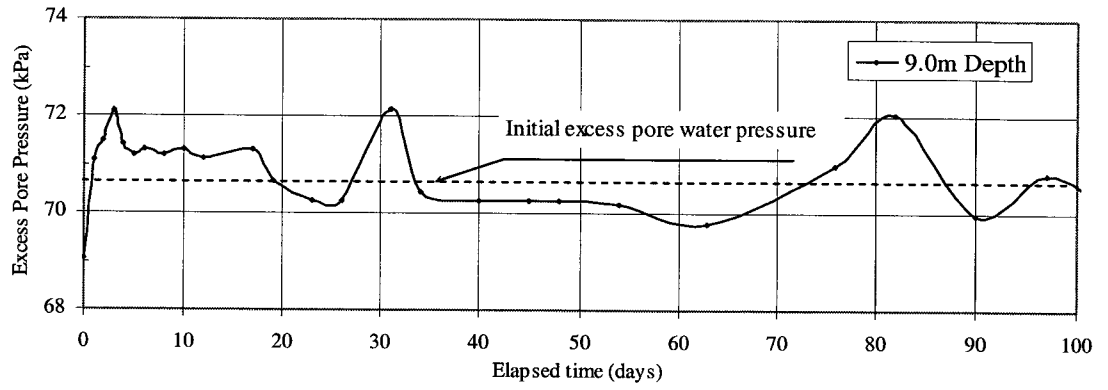
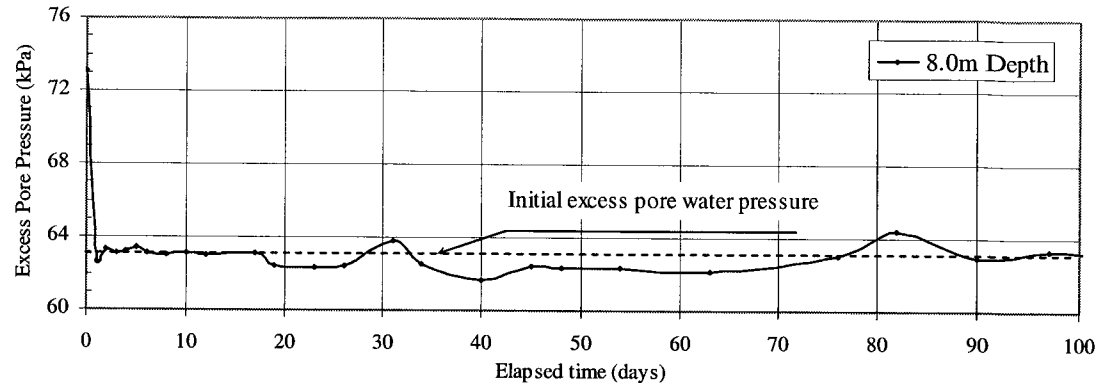


Figure 6.7 Initial excess pore water pressure measurements (continued)

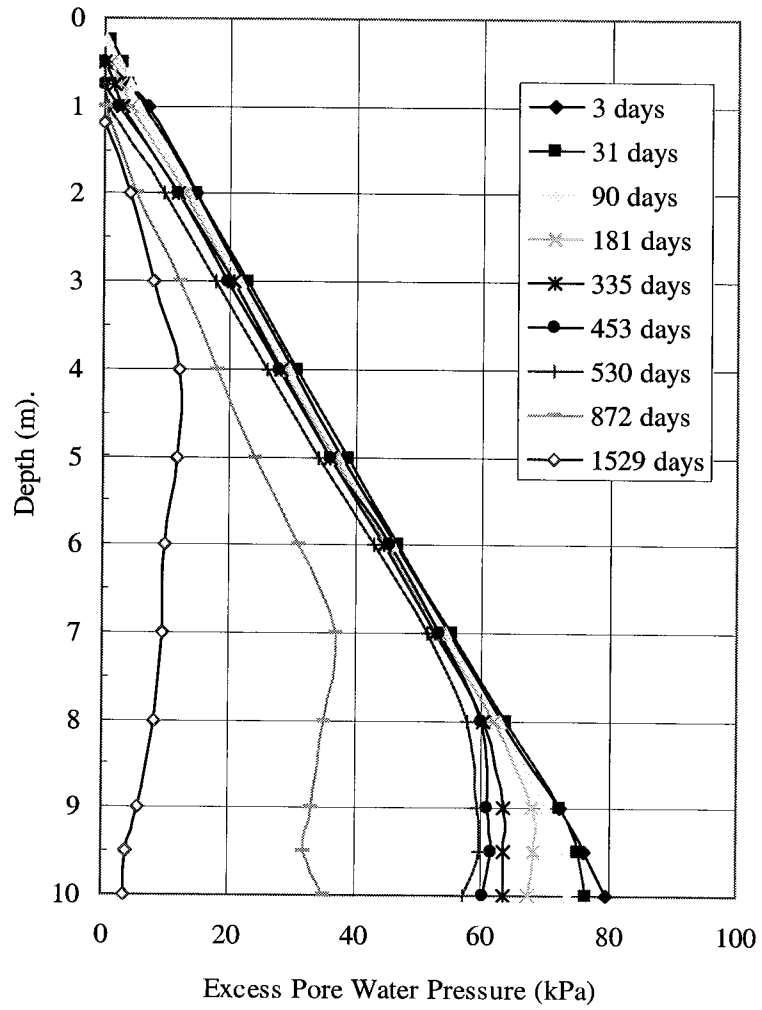


Figure 6.8 Excess pore water measurements in Standpipe 3

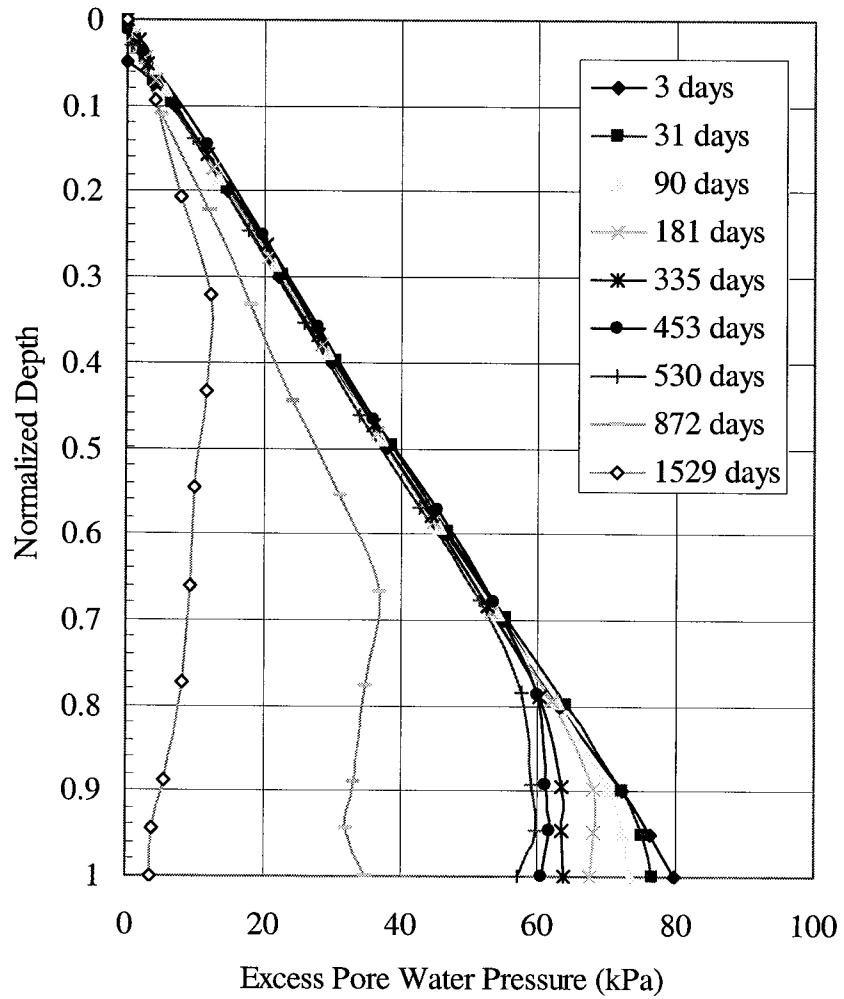


Figure 6.9 Normalized depth of Excess pore water pressure in Standpipe 3

6.5 Effective Stress Calculations

Due to the absence of good measurements of the solids content, effective stress profiles can not be obtained directly. In order to obtain the effective stress profiles, the interface settlement is used to calculate the average solids content at different times. Assuming that the solids content is constant throughout the depth of the standpipe, the total stress can be calculated. The calculated total stresses are then subtracted by the measured pore water pressures to obtain the effective stress profiles.

To evaluate the assumption that the solids content was constant with depth, the relationship in Figure 6.5 was used to calculate the solids content profile at the end of consolidation. Figure 6.10 shows the assumed uniform solids content profile and the actual solids content profile; the difference is not large. For further comparison, the relationship in Figure 6.5 was used in a finite strain consolidation program to calculate the effective stress profile at 100% consolidation. This calculated profile fell on the top of the effective stress profile in Figure 6.15 which was calculated using the constant solids content assumption. This assumption is therefore valid for this standpipe.

Figures 6.11, 6.12, 6.13, 6.14 and 6.15 show total stresses, effective stresses and pore pressures at five different times which are 3 days, 335 days, 872 days, 1529 days and 100% consolidation respectively. From Figures 6.9 and 6.12, it is observed that the effective stress starts to develop almost immediately at the bottom of the standpipe and it has significantly developed throughout the depth of the standpipe after about 500 days. Volume decrease by creep compression does not appear significant in Standpipe 3 after 229 days.

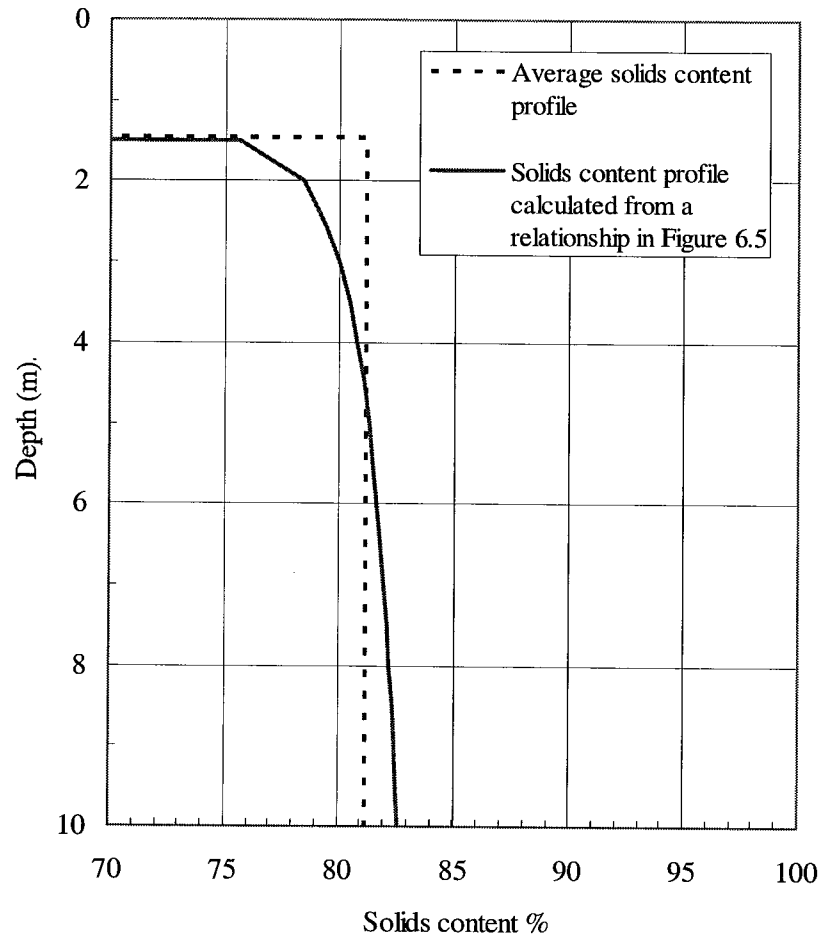


Figure 6.10 Solids content profiles at 100% consolidation

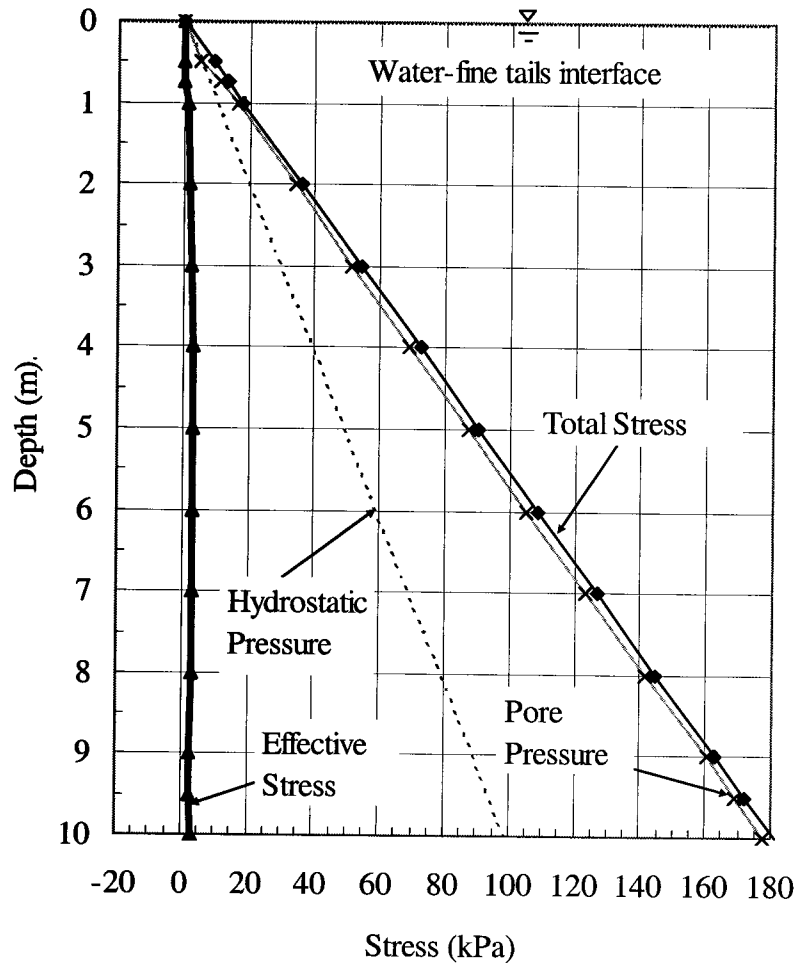


Figure 6.11 Total stress, pore pressure and effective stress profiles at 3 days

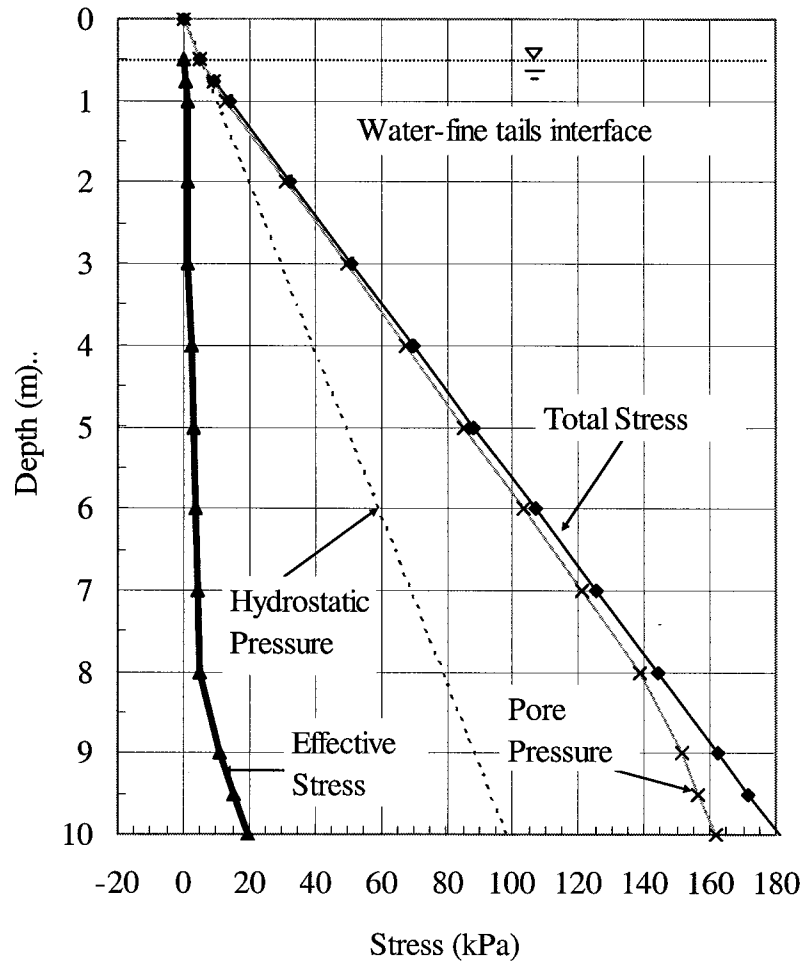


Figure 6.12 Total stress, pore pressure and effective stress profiles at 335 days

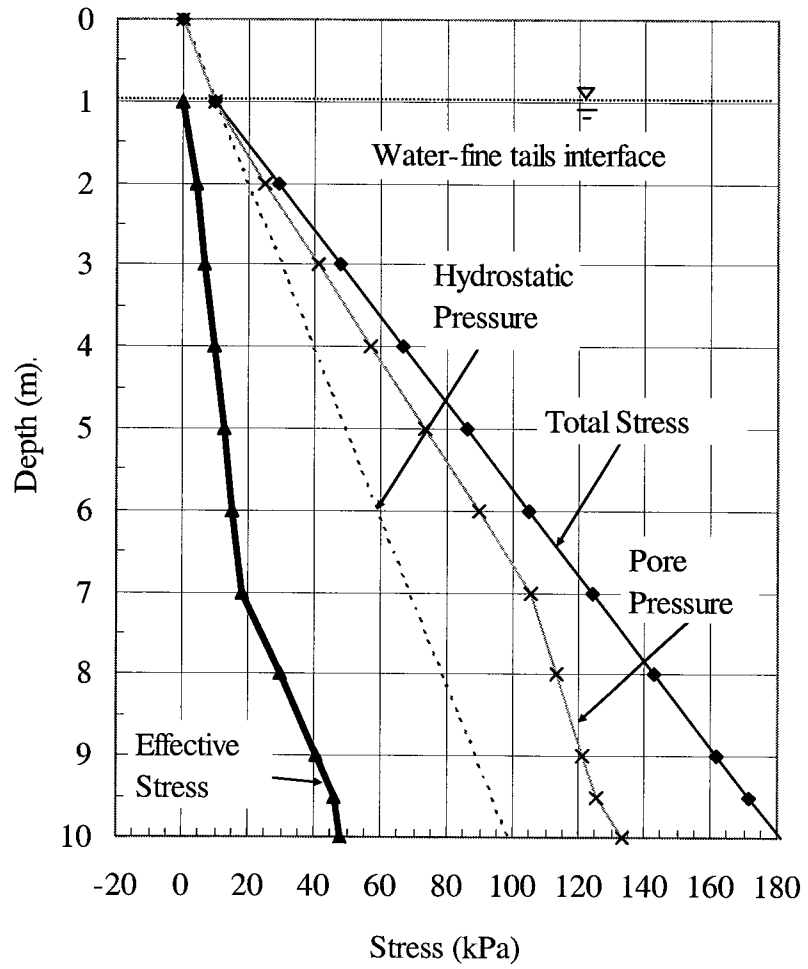


Figure 6.13 Total stress, pore pressure and effective stress profiles at 872 days

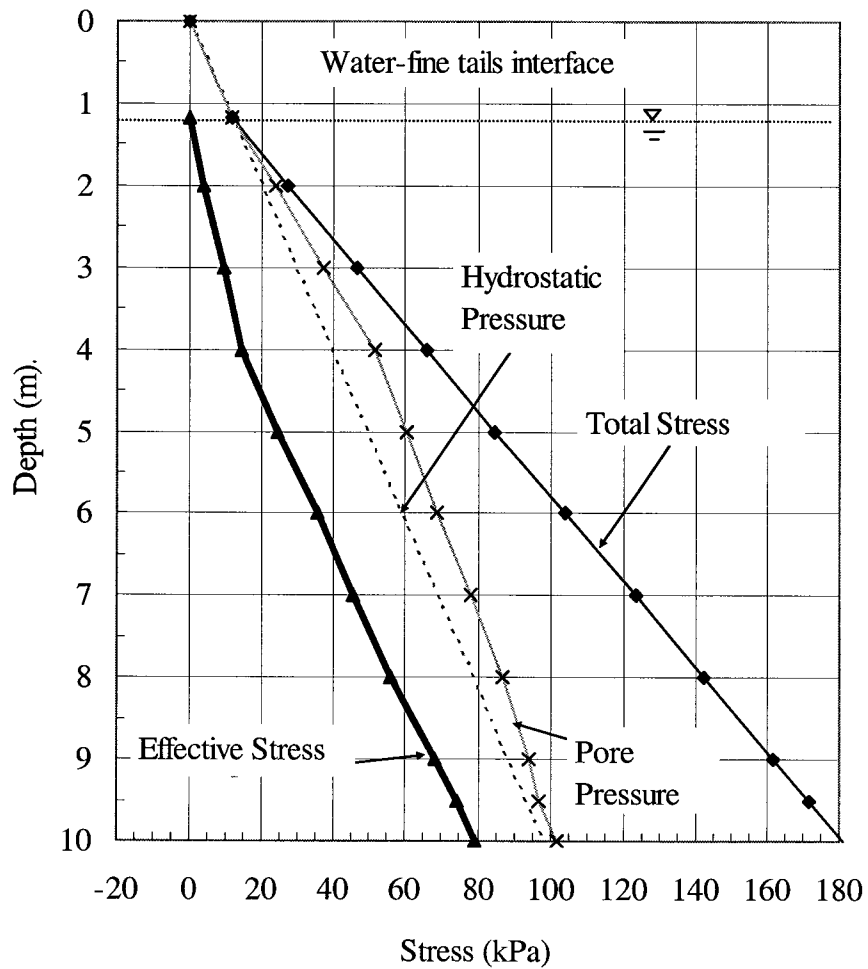


Figure 6.14 Total stress, pore pressure and effective stress profiles at 1529 days

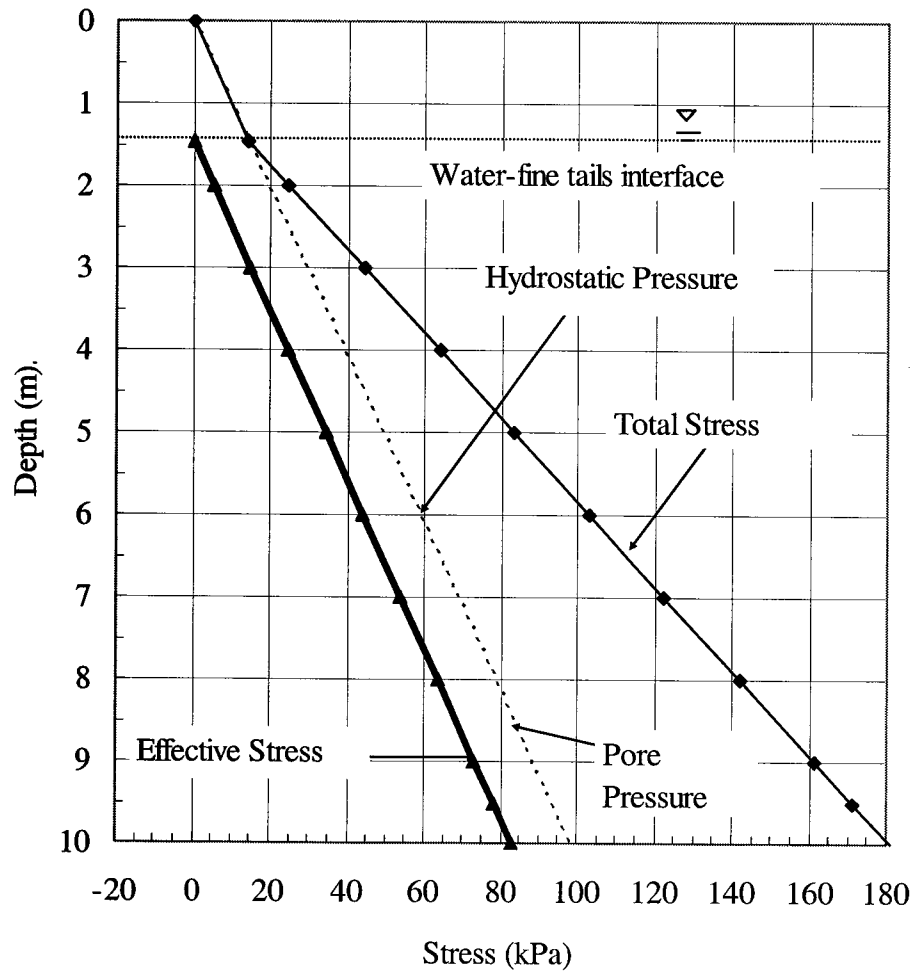


Figure 6.15 Total stress, pore pressure and effective stress profiles at 100% consolidation

6.6 Comparison of settlement in Standpipes 1, 2 and 3.

In section 5.2, a comparison was made of the rate and magnitude of settlement for the first two years of Standpipes 1 and 2. Although values of settlement are given, the comparison is qualitative not quantitative. As shown in Figure 3.2 and Table 3.2, the three standpipes varied in not only sand content but also in solids content and fines/fines+water ratio. Comparison of change in volume must be made with a consistent parameter not a combination of three parameters.

Figure 3.2 also shows that all standpipes are in the fines matrix region; the sand grains are not touching but floating in the matrix of fines and water. The fines/fines+water ratio or the fines void ratio which are directly related will govern the behaviour of all three standpipe materials.

The increase of solids contents over the initial two year period is shown for all three standpipes (Figure 6.16). This length of comparison was chosen not only because the Standpipe 2 test ended after 2 years but also because consolidation started to dominate the settlement of Standpipe 3 after this period. Normally a higher solids content soil would show less compression but Figure 6.16 shows the higher the initial solids content of the tailings, the faster the rate of increase in solids.

The explanation for this comparison of rate of increase in solids is that the fines solids are governing the behaviour not the total solids. The sand content in the fines matrix acts as an internal surcharge and the greater the amount of sand, the faster the rate of compression of the fines matrix. This behaviour is best shown in Figure 6.17 where the changes in fines void ratios with time are plotted. The slopes of the settlement plots in Figure 6.17 are plotted against sand content in Figure 6.18. An excellent correlation between the amount of sand in the mix and the compression rate of the fines matrix is shown.

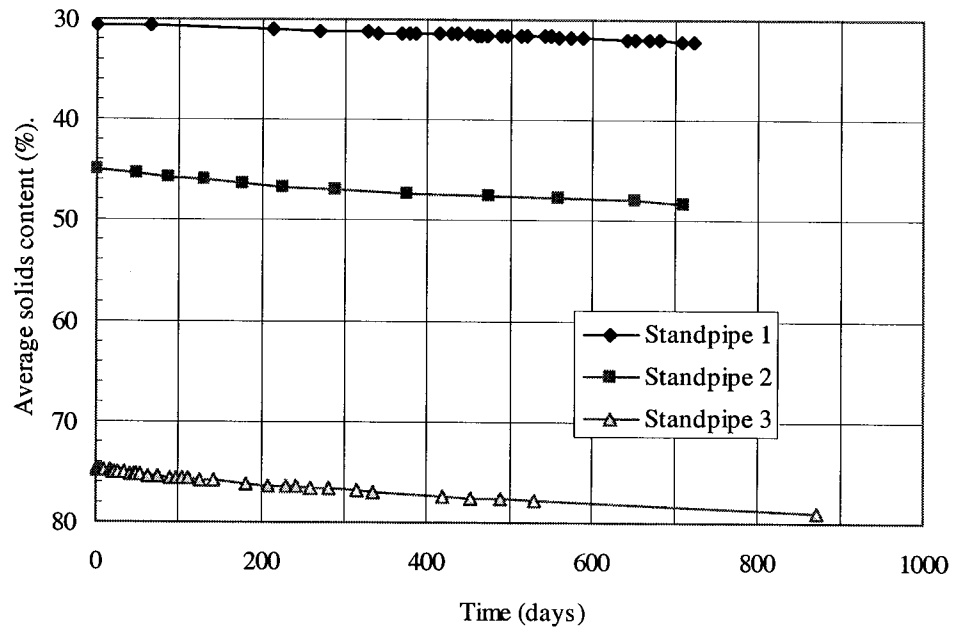


Figure 6.16 Solids content increases with time

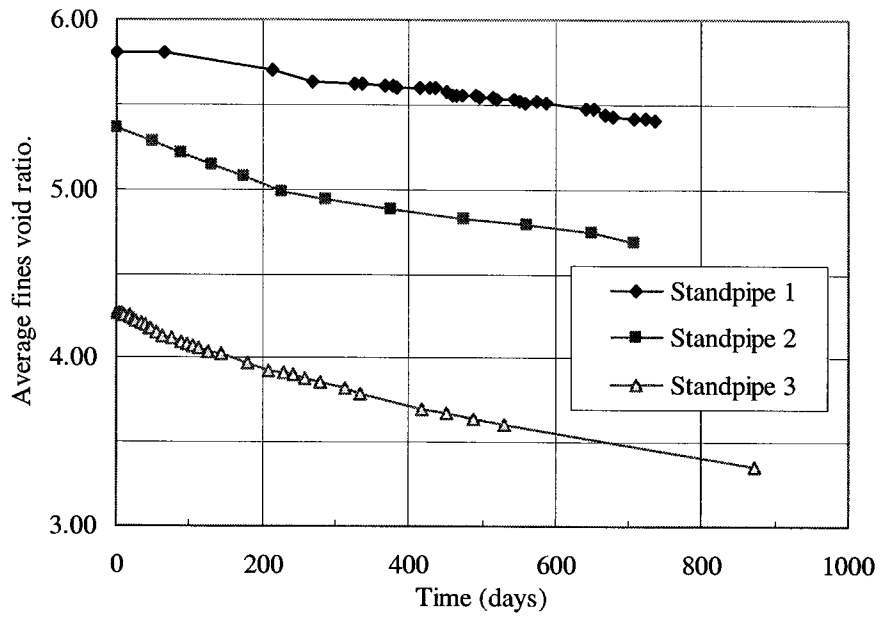


Figure 6.17 Fines void ratio changes with time

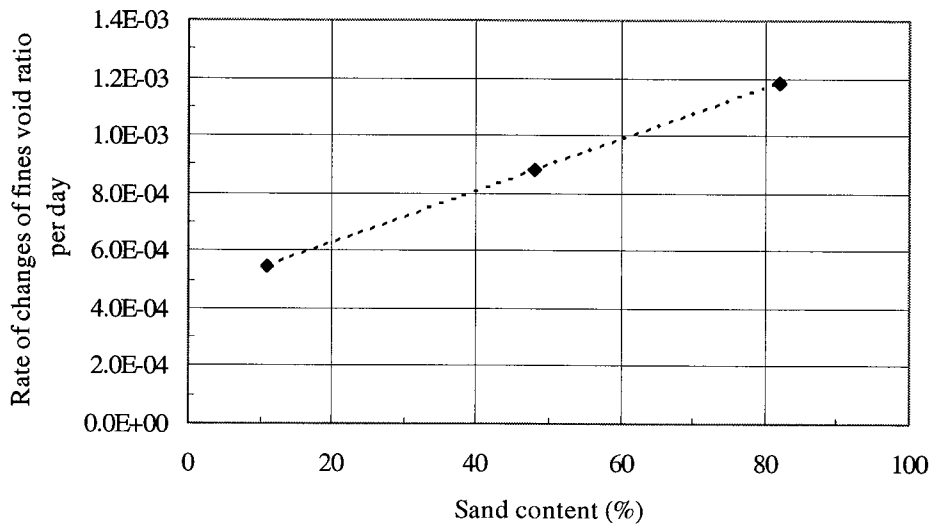


Figure 6.18 Rate of compression of fines matrix with sand content

6.7 Summary

Adding tailings sand to the mature fine tailings can produce a mix which is less compressible than the pure mature fine tailings and would appear to consolidate significantly fast enough that reclamation of the tailings pond surface would be possible.

Standpipe test 3 was conducted to investigate the effect of a high amount of sands on the consolidation behaviour of the mature fine tailings. Adding sand increases the density of the slurry and therefore should speed self-weight consolidation. The test continued for 12.2 years when consolidation was completed.

The following observations and conclusions on the standpipe measurements have been reached.

1. Standpipe 3 contained a MFT-tailings sand mix with an initial solids content of 74.8% that was 10% clay-size, 8% silt-size and 82% sand.
2. The major minerals in the standpipe mix are 87% quartz and other rock forming minerals and 13% clay minerals. The clay-size material contains equal amounts of kaolinite and illite. About one third of the silt-size material is large aggregates or booklets of kaolinite.
3. The bitumen content of the mix was 1.2 % of the total mass and the specific gravity of the solids was 2.58.
4. The interface settlement rate shows a discrete change at around 7 years caused by the sand particles contacting at a solids content of about 79%. At higher solids, the sand structure must be compressed as well as the fines-water matrix.
5. The average solids content increased from its initial value of 74.8% to 81.2% at the end of compression.
6. Excess pore water measurements and effective stress profiles show that significant pore pressure dissipation started immediately at the bottom of the standpipe and it significantly developed throughout the depth of the standpipe at around 500 days.

7. The settlement rate can be monitored through the change of fines void ratio. The rate of compression of the fines matrix from the three standpipes shows that the higher the sand content, the faster the decrease in fines void ratio.

The effect of the addition of sand appears to be that it acts like an internal surcharge which has a role in self-weight consolidation. Therefore by adding sand to MFT and using a mix design so there will be no segregation, the MFT- tailings sand mix will consolidate faster and more than the consolidation of the mature fine tailings. However, the creep mechanism which appears to be related to the thixotropy of the MFT will still be there. This is because the sand is only floating in the fines matrix and has little to do with the interparticle reaction of the fines. The amount of creep depends on time and the state of the fines void ratio. The material in Standpipe 3 compressed rapidly with a small value of fines void ratio, therefore, the effects of creep on this material was considered low compared to that in the MFT.

7. Consolidation Modeling of Thixotropic Slurries

Analytical predictions of the rate and magnitude of settlement of deposited oil sands tailings slurries generally overestimate how fast pore pressures will dissipate. Field deposits of nonsegregating tailings to mature fine tailings show continued high pore pressures near the surface which impede surface reclamation.

In geotechnical analyses which predict the consolidation behaviour of soft soils a finite strain theory is used. Effective stress-void ratio and void ratio-hydraulic conductivity relationships, determined from laboratory large strain consolidation tests, are used in the finite strain predictions. This theory, however, cannot predict the full range of sedimentation, consolidation and pore pressure dissipation which occurs in large scale deposits of thixotropic tailings slurries.

In this chapter, the large strain consolidation test and test results of materials from the large ten meter standpipes are presented. A review and discussion on the use of the large strain consolidation theory with the thixotropic tailings slurries is presented by comparing the 10 meter standpipe measurements with finite strain consolidation predictions.

7.1 Consolidation and Hydraulic Conductivity Tests

The large ten meter high standpipe tests presented previously provide valuable information for validating a consolidation model. For soft soils or slurry material that undergo so much volume change, the infinitesimal consolidation theory – Terzaghi consolidation theory - is not valid and the finite strain consolidation theory is widely used. To be able to use the finite strain consolidation theory, compressibility and hydraulic conductivity relationships must be obtained from a consolidation test.

Due to the large volume change that takes place the infinitesimal theory does not correctly calculate the hydraulic conductivity from consolidation-time measurements and the hydraulic conductivity must be directly measured. Therefore, a standard consolidation

test can not be used. To overcome these problems, large strain consolidation testing apparatus is used to capture the consolidation characteristics of slurry materials. The large strain consolidation test provides compressibility (the void ratio-effective stress relationship) and hydraulic conductivity (the hydraulic conductivity - void ratio relationship) that are used with the finite strain consolidation model. In this section, details of the large strain consolidation and hydraulic conductivity test for fine tailings are presented. The results and discussions of a consolidation test on a fine tailings sample are also shown as an example.

7.1.1 Consolidation testing of oil sands fine tailings

In this section, several types of consolidation tests are discussed and the large strain consolidation test for oil sands fine tailings is presented.

A problem with a consolidation test on oil sands fine tailings is that this slurry like material has a high initial water content or void ratio and thus will have a large volume change during consolidation. The standard oedometer test is developed for small-strain consolidation problems and uses small-strain theory. In this oedometer test, constant loads are applied to the sample, and the settlement with time is measured for each load. This test allows a relationship between void ratio and effective stress to be measured and the relationships between hydraulic conductivity and void ratio to be calculated by using small strain theory. The large strain that takes place during consolidation makes the standard oedometer test inappropriate for consolidation testing of oil sands fine tailings.

7.1.1.1 Improved consolidation testing

Several testing techniques have been developed to overcome the problem of the long test duration of the large-strain oedometer test. Such tests include the constant rate of deformation test (CRD) by Lee (1981), the constant hydraulic gradient test (CHG) by Lowe et al. (1969), and the constant rate of loading test (CRL) by Aboshi et al. (1979). The mentioned tests are considered more rapid than the step-loading oedometer test.

However these tests adapt the small strain theory and therefore are restricted by the assumptions (Znidarcic et al. 1984).

In the CHG test, through the use of a feedback system, the loading rate is continually adjusted such that there is a constant gradient within the sample. The assumptions used in this test include small strain, constant permeability, a linear compressibility relationship and a constant void ratio throughout the specimen (Znidarcic et al. 1984). In the CRD test, the assumptions used for evaluating testing data are small strain, constant coefficient of consolidation, and assumptions regarding the relationships between either the void ratio and time or the void ratio distribution in the specimen. Neither of the void ratio relationship assumptions can be validated (Znidarcic et al, 1984). For the CRL test, it has similar assumptions and restrictions.

An inter-connected consolidometer has been developed (Imai, 1992) in which several thin sub specimens can be prepared in individual consolidation cells which are connected successively. During consolidation, the settlement of each specimen and the pore water pressure between adjacent sub specimens are measured continually, and vertical distributions of void ratio and effective stress in the specimen and their changes with time are obtained by calculation. To evaluate the hydraulic conductivity, the direct measurement of hydraulic gradient and the velocity of water at different locations in the specimen are performed. From this test the effective stress-void ratio relationship and the hydraulic conductivity-void ratio relationship can be obtained.

The above consolidation tests, except the inter-connected consolidometer (Imai, 1992), with their analyses have been developed for soils that obey the assumptions of Terzaghi's infinitesimal consolidation theory. Therefore they are not applicable to highly compressible soils such as oil sands fine tailings. At the Geotechnical Centre at the University of Alberta, a step loading large strain consolidation test has been developed and used to determine consolidation characteristics of highly compressible soils.

7.1.1.2 The University of Alberta Geotechnical Centre large strain consolidation test

Large strain consolidation tests or slurry consolidation tests have been developed in the Geotechnical Centre to allow large deformations during consolidation and to allow hydraulic conductivity to be measured. This test is a step loading test similar to the standard oedometer test which allows void ratio – effective stress to be measured. Between each loading step, a hydraulic conductivity test is conducted to determine hydraulic conductivity at a specific void ratio which is then used to develop the hydraulic conductivity – void ratio relationship.

7.1.1.2.1 Large strain consolidation test procedure

The test procedure for the large strain consolidation test presented here is the 2003-2004 test procedure used in the Geotechnical Centre at the University of Alberta. The tested material shown in this section is mature fine tailings and Table 7.1 shows the initial properties of this material. The detailed procedure is:

1. Prepare required volume of sample, about 2 L, to the desired water content.
2. Set up the consolidation cell (Figure 7.1) and saturate the base and the permeability tube with tailings water. The tube is leveled at the same elevation as the outlet port. The valve of the tube is closed after the tube is filled.
3. Start the test with the top plate of the cell off and place the sample in the cell to a designated height (generally 9 cm.). During this step, it must be ensured that there is no leakage around the base. The bottom seal on the plexiglas cell must be well greased and while one of the operators pours the sample in the cell, another should hold the plexiglas cell down. After the sample has reached the desired level, tailings water is poured carefully to reach about 5 cm. above the sample. During sample filling take 2 samples of the tailings for water content determination. Place a presoaked filter paper on the top of the sample ensuring that it fits tight around the circumference.
4. The piston rod is clamped on the top plate with the bottom of the piston about 1 cm above the sample. The top plate is then bolted on. During this step, the top plate must be put on rapidly with care not to introduce load on the sample. The water level

should rise to the level of the outlet port at this time. If not, add more tailings water to reach the level of the outlet valve.

5. The LVDT is then set on the LVDT bar on the piston rod. The piston rod is unclamped and the piston is lowered on the top of the sample. The approximately 1 cm movement of the LVDT is monitored and the time of the piston contact with the sample is noted. Release the piston. The sample height and the excess pore water pressure are recorded with time. The operators must observe if there is any sample material squeezing out past the filter paper around the circumference of the piston. This first stress is composed of the buoyant self-weight of the sample at mid-height, the piston, the piston rod, the LVDT bar and the piston adapter. This test setup is shown in Figure 7.1.
6. Alternately, if the water content of the tailings is very high, the sample is allowed to settle under self-weight and the settlement is monitored manually on a scale. The stress for this settlement is assumed to be the buoyant self-weight at the mid-height of the sample. Very high water content tailings will usually undergo hindered sedimentation at the beginning of settlement. The rate of hindered sedimentation is used to calculate the hydraulic conductivity of the sample at its initial void ratio. A hydraulic conductivity test with a very low hydraulic gradient can also be performed at the end of self-weight consolidation before the piston load is applied. The next applied stress is then the system outlined in Paragraph 5.
7. After the settlement finishes (excess pore water pressure is zero or the LVDT reads the end of primary consolidation), a hydraulic conductivity test is performed with a designate head of water (see hydraulic conductivity test for details).
8. Add dead loads on the piston doubling the stress each time to reach 8 kPa (Figure 7.2). See Table 7.2 for a list of weights to be used. Perform a hydraulic conductivity test after each load. See Table 7.4 for a list of the head to be used. The dead load procedure is now finished.
9. The cell is then put into the loading frame and the sample is loaded with stresses of 15, 30, 60, 120, 250, 500 and 1000 kPa from a bellofram (Figure 7.3). See Table 7.3 for the bellofram air pressure to be used. The sample height and the excess pore water

pressure are recorded with time. After the settlement finishes at each load, a hydraulic conductivity test is performed.

10. After loading is finished, the sample is unloaded by reducing the stress from 1000 to 250, 60, 15 and 4 kPa followed by the piston load. Hydraulic conductivity tests are not performed during unloading.
11. When the unloading test is finished, the sample is taken out layer by layer to measure the variation in water content in the sample and to determine its average water content and void ratio.

Table 7.1 MFT sample for large strain consolidation test

Initial Water content, w	226.8 %
Initial Solids content, s	30.6 %
Specific gravity, G_s	2.28
Void ratio, e	5.17
Density, ρ	1.21 g/cm ³
Total Unit Weight, γ	11.84 kN/m ²
Initial Sample Height, H	9.00 cm
Effective stress at bottom of sample from self-weight $= (\gamma - \gamma_w) \cdot H$	~0.18 kPa
Effective stress at mid-height of sample from self-weight $= (\gamma - \gamma_w) \cdot H/2$	~0.09 kPa

Table 7.2 Dead load

Load No.	Accumulated Effective Stress on sample (kPa)	Incremental Effective Stress (kPa)	Additional submerged Weight (kg)	Accumulated Total stress (kPa)	Incremental Total Stress (kPa)	Additional Total weight (kg)	Remarks
0	0.09	0.09	-	0.53	0.53	-	self weight at mid-height
1	0.72	0.63	0.98	1.53	1.00	1.57	a piston + plastic tube + LVDT rod + Piston Adaptor
2	2.05	1.44	2.26	2.86	1.44	2.26	Loading plate is on and the piston adaptor is off
3	3.96	1.91	3.00	4.77	1.91	3.00	Weight
4	8.04	4.08	6.40	8.85	4.08	6.40	Weight

Table 7.3 Bellofram load

Load No.	Effective Stress on sample(kPa)	Additional cell Stress needed (kPa)	Incremental Bellofram Stress (kPa)	Applied Bellofram stress (kPa)	Applied Bellofram Stress (psi)	Remarks
5	16	15.28	10.13	10.13	1.47	Take Dead Load 2, 3, and 4 off the cell and move the cell into the loading frame, the remaining effective stress is 0.91 kPa from the dead load
6	32	16	10.60	20.73	3.01	
7	64	32	21.20	41.93	6.08	
8	128	64	42.41	84.34	12.23	
9	256	128	84.82	169.16	24.53	
10	500	244	161.68	330.84	47.97	
11	1000	500	331.31	662.14	96.02	
12	256	-744	-492.99	169.16	24.53	unloading
13	64	-192	-127.22	41.93	6.08	unloading
14	16	-48	-31.81	10.13	1.47	unloading
15	4	-	-	-	-	Load 3 Dead load
16	0.91	-	-	-	-	Load 1 Dead load

Table 7.4 Maximum head difference to be used for a hydraulic conductivity test

Load No.	Total Sample weight (kPa)	Total deadload or Bellofram load (kPa)	Total Stress at the bottom of sample (kPa)	Max Head * Difference (m)	Max Head* Difference (cm)
0	1.06	0.00	1.06	0.02	1.85
1	1.06	1.00	2.06	0.12	12.00
2	1.06	2.33	3.39	0.26	25.59
3	1.06	4.24	5.31	0.45	45.08
4	1.06	8.32	9.39	0.87	86.68
5	1.06	16.28	17.35	1.68	167.83
6	1.06	32.28	33.35	3.31	330.93
7	1.06	64.28	65.35	6.57	657.12
8	1.06	128.28	129.35	13.10	1309.52
9	1.06	256.28	257.35	26.14	2614.31
10	1.06	500.28	501.35	51.02	5101.57
11	1.06	1000.28	1001.35	101.98	10198.41

* The maximum head difference is the head that equals the total stress. A larger head would result in quicking or piping in the sample. Although the head can be greatly increased when the applied stress is high, this is not necessary and a reasonable flow rate can be achieved at low void ratios with a head difference of less than 0.5 m.

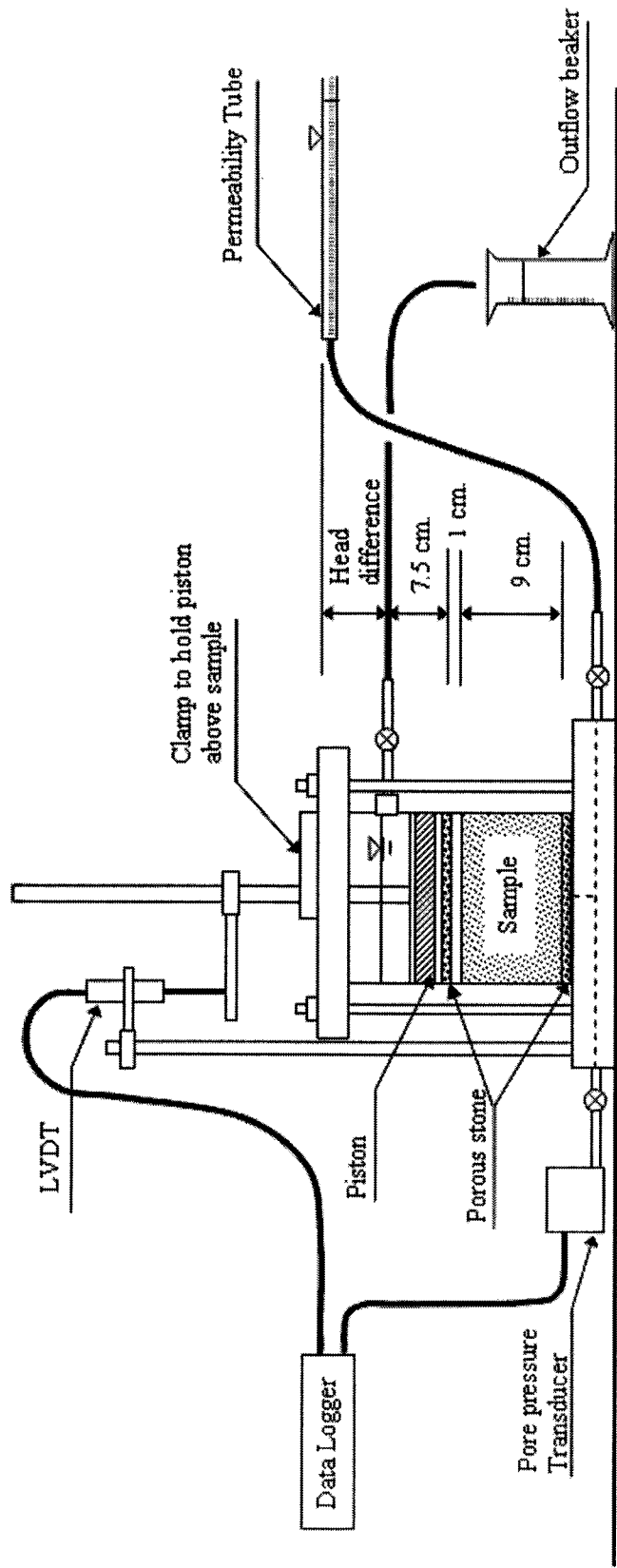


Figure 7.1 Initial set up of the large strain consolidation test before loading sample

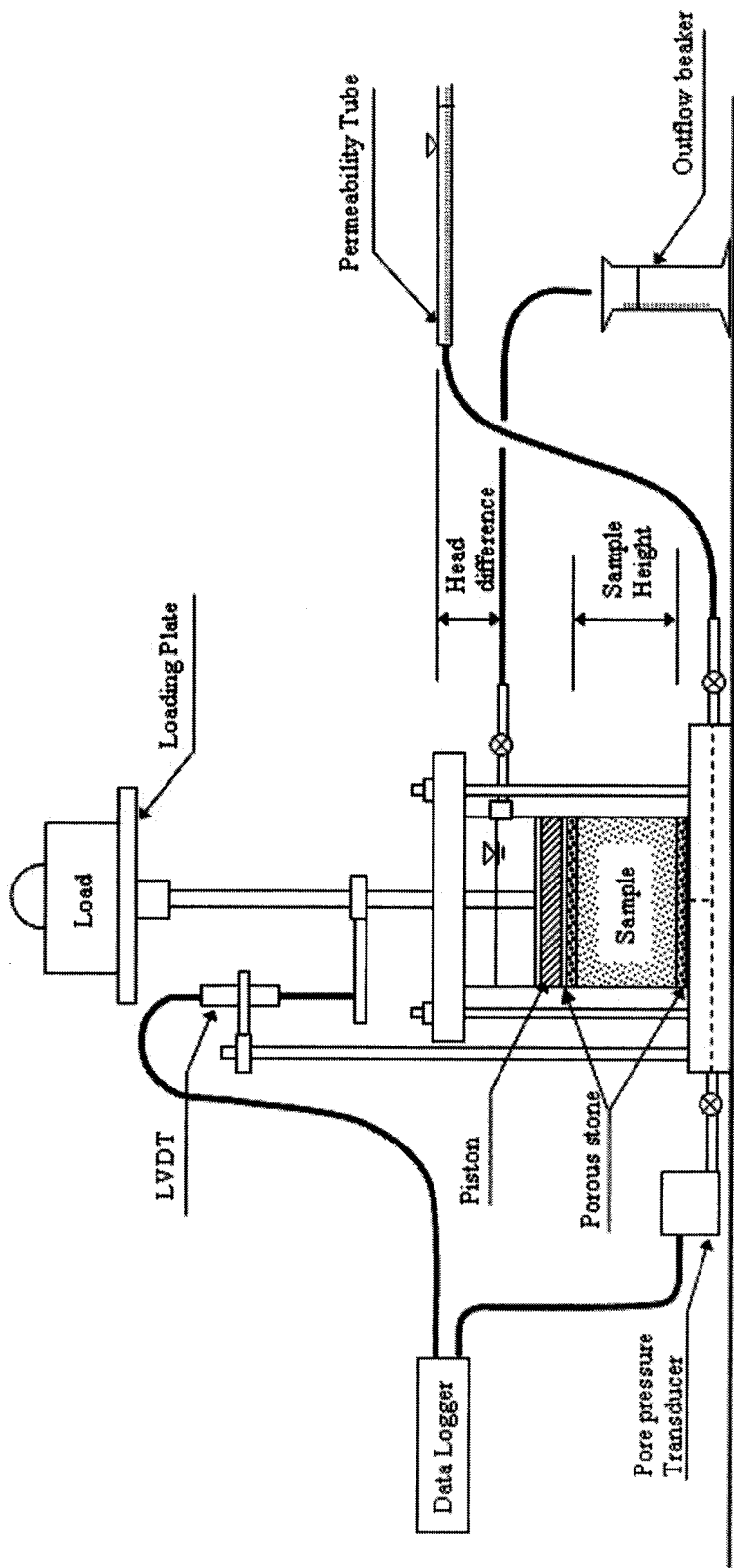


Figure 7.2 Sample loaded with piston and dead loads up to about 8 kPa

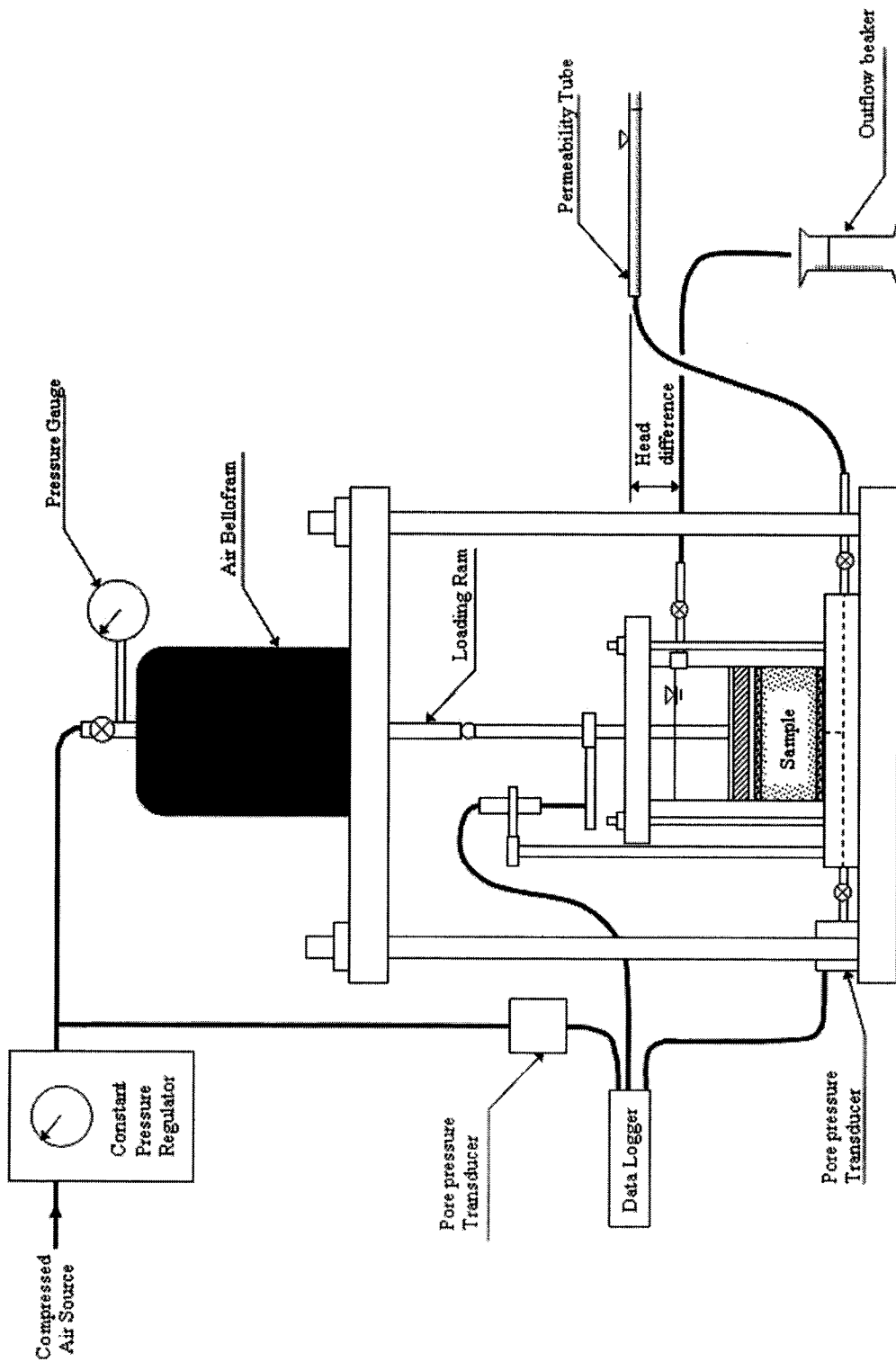


Figure 7.3 Sample in loading frame and loaded by bellofram up to 1000 kPa.

7.1.2 Hydraulic conductivity test

There are several methods available to determine the hydraulic conductivity – void ratio relationship in the laboratory. Hydraulic conductivity can be determined either directly or indirectly. The direct method involves forcing a permeant through a specimen and monitoring the rate of flow, or the hydraulic head changes induced by it. Indirect methods of determining hydraulic conductivity are done by inverting a consolidation theory and applying it to data obtained from a consolidation test. The different testing methods are reviewed in this section and a method used for the oil sands fine tailings is presented.

7.1.2.1 Indirect methods of determining hydraulic conductivity

Indirect methods of determining hydraulic conductivity as mentioned above use the inverted consolidation theory with data from a consolidation test. Several kinds of consolidation tests available to be used are the step loading test, controlled gradient test, constant rate of deformation test and constant rate of loading test. The most common method of determining hydraulic conductivity is by inverting Terzaghi's consolidation theory. The method has been used for engineering practice however an assumption of the theory - hydraulic conductivity is a constant – is unacceptable for the large volume change in some materials such as the oil sands fine tailings or highly compressible clays.

Several authors have proposed the indirect measurement of permeability using finite strain consolidation theory (Tan et al. 1988, Znidarcic et al. 1986, Been and Sills 1981). All these studies suffer from the restrictive assumptions made to solve the equations by limiting their application to constant material properties.

Indirect methods of determining hydraulic conductivity have been found to be unacceptable because of experimental procedures (eg. high strain rates) and analytical reasons (assumption of a constant permeability). As a result, only the direct measurement of hydraulic conductivity has been used in this study.

7.1.2.2 Direct methods of determining hydraulic conductivity

7.1.2.2.1 Constant head and falling head test

There are two common methods of directly determining the hydraulic conductivity of soil which are the constant head and the falling head permeability tests. These two methods have been widely used in geotechnical laboratories because of their simplicity in apparatus, procedure and evaluation of data. The constant head is most reliable and accurate for relatively permeable soils, such as sand, where the quantity of discharge is rather large. For most fine grained soils the falling-head permeability test gives results that are better than those of the constant head type because of the slow flow rate.

The disadvantages of these two methods were discussed by Hardcastle and Mitchell (1974) and Olsen et al. (1985). In both methods, flow rates are obtained by conventional volume measurement techniques where the maximum resolution is of the order of 10^{-3} ml (Suthaker, 1995). For this resolution, accurate measurements of hydraulic conductivity of soil with low permeability can be achieved only if the imposed gradients are very high or the tests last for a long time. If the burettes are replaced by capillary tubes in order to increase resolution, contamination of the tubes may lead to a non-zero contact angle between the water and the glass which will affect the imposed gradient and produce erroneous results (Olsen and Daniel 1981).

The large imposed gradient will usually produce a large variation of effective stress in the sample causing it to become less homogeneous (Aiban and Znidarcic 1989). In the falling head test, the hydraulic gradient changes continuously with time. Therefore, the falling head test is always done in a transitional state and the effective stress within the sample changes continuously which will change the volume and as a result the permeability is changed. Analysis of the falling head test accounts for the change of hydraulic gradient but not the volume. Several modifications have been proposed for falling head tests such as rising tail water test and the automatic falling head permeameter test but all use the same falling head test principle (Daniel, 1989 and Tan, 1989).

7.1.2.2.2 Flow pump test

Olsen (1966) proposed the flow pump test technique for determining hydraulic conductivity of fine grained soils. This test uses the constant quantity of flow through a specimen by a pump and uses a differential pressure transducer to determine hydraulic gradient in the specimen. A very slow rate must be applied for this test (Olsen et al 1985). It is reported by Aiban and Znidarcic (1989) that this test gives the same hydraulic conductivity values as the constant head test when a sample is tested under similar conditions.

7.1.2.2.3 Restricted flow test

Sills et al. (1986) proposed a restricted flow test which can continuously measure hydraulic conductivity during consolidation and also had a separate hydraulic conductivity measurement at the beginning and the end of a consolidation test. This test can be done by applying total stress to one face of a specimen. The drainage is allowed only on this face through a restrictor. Pore pressures at both ends of the specimen are measured using transducers. The hydraulic gradient can be calculated using sample height and pore pressure difference at anytime, and the flow rate can be obtained from a direct measurement or calculated from the compression of a specimen. The main difficulty of this test is achieving an accurate measurement of pressure difference between drained and undrained faces especially when there is a small different of pressure between the two faces. A differential transducer may be used to measure the difference of pore pressure directly.

7.1.2.2.4 Seepage test

The seepage test is done by passing fluid (water) through a specimen by an application of a constant head difference across the specimen. The pore pressure distribution within the specimen is measured at different points, the flow through the specimen is measured, and the test continues until steady state pore pressure readings are obtained. After the steady state condition is established, the flow is stopped and the specimen is sliced to determine the void ratio distribution. Material balance calculations must be used along with the measured void ratio to determine the exact void ratio. From

the pore pressure distribution, the hydraulic gradient can be calculated, and by using the measured flow rate, hydraulic conductivity can be obtained.

7.1.2.3 Hydraulic conductivity test on the oil sands fine tailings

The hydraulic conductivity test on the oil sands fine tailings used in the Geotechnical Centre at the University of Alberta is a constant head test. The test is chosen based on the advantages of the use of a small hydraulic gradient to measure hydraulic conductivity during the consolidation test and the ability to study time flow effects. The consolidation test is performed in a slurry consolidometer. This apparatus was designed so the hydraulic conductivity measurements can be performed at different void ratios after each consolidation load increment.

7.1.2.3.1 Testing equipment

The upward flow constant head hydraulic conductivity test equipment shown in Figures 7.1, 7.2 and 7.3 is composed of a long permeability tube (I.D. of 5 mm) with a scale, a permeability tube holder to hold and change the head difference, and a rubber tube to connect the consolidometer to the permeability tube.

7.1.2.3.2 Test procedure

This following test procedure is based on the 2003-2004 large strain consolidation and hydraulic conductivity test.

1. Flush the system with the tailings water.
2. The valve on the permeability tube is closed after filling.
3. The inflow tube must have enough water in it so enough readings can be obtained.
4. The valve on the outflow is left open to let the water in the cell adjust itself to this level. The outflow water level is then at the outflow valve. A beaker is placed to collect the outflow water during the test. The beaker must be weighed before and after each hydraulic conductivity test to obtain a volume of outflow.
5. The inflow tube or the bottom flow is then raised to the desired elevation. See Table 7.4. The vertical difference between the inflow tube and the outflow valve is the head

- difference. Then open the inflow valve. The hydraulic conductivity test commences here. The inflow and the pore water pressure at the bottom and time are measured.
6. The operators must keep an eye on the sides of the sample to check if there is any piping happening. If the hydraulic gradient is too high there may be piping.
 7. During testing, plot the calculated incremental hydraulic conductivity with total elapsed time and continue the test until the hydraulic conductivity is stable. The test is finished after the hydraulic conductivity becomes stable.
 8. Turn the bottom valve (inflow valve) off at the end of the test. The top valve (outflow valve) is left open to control the top elevation of the water.

7.2 Consolidation Test and Hydraulic Conductivity Test Results

As stated previously, the finite strain consolidation theory used for consolidation modeling of slurry materials needs the compressibility and hydraulic conductivity of the modeled material. In this section, the two important relationships; effective stress-void ratio and hydraulic conductivity-void ratio from large strain consolidation tests for the tailings materials from all 3 ten meter standpipes are presented.

7.2.1 Effective stress-void ratio relationship

An effective stress-void ratio relationship can be determined from a large strain consolidation test by calculating the void ratio from the measured settlement and calculating the effective stress from the applied pressure. Figure 7.4 shows the compressibility of all the materials from the 3 large standpipes.

For mature fine tailings, the effect of initial void ratio is substantial in the low effective stress range that exists in the tailings ponds. The compressibility of the mature fine tailings, therefore, is dependent on the initial void ratio of the sample. In soil mechanics, for young or newly deposited soils, there is supposed to be no preconsolidation pressure. From Figure 7.4 it can be seen that all slurry samples show a preconsolidation pressure then a virgin compression state. The mature fine tailings are not overconsolidated soils; they are underconsolidated and therefore should follow the virgin compression line irrespective of the initial void ratio. This behaviour is not found in

normal slurries. As discussed in Chapter 3, the thixotropic gel strength is the reason for the oil sands slurry to behave like overconsolidated soils. Therefore, a consolidation model used for this class of material has to consider the effect of thixotropic gain in strength.

For MFT-tailings sands mixes of 48% sand and 82% sand, the effect of thixotropy is less noticeable due to the lower void ratio from the high sand content.

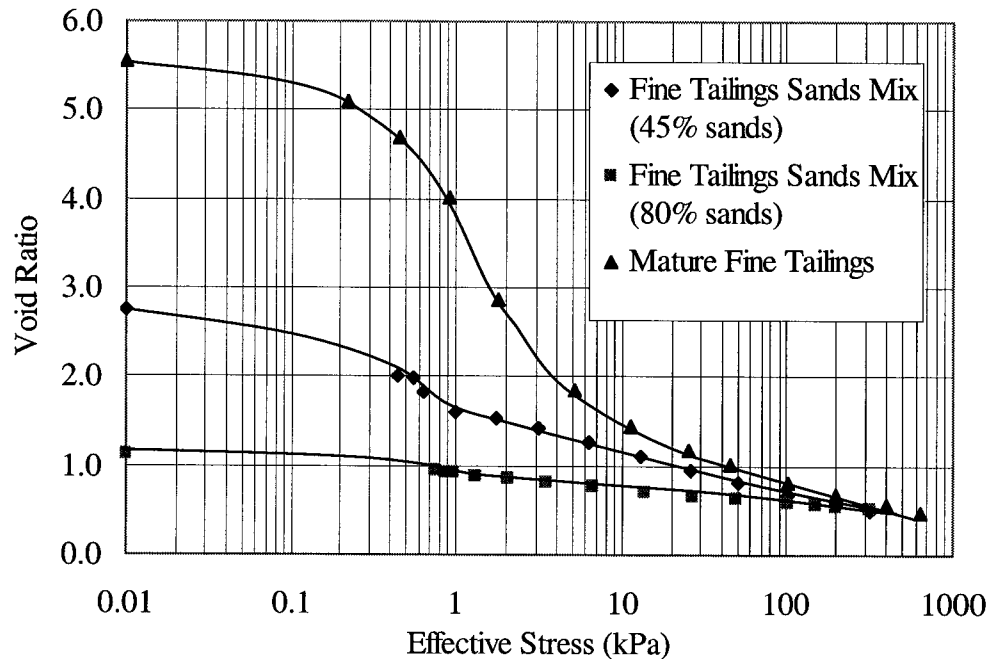


Figure 7.4 Compressibility of oil sands tailings (Modified from Pollock, 1988)

Considering the MFT-tailings sand mix with 80% sand at 70% solids, the above relationship obtained from the large strain consolidation test will be different from the material in Standpipe 3 which has 82% sand at 74.8% solids. Therefore it is necessary to slightly modify this relationship to obtain a relationship for the material in the standpipe. In Figure 7.5, 38 large strain consolidation tests performed on Syncrude and Suncor tailings with different additives are presented. The properties of the tailings vary with solids contents of 51 to 65% and fines contents of 14 to 30% and with different additives (gypsum, phosphogypsum, lime, acid/lime, acid/flyash, alum).

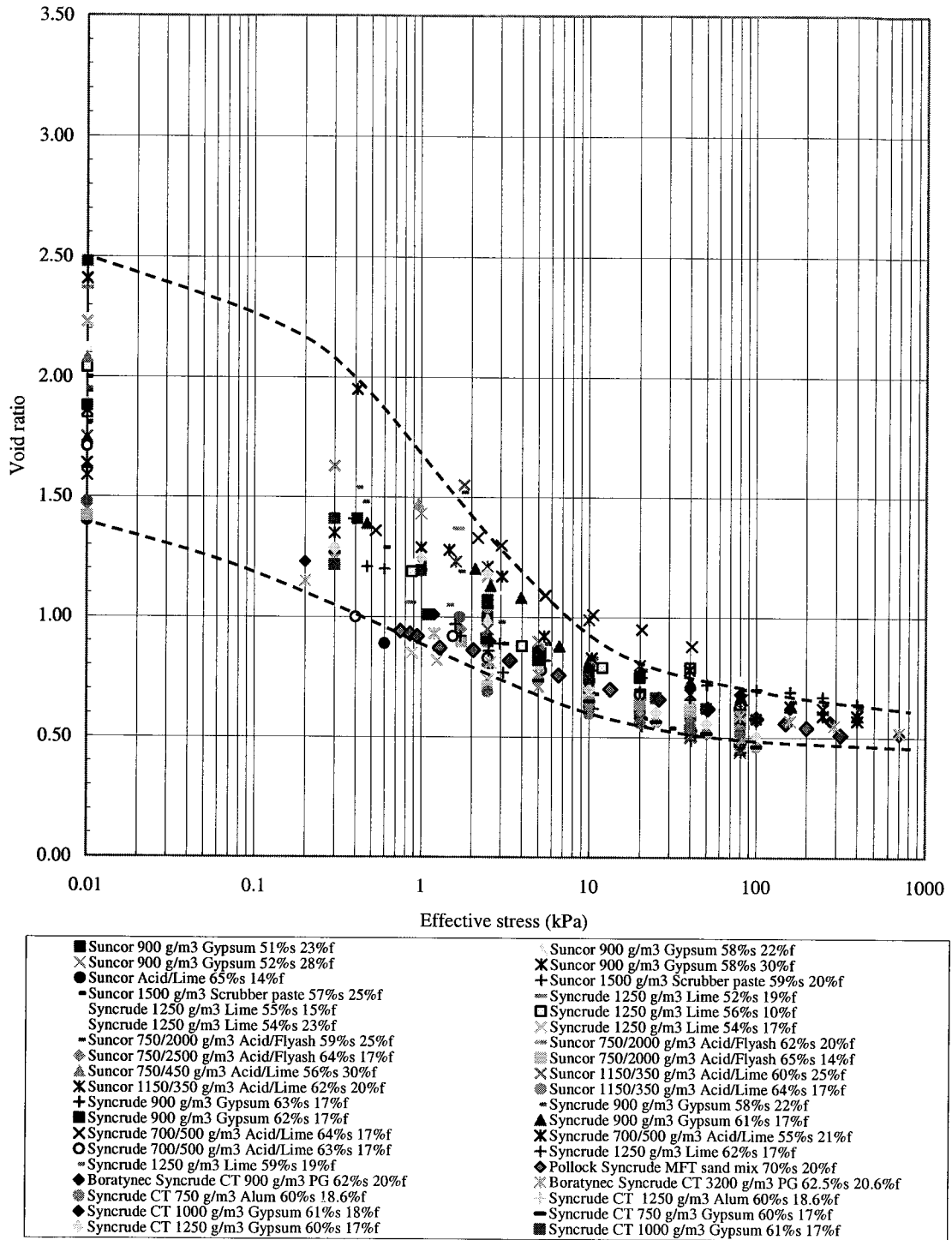


Figure 7.5 Compressibilities of fine tailings with sand

Upper and lower boundaries for all these materials are drawn (Figure 7.5). Clearly, there is a considerable spread between upper and lower boundaries. This shows that the

compressibility of the MFT-tailings sand mix can vary significantly depending on initial conditions (solids contents and fines) and different type/amount of additives in the tailings. However from our experience there is very little to no difference in compression curves for the different additives when the vertical applied effective stress is over 10 kPa (Figures 7.6 to 7.9). Therefore, some of the tests from Figure 7.5 have been selected based on initial solids content and fines content and are plotted in Figure 7.10 to achieve the best trend for the compressibility relationship.

In Figure 7.10, the effective stress-void ratio relationship of MFT-tailings sand mix still varies quite a bit and tends to become more compressible as the fines decreases from 20 to 17%. The compressibility relationship of Standpipe 3 material should have lower void ratios due to the higher initial solids content (74.8% solids) than the large strain consolidation test on the MFT-tailings sand mix with 80% sand and 69.7% solids in Figure 7.4. Therefore, the compressibility of the MFT-tailings sand mix with 82% sand in Standpipe 3 should fall in this set of data but below the compressibility of MFT-tailings sand mix with 80% sand. The approximated compressibility of the Standpipe 3 material is shown in the figure.

From Figures 7.4 and 7.10, the void ratio-effective stress relationships for the three tailings materials, MFT, MFT-tailings sand mix with 48% sand and MFT-tailings sand mix with 82% sand, can be expressed in equations 7.1, 7.2, and 7.3 respectively.

$$e = 28.71 \cdot \sigma'^{(-0.3097)} \quad (7.1)$$

$$e = 7.256 \cdot \sigma'^{(-0.2052)} \quad (7.2)$$

$$e = 1.670 \cdot \sigma'^{(-0.09929)} \quad (7.3)$$

Where e is void ratio and σ' is effective stress in Pascals.

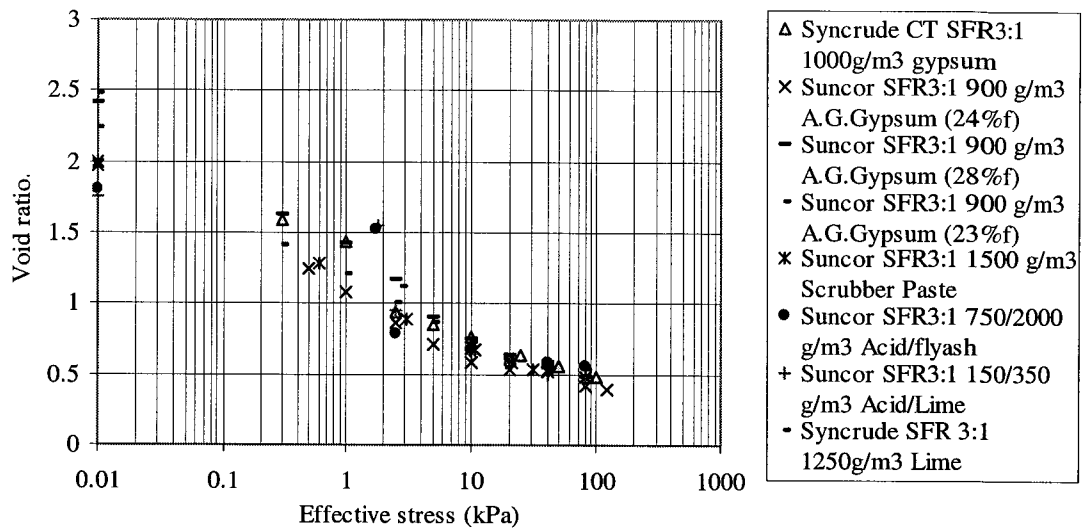


Figure 7.6 Compressibility of oil sand tailings SFR 3:1 with different additives

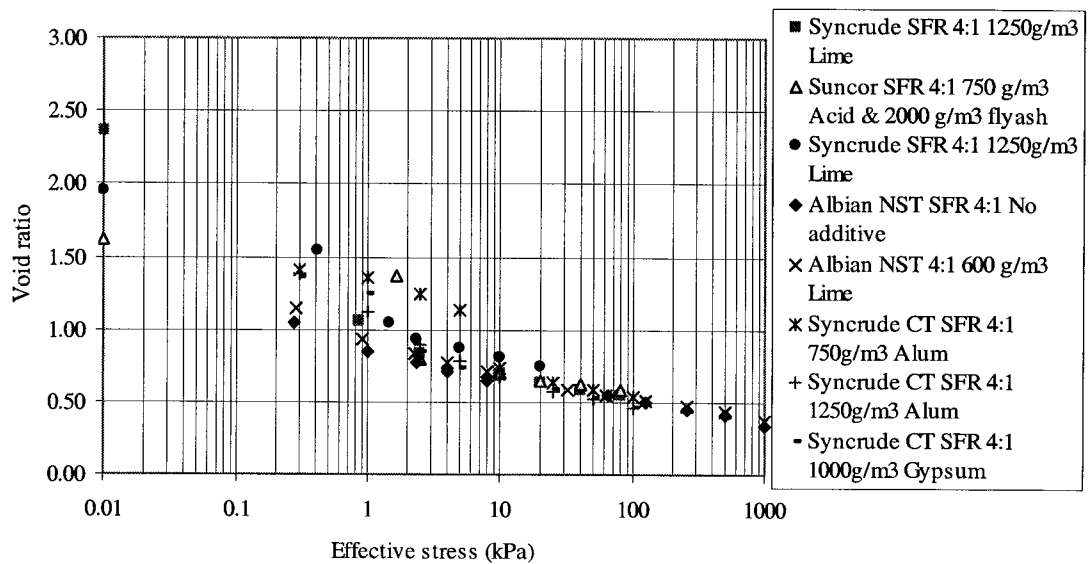


Figure 7.7 Compressibility of oil sand tailings SFR 4:1 with different additives

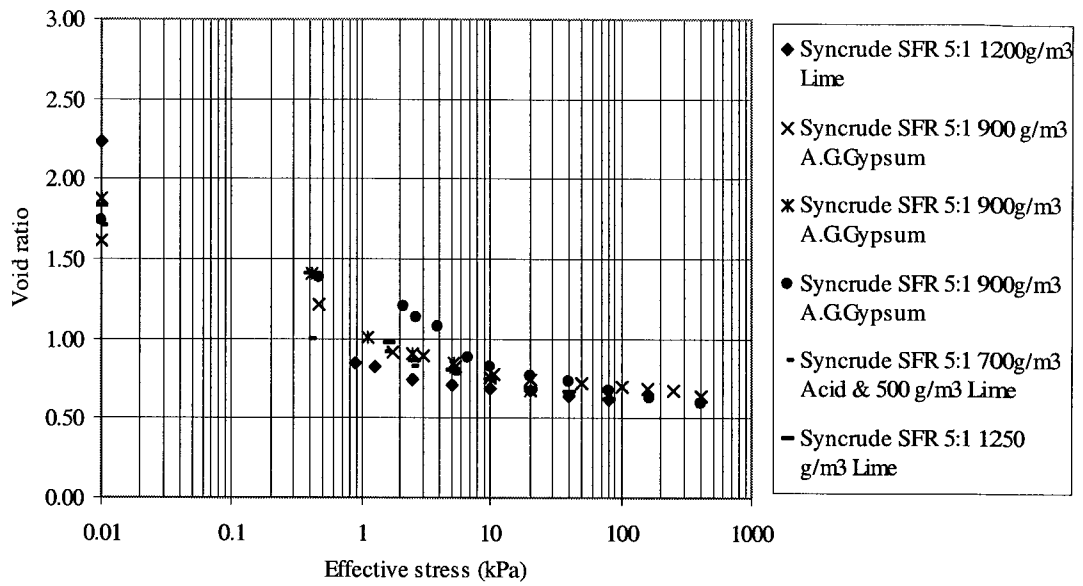


Figure 7.8 Compressibility of oil sand tailings SFR 5:1 with different additives

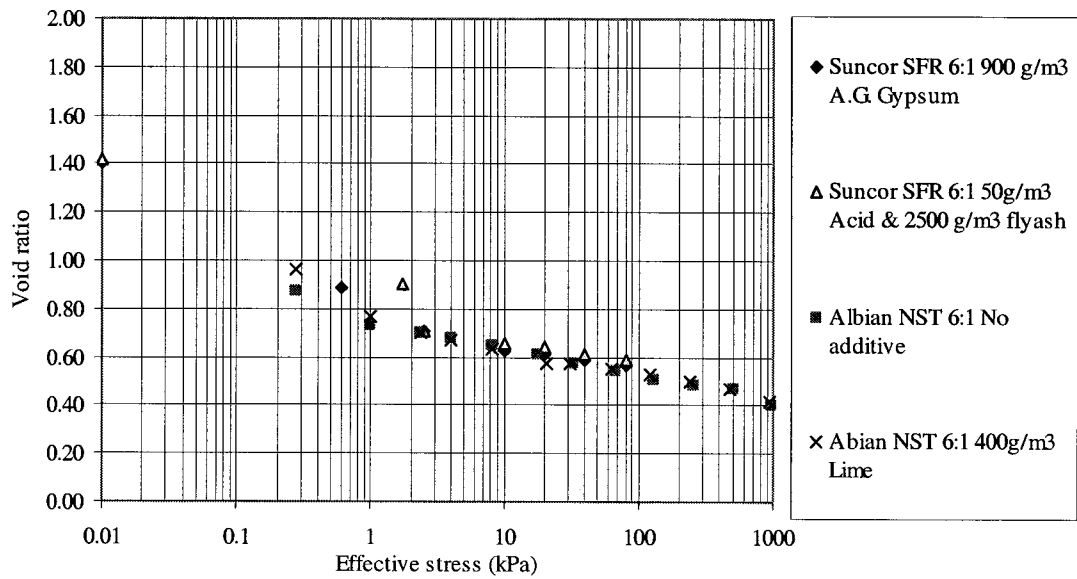


Figure 7.9 Compressibility of oil sand tailings SFR 6:1 with different additives

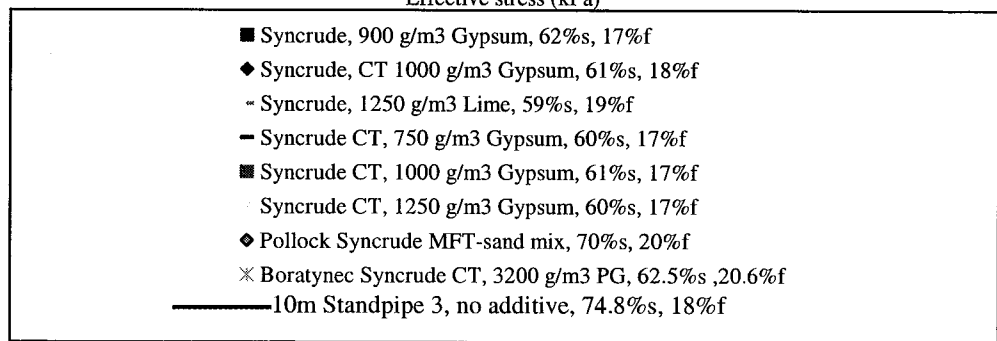
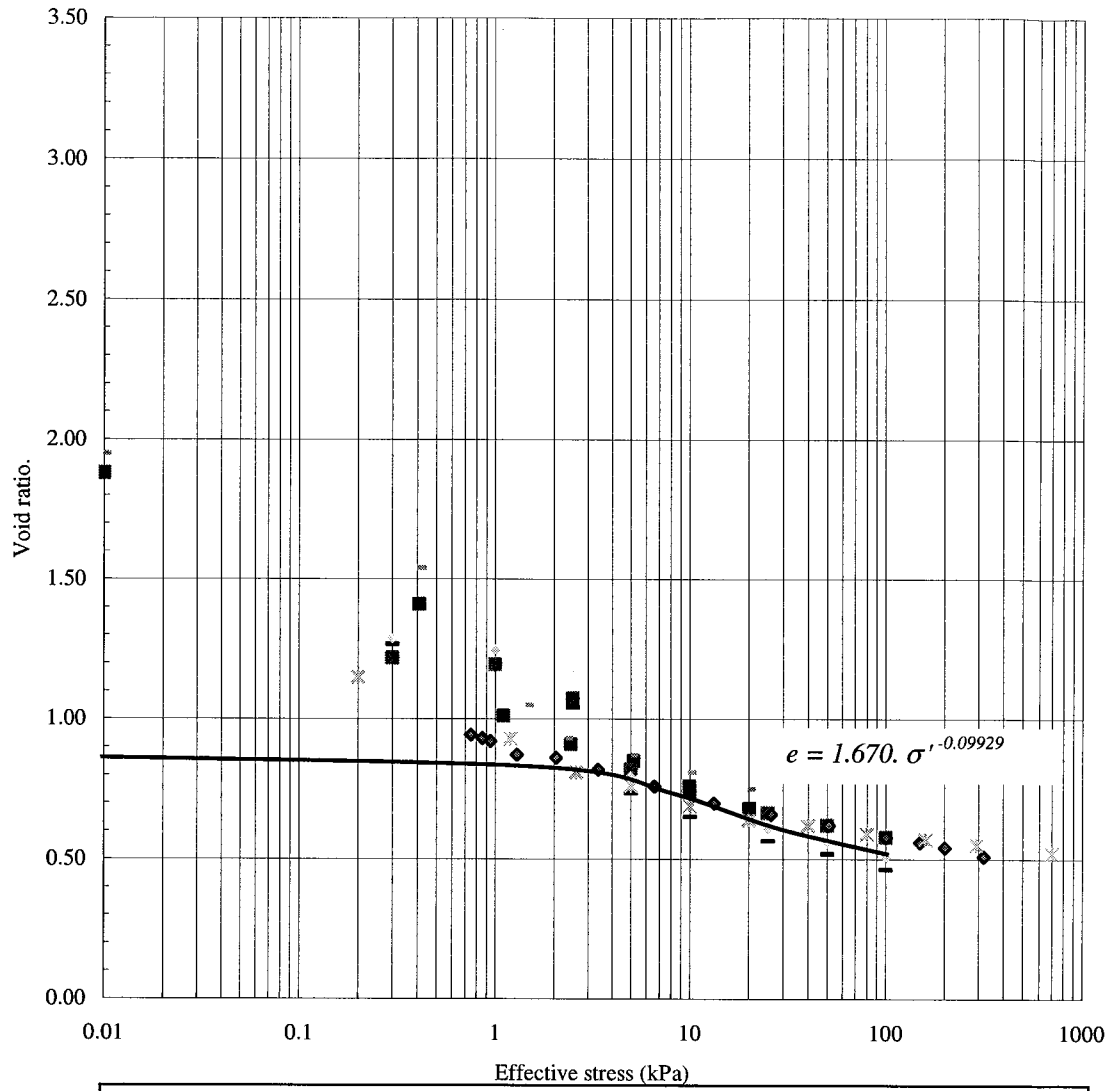


Figure 7.10 Selected compressibilities of fine tailing with sands

7.2.2 Hydraulic conductivity-void ratio relationship

Figure 7.11 shows 11 tests of hydraulic conductivity values for different samples of mature fine tailings. Unlike the void ratio-effective stress behaviour, hydraulic conductivity-void ratio behaviour is not influenced by the initial void ratio. This suggests that the thixotropic gel strength does not significantly change the pore system of the slurry; therefore the effect of thixotropic gel strength on the hydraulic conductivity is not significant. However more investigation is suggested.

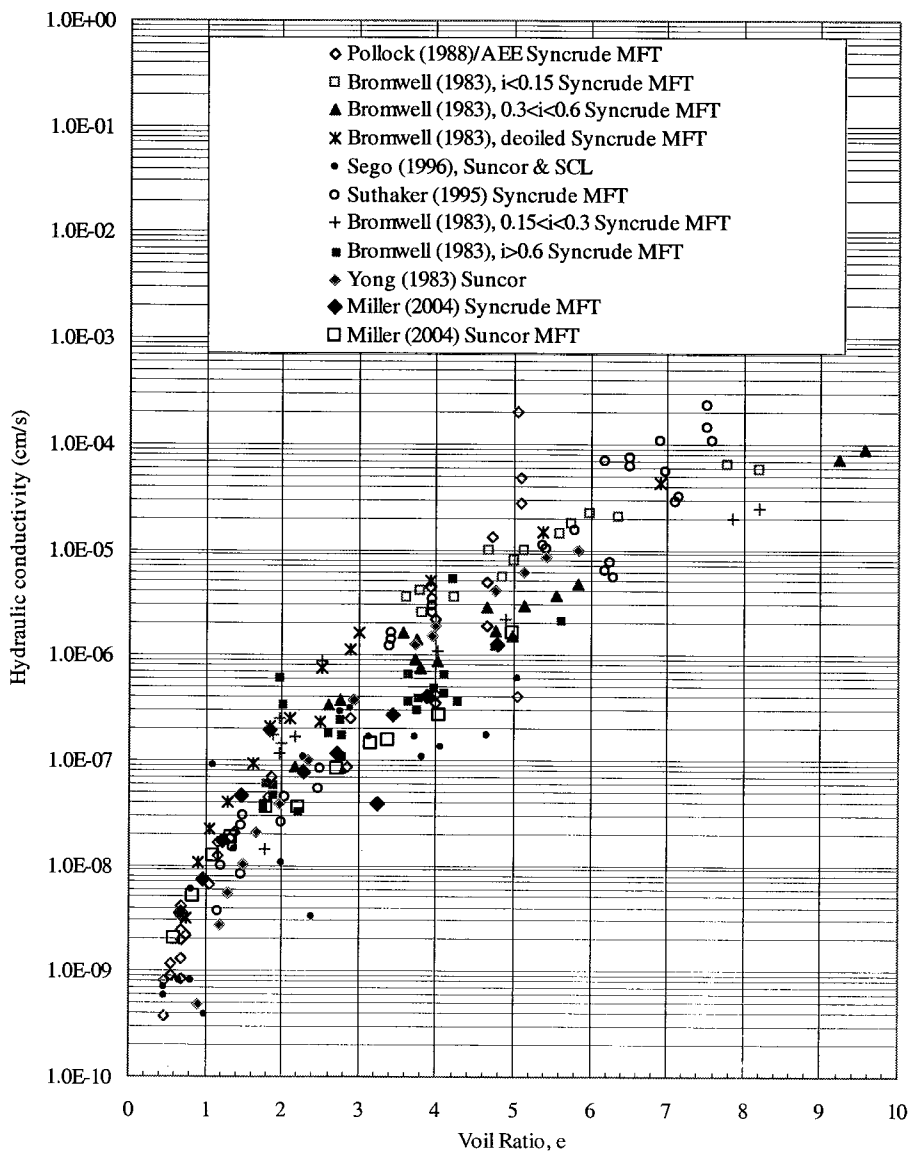


Figure 7.11 Hydraulic conductivities of mature fine tailings

In Figure 7.12, the hydraulic conductivity of the materials from all 3 standpipes (Pollock, 1988) are shown. It has been found that in MFT-tailings sand mixes, when all data are put in a fines void ratio format, all data points fall on a line. The fines void ratio is defined as:

$$e_f = \frac{e \times G_f}{G_s \times f} \quad (7.4)$$

Where

- e_f = Fines void ratio
- e = Void ratio
- G_f = Specific gravity of fines (fines and attached bitumen)
- G_s = Specific gravity of solids (sand, fines and attached bitumen)
- f = Fines content

This means the hydraulic conductivity is controlled by the fines content. A best fit line is plotted for this data and its equation is shown. The influence of the sand on the hydraulic conductivity appears to be only as a filler, which decreases the fines concentration for a given volume. Therefore, in terms of total void ratio, the hydraulic conductivity changes with changes in the sand content.

From Figure 7.12, by knowing the amount of fines in each standpipe material, and using the hydraulic conductivity – fines void ratio equation, the hydraulic conductivity – void ratio relationships of the materials in the ten meter standpipes can be obtained (Figure 7.13).

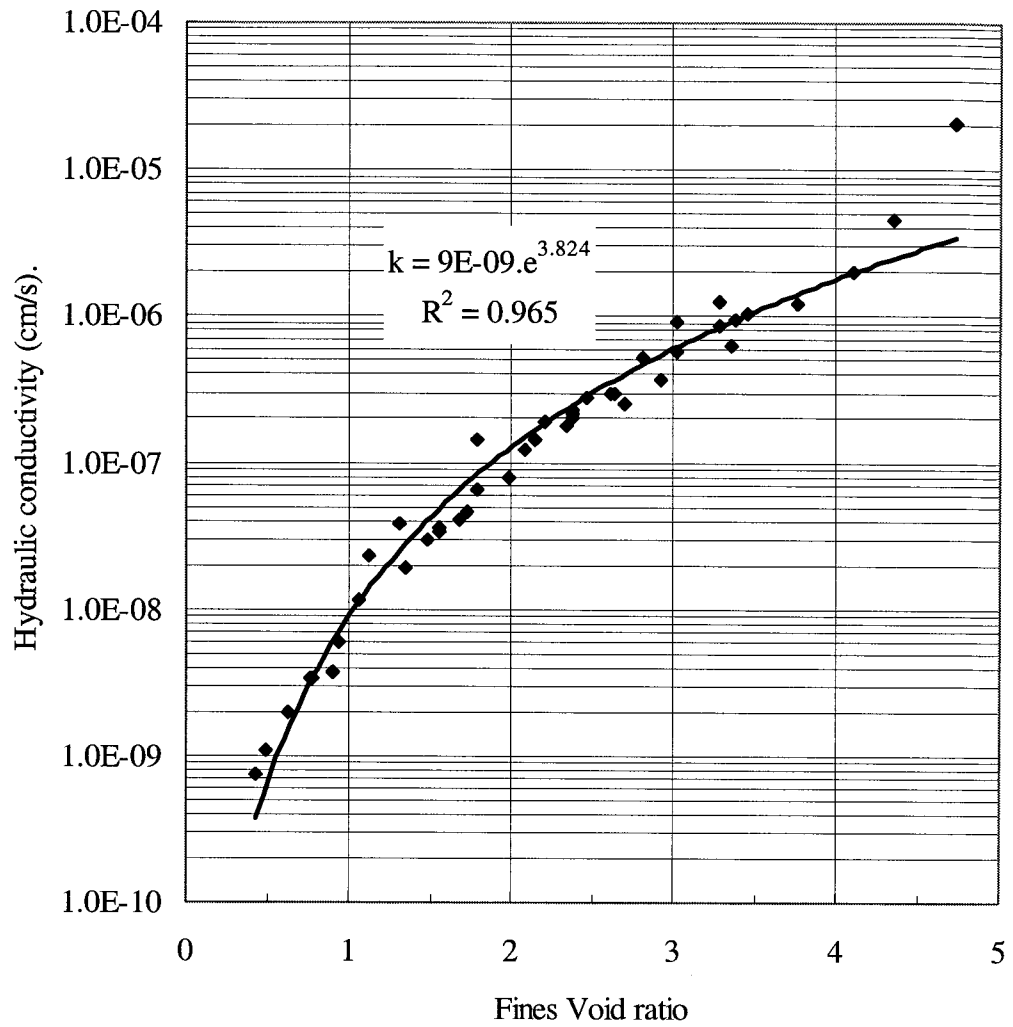


Figure 7.12 Hydraulic conductivity - fines void ratio relationship of tailings materials in the ten meter standpipes

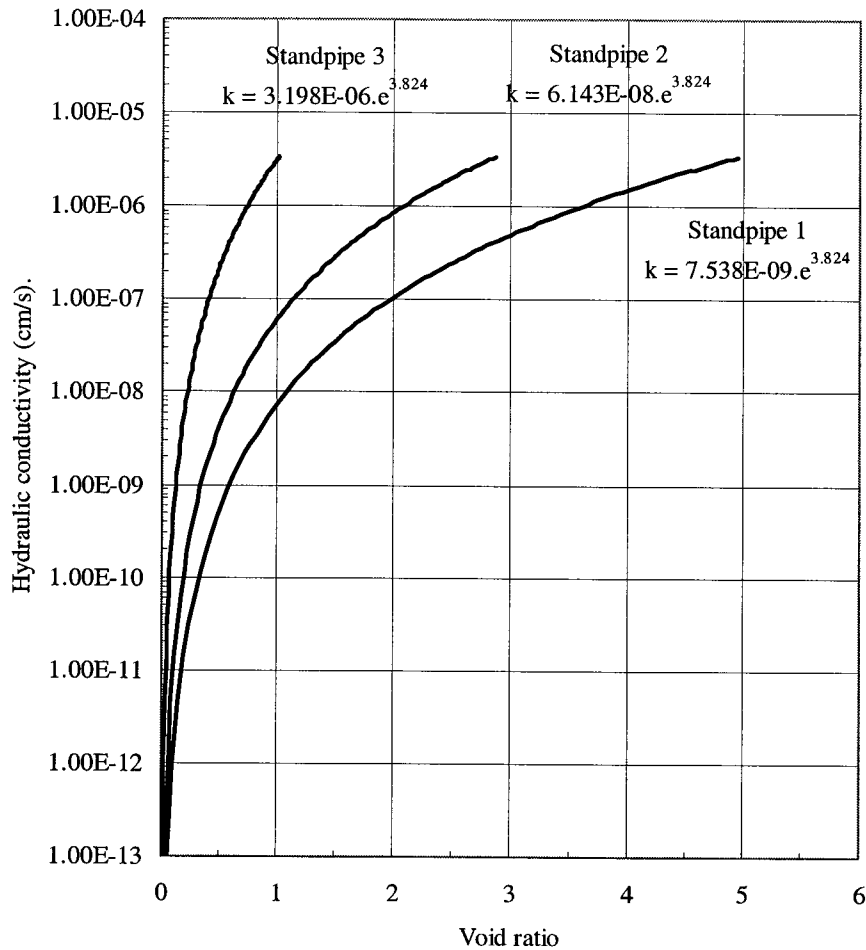


Figure 7.13 Hydraulic conductivity – void ratio relationships for the tailings materials in the ten meter standpipes

The chosen relationships in Figures 7.12 and 7.13, however, need to be compared with other sets of data to strengthen the confidence of using these relationships. Some available data on Syncrude and Suncor fine tailings-sand mixes have been chosen for this purpose based on the similarity of the mineralogy of the materials

In Figure 7.14, hydraulic conductivity-void ratios from 36 tests of oil sand tailings materials are shown. As the fines content varies between 14% and 30% the data is very

scattered. By changing the void ratio to fines void ratio, Figure 7.15 is obtained. Although the fines void ratio is used, the data set is still varying and difficult to interpret. This may be a result of different additives, amount of additives and/or the particle size distribution of the fines (that is the amount of clay in the fines). Also, test procedures and experiment difficulties can contribute to some distortion to the data set. It can be seen that the effect of these variables becomes smaller as the soils approach a lower void ratio. This would indicate that it is the additive variations that are affecting the hydraulic conductivity.

To compare with data obtained from the ten meter standpipe materials, several large strain consolidation tests are selected based on type of additives that appear to have the least effects on the hydraulic conductivity and the results are shown in Figure 7.16. The tests show very good agreement to the chosen hydraulic conductivity-void ratio relationship for the ten meter standpipe material in Figure 7.12. Therefore the hydraulic conductivity-void ratio relationships shown in Figure 7.13 are considered satisfactory and represent the hydraulic conductivity of the oil sand tailings without any additive.

From Figure 7.13, the hydraulic conductivity-void ratio relationships of the three standpipe tailings materials, MFT, MFT-tailings sand mix with 48% sand and MFT-tailings sand mix with 82% sand, can be expressed with equations 7.5, 7.6, and 7.7 respectively.

$$k = 7.538E - 9.e^{(3.824)} \quad (7.5)$$

$$k = 6.143E - 8.e^{(3.824)} \quad (7.6)$$

$$k = 3.198E - 6.e^{(3.824)} \quad (7.7)$$

Where k is hydraulic conductivity in cm/s and e is void ratio.

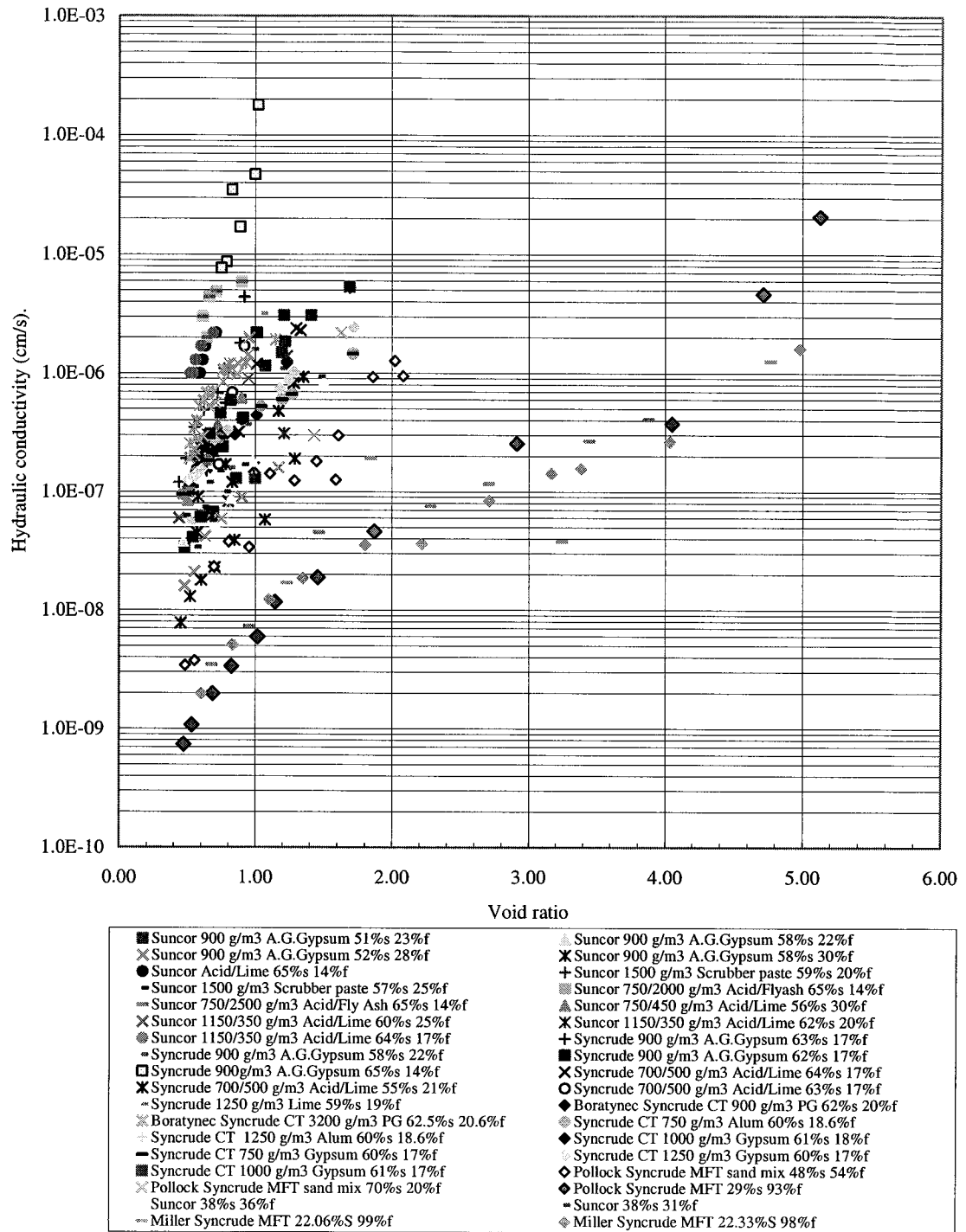


Figure 7.14 Hydraulic conductivity – void ratio of various oil sands tailings materials

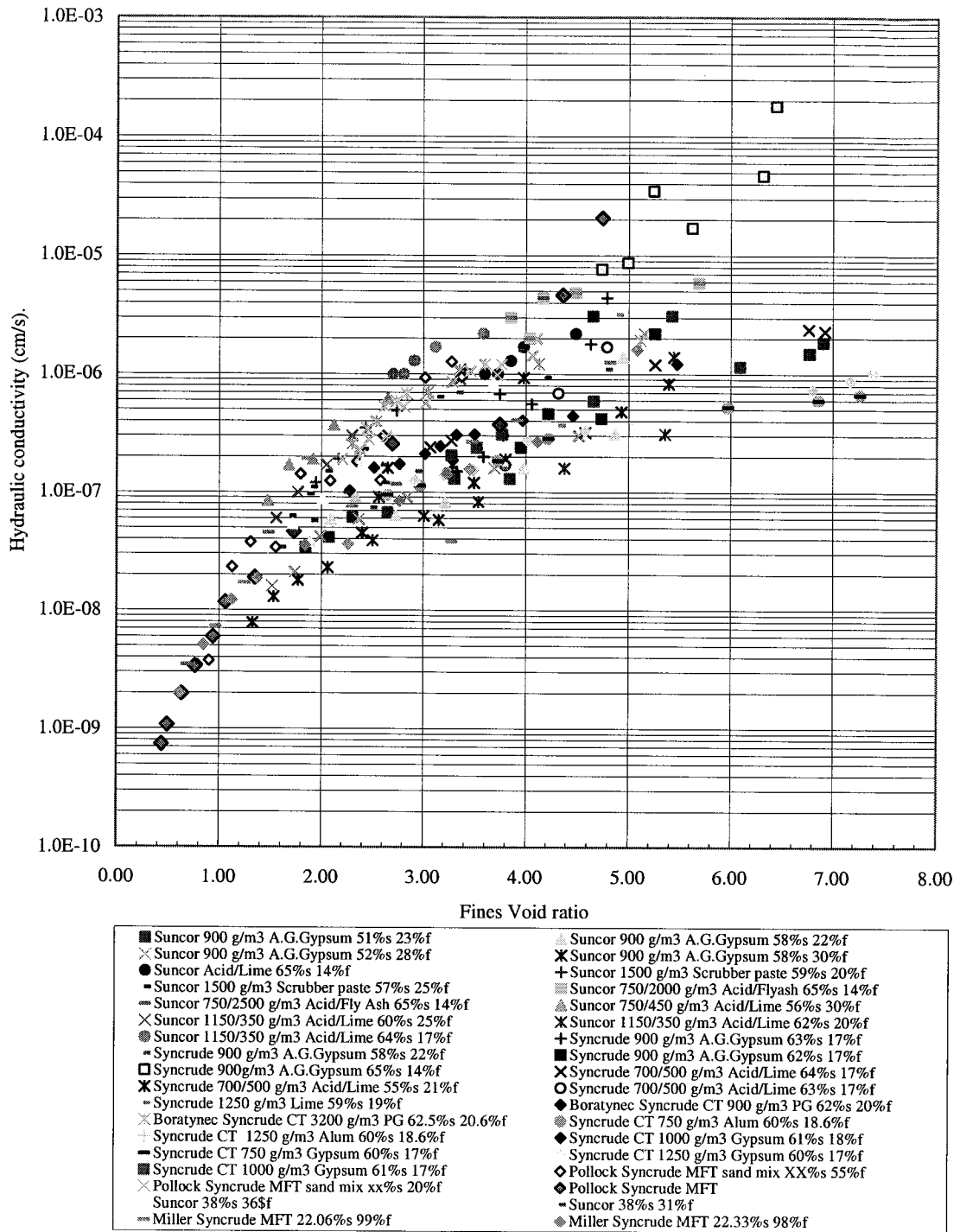
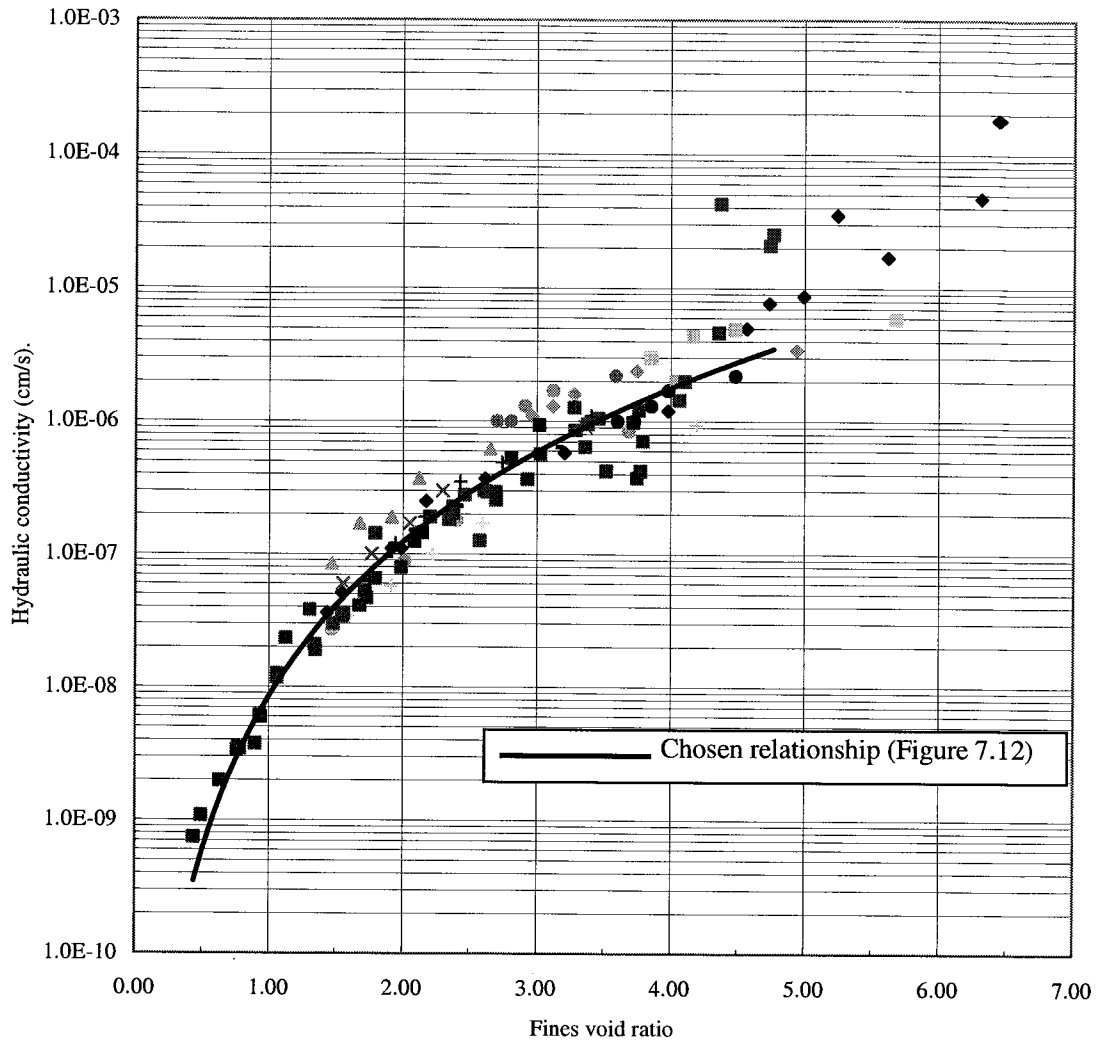


Figure 7.15 Hydraulic conductivity – fines void ratio of various oil sands tailings materials



◆ Suncor 900g/m3 A.G.Gypsum 57% <i>s</i> 24% <i>f</i>	◆ Syncrude 900g/m3 A.G.Gypsum 65% <i>s</i> 14% <i>f</i>
+ Suncor 1500g/m3 Scrubber paste 59% <i>s</i> 20% <i>f</i>	- Suncor 1500g/m3 Scrubber paste 57% <i>s</i> 25% <i>f</i>
▲ Suncor 750/450 g/m3 Acid/Lime 56% <i>s</i> 30% <i>f</i>	× Suncor 1150/350 g/m3 Acid/Lime 60% <i>s</i> 25% <i>f</i>
⊗ Suncor 1150/350 g/m3 Acid/Lime 64% <i>s</i> 17% <i>f</i>	● Suncor 700/450 g/m3 Acid/Lime 65% <i>s</i> 14% <i>f</i>
⊗ Suncor 38% <i>s</i> 36% <i>f</i>	+ Suncor 38% <i>s</i> 31% <i>f</i>
◇ Suncor 750/2500 g/m3 Acid/Fly Ash 64% <i>s</i> 17% <i>f</i>	≡ Suncor 750/2500 g/m3 Acid/Fly Ash 65% <i>s</i> 14% <i>f</i>
■ 10m Standpipe materials (Pollock 1988)	

Figure 7.16 Hydraulic conductivity – fines void ratio of chosen oil sands tailings materials

7.3 Theories of Consolidation

Consolidation of fine grained soils is one of the major aspects of geotechnical engineering. It was studied and developed as a major subdiscipline of civil engineering, known initially as soil mechanics. The original consolidation theory was developed by Karl Terzaghi, who dominated the geotechnical engineering profession for the first forty five years of its life. The theory is still valid and is used for almost all consolidation problems in geotechnical engineering. Terzaghi's work was the first starting place of all studies of consolidation as well as other subjects related to the deformation of porous media with flowing fluid through the medium.

All oil sands fine tailings, however, undergo large deformations during consolidation and thus the Terzaghi infinitesimal strain consolidation theory is not applicable and the finite strain consolidation theory is used. In this section, the finite strain consolidation theory is presented.

7.3.1 Finite Strain Theory

It is noted that the scope of this thesis is not to develop a new numerical model or theory but to suggest modifications for the use of the finite strain consolidation theory so it becomes adequate in predicting fine tailings consolidation behaviour.

Large Strain Slurry Consolidation Software for Mine Tailings - Deltaic Deposits - Soft Soils or "FSconsol Version 2.5" of GWP Software Inc provided by Gord Pollock is used for consolidation prediction in this thesis. The program which has been developed mainly by Pollock (1988) is based on the reformulation of the governing equation (Gibson, England, and Hussey, 1967) in term of excess pore pressure instead of void ratio presented by Somogyi (1980).

Somogyi gives the continuity of fluid flow relationship:

$$\frac{\partial}{\partial z} \left[-\frac{k}{\gamma_f (1+e)} \frac{\partial u}{\partial z} \right] + \frac{de}{d\sigma'} \frac{\partial \sigma'}{\partial t} = 0 \quad (7.8)$$

A time dependent effective stress equation is as following.

$$\frac{\partial \sigma'}{\partial t} = (D_R - 1) \gamma_f \frac{d(\Delta z)}{dt} - \frac{\partial u}{\partial t} \quad (7.9)$$

where D_R is the relative density and Δz is the material coordinate difference between the surface and the point of interest. By combining equations 7.8 and 7.9, the governing equation for the excess fluid pressure is obtained.

$$\frac{\partial}{\partial z} \left[\frac{k(e)}{\gamma_f (1+e)} \frac{\partial u}{\partial z} \right] + \frac{\partial e}{\partial \sigma'} \left[(D_R - 1) \gamma_f \frac{d(\Delta z)}{dt} - \frac{\partial u}{\partial t} \right] = 0 \quad (7.10)$$

Somogyi then uses the power law form to handle the nonlinearity of void ratio-effective stress and hydraulic conductivity-void ratio relationships.

$$e = A \sigma'^B \quad (7.11)$$

$$k = C e^D \quad (7.12)$$

where A , B , C and D are curve fitted constants. The governing equation 7.10 is then changed to

$$\frac{\partial u}{\partial t} + \frac{\sigma'^\beta}{a} \left(\frac{k}{1+e} \right) \frac{\partial^2 u}{\partial z^2} + \frac{\sigma'^\beta}{a} \frac{\partial \left(\frac{k}{1+e} \right)}{\partial z} \frac{\partial u}{\partial z} = \gamma_b \frac{d(\Delta z)}{dt} \quad (7.13)$$

where

$$\gamma_b = \gamma_s - \gamma_f$$

$$a = AB \gamma_f$$

$$\beta = 1 - B$$

Somogyi chooses a fully implicit central finite difference method due to its stability to solve equation 7.13. The disadvantage of this method is that it needs to know u , σ' , e and k at the next time step in order to calculate the present time. To overcome this problem, the present time step is put to the next time step with a very small increment of time step to insure that little variation will occur. Somogyi states that the stability of the implicit finite difference method will cause the error introduced by this approximation to decay. The governing equation 7.13 in terms of differences becomes

$$S_{i,j}\delta(K_{i,j} + D_{i,j})u_{i+1,j+1} + (1 - 2S_{i,j}K_{i,j}\delta)u_{i,j+1} + S_{i,j}\delta(K_{i,j} - D_{i,j})u_{i-1,j+1} = u_{i,j} + \gamma_b \Delta z \quad (7.14)$$

where

$$S_{i,j} = \frac{\sigma'_{i,j}}{a}$$

$$K_{i,j} = \frac{k_{i,j}}{(1 + e_{i,j})}$$

$$D_{i,j} = \frac{1}{4} \left(\frac{k_{i+1,j}}{1 + e_{i+1,j}} - \frac{k_{i-1,j}}{1 + e_{i-1,j}} \right)$$

$$\delta = \frac{\Delta t}{(\Delta z)^2}$$

i is the material coordinate index, j is the time index, Δt is the time increment, and Δz is the material coordinate increment.

For the boundary condition, at an impermeable lower boundary which has $v_s = v_f = 0$, which will cause Darcy's law to yield $\partial u / \partial z = 0$, becomes in the term of differences $u_{i+1} = u_{i-1}$. For a permeable boundary, it simply sets the excess pore water pressure to zero. For the pond filling problem, the upper boundary will be defined by an immediate solids content which defines the break between sedimentation and consolidation. At this solids content an initial void ratio, effective stress, and hydraulic conductivity can be calculated. The excess fluid pressure at the boundary is set to be zero.

For a standpipe analysis where the initial filling is assumed to be instantaneous, the void ratio throughout the depth is assumed to be constant and the excess fluid pressure is equal to the linear buoyant stress distribution at time $t = 0$.

Once the initial and boundary conditions are satisfied, the governing equation can be solved. When excess fluid pressure is obtained, effective stress, void ratio and hydraulic conductivity can be calculated. The void ratio is then used to calculate the height of the consolidating mass. It is noted that the material parameters A , B , C , and D from laboratory testing are very important, the accuracy of the finite strain theory depends on these parameters.

7.3.1.1 Finite strain consolidation model and variation of input relationships

Suthaker (1995) evaluated how the change of compressibility and hydraulic conductivity relationships affect the consolidation prediction in an oil sands tailings deposit. It was concluded that if the compressibility of the fine tailings in the disposal pond is different from that used in the model, the settlement may not substantially vary from the prediction. The variation in hydraulic conductivity, however, has a strong impact on the prediction of settlement rate but no effect on the ultimate amount of settlement. The general behaviour of the finite strain consolidation model for interface settlement prediction is demonstrated in Figures 7.17, 7.18, 7.19 and 7.20. These predictions are based on an initial solids content of 30%, an initial height of 10 m and the finite strain parameters in Table 7.5.

Table 7.5 Finite strain parameters

Case	Multiplying factor	Compressibility (Pa)		Hydraulic conductivity (cm/s)	
		A	B	C	D
1	1.0	28.71	-0.3097	7.54E-09	3.824
2	1.5	43.07	-0.3097	7.54E-09	3.824
3	2.0	57.42	-0.3097	7.54E-09	3.824
4	1.5	28.71	-0.3097	1.13E-08	3.824
5	2.0	28.71	-0.3097	1.51E-08	3.824

From a demonstration of a short term analysis (Figures 7.17 and 7.18), the compressibility variations do not have any influence in the first 5 years but the variations in the hydraulic conductivity relationship have a strong influence on the predicted rate and amount of settlement. For a long term analysis (Figure 7.19 and 7.20), where the ultimate settlement is concerned, the variations of compressibility become very important and have a strong influence on a final settlement amount. On the other hand, the variations in the hydraulic conductivity relationship do not have any effect on the final settlement.

It is important to understand that even though there is a small effect on short term prediction by a variation of compressibility in fine tailings or in a MFT-tailing sand mix, there is a significant effect on the long term prediction or at the end of consolidation. This means that for a creep material and for high hydraulic conductivity materials in which consolidation finishes in a short period, a compressibility relationship used in the finite strain model becomes important in order to correctly estimate the ultimate settlement.

To predict the rate and amount of settlement in the short and medium term correctly, that is the first 30 years, in a tailings pond or in the 10 m standpipes, the hydraulic conductivity relationship dominates and must be correctly defined. This need is the reason for the detailed analyses of hydraulic conductivity relationships in the preceding sections of this thesis.

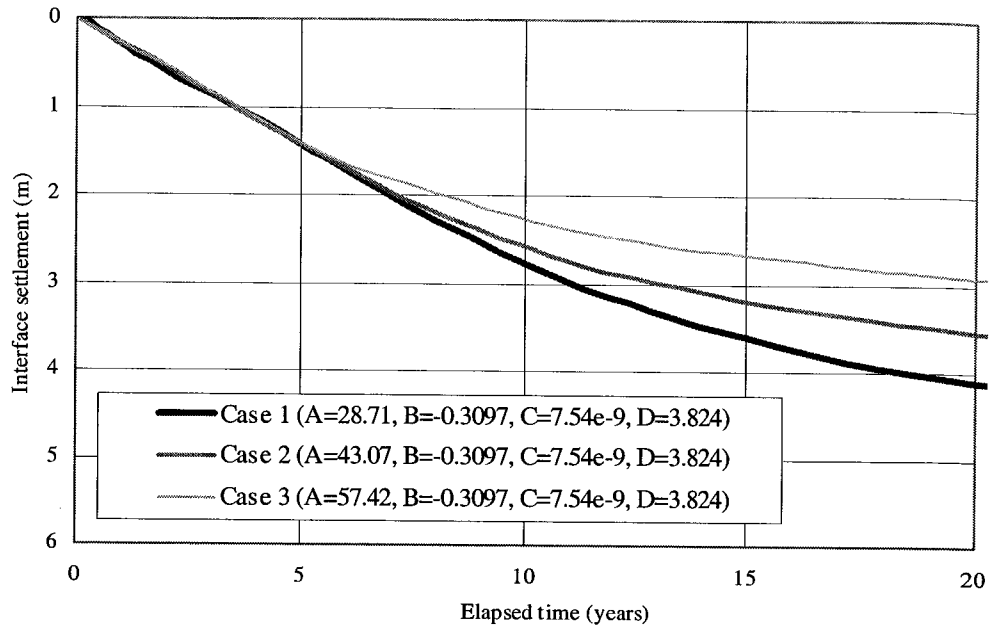


Figure 7.17 Varied Compressibility and interface settlement prediction for short term

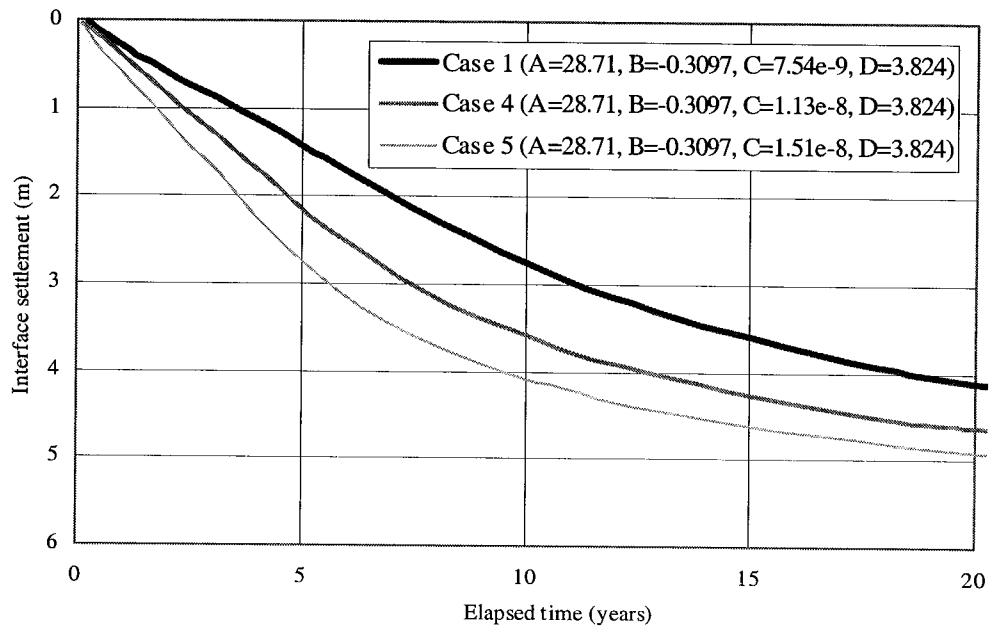


Figure 7.18 Varied hydraulic conductivity and interface settlement prediction for short term

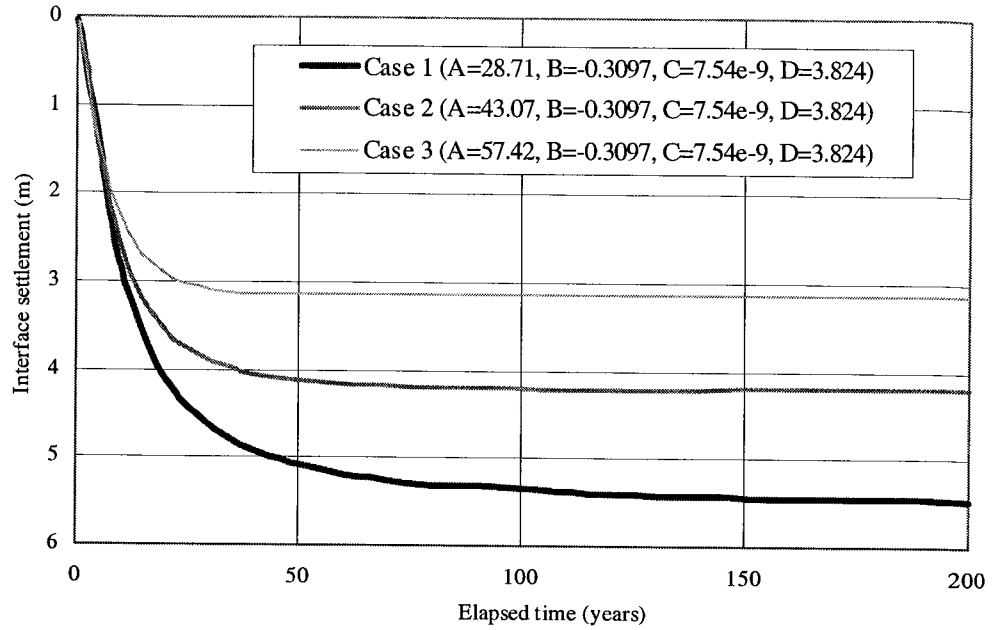


Figure 7.19 Varied Compressibility and interface settlement prediction for long term

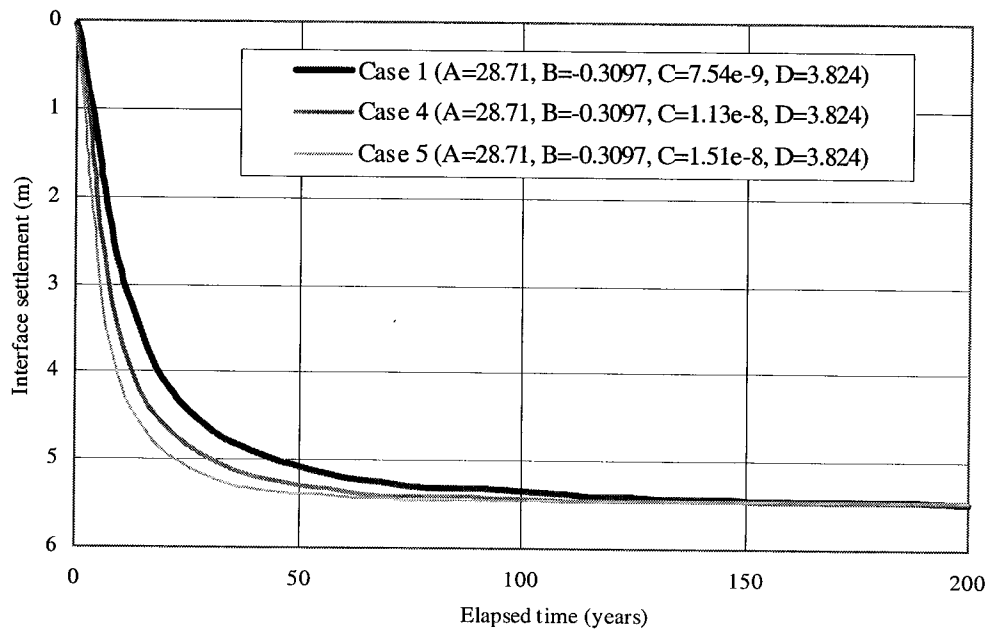


Figure 7.20 Varied hydraulic conductivity and interface settlement prediction for long term

7.4 Stress- Strain-Strain Rate Relationship for the Compressibility of Clays

Before proceeding with the analysis of finite strain consolidation theory, an important discussion about the effect of rate of strain, which will be used in the consolidation prediction, must be drawn.

The stress-strain behaviour of many lightly overconsolidated clays is quite strongly time dependent. For example, the preconsolidation pressure and the undrained shear strength are found to be strongly dependent in the field on the speed of loading or in the laboratory on the rate of straining. This topic was presented by Bjerrum (1967) who proposed that the compression of clays be divided into two components; instantaneous compression and delayed compression (Figure 7.21). The instantaneous compression means an increase in effective stress is instantaneously transferred to the clay skeleton and the delayed compression means a reduction of the soil volume under constant vertical effective stress. Previous analyses recognized that secondary consolidation was a creep phenomenon that resulted in a reduction of soil volume under constant vertical effective stress. Bjerrum's extension proposed that creep was also occurring during primary consolidation. Regarding time, it was argued that the compressibility characteristics of clays can not be described by a single e - $\log p$ curve, but by a family of similar curves each of which corresponds to a specific time of loading as shown in Figure 7.22.

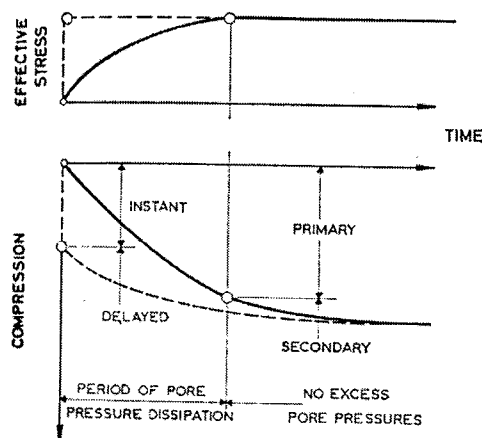


Figure 7.21 Instant and delayed compression compared with primary and secondary compression (Modified from Bjerrum 1967).

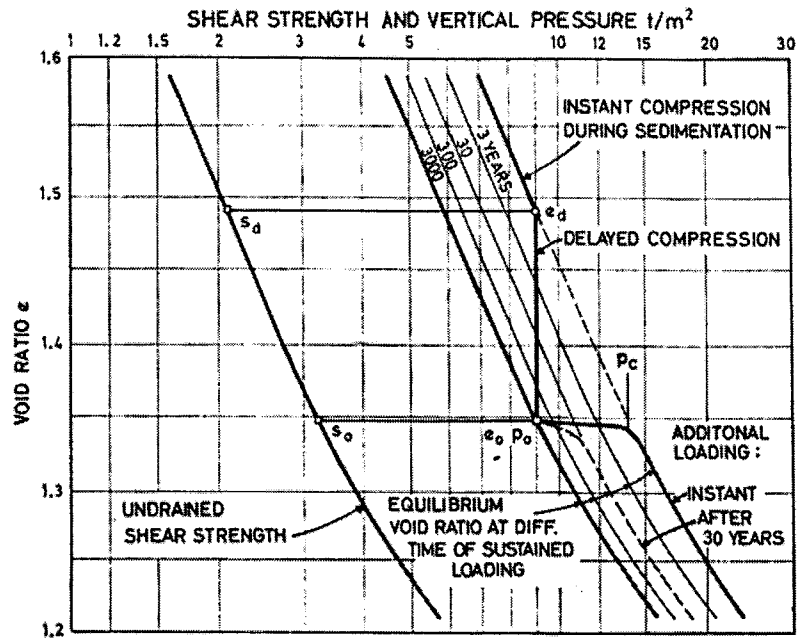


Figure 7.22 Compressibility and shear strength of clay exhibiting delayed consolidation (Modified from Bjerrum 1967).

From Figures 7.21 and 7.22, it can be seen that instant compression can be achieved only at the drainage boundary where the pore pressure can dissipate instantaneously. For soil below this drainage boundary the time of dissipation will be different and this will consequently lead to a different e - $\log p$ curve in a single homogeneous clay layer. This concept is supported by laboratory measurements (Imai and Tang, 1992, Imai and Hawlader, 1997). It is clear from this concept that a single compression curve or a constitutive equation in a form of $f(e, \sigma', t) = 0$ can only be used to approximate consolidation behaviour of a whole clay layer.

A recent development of this subject is presented by Yin and Graham (2000) who use Bjerrum's original idea (Bjerrum, 1967) to develop an Elastic Viscoplastic Model. They show that settlement is a combination of instant compression and delayed compression. Delayed compression is solely caused by the effect of creep. The higher the creep parameter, the greater the effect of strain rate, or the slower the strain rate, the greater the amount of creep.

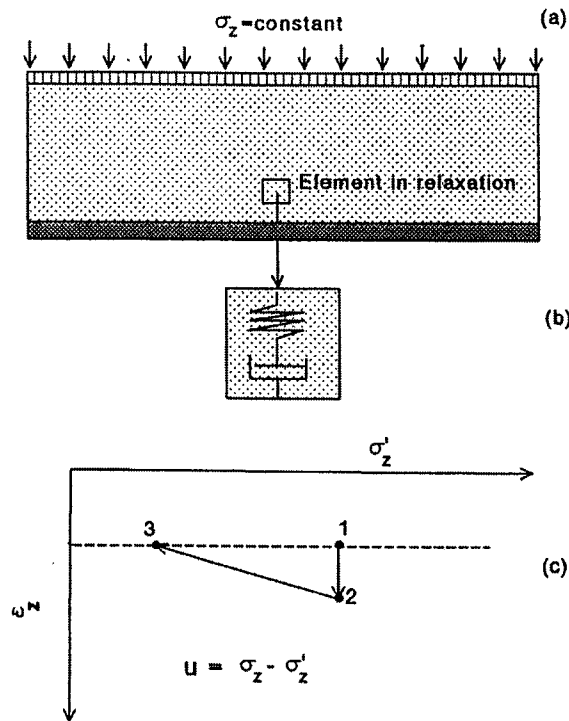


Figure 7.23 Schematic of pore water pressure increase during relaxation (a) A consolidating layer (b) an element in relaxation (c) Stress-strain state in relaxation (Modified from Yin et al. 1994)

From the Elastic Viscoplastic constitutive model, Yin et al. (1994) show that soils with significant creep behaviour (or secondary compression) can have pore water pressures that increase some time after the loading is applied. This phenomenon is explained by Figure 7.23a showing a schematic of a layer of clay consolidating under constant loading σ_z . The top of the layer is drained and the bottom is undrained. Assume that the clay was fully consolidated before the loading was added, that is, u_e was zero at time zero time. When the load is increased, the excess pore water pressure is increased by the same amount after zero time. The excess pore water pressures will then start to dissipate. The water near the drained boundary starts to drain. The water near the top of the layer of the drained boundary will come out first, at the same time the water in the interior remains immobile for some time. From Figure 7.23b, at a position near the undrained boundary, the water in the mass and therefore the volume of the mass, remains unchanged for sometime after loading. This means that the element near the undrained

boundary is in a state of relaxation where the volume remains constant but the effective stress decreases. In relaxation at a constant volume and constant total stress, decreases in effective stress in the soil skeleton must be balanced by increases in pore water pressure. Figure 7.23c explains this process qualitatively. The stress-strain state of the element is at point 1 at some time after loading. Since the behaviour of the clay is viscous, the soil skeleton is tending to creep with time from point 1 to point 2. However, since water in the element has not yet started to move, the vertical strain is constant. This implies that the stress-strain state can not move from point 1 to point 2 but instead must unload elastically to point 3 at the same strain. Here expansive elastic strains are equal and opposite of plastic creep strains. The decreases in vertical effective stress produce increases in pore water pressure (Yin et al. 1994).

With the above discussion, it can be explained, for example, that for the 10 m Standpipe 1 which exhibits significant creep behaviour, the increase in the excess pore water pressure at the beginning of the test is due to creep which is significant after the thixotropic gel strength builds up. The slow bond yielding or creep behaviour most likely generates increases of excess pore water pressure and at the same time pore water pressure dissipation slowly occurs and is governed by the hydraulic conductivity and length of drainage path. Overall excess pore water pressure behaviour, therefore, is a combination of creep inducing pore water pressure and dissipation of pore water pressure controlled by hydraulic conductivity.

The elastic viscoplastic model of Yin (1994) is a significant development and provides a good understanding of the effect of strain rate on compressible clays based on physics and mathematics. However, it is a small strain theory, hydraulic conductivity is assumed to be constant and compressibility is assumed to be linear. Therefore the theory can not be applied for a large deformation analysis such as consolidation of slurries.

Another interesting discussion regarding effect of strain rate on consolidation behaviour is given by Leroueil et al. (1985). It is shown that there exists a unique stress-strain-strain rate relationship. The effective stress-strain is normalized by

preconsolidation pressure and used for a rheological model for natural clays. This rheological behaviour of natural clays is described by the two equations shown below.

$$\sigma'_p = f(\epsilon'_v) \quad (7.15)$$

$$\sigma'_v / \sigma'_p = g(\dot{\epsilon}'_v) \quad (7.16)$$

Once these two relationships are known for a given soil, any stress-strain-strain rate relationship for the soil may easily be constructed as shown in Figure 7.24.

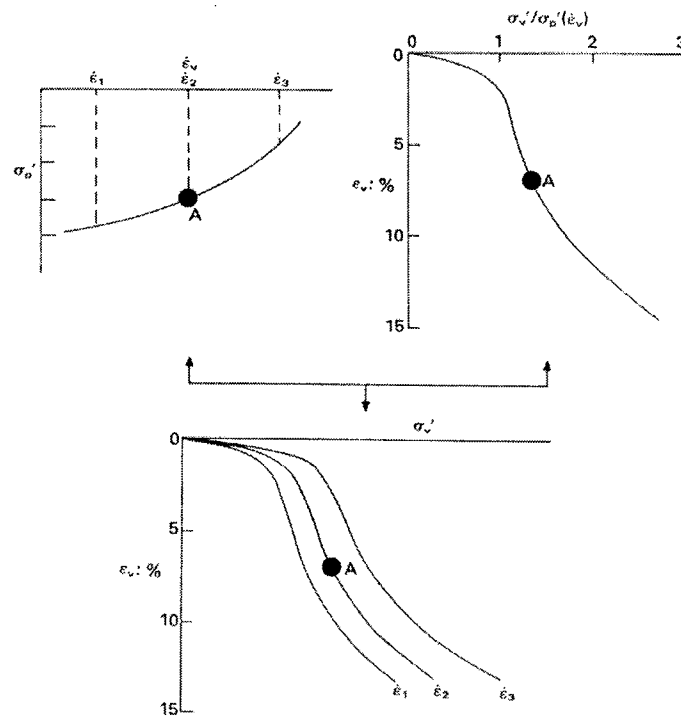


Figure 7.24 Suggested rheological model (Modified from Leroueil et al. 1985)

All of these concepts are important for the oil sand fine tailings material due to laboratory and field evidence of creep behaviour. Laboratory testing has shown that the fine tailings have a very high creep parameter and the ratio of C_α to C_c is 0.085 which is high and similar to other organic soils (Suthaker, 1995). Therefore these materials must show significant creep behaviour. Moreover, from the ten meter standpipe test 1, it is shown that volume decrease happens under zero or a very low constant effective stress. This can be explained, considering that the thixotropic gel strength overconsolidates the

soil structure which will then not consolidate until an effective stress larger than the over consolidation stress is applied. The settlement is caused by the whole soil structure reducing in volume by creep. The slow pore pressure dissipation observed with almost no gain in effective strain results from a combination of creep inducing pore pressure and a slow dissipation of pore pressure due to low hydraulic conductivity.

As a result, settlement predictions of the oil sand fine tailings must include thixotropy and creep in the analysis. From this concept, the compatibility of the present consolidation model (the finite strain consolidation model) on predicting settlement of the oil sand fine tailings will be demonstrated and discussed. The predictions will be compared with the data from the 10 m standpipes.

7.5 Consolidation Modeling by Finite Strain Consolidation Theory

7.5.1 Consolidation prediction of the ten meter Standpipe 1

For the ten meter Standpipe 1, the use of FSconsol or a finite strain consolidation program will be demonstrated along with a consideration of strain rate that affects the compressibility behaviour of thixotropic slurries.

The discussion in this section is based on the concept that the average strain rate can be calculated from the total strain divided by time at the end of primary consolidation. The average strain rate from a consolidometer test is very high compared to the 10 m standpipe thus the consolidometer compressibility test results overestimate the void ratio-effective stress relationship of the 10 m standpipe and need to be modified. In order to improve a compressibility function for the fine tailings, a normalized stress-strain relationship is developed for use for any average strain rate as explained in the following section.

7.5.1.1 Procedure to obtain void ratio – effective stress relationship

The consolidometer test average strain rate is calculated from the total test time and the total strain. For a 10 m standpipe, the rectangular hyperbolic method (Sridharan et al. 1987) is used to find the approximate end of creep compression. Then time and

strain at this stage are used to calculate the average strain rate. The results are shown in Table 7.6.

Table 7.6 Average strain rate results

Test	Average strain rate (min^{-1})
The 10 m standpipe 1	1.73×10^{-6}
Consolidometer	1.60×10^{-4}

From the Table 7.6, the strain rate of the 10 m standpipe is approximately 100 times smaller than that of the consolidometer test. This implies that the real strain or compressibility of the 10 m standpipe should be at smaller effective stresses than those in the consolidometer. To investigate this compressibility behaviour, the effective stress and strain of the 10 m standpipe and the consolidometer are plotted in Figure 7.25.

In Figure 7.25, the data points for the standpipe are very scattered and must be identified for different strain rates. An assumption is made that for a small change in effective stress, the strain rate should not vary significantly. Therefore in Figure 7.25, the most probable stress state lines are drawn through the 10 m standpipe data. The upper line is the consolidometer test, the middle line is the 10 m standpipe for effective stresses higher than ~ 0.5 kPa and the bottom line is the 10 m standpipe for stresses lower than ~ 0.5 kPa and close to zero. This means that the above assumption has been used to draw lines of different rate of strain. From these results stress-strain relationships are developed based on the observed data from the standpipe.

The stress-strain curves are then normalized by their preconsolidation pressures as shown in Figure 7.26. All the data falls into a thin band of data and an average curve is drawn. Leroueil et al. (1985) showed that in natural clays, there exists a narrow band of data of preconsolidation pressure and strain rate. In Figure 7.27, the average strain rate calculated is plotted with preconsolidation pressure similar to those performed by Leroueil et al. (1985). This diagram shows that for different rates of strain, different preconsolidation pressures will be obtained.

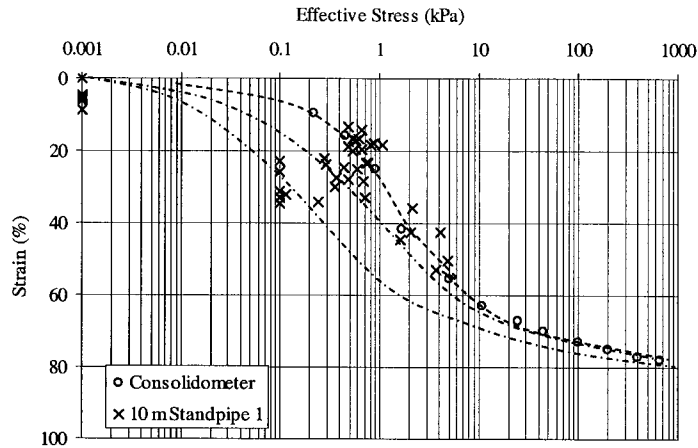


Figure 7.25 Stress-strain curve

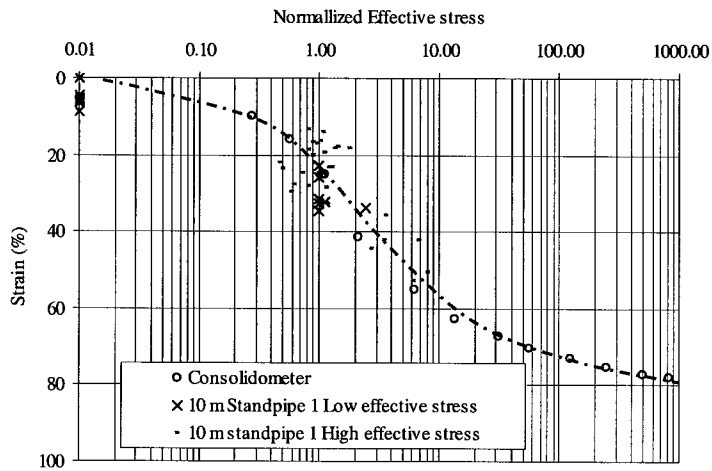


Figure 7.26 Normalized stress-strain curve

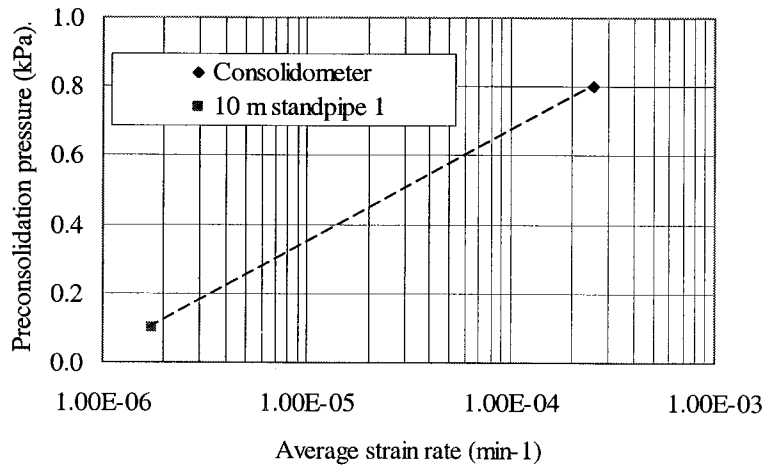


Figure 7.27 Preconsolidation-average strain rate

From Leroueil's findings, the relationship of strain rate and preconsolidation pressure is non linear but concave downward. Here the relationship is assumed to be linear due to the very small range of over consolidation stresses which are between 0 and 1 kPa. At this point a normalized stress strain relationship for any strain rate has been developed. To estimate the strain rate of the fine tailings, data from the 10 meter standpipe 1, 2 meter standpipes (from Suthaker, 1995) and consolidometer tests of the fine tailings are plotted together in 3D space in Figure 7.28.

From Figure 7.28, it can be seen that the surface tends to flatten off when the height of a deposit gets deeper. This trend indicates that for a deeper deposit (>10 m), strain and time may not be very much different from the 10 meter standpipe. This implies that the average strain rate as well as the compressibility of the deeper deposit might be similar to that of the 10 meter standpipe.

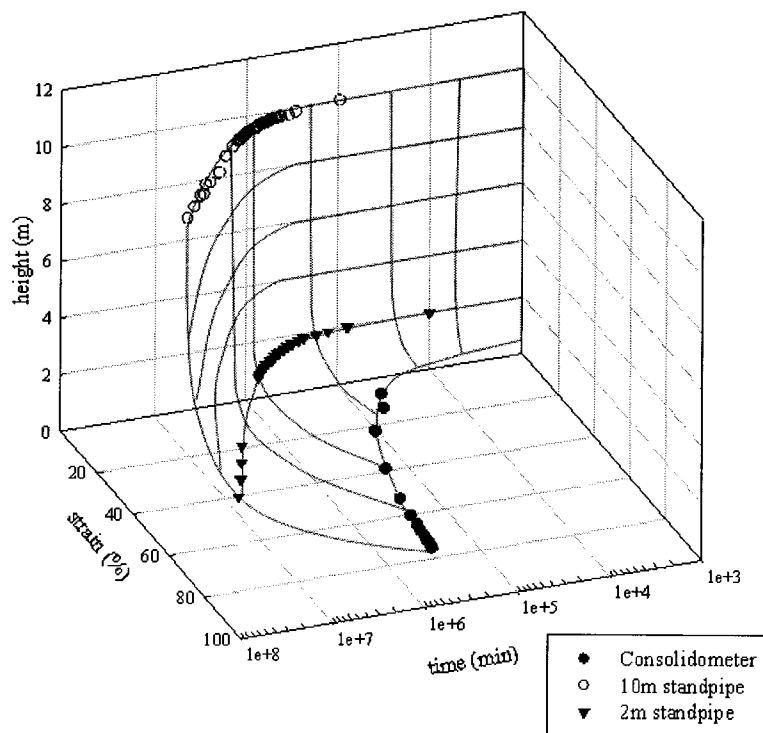


Figure 7.28 Strain – time –sample height

From Figure 7.28 the approximate rate of strain can be obtained for any sample height from 2 to 10 meters. The approximate strain rates are then used in Figure 7.27 to obtain the preconsolidation pressures. The preconsolidation pressures will be used to obtain average effective stress-strain relationships at the specific average strain rates from the normalized curve in Figure 7.26. A stress-strain relationship is then converted to an effective stress-void ratio relationship and use in a finite strain consolidation model to predict the settlement of the slurry.

7.5.1.2 Finite strain consolidation input parameters and analysis results

The finite strain consolidation theory uses two important functions which are void ratio-effective stress and hydraulic conductivity-void ratio. These functions were discussed earlier in Section 7.3.1.

For the 10 m standpipe, the heights are put in Figure 7.28 and the strain rate is calculated as $1.5E-6 \text{ min}^{-1}$. From these strain rates, the diagram in Figure 7.27 is used to obtain the preconsolidation pressure which is 0.10 kPa.

Then from the normalized curve, the stress-strain relationship of the 10 m standpipe is obtained and it is converted to a void ratio-effective stress plot (Figures 7.29 and 7.30). The compressibility relationship from the consolidometer is also shown in these figures. Clearly the effect of strain rate shifts the compressibility relationship to the left of the consolidometer measured value by an order of magnitude.

The relationship shown for the 10 m standpipe in Figure 7.29 models well the performance of the standpipe during its 21 years of settlement. The void ratio has decreased from its initial value of 5.17 to 3.34 with no measurable development of effective stress. The model indicates that the void ratio must decrease to a value approaching 2 before significant effective stresses will develop. The average void ratio in the bottom half meter is now 2.65 and effective stresses at this depth are starting to develop.

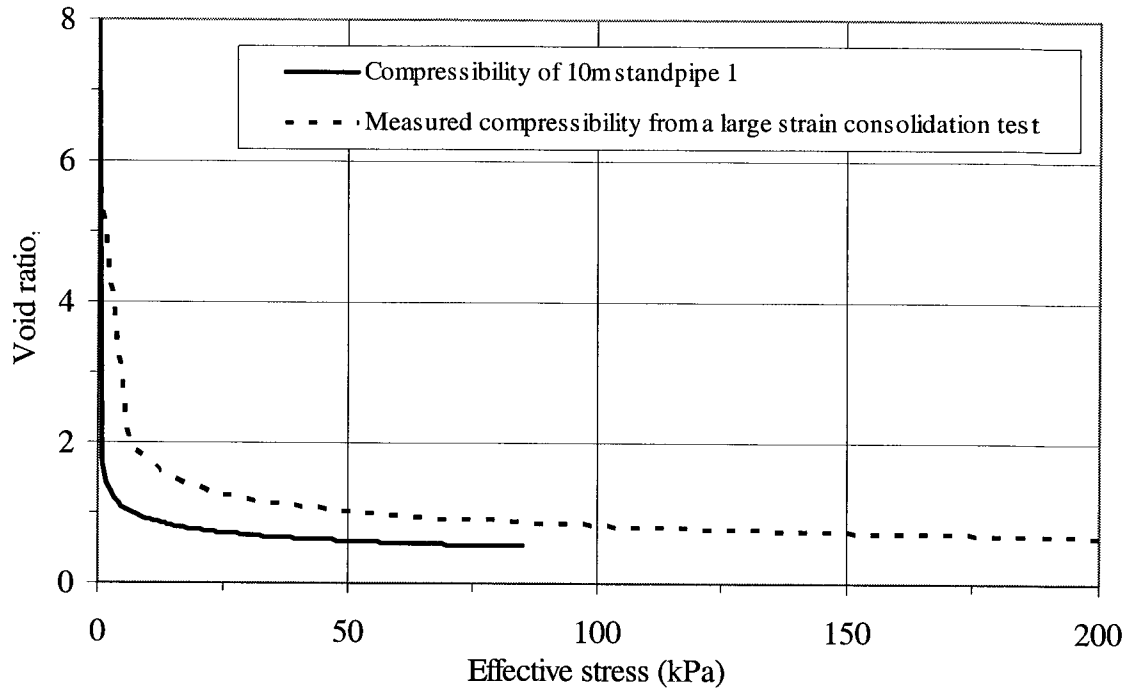


Figure 7.29 The 10 m standpipe void ratio-effective stress arithmetic curve

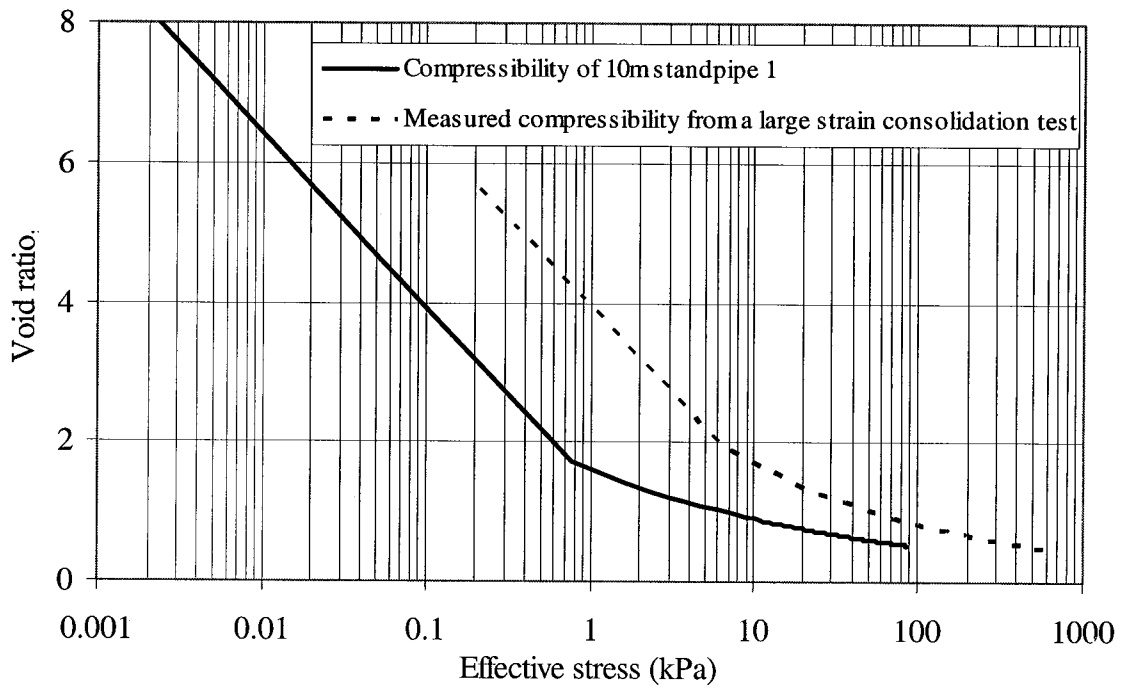


Figure 7.30 The 10 m standpipe void ratio-effective stress log curve

Finite strain consolidation parameters according to equations 7.11 and 7.12 are obtained from Figures 7.30 and 7.13 and shown in Table 7.7. The parameters in Table 7.7 are used in the finite strain consolidation program and the results of the consolidation prediction of Standpipe 1 are shown in Figures 7.31 to 7.35.

Table 7.7 Finite strain parameters in pascals and m/s for Standpipe 1

Test	A	B	C	D
10m standpipe 1 (modified compressibility)	9	-0.25	7.538e-11	3.824
10m standpipe 1 (measured compressibility)	28.71	-0.3097	7.538e-11	3.824

Figures 7.31 to 7.35 compare consolidation predictions and observations. The results show that by using the strain rate approach the interface settlement prediction is not improved as expected. This is probably because the rate of strain is controlled by the hydraulic conductivity relationship and not by the compressibility function. However, the calculated effective stresses and excess pore water pressure profiles tend to be closer to the actual values than those calculated by previous researchers (Pollock, 1988, Suthaker, 1995 and Masala, 1998).

It can be explained that the change of the compressibility is intended to mimic the average effective stress – void ratio curve for an average strain rate. The curve reflects the average change in void ratio with gain in effective stress with the average rate of strain that would occur. By using the power fit to the curve the function does miss the over consolidation stress and therefore the actual performance can not be fully modeled by the present finite strain consolidation model. However, by including an over consolidation stress, the settlement would not be significant. Also, the settlement of the fine tailings is caused by creep which is not included in the finite strain consolidation theory. The finite strain consolidation program has a creep option that allows creep analysis, however, it does this by modifying settlement at every time step during the consolidation process, that is, during pore pressure dissipation. As the creep is not inducing any excess pore water pressure in the model and the creep behaviour is not a constant in a real case but get less when soils approach a higher solids content, the creep option has to be more complex. However, the modified compressibility does show slow

dissipation of excess pore water pressure and slow gaining in effective stress similar to measurements in Standpipe 1.

It would appear from the discussion on creep in Section 2.3.4 and from Figure 2.19 that the settlement rate is controlled by creep. This conclusion is based on the assumption that the hydraulic conductivity is large enough that it does not restrict the water flow from creep. The hydraulic conductivity relationship shown in Figure 7.13 meets this assumption. When this hydraulic conductivity relationship is used in the finite strain consolidation theory, the settlement rate of the interface is overpredicted (Figure 7.31). However, a slight change of the hydraulic conductivity-void ratio relationship can make the prediction work. The hydraulic conductivity function for the mature fine tailings material requires further research work to investigate the flow characteristic of the process water through the fines matrix for different matrix structures resulting from thixotropy and creep. For this research, however, the chosen hydraulic conductivity relationship appears appropriate and can be used with confidence.

In summary, the finite strain consolidation theory lacks thixotropy and creep behaviour that control the rate and amount of settlement and the excess pore water pressure dissipation rate. As a result, it is inadequate to predict the consolidation behaviour of the thixotropic MFT in Standpipe 1.

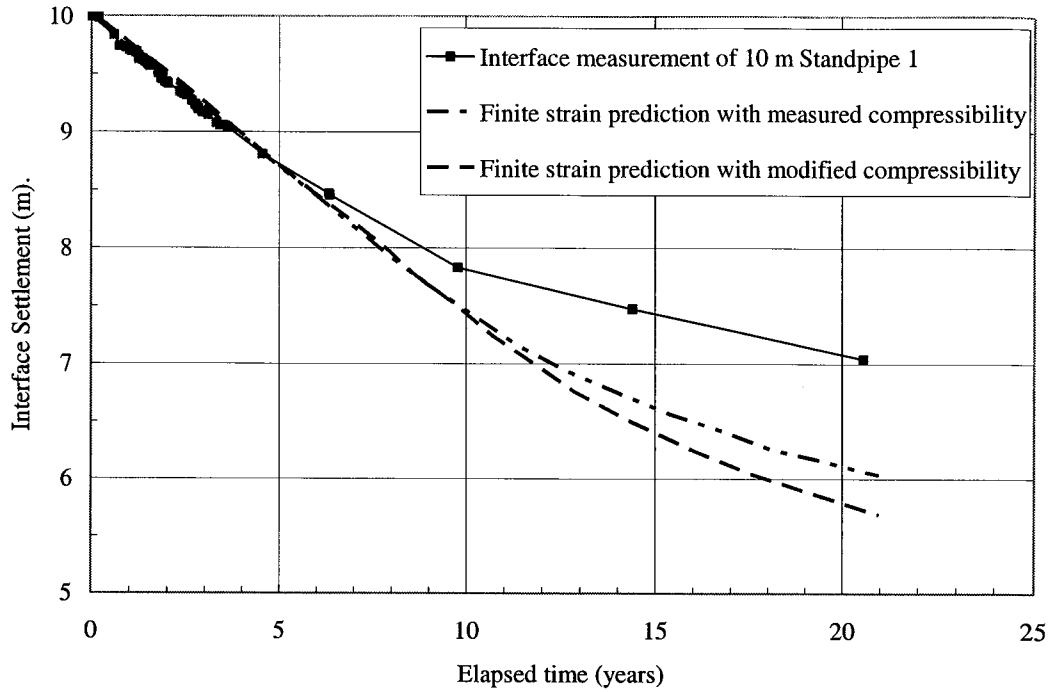


Figure 7.31 Interface settlement for 10 m standpipe 1

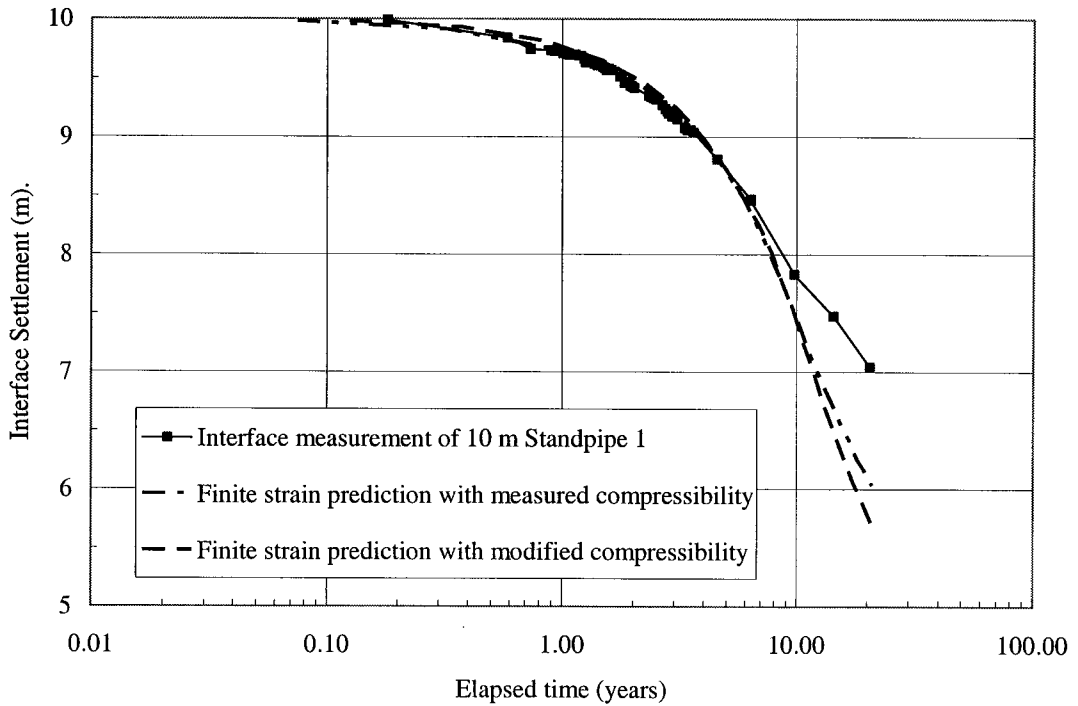


Figure 7.32 Interface settlement for 10 m standpipe 1 (log time)

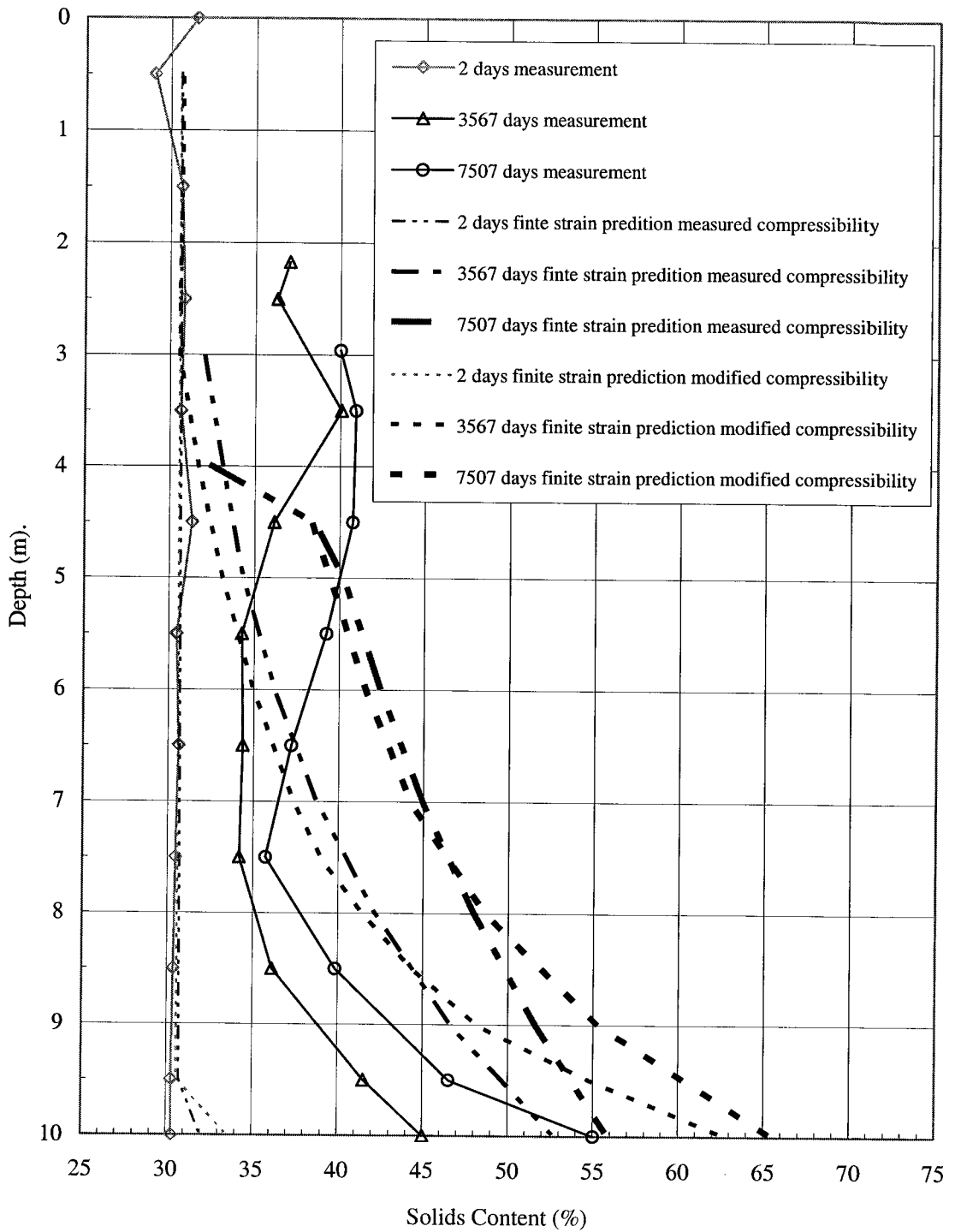


Figure 7.33 Solids content profile for 10 m standpipe 1

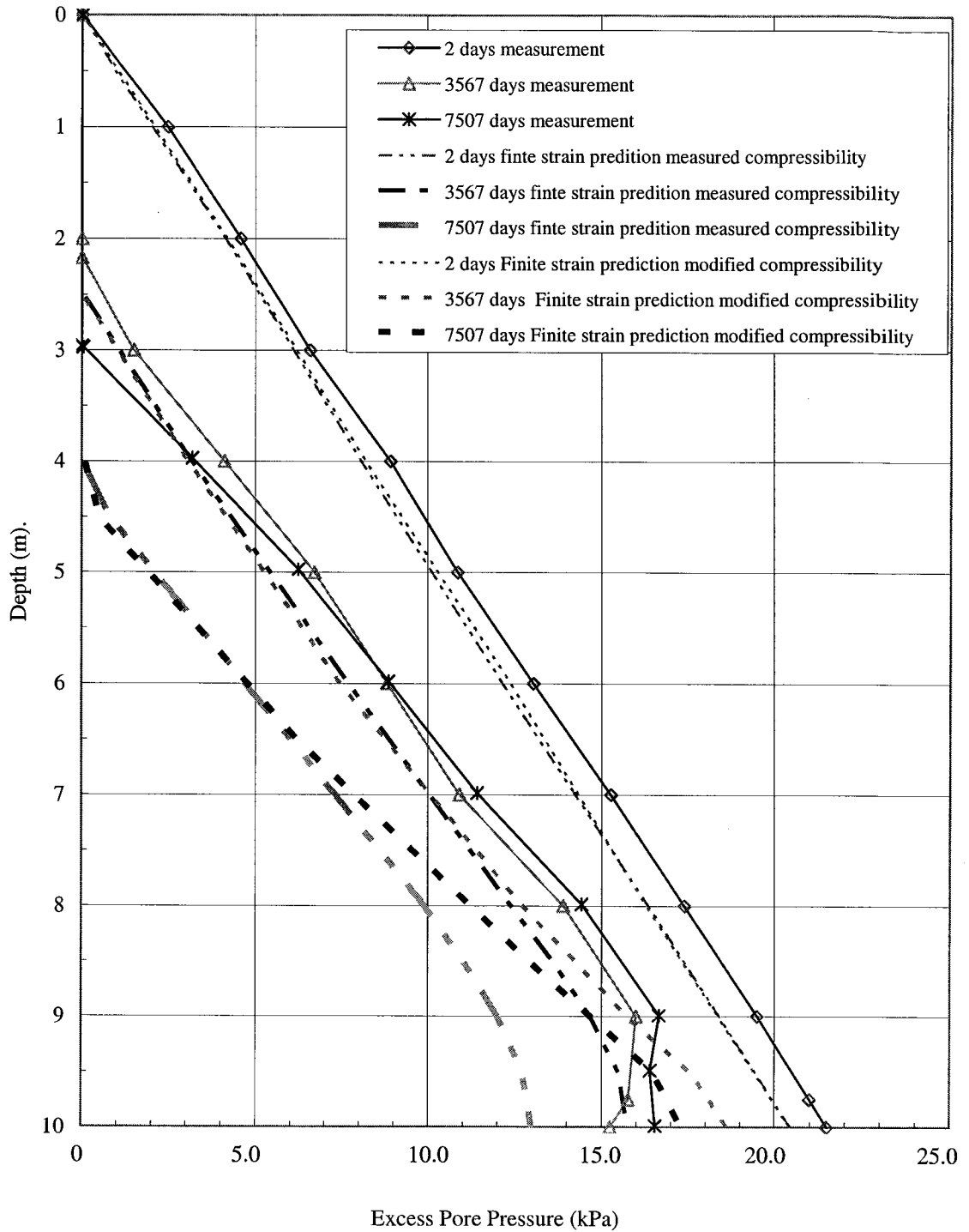


Figure 7.34 Excess pore water pressure profile for 10 m standpipe 1

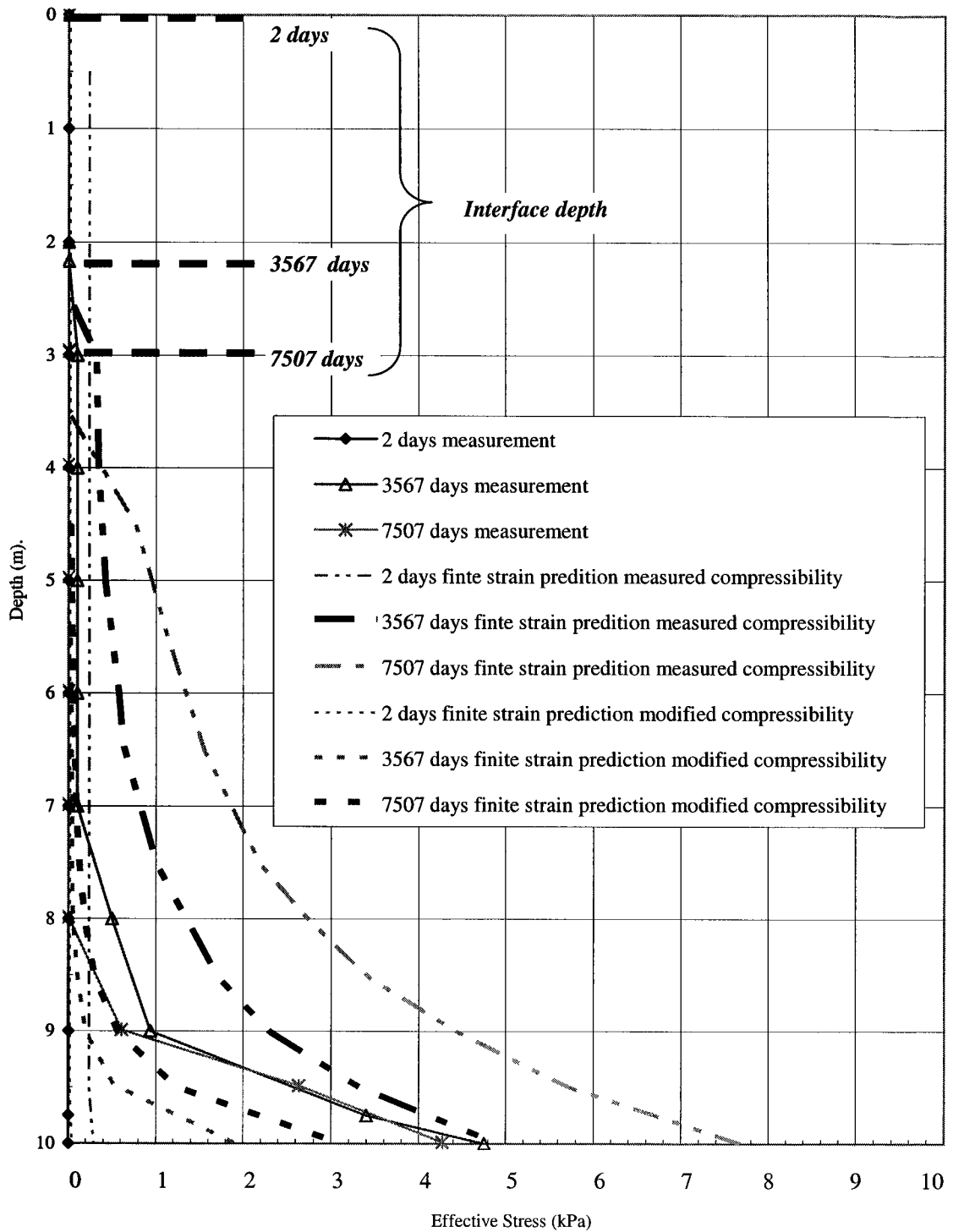


Figure 7.35 Effective stress profile for 10 m standpipe 1

7.5.2 Consolidation prediction of the ten meter Standpipe 2

For Standpipe 2 which contains a MFT-tailings sand mix with 48% sand, there is inadequate data to interpret the effect of strain rate, so no change in the compressibility relationship can be made. In this section, the finite strain consolidation parameters (Table 7.8) are simply used in the finite strain consolidation model. The analyzed data is compared with the observations as shown in Figures 7.36 to 7.40.

Table 7.8 Finite strain parameters in pascals and m/s for Standpipe 2

Test	A	B	C	D
10 m standpipe 2	7.256	-0.2052	6.143e-10	3.824

The measured interface settlement as discussed in Chapter 5 shows a discrete change in the settlement rate and it was postulated by Scott and Chichak (1985b) that it is related to sand segregation in the top 30 cm of the standpipe. The predicted interface settlement from the finite strain consolidation model (Figures 7.36 and 7.37) compares well with the settlement at the end of the observational period but not prior to this point. The measured data is not adequate to draw a conclusion on the performance of this standpipe.

From the solids content comparison (Figure 7.38), the erratic measured data may suggest problems with the sampling of this high sand content material. It is suggested that other methods of solids content measurement should have been used. The excess pore water pressure comparison (Figure 7.39) shows good agreement between observation and prediction but as expected the prediction at the top of the profiles shows some distortion which can be an effect of the segregation of sands. However, again the period of prediction is too short to draw any conclusion. The effective stress comparison (Figure 7.40), as a result of erratic solids content profiles, shows odd behaviour although the average results near the bottom are the right order of magnitude.

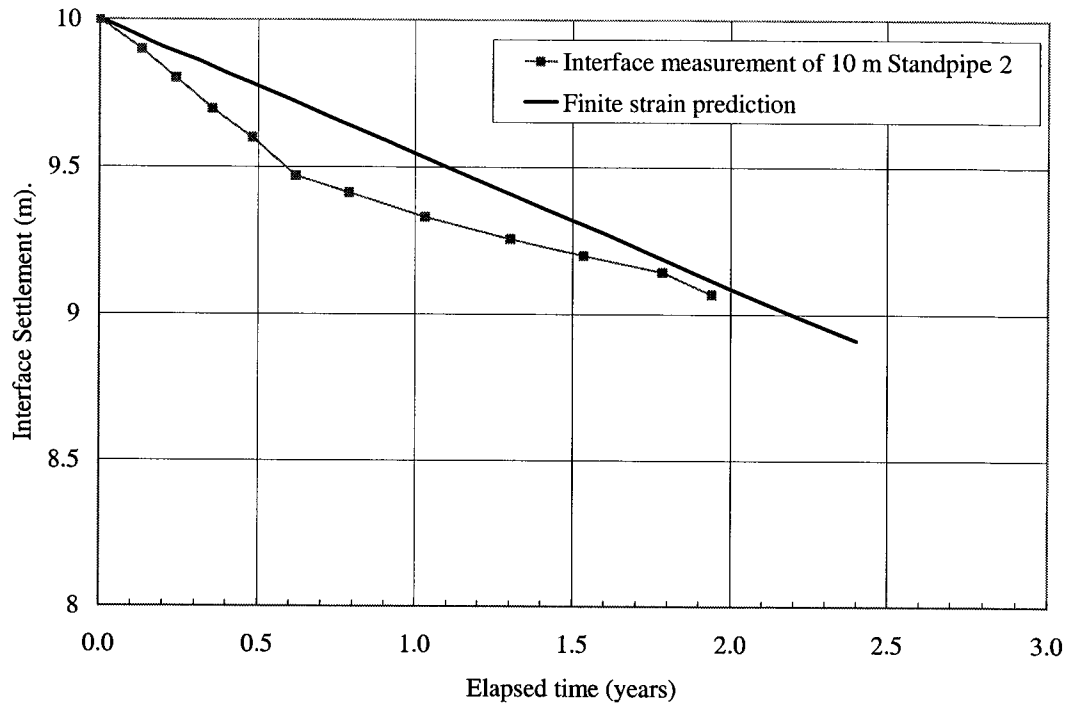


Figure 7.36 Interface settlement for 10 m standpipe 2

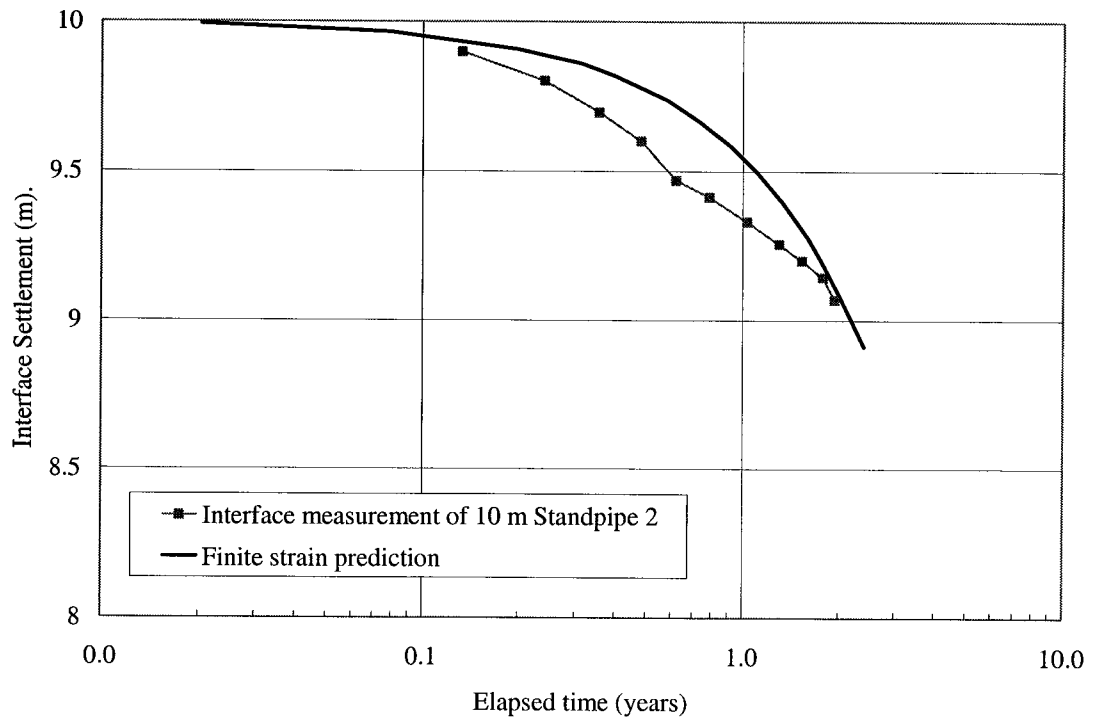


Figure 7.37 Interface settlement for 10 m standpipe 2 (log time)

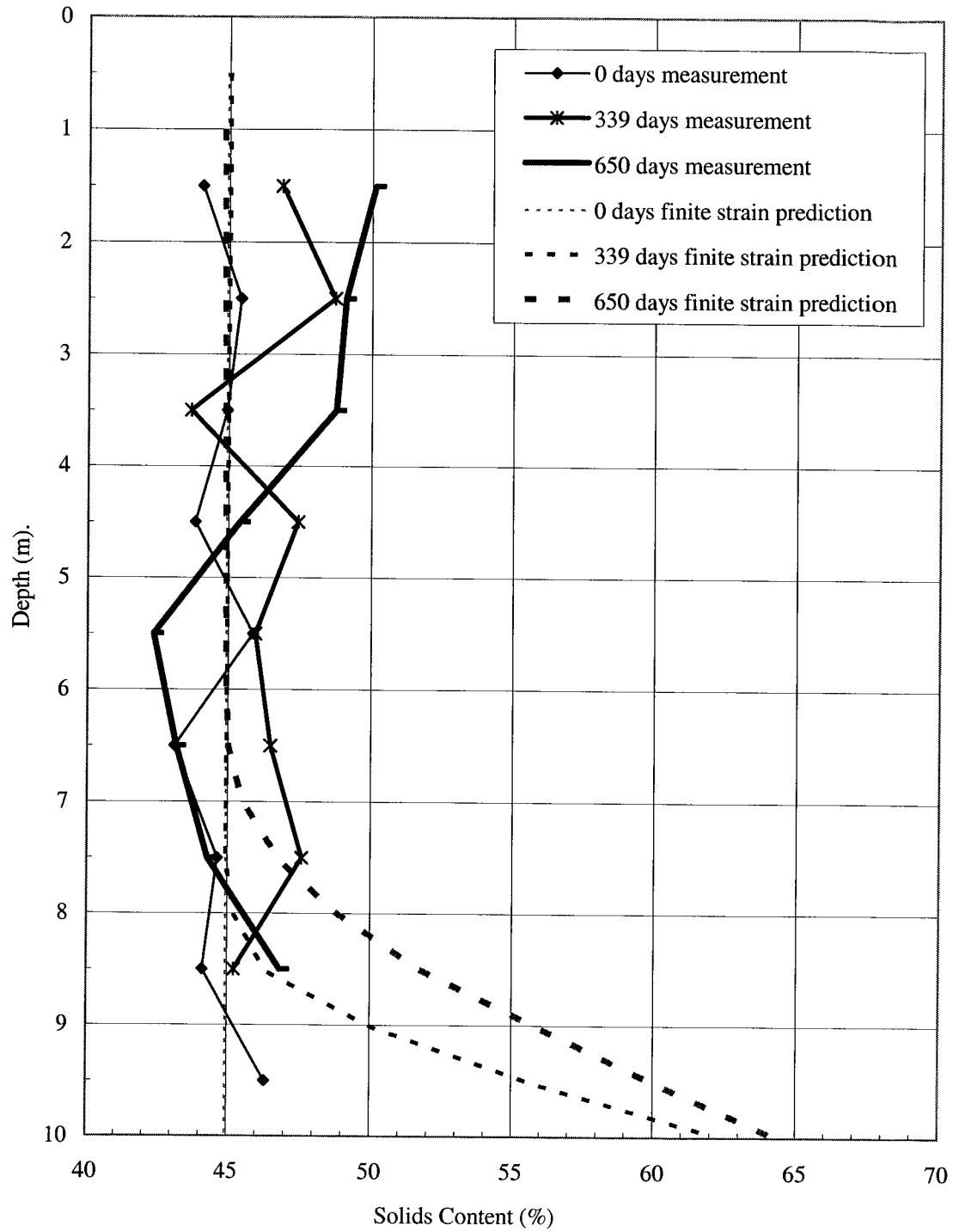


Figure 7.38 Solids content profile for 10 m standpipe 2

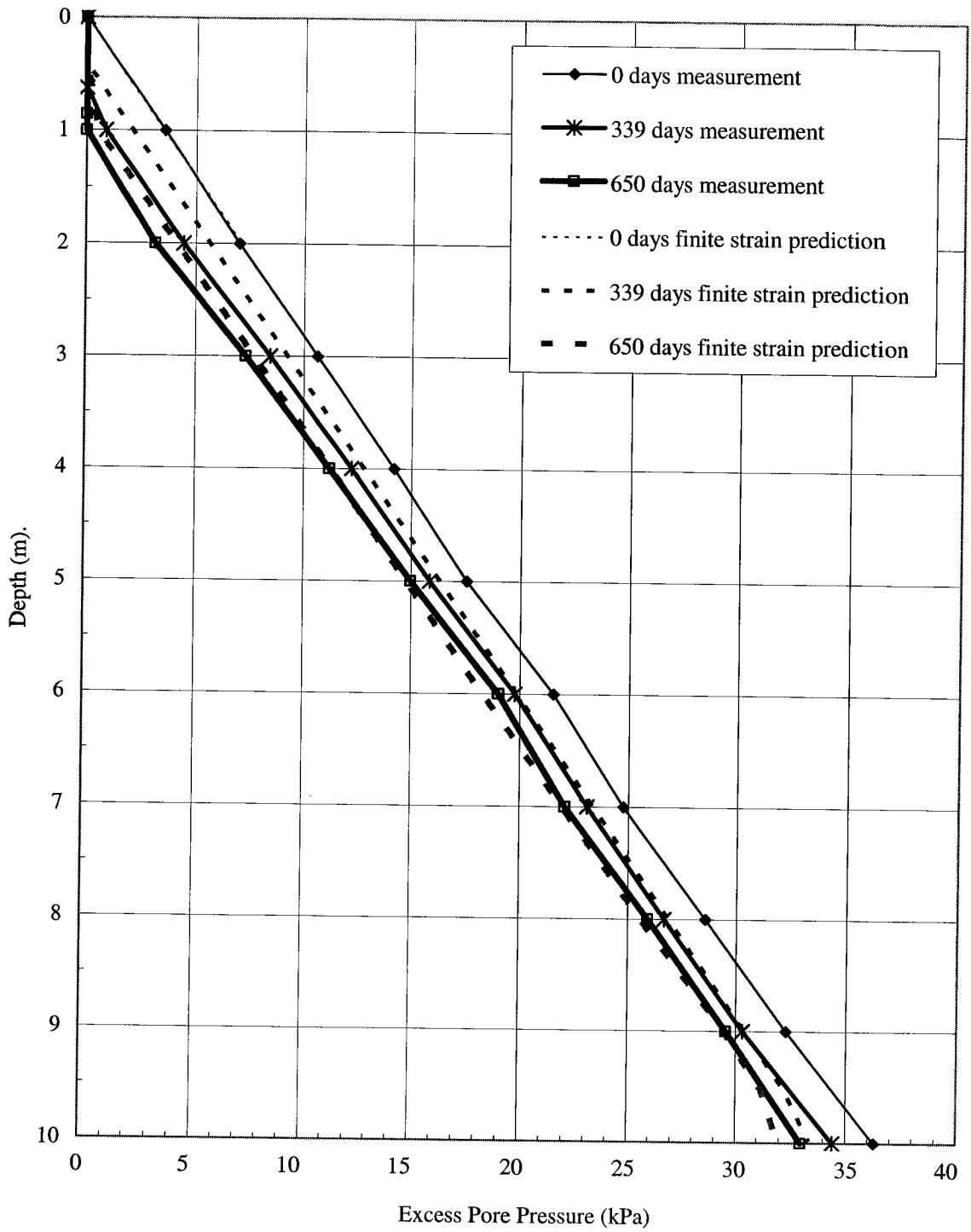


Figure 7.39 Excess pore water pressure profile for 10 m standpipe 2

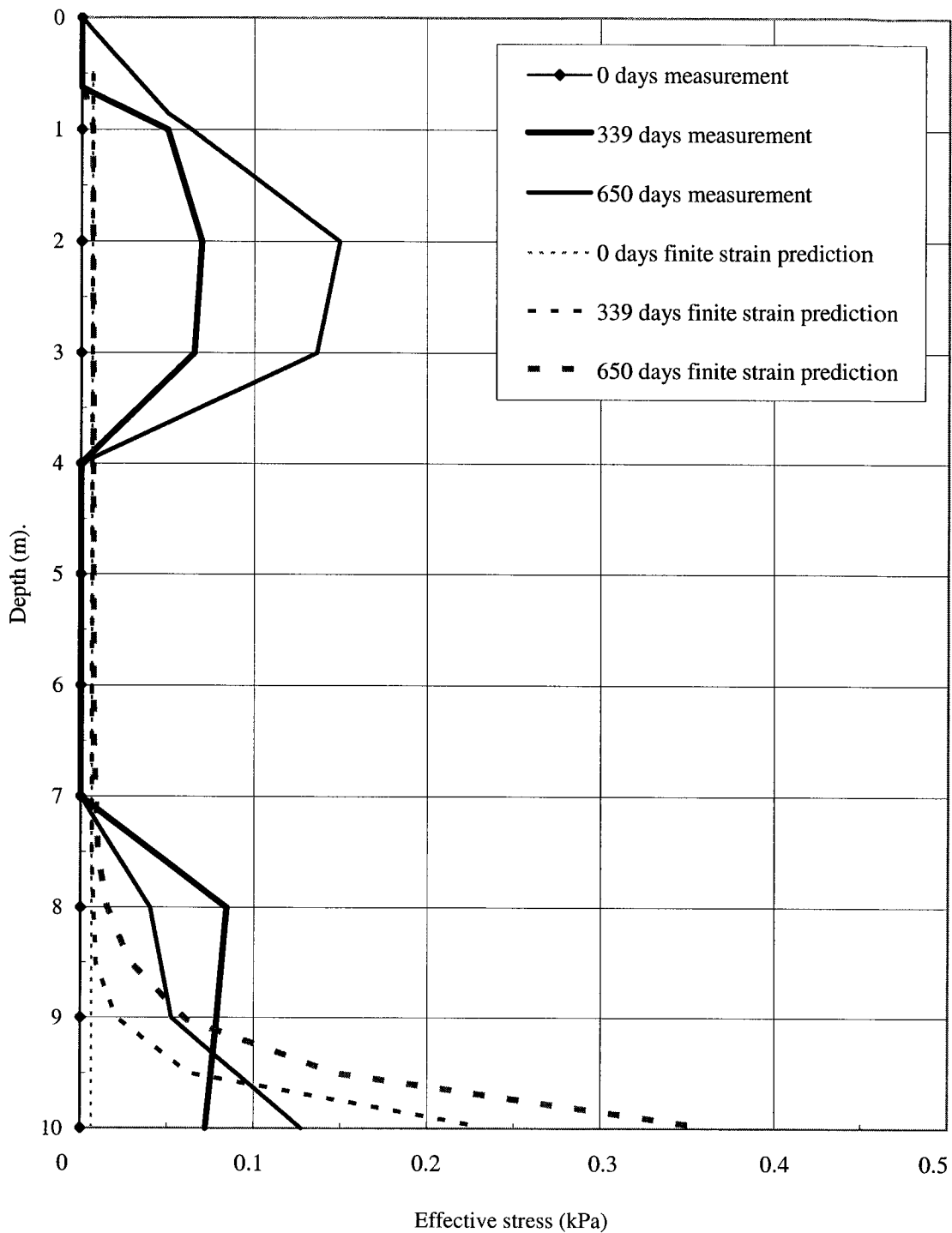


Figure 7.40 Effective stress profile for 10 m standpipe 2

7.5.3 Consolidation prediction of the ten meter Standpipe 3

Similar to Standpipe 2, Standpipe 3 is filled with a MFT-tailings sand mix but with a greater sand content of 82%. A correction of compressibility is made based on available test data from a large strain consolidation test which contains slightly less sand from that in Standpipe 3.

The compressibility relationship of the material is based on the set of data in Figures 7.4 and 7.10. From Standpipe 1, it has been concluded that the strain rate affects the consolidation prediction. For Standpipe 1, a change in compressibility of approximately an order of magnitude lower than the measured value from a large strain consolidation test was required. However, the effect will be different for Standpipe 3 because it contains much more sand. This implies that the slurry should creep less which would have less effect on the rate of compression. However, from the available data, no conclusion on the effect of strain rate can be drawn.

The set of data in Section 7.2.1 suggests that the compressibility of the MFT-tailings sand mix of 82% sand in Standpipe 3 is likely to fall in this set of data but less than the compressibility of the MFT-tailings sand mix with 80% sand. The selected relationship and the relationship achieved from a large strain consolidation test are compared (Figure 7.41). It is suggested that it is more reasonable to use this selected relationship rather than the measured value because the initial solid content of Standpipe 3 is higher (which implies that the compressibility relationship should be lower than the measured one). Other tests (Figure 7.10) with fines contents similar to the material in the standpipe fall lower than the measured value at effective stresses larger than about 2 kPa. Any strain rate effect will tend to move the compressibility relationship lower than the measured value as well. Therefore the selected finite strain parameters are those in Figure 7.41 and are shown in Table 7.9.

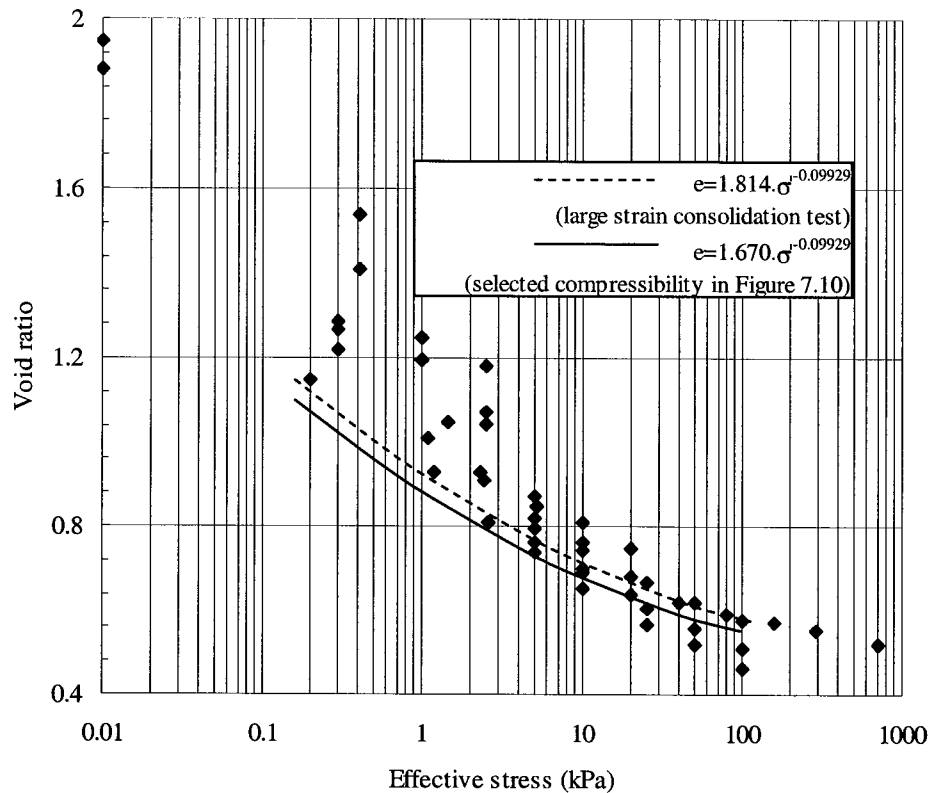


Figure 7.41 Measured and selected compressibility relationship of Standpipe 3

Table 7.9 Finite strain parameters in pascals and m/s for Standpipe 3

Test	A	B	C	D
10m standpipe 3 (measured compressibility)	1.814	-0.09929	3.198e-8	3.824
10m standpipe 3 (modified compressibility)	1.670	-0.09929	3.198e-8	3.824

Figures 7.42 and 7.43 show the comparison of interface settlement in arithmetic and log time plots respectively. The excess pore water pressure profile comparison is shown in Figure 7.44. Due to the difficulty of measuring the solids content of the high sands content material in Standpipe 3, measurement of solids content was stopped early after the standpipe was initiated and no measurement values exist after 229 days that can be used for a calculation of solids content profiles and total stress profiles. However, the

average solids content and average density are known at later time periods and the excess pore pressure distribution is also known. This data can be used to approximate the measured effective stress profiles in Figure 7.45 (Section 6.5).

In Figures 7.42 and 7.43, the selected compressibility gives a better prediction with the standpipe settlement than the relationship measured in the large strain consolidation test. However, the prediction appears to consolidate faster around 4 years which may reflect an error in the measured interface location at this time. The prediction and observation settlements are similar at the end of consolidation progress with about 1.46 m of settlement. In general, as one would expect, this slurry behaves more like a normal soil because the large amount of sand would be expected to subdue the effects of thixotropy and creep. The creep in Standpipe 3 however may be different from that in Standpipes 1 and 2; it depends on how much the thixotropic gel strength affects the settlement behaviour. In other words, the sand particles can reduce the effect of thixotropy (less effect on over consolidation stress) therefore the soil particle interaction may be different. As a result, there would be different creep behaviour.

In the excess pore pressure comparison (Figure 7.44), the selected compressibility relationship predicts the actual general shape and location of the data measured in the standpipe. The approximated effective stress profiles and the predicted effective stress profiles (Figure 7.45) also show good agreement. Therefore, the finite strain consolidation prediction has been able to model the consolidation progress of the MFT-tailings sand mix in Standpipe 3.

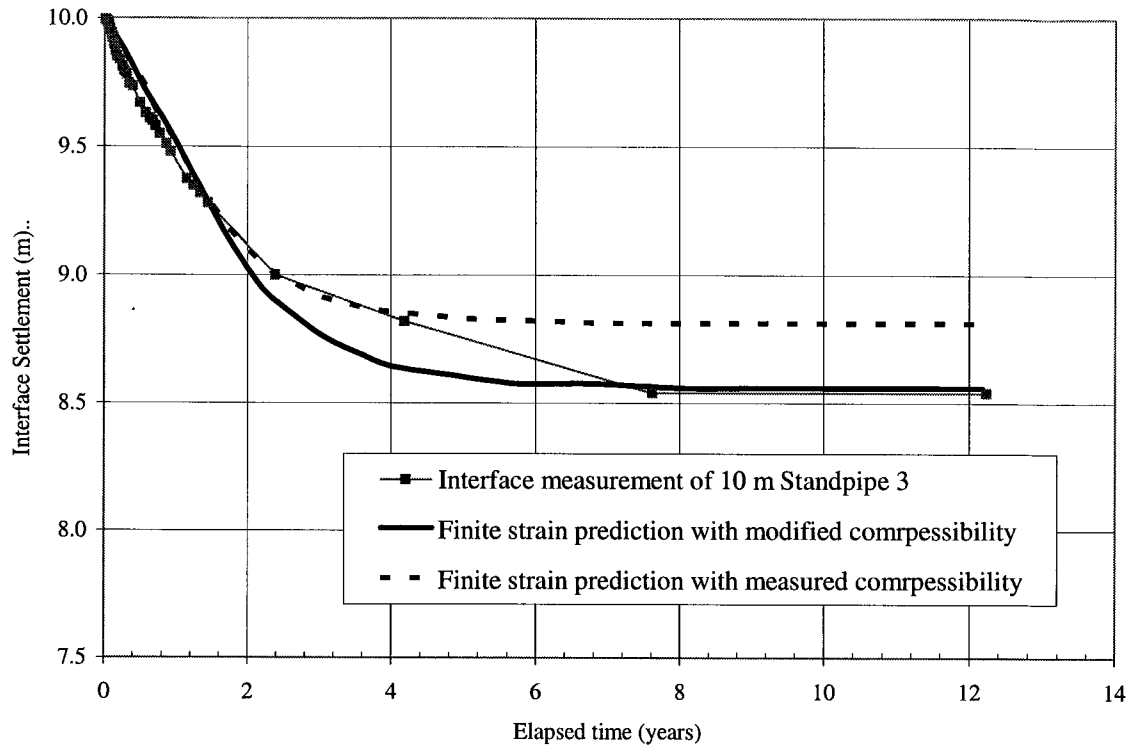


Figure 7.42 Interface settlement for 10 m standpipe 3 (arithmetic time)

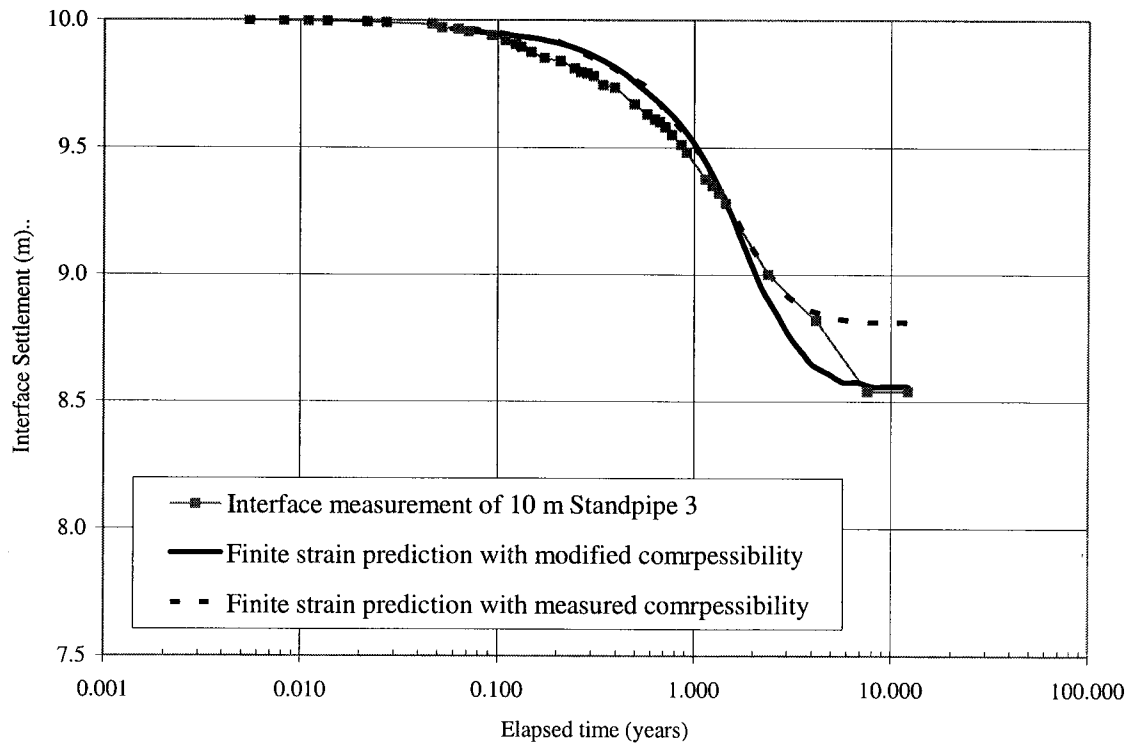


Figure 7.43 Interface settlement for 10 m standpipe 3 (log time)

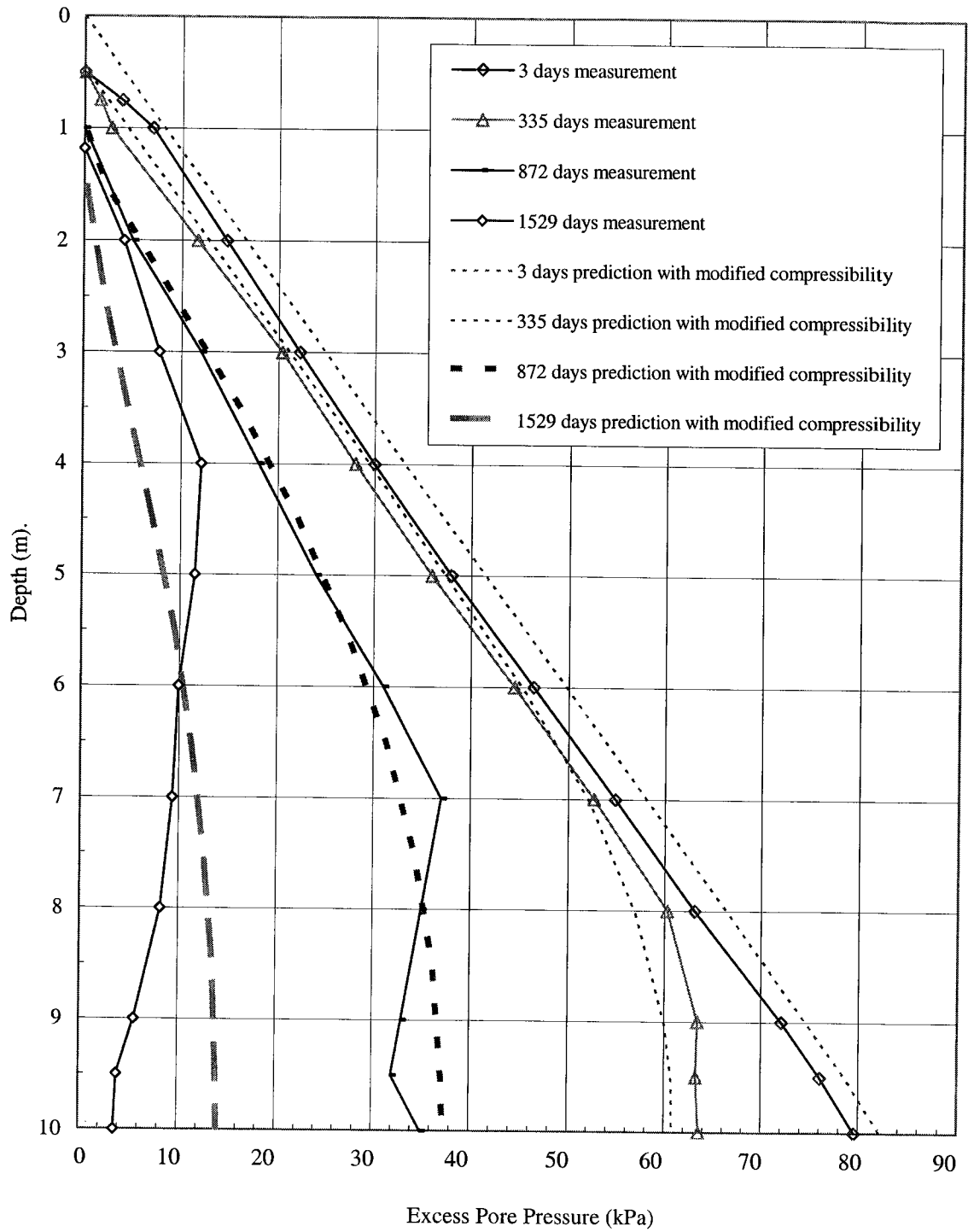


Figure 7.44 Excess pore water pressure profile for 10 m standpipe 3

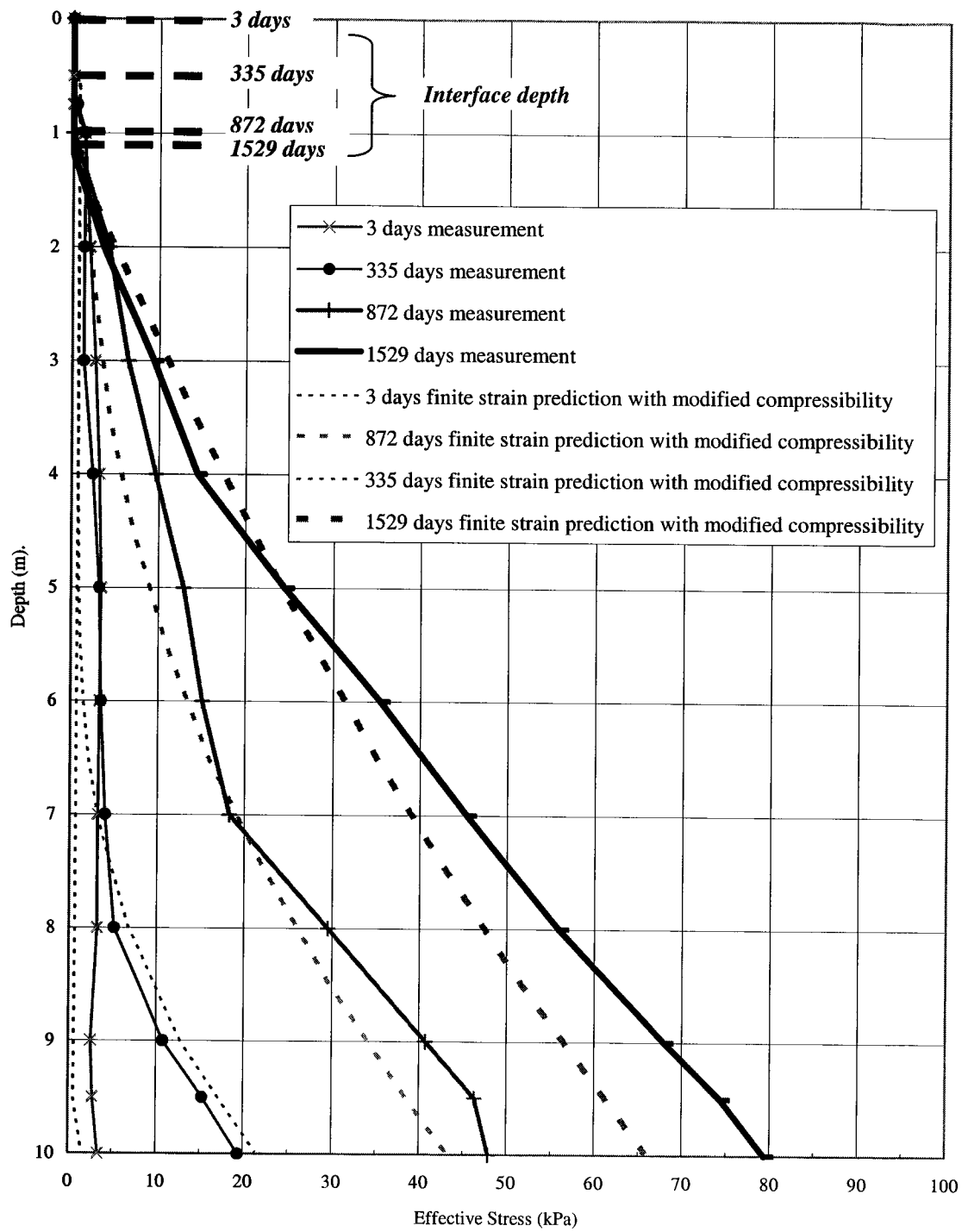


Figure 7.45 Effective stress profile for 10 m standpipe 3

7.6 Summary

Experimental equipment and procedures for the large strain consolidation test at the University of Alberta and test results of such tests on oil sands tailings materials are presented in this chapter. The use of the large strain consolidation theory with experimental relationships for the oil sand tailings is presented by comparing the 10 meter standpipes measurements with finite strain consolidation predictions.

The following observations and conclusions on the consolidometer test, on the compressibility, and hydraulic conductivity relationships for oil sands tailings materials and on consolidation modeling for the oil sands tailings have been reached.

1. Large strain consolidation test and the test results

- Compressibility of the oil sands tailings is influenced by the initial void ratio and shows a preconsolidation pressure which is not found in normal slurries, believed to be the effect of thixotropy.
- The compressibility of the oil sands tailings can vary significantly depending on initial conditions and on different type and amount of coagulants in the tailings.
- Observations show very little to no difference in compression curves for the different additives when the vertical applied effective stress is over 10 kPa.
- Hydraulic conductivity of the oil sand tailings is not influenced by the initial void ratio.
- The influence of the sand on the hydraulic conductivity appears to only decrease the fine concentration for a given volume. The hydraulic conductivity is controlled by the fines-water ratio.
- Void ratio-effective stress and hydraulic conductivity-void ratio relationships for the tailings materials in the 10 m standpipes have been determined. The chosen relationships appear appropriate and can be used with confidence.

2. Finite strain consolidation

- For short term analysis, variations in the compressibility relationship have little influence on the interface settlement prediction. The compressibility relationship becomes important to estimate the ultimate settlement correctly.
- Variations in the hydraulic conductivity relationship have a strong influence on the predicted rate and amount of settlement for short term analysis. These variations, however, have no effect on the final settlement.
- The influence on settlement rate and magnitude by creep and thixotropy is not included in the finite strain consolidation theory.

3. Prediction of compression behaviour of MFT

- The compressibility function has been empirically modified to incorporate the time effect into the stress-strain relationship.
- The modification of the compressibility is intended to simulate the average effective stress – void ratio relationship for an appropriate average strain rate. The modified compressibility shows a slow dissipation of excess pore pressure and a slow gain in effective stress similar to that observed in the standpipe test.
- The power fit to the compressibility curve misses the over consolidation stress and therefore the actual performance can not be fully modeled by the present finite strain consolidation model. By including an over consolidation stress, the settlement would not be significant, which also does not predict the actual performance.
- It would appear that the settlement rate is controlled by creep. This conclusion is based on the assumption that the hydraulic conductivity is large enough that it does not restrict the rate of water flow during creep. Further research is needed.
- A slight change of the hydraulic conductivity relationship can make the interface settlement prediction match the actual performance. However, the modification of the hydraulic conductivity relationship for these tailings requires further research to investigate the flow characteristic of the process

water through the fines matrix for different matrix structures resulting from thixotropy and creep.

4. MFT-tailings sand mix with 48% sand

- The predicted interface settlement generally agrees with the actual settlement to the end of the two year observational period.
- The excess pore water pressure prediction shows good agreement with the measurements. Some distortion near the surface is observed which is suspected to be caused by the segregation of sand.

5. MFT-tailings sand mix with 82% sand

- The compressibility function of this material has been modified to correct for the difference in initial properties of the material tested in Standpipe 3 and in the large strain consolidometer test.
- The prediction with the finite strain consolidation theory closely forecasts the measured interface settlement.
- The finite strain model predicts the actual general shape and location of the material properties measured pore water pressures and the estimated effective stresses in the standpipe.
- The large amount of tailings sand subdues the effects of thixotropy and of creep and the high solids content that make these tailings behave more like a normal soil. Therefore, the finite strain consolidation prediction has been able to model the consolidation progress of this material.

The finite strain consolidation theory which does not have any thixotropic and creep behaviour incorporated in the formulations will never be able to fully predict the consolidation behaviour of the high void ratio thixotropic slurries. Such a model must incorporate not only the effective stress-void ratio and the void ratio-hydraulic conductivity relationships for the material but also the thixotropic gain in strength and the excess pore water pressure maintained by creep behaviour.

8 Summary, Conclusions and Recommendations

8.1 Summary

The oil sands mining operations in Alberta produce large volumes of fine tailings. After the fine tailings settle to about 30% solids, it exhibits significant cohesion and does not appear to be consolidating in the tailing ponds. Volume reduction appears to be taking place by a creep mechanism.

To investigate these phenomena, large ten meter standpipe tests have been performed to study the self-weight consolidation behaviour of the oil sands tailings. There are a total three tests. The first test is Standpipe 1 which is filled with the MFT and has been monitored for over 22 years. Although the MFT has compressed 3 meters by self-weight, very little or no effective stresses have developed. The second test is Standpipe 2 filled with a MFT-tailings sand mix with 48% sand and the third test is Standpipe 3 filled with a MFT-tailings sand mix with 82% sand. These two latter standpipe tests were conducted to study the effects of sand on the compression behaviour.

The objectives of this research were to study and document the compression behaviour of the oil sand tailings in the ten meter standpipe tests which include mature fine tailings (MFT) and MFT-tailings sand mixes. This research also includes the use of a finite strain consolidation theory to model the compression behaviour of these materials in the 10 m standpipes and to provide limitations and suggestions on using the finite strain theory.

8.2 Observations and Conclusions

The observations and conclusions by Chapter are:

Chapter 2

1. During the mature fine tailings stage, the fine tailings form a fines matrix that has a structure which is overconsolidated and resulting in a resistance to a reduction in volume.

2. The fine tailings compression behaviour appears to be affected by the thixotropic gain in strength. The reduction of volume under little or no effective stress appears to be caused by creep.

Chapter 3

1. The large ten meter standpipe tests at the University of Alberta have been performed to understand the self-weight consolidation behaviour of the oil sand tailings.
2. A total of three standpipe tests have been conducted with different tailings materials (MFT, MFT-tailings sand mix of 48% sand and MFT-tailings sand mix of 82% sand). Only the MFT standpipe is currently under observation.

Chapter 4

1. Particle size profiles show that no segregation of coarse particles has occurred in the 1985 to 2003 period.
2. The clay-sized ($<2 \mu\text{m}$) minerals in the MFT are entirely kaolinite and illite in approximately equal amounts. Some of the kaolinite is in the form of aggregates and booklets which appear as silt-size ($45 \mu\text{m} - 2 \mu\text{m}$) particles.
3. The repulsive and attractive forces between the clay particles dominate the behaviour of the fine tailings-water structure. This appears to be mainly caused by the presence of sodium and bicarbonate ions in the tailings water.
4. Conductivity and pH in 2000 were similar to those in the Syncrude and Suncor tailings ponds measured in 1992, indicating that no significant changes in water chemistry in the standpipe occurred during this period.
5. The lack of methanogens in the MFT indicates gas generation should be negligible and no gas bubbles have been observed in the standpipe. Measurements in 2003 indicate the potential for microbial activity which produces gas at the surface of the MFT.
6. MFT which is predominately kaolinite exhibits a very high thixotropic gain in strength. This is caused by the addition of a dispersing agent during the extraction process and the presence of bicarbonates and bitumen.

7. MFT at solids contents of 33 and 40% has overconsolidation stresses of 2.9 kPa and 8.8 kPa, respectively, because of thixotropy. Therefore fine tailings deposits at these solid contents must have vertical effective stresses greater than these amounts for significant consolidation to take place. Settlement that takes place at lower effective stresses must be mainly caused by creep phenomenon.
8. The solids content in the 10 m standpipe is increasing fairly uniformly with depth and only the bottom meter appears to be consolidating. The average solids content has increased from 30.6 to 40.6% during the 21 years.
9. Pore water pressure measurements in the standpipe have shown that the settlement and decrease in void ratio are not due to consolidation but are a creep phenomenon at a constant effective stress of zero.

Chapter 5

1. The average solids content increased from its initial value of 45% to its 2-year value of 48.3%.
2. Solids content and fines content profiles showed possible sand segregation from the middle third of the standpipe to the lower third and an increase in solids in the top third of the standpipe, possibly from consolidation.
3. Excess pore water pressures show there was little significant effective stress in the standpipe after 650 days. It appears that creep compression took place in this MFT-tailings sand mix, as in the mature fine tailings in Standpipe 1.

Chapter 6

1. The interface settlement rate shows a discrete change at around 7 years caused by the sand particles contacting at a solids content of about 79%. At higher solids, the sand structure must be compressed as well as the fines-water matrix.
2. The average solids content increased from its initial value of 74.8% to 81.2% at the end of consolidation.
3. Excess pore water pressures and effective stress profiles show that significant pore pressure dissipation started immediately at the bottom of the standpipe and significantly developed throughout the depth of the standpipe at around 500 days.

4. The settlement rate can be monitored through the change of fines void ratio. The rate of compression of the fines matrix from the three standpipes shows that the higher the sand content, the faster the decrease in fines void ratio.

Chapter 7

1. Large strain consolidation test and the test results

- The compressibility of the oil sands tailings can vary significantly depending on initial conditions and on different type and amount of coagulants in the tailings.
- Observations show very little to no difference in compression curves for the different additives when the vertical applied effective stress is over 10 kPa.
- Void ratio-effective stress and hydraulic conductivity-void ratio relationships for the tailings materials in the 10 m standpipes have been determined. The chosen relationships appear appropriate and can be used with confidence.

2. Finite strain consolidation

- For short term analysis, variations in the compressibility relationship have little influence on the interface settlement prediction. The compressibility relationship becomes important to estimate the ultimate settlement correctly.
- Variations in the permeability relationship have a strong influence on the predicted rate and amount of settlement for short term analysis. These variations, however, have no effect on the final settlement.

3. Prediction of compression behaviour of MFT

- The compressibility function has been empirically modified to simulate the average effective stress – void ratio relationship for an appropriate average strain rate. The modified compressibility shows a slow dissipation of excess pore pressure and a slow gain in effective stress similar to that observed in the standpipe test.
- By using the power fit to the compressibility curve the finite strain model misses the over consolidation stress and therefore the actual performance can not be fully modeled by the present finite strain consolidation model.

- It would appear that the settlement rate is controlled by creep, based on the assumption that the hydraulic conductivity is large enough that it does not restrict the rate of water flow during creep.
 - A slight change of the permeability relationship can make the interface settlement prediction match the actual performance.
4. MFT-tailings sand mix with 48% sand
- The predicted interface settlement generally agrees with the actual settlement to the end of the two year observational period.
 - The excess pore water pressure prediction shows good agreement with the measurements. Some distortion near the surface is observed which is suspected to be caused by the segregation of sand.
5. MFT-tailings sand mix with 82% sand
- The finite strain model can predict the measured interface settlement, the measured excess pore pressures and the effective stresses in the standpipe.
 - The large amount of tailings sand subdues the effects of thixotropy and of creep and the high solids content that make these tailings behave more like a normal soil. Therefore, the finite strain consolidation prediction has been able to model the consolidation progress of this material.

8.3 Major Conclusions of Research Project

1. MFT Standpipe with 89% fines:

- Particle size profiles show that no segregation of coarse particles has occurred in the 1985 to 2003 period.
- MFT which is predominately kaolinite exhibits a very high thixotropic gain in strength. This is caused by the addition of a dispersing agent during the extraction process and the presence of bicarbonates and bitumen.
- MFT at solids contents of 33 and 40% has overconsolidation stresses of 2.9 kPa and 8.8 kPa, respectively, because of thixotropy. Therefore fine tailings deposits at these solid contents must have vertical effective stresses greater than these amounts for significant consolidation to take place. Settlement that takes place at lower effective stresses must be mainly caused by creep phenomenon.

- The solids content in the 10 m standpipe is increasing fairly uniformly with depth and only the bottom meter appears to be consolidating. The average solids content has increased from 30.6 to 40.6% during the 21 years.
- Pore water pressure measurements in the standpipe have shown that the settlement and decrease in void ratio are not due to consolidation but are a creep phenomenon at a constant effective stress of zero.
- By using the power fit to the compressibility curve the finite strain model misses the over consolidation stress and therefore the actual performance can not be fully modeled by the present finite strain consolidation model.

2. MFT –Tailings sand Standpipe with 82% sand:

- The interface settlement rate shows a discrete change at around 7 years caused by the sand particles contacting at a solids content of about 79%. At higher solids, the sand structure must be compressed as well as the fines-water matrix.
- The finite strain model can predict the measured interface settlement, the measured excess pore pressures and the effective stresses in the standpipe.
- The large amount of tailings sand subdues the effects of thixotropy and of creep and the high solids content that make these tailings behave more like a normal soil. Therefore, the finite strain consolidation prediction has been able to model the consolidation progress of this material.

3. Comparison of the 3 standpipes settlements:

- The settlement rate can be monitored through the change of fines void ratio. The rate of compression of the fines matrix from the three standpipes shows that the higher the sand content, the faster the decrease in fines void ratio.

8.4 Recommendations for Further Study

Investigation on the compression behaviour of the mature fine tailings in Standpipe 1 should be continued for further evaluation.

The sampling method and equipment should be improved to be able to measure the density of tailings more precisely especially for material that has high solids and sands contents

The tailings material in Standpipe 3 should be sampled for a solids content profile. Coring of the standpipe may be possible for this high solids material.

A series of constant rate of strain consolidation tests should be performed on tailings samples to improve understanding of the effect of creep and effect of strain rate on compressibility. This should improve confidence for the use of a finite strain consolidation model.

For large strain consolidation tests, it is suggested to also measure pore pressure and total stress at the bottom of specimen in order to provide verification of measured hydraulic conductivity and applied stresses.

The thixotropy of oil sand tailings is suspected to have an effect on the movement of pore water through the void system due to the fact that the soil structure can be different depending on loading conditions. It is also suggested to conduct permeability tests on oil sand tailings samples at different ages and with different sand content.

For thixotropic tailing slurries, the finite strain consolidation theory needs to be improved by incorporating the effects of thixotropy and creep into the formula. This would require a reformulation of the governing equations.

Bibliography

- Aboshi, H., Toshikuni, H., and Maruyama, S., 1978. Constant loading rate consolidation test. *Soils and Foundations*, Vol. 10, No. 1, pp. 43-56.
- AGRA, 1997. Progress on MFT Modeling. Report to Syncrude Canada Ltd., AGRA Earth & Environmental limited, Edmonton, Alberta, 29p.
- AGRA, 1997. Large Strain Consolidation Analysis of Composite Tailings Oedometer Tests. Report to Syncrude Canada Ltd., AGRA Earth & Environmental limited, Edmonton, Alberta, 14p.
- Aiban, S.A., and Znidarcic, D., 1989. Evaluation of the flow pump and constant head techniques for permeability measurements, *Geotechnique*, Vol. 39, No. 4, pp. 655-666.
- American Public Health Association. 1985. Standard methods for the examination of water and wastewater. 16th Edition.. New York, N.Y. pp. 880–882.
- Banas, L., 1991. Thixotropic Behaviour of oil sands tailings sludge, MS.c. Thesis, University of Alberta, Edmonton, Canada.
- Baver, L.D., 1956. Soil physics, Fourth Edition, Wiley & Sons, 498 p.
- Been, K., 1980. Stress Strain Behaviour of a cohesive Soil Deposited Under Water. Ph.D. Thesis, University of Oxford, Oxford, United Kingdom.
- Been, K. and Sills, G.C., 1981. Self Weight Consolidation of Soft Soils: An experimental and Theoretical Study. *Geotechnique*, Vol. 31, No. 4, pp. 519-535.
- Bently, S.P., 1979. A Viscosity Assessment of a Remoulded Sensitive Clay, *Canadian Geotechnical Journal*, Vol. 212, pp. 414-419.
- Berkowitz, N. and Speight, J.G., 1975. The Oil Sands of Alberta. *Fuel*, Vol. 54, pp.138-149.
- Bjerrum, L., 1967. Seventh Rankine lecture, Engineering geology of Norwegian normally consolidated marine clays as related to the settlements of buildings, *Geotechnique*, Vol. 17, No. 2, pp. 81-118.
- Boratynec, D., 2003. Fundamentals of Rapid Dewatering of Composite Tailings, MS.c. Thesis, University of Alberta, Edmonton, Canada.
- Burchfield, T.E. and Hepler, L.G., 1979. Some Chemical and physical Properties of Tailings Water from Oil Sands Extraction Plants. *Fuel*, Vol. 58, pp. 745-747.

- Camp, F.W., 1977. Processing Athabasca Tar Sands - Tailings Disposal. Canadian Journal of Chemical Engineering, Vol. 55, Oct., pp. 581-591.
- Cargill, K.W., 1982. Consolidation of Soft Layers by Finite Strain Analysis. U.S. Army Engineer Waterways Experimentation Station. Vicksburg, Mississippi, Miscellaneous Paper GL-82-3.
- Cargill, K.W., 1984. Prediction of Consolidation of Very Soft Soil. Journal of Geotechnical Engineering, Vol. 110, No. 6, pp. 775-795.
- Carrier III, W. D., Bromwell, L.G., and Somogyi, F., 1981, Slurried Mineral Wastes: Physical Properties Pertinent to Disposal, Presented at the ASCE National Convention, October, St. Louis.
- Cernica, J.N., 1995. Geotechnical Engineering: Soil mechanics. Wiley & Sons, 453 p.
- Chalaturnyk, R.J., J.D. Scott and B. Ozum, 2004. Environmentally Acceptable Deposition of Oil Sands Tailings, SWEMP 2004, 8th International Symposium on Environmental Issues and Waste Management in Energy and Mineral Production May 17-20, 2004 Antalya, Turkey, 6p.
- Chatterji, P. K., and Morgenstern, N. R. 1989. A Modified Shear Strength Formulation for Swelling Clay Soils. Submitted to Symposium on Physico-Chemical Aspects of Soil, Rock and Related Materials, St. Louis, Missouri, pp. 118-135.
- Daniel, D.E., 1989. A note on falling headwater and rising tail water permeability tests, Geotechnical Testing Journal, Vol. 12, No. 4, pp.308-310.
- Ripple, C. D., and Day, P. R., 1966. Suction responses due to shear of dilute montmorillonite-water pastes, Clays and Clay Minerals, Vol. 14, pp. 307-316.
- Dusseault, M.B., 1977. The Geotechnical Characteristics of Oil Sands. Ph.D. Thesis, University of Alberta, Edmonton, Canada.
- Elder, D.M., 1985, Stress strain and strength behaviour of very soft soil sediment, D.Phil. Thesis, Oxford University, U.K.
- EUB (Alberta Energy and Utilities Board) Statistical Series (ST) 2004-98, 2004, "Alberta's Reserves 2003 and Supply/Demand Outlook 2004-2013), www.eub.gov.ab.ca.
- EUB (Alberta Energy and Utilities Board) Report 2003-A, 2003 "Athabasca Wabiskaw-McMurray Regional Geological Study), www.eub.gov.ab.ca.

- Fedorak, P.M., Coy, D.L., Salloum, M.J. and Dudas, M.J., 2002. Methanogenic potential of tailings samples from oil sands extraction plants, *Canadian Journal of Microbiology*. Vol. 48, pp 21-33.
- FTFC (Fine Tailings Fundamentals Consortium), 1995 “Vol I, Clark Hot Water Extraction Fine Tailings” In: *Advances in Oil Sands Tailings Research*, Alberta Department of Energy, Oil Sands and Research Division, Publisher.
- Fuhr, B., Powter, C., Taplin, D., and Rose, D., 1993, *Catalogue of Technologies for Reducing the Environmental Impact of Fine Tails from Oil Sand Processing Proceedings*, Fine Tailings Symposium, Oil Sands Our Petroleum Future Conference, April 4-7, Edmonton, Alberta.
- Gibson, R.E., 1958. The Progress of Consolidation in a Clay Layer Increasing in Thickness with Time. *Geotechnique*, Vol. 8, pp. 171-182.
- Gibson, R.E., England, G.L., and Hussey, M.J.L., 1967. The Theory of One-Dimensional Consolidation of Saturated Clays I, Finite Non-Linear Consolidation of Thin Homogeneous Layers. *Geotechnique*, Vol. 17, pp. 261-273.
- Gibson, R.E., Schiffman, R.L., and Cargill, K.W., 1981. The Theory of One-Dimensional Consolidation of Saturated Clays II, Finite Non-Linear Consolidation of Thick Homogeneous Layers. *Canadian Geotechnical Journal*, Vol. 18, pp. 280-293.
- Guo, C., Chalaturnyk, R.J., Scott, J.D. and MacKinnon, M., 2004. Densification of Oil Sands Tailings by Biological Activity. *Proceedings of the 57th Canadian Geotechnical Conference*, October 24-27, Quebec, Montreal.
- Guo, C., Chalaturnyk, R.J., Scott, J.D. and Mackinnon, 2004. Effect of Biological generation on oil sands fine tailings. *CIM Edmonton 2004 Conference*, May 9-12, Edmonton, Alberta.
- Guo, C., Chalaturnyk, R.J., Scott, J.D., Mackinnon, M. and Cyre, G., 2002. Geotechnical field investigation of the rapid densification phenomenon in oil sands mature fine tailings (MFT). *55th Canadian Geotechnical Conference*, Niagara Falls, Ontario, October 20-23.
- Hocking, M.B. and Lee, G.W., 1977. Effect of Chemical Agents on Settling Rates of Sludge from Effluent of Hot-Water Extraction of Athabasca Oil Sands. *Fuel*, Vol. 56, July, pp. 325-333.
- Holowenko, F. M., MacKinnon, M.D., and Fedorak, P.M., 2000. Methanogens and sulfate-reducing bacteria in oil sands fine tailings wastes, *Canadian Journal of Microbiol*, 46, p. 927-937.

- Ignasiuk, T.M., Kotlyar, L., Longstaffe, F.J., Strausz, O.P., and Montgomery, D.S., 1982. Separation and Characterization of Clay from Athabasca Asphaltene. *Fuel*, Vol. 62, March, pp. 353-362.
- Imai, G., 1981. Experimental studies on sedimentation mechanism and sediment formation of clay materials. *Soils and Foundations*, Japanese Society of Soil Mechanics and Foundation Engineering, Vol. 21, No. 1, March, pp. 7-20.
- Imai, G. and Hawlader, B.C., 1997. An elastio-viscoplastic analysis of self weight consolidation. *Computer Methods and Advances in Geomechanics*, pp. 1065-1070.
- Imai, G. and Tang, Y. X., 1992. A constitutive equation of one-dimensional consolidation derived from inter-connected tests. *Soils and Foundation*, Japanese Society of Soil Mechanics and Foundation Engineering, Vol. 32, No. 2, June, pp. 83-96.
- Kessick, M.A., 1978. Clay Slimes from the Extraction of Alberta Oil Sands, Florida Phosphate Matrix and Other Mined Deposits. *Waste Treatment*, Feb., 9 p.
- Lee, K., 1981. Consolidation with constant rate of deformation. *Geotechnique*, Vol. 31, pp. 295-329.
- Leroueil, S., Kabbaj, M., Tavenas, F., and Bouchard, R., 1985. Stress-strain-strain rate relation for the compressibility of sensitive natural clays. *Geotechnique*. Vol. 35, No. 2, pp. 159-180.
- Locat, J., Berube, M.A., and Chagnon, J.Y., 1985. The mineralogy of sensitive clays in relation to some engineering geology problems- An Overview, *Applied Clay Science*, Vol.1, No. ½, pp. 193-205.
- Lowe, J., Jonas, E., and Obrician, V., 1969. Controlled gradient consolidation test. *ASCE Soil Mechanics and Foundation Division*, Vol. 95, SM 1, pp. 77-97.
- Masala, S., 1998, Numerical Solution of sedimentation and consolidation of fine tailings, MSc Thesis, University of Alberta, Edmonton, AB.
- Mesri, G, 1975, New design procedure for stability of soft clays, Discussion, *Journal of Geotechnical Engineering*, American Society of Civil Engineers, Vol.101, No. GT4, pp. 1090-1093.
- Miller, W.G., 2004, personal communication.
- Mitchell, J. K., 1960, Fundamental aspects of thixotropy in soils, *Journal of Soil Mechanics Foundations Divisions American Society of Civil Engineers*, 83(3), pp. 19-52.

- Mitchell, J. K., 1993, *Fundamentals of Soil Behaviour*, Second Edition, Wiley, New York, 436 p.
- Moretto, O., 1948. Effect of Natural Hardening on the Unconfined Compression Strength of Remoulded Clays, *Proceedings, 2nd International Conference on Soil Mechanics*, Vol. 1.
- Morgenstern, N.R., and Scott, J. D., 1995. "Geotechnics of Fine Tailings Management." *GeoEnvironment 2000, ASCE Specialty Conference, New Orleans*, 46(2) 1663-1683.
- Myint, W.B., Wong, K.S., Victor, C., The, C.I., 2003. Compression Tests of Ultra-Soft Soil Using an Hydraulic Consolidation Cell. *Geotechnical Tesing Journal*, Vol. 26, No. 3.
- Olsen, H.W., 1996. Darcy's law in saturated kaolinite, *water Resources Research*, Vol. 2, No. 6, pp. 287-295.
- Olsen, H.W., Nichols, R.W., and Rice, T.L. 1985. Low gradient permeability measurements in a triaxial system, *Geotechnique*, Vol. 35, No. 2, pp. 145-157.
- Olsen, R.E., and Daniel, D.E., 1981. Measurement of hydraulic conductivity of fine grained soils, In *permeability and ground water contaminant transport*, Edited by T.F. Zimmie and C.O. Riggs. American Society for Testing and Materials, Special Technical Publication 746, pp. 18-64.
- Osipov, V.I., Nikolaeva, S. K., and Sokolov, V.N., 1984. Microstructural changes associated with thixotropic phenomena in clay soils. *Geotechnique*, Vol. 34, No. 2, pp. 293-303.
- Pollock, G., 1988. *Large Strain Consolidation of Oil Sand Tailings Sludge*, MS.c. Thesis, University of Alberta, Edmonton, Canada.
- Prasad, B.D. and Joshi, R.C., 1985. Tailings Pond Bitumen Extraction and Sludge Solidification. *Third International Conference on Heavy Crude and Tar Sands, UNITAR/UNDP Information Centre for Heavy Crude and Tar Sands, Long Beach, California, July 22-31, Preprint, Vol. 2, 17 p.*
- Ripmeester, J.A. and Sirianni, 1981, A.F., 1981. Recovery of Water and Bitumen from the Athabasca Oil Sands Tailings Ponds. *Canadian Journal of Petroleum Technology*, Jan-March, pp. 131-133.
- Schiffman, R.L., Pane, V., and Gibson, R.E., 1984. The theory of One-Dimensional Consolidation of Saturated Clays IV. An overview of Nonlinear Finite Strain Sedimentation and Consolidation, *Sedimentation/Consolidation Models*, Edited by R.N.Yong and F.C.Townsend, ASCE, pp. 1-29.

- Schiffman, R.L., 2001. Theories of Consolidation. University of Colorado Press, 570p.
- Scott, J.D., Chalaturnyk, R.J., and Jeeravipoolvarn, S., 2004, "Settlement of Tailings Slurries by Creep Compression", CIM Edmonton 2004 Conference. May 9-12, Edmonton, Alberta.
- Scott, J.D., Chalaturnyk, R.J., and Jeeravipoolvarn, S., 2004, "Fine Tailings Decrease in Volume by Creep Compression", Proceedings of the 57th Canadian Geotechnical Conference, October 24-27, Quebec, Montreal
- Scott, J.D., and Chichak, M.F., 1985a. Large Sludge Standpipe Consolidation Test 1, Progress Report to February, 1985. Sludge Standpipe Testing Contract Agreement C2919-55 for Syncrude Canada Lts., June, 60 p.
- Scott, J.D., and Chichak, M.F., 1985b. Large Sludge Standpipe Consolidation Test 2, Final report. Sludge Standpipe Testing Contract Agreement C4884-55 for Syncrude Canada Lts., June, 62 p.
- Scott, J.D., and Chichak, M.F., 1985c. Large Sludge Standpipe Consolidation Test 3, Progress Report to September, 1985. Sludge Standpipe Testing Contract Agreement C4884-55 for Syncrude Canada Lts., June, 46 p.
- Scott, J. D., and Dusseault, M.B., 1980. Behaviour of Oil Sands Tailings. Proceedings of the 33rd Canadian Geotechnical Conference, Calgary, Alberta, p. 35.
- Scott, J. D., and Dusseault, M.B., 1982. Behaviour of Oil Sand Tailings Sludge. 33rd Annual Technical Meeting of the Petroleum Society of the Canadian Institute of Mining and Metallurgy, Calgary, Alberta, June, Paper no. 82-33-85, 19 p.
- Scott, J. D., and Dusseault, M.B. and Carrier III, W.D., 1985, Behaviour of the clay/bitumen/water sludge system from oil sands extraction plants, Journal of Applied Clay Science, 1, pp. 207-218.
- Scott, J. D., and Dusseault, M.B. and Carrier III, W.D., 1986, Large-scale self weight consolidation testing, Consolidation of soils: Testing and Evaluation, ASTM SPT 892, pp. 500-515.
- Scott, J. D., Liu, Y., and Caughill, D.L., 1993. Total Tailings Disposal Research Program Report 10: Summary Report on Total Tailings Disposal Research Program submitted to Syncrude Canada Ltd, December 16th, 1993.
- Seed, H.B., and Chan, C.K., 1957. Thixotropic Characteristics of Compacted Clays. Journal of Soil Mechanics : Foundation Division., ASCE, Vol. 83. SM 4, pp. 1-35.

- Sill, G.C., Hoare, D.L., and Baker, N., 1986. An experimental assessment of the restricted floe consolidation test, Consolidation of Soils, ASTM STP 892, R.N. Yong and F.C. Townsend, Eds., American Society for Testing and Materials, Philadelphia, 1986, pp. 7-70.
- Skempton, A.W. and Northey, R.D., 1952. The sensitivity of clays, *Geotechnique*, Vol.3, No. 1, pp. 203-208.
- Somogyi, F., 1980. Large Strain Consolidation of Fine Grained Slurries. Presented at the Canadian Society for Civil Engineering, Winnipeg, Manitoba, May 29-30.
- Somogyi, F., Carrier III, W.D., Lawver, J.E., and Beckman, J.F., 1984. Waste Phosphatic Clay Disposal in Mine Cuts. Sedimentation/Consolidation Models – Prediction and Validation, American Society of Civil Engineers, New York, pp. 545-564.
- Somogyi, F., Keshian, B., Beomwell, L.C., and Carrier III, W.D., 1981. Consolidation Behaviour of Impounded Slurries. Presented at Annual Spring Convention, ASCE, New York.
- Sridharan, A., and Rao, A. S., 1982. Mechanisms controlling the secondary compression of clays, *Geotechnique*, Vol. 32, No. 3, pp. 249-260.
- Sridharan, A., Murthy, N. S. and Prakash, K., 1987. Rectangular hyperbola method of consolidation analysis, *Geotechnique*, Vol. 37, No. 3, pp. 355-368.
- Suthaker, N. N., 1995. Geotechnics of Oil Sand Fine Tailings, Ph.D. Thesis, University of Alberta, Edmonton, Canada.
- Suthaker, N. N., Scott, J.D., and Miller, W.G., 1997. The first fifteen years of a large scale consolidation test, Proceedings of the 50th Canadian Geotechnical Conference, October 20-22, Ottawa, ON, pp. 476-483.
- Tan, T.S., and Scott, R.F., 1988. Finite strain consolidation a study of convection. *Soils and Foundations*, Vol. 28, No. 4, pp. 64-74.
- Tan, S.A., 1989. A simple automatic falling head permeameter, *Soils and Foundations*, Vol. 29, No. 1, pp. 161-164.
- Tan, T.S., 1995 "From sedimentation to consolidation: A geotechnical perspective." in Proceedings, International Conference on Compression and Consolidation of Clayey Soils, May, 1995, Hiroshima, Japan, Yoshikuni and Kusakabe (eds), Balkema, pp. 937-948. (Keynote Lecture)
- Tan, T.S., Yong, K.Y., Leong, E.C and Lee, S.L., 1990b. Behaviour of clay slurry. *Soils and Foundations*, Vol. 30, No. 4, pp. 105-118.

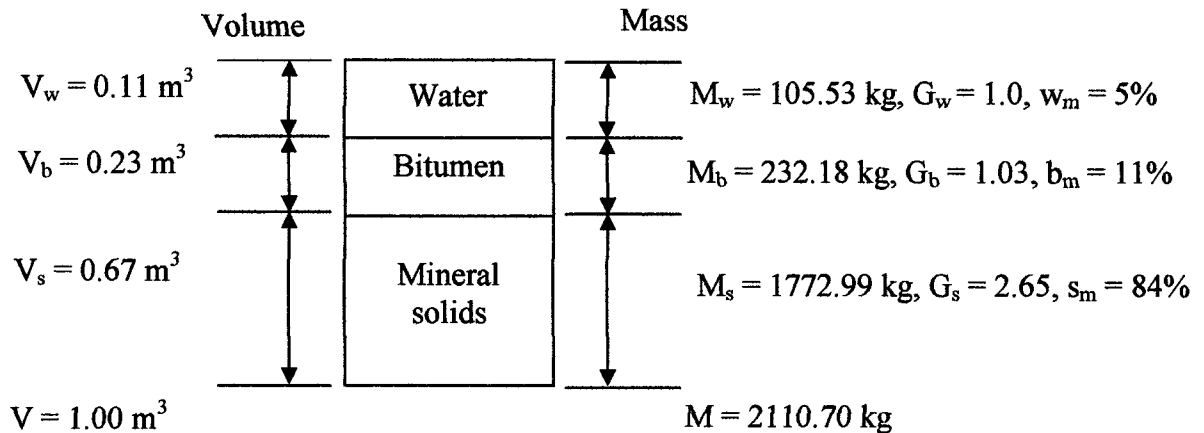
- Tang, J., Biggar, K.W., Scott, J.D., and Segoo, D.C., 1997, Examination of Mature Fine Tailings Using a Scanning Electron Microscope, 50th Canadian Geotechnical Conference, Ottawa, Ontario, October 20-22, pp. 746-754.
- Tang, J., 1997. Fundamental Behaviour of Composite Tailings. MS.c. Thesis, University of Alberta, Edmonton, Canada.
- Terzaghi, K., Peck, R. B., and Mesri, G, 1996, Soil Mechanics in Engineering Practice, Third Edition, John Wiley & Sons, Inc., 549 p.
- Terzaghi, K., 1943. Theoretical Soil Mechanics, John Wiley and Sons, Inc., New York, New York, 510 p.
- Touhidi-Baghini, A.,1998. Absolute Permeability of McMurray Formation Oil Sands at Low Confining Stresses, Ph.D. Thesis, University of Alberta, Edmonton, Canada.
- Tovey, P. S. a. N. K., 1980, Electron microscopy of soils and sediments: techniques, Clarendon Press, Oxford, 264 p.
- Tovey, P. S. a. N. K., 1980, Electron microscopy of soils and sediments: examples, Clarendon Press, Oxford, 264 p.
- Van Olphen, H., 1977. An Introduction to Clay Colloid Chemistry. John Wiley and Sons, Wiley-Interscience, 2nd Edition., New York, 318 p.
- Yin, J.H., Zhu, J.G., and Graham, J., 2002. A new elastic viscoplastic model for time-dependent behaviour of normally and overconsolidated clays: theory and verification. Canadian Geotechnical Journal, Vol. 39, No.4, pp. 157-173.
- Yin, J.-H., and Graham, J., 1989. Viscous-elastic-plastic modelling of one-dimensional time-dependent behaviour of clays. Canadian Geotechnical Journal, Vol. 26, 199-209.
- Yin, J.-H., and Graham, J., 1994. Equivalent times and one-dimensional elastic viscoplastic modelling of time-dependent stress-strain behaviour of clays. Canadian Geotechnical Journal, Vol. 31, pp. 42-52.
- Yin, J.-H., and Graham, J., 1999. Elastic visco-plastic modelling of time-dependent stress-strain behaviour of soils. Canadian Geotechnical Journal, Vol. 36, No.4, pp. 736-745.
- Yin, J.H., Zhu, J.G., and Graham, J., 2002. A new elastic viscoplastic model for time-dependent behaviour of normally and overconsolidated clays: theory and verification. Canadian Geotechnical Journal, Vol. 39, No.4, 157-173.

- Yong, R.N., Sheeran, D.E., Sethi, A.J., and Erskine, H.L., 1982. The Dynamics of Tar-Sand Tailings. Proceedings of the 33rd Annual Technical Meeting of the Canadian Institute of Mining and Metallurgy, Calgary, Alberta, June, Paper no. 82-33-42, 6p.
- Znidarcic D., Croce, P., Pane, V., Ko, H.W., Olsen, H. W., and Schiffman, R.L., 1984. The theory of one-dimensional consolidation of saturated clays, III, existing testing procedures and analyses. Geotechnical Testing Journal, Vol. 7, No. 3, pp. 123-133.

Appendix A – Estimation of Oil Sands Tailings Stream Volume

In the mineable oil sands area north of Fort McMurray (EUB, 2004) the average bitumen content is 9.7%. In the areas being mined, however, the bitumen content averages 11% (Scott et al. 1993). The porosity of these rich oil sands is approximately 33% with bitumen occupying 68% of the pore volume and connate water occupying the other 32%. Little to no gas is in the voids of the in place, undisturbed oil sands. The bitumen, however, is generally saturated with gas which comes out of solution when the oil sands are unloaded by surface mining. The phase diagram below shows the mass and volume of each component of the in place oil sands.

In place oil sands

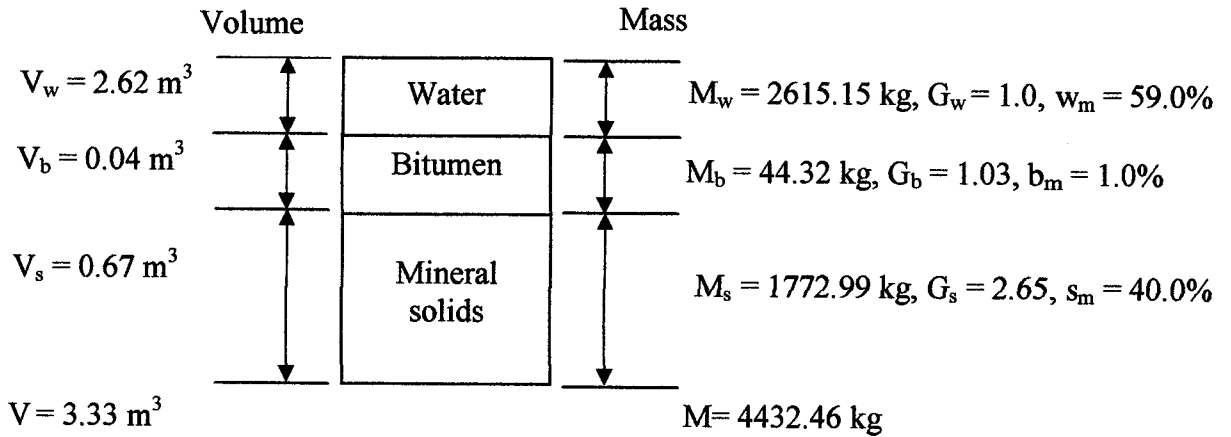


The volume of produced tailings depends on the extraction process, the fines content of the oil sands, the addition of other waste streams and the amount of water required for pipeline transportation. The solids content of the tailings will vary from 40% to 60% at different extraction plants at different stages of mining (Scott et al. 1993 and Scott et al. 1994).

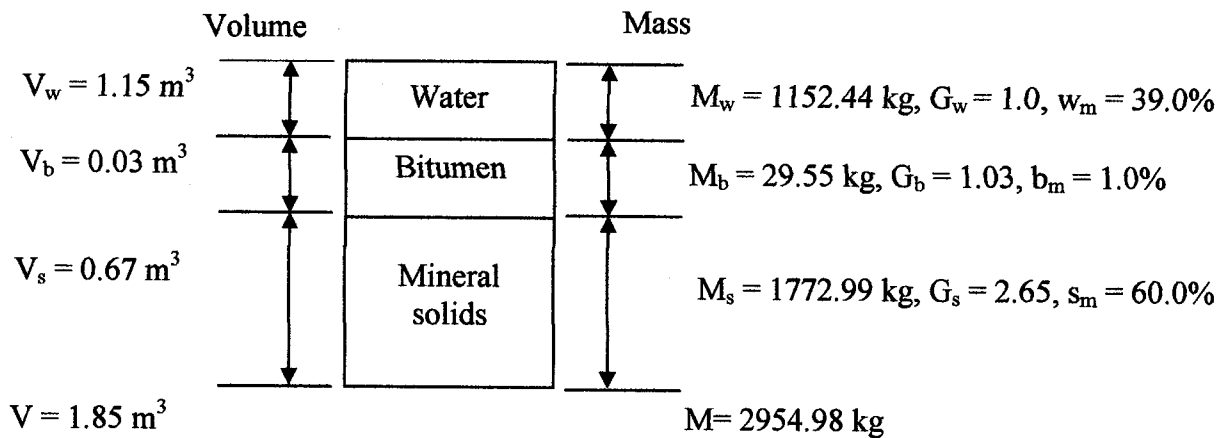
Based on the mass of solids in the in place oil sands and the solids contents of the tailings streams the following two phase diagram are shown for 40% solids and 60% solids, respectively. The bitumen content of the tailings varies between 0.5% and 2% and a typical amount of 1% is included in the phase diagrams.

Tailings streams

40% solids content



60% solids content



From the above phase diagrams, 1.0 m^3 of in place oil sands results in a volume of tailings at 40% solids of 3.3 m^3 and a volume of tailings at 60% solids of 1.9 m^3 .